


2006

Novel Cancer Therapeutics, the Generation of ROS, and Cell Survival

Clint Mitchell

Virginia Commonwealth University

Follow this and additional works at: <http://scholarscompass.vcu.edu/etd>

 Part of the [Biochemistry, Biophysics, and Structural Biology Commons](#)

© The Author

Downloaded from

<http://scholarscompass.vcu.edu/etd/1245>

This Dissertation is brought to you for free and open access by the Graduate School at VCU Scholars Compass. It has been accepted for inclusion in Theses and Dissertations by an authorized administrator of VCU Scholars Compass. For more information, please contact libcompass@vcu.edu.

Novel Cancer Therapeutics, the Generation of ROS, and Cell Survival

A dissertation submitted in partial fulfillment of the requirements for the degree of
Doctor of Philosophy at Virginia Commonwealth University.

By:

Clint Mitchell
Master of Science
Virginia Commonwealth University
Richmond, VA 2005

Director: Paul Dent Ph.D.,
Professor, Biochemistry

Virginia Commonwealth University
Richmond, Virginia
August, 2006

Acknowledgement

I would like to thank my parents and friends for their continual support. I would also like to thank Dr. Adly Yacoub, Dr. Song-Iy Han, Dr. Margaret Park, and Dr. William Hawkins for their expertise and patience with me throughout this continual learning process. My sincere appreciation goes to the members of my committee for their time and encouragement. I do not have the words to express my thanks to Dr. Paul Dent for his unending support of my ever-changing goals and aspirations, so a simple thank you will have to do.

Table of Contents

List of Tables.....	vii
List of Figures.....	viii
List of Abbreviations.....	xiii
Abstract.....	xv
Chapter One: Introduction.....	1
1.1.1 – Background on Renal Cell Carcinoma.....	1
1.1.2 – Gene Therapy and MDA-7.....	2
1.1.3 - Cellular Signaling Pathways Involved in Apoptosis.....	4
1.1.4 – Background on Reactive Oxygen Species (ROS).....	17
1.1.5 – Erb-B Receptors Interact with the Intrinsic/Extrinsic Pathways.....	20
1.1.6 – Background on MAPK Pathways.....	24
1.2.1 – Background on Glioblastoma Multiforme and MDA-7 Review.....	39
1.2.2 – Mechanisms Involved in Cell Cycle Control.....	41
1.2.3 – Cell Cycle Regulation.....	50
1.3.1 – Background on Hepatocellular Carcinoma.....	56
1.3.2 – Role of Bile Acids in the Liver.....	58
1.3.3 – Fas Receptor Review and Endoplasmic Reticulum Functionality.....	61
1.3.4 – Endoplasmic Reticulum (ER) Stress Response.....	61
1.3.5 – Heat Shock Protein Background.....	64
1.3.6 – Geldanamycin Background.....	76

1.4.1 – Objective: Renal Cell Carcinoma and MDA-7.....	78
1.4.2 – Objective: Glioblastoma Multiforme and MDA-7.....	79
1.4.3 – Objective: Hepatocellular Carcinoma, Bile Acid, and 17-AAG.....	80
Chapter Two: Materials and Methods.....	82
2.1 – Materials.....	82
2.2 – Cell Culture.....	83
2.3 – Primary Culture of Rodent Hepatocytes.....	84
2.4 – Generation of Rho-zero HuH7 Cells.....	84
2.5 – Generation of Adenovirus Ad.mda-7 and Synthesis of GST-MDA-7.....	85
2.6 – Recombinant Adenovirus Vectors: generation, titering <i>in vitro</i> infection.....	86
2.7 – Poly-L-lysine Adenoviral Vectors: Infection <i>In Vitro</i>	88
2.8 – Ionizing Radiation Exposure.....	90
2.9 – Cell Homogenization and Protein Assay Analysis.....	90
2.10 – SDS Poly-Acrylamide Gel Electrophoresis and Western Blot Analysis...91	
2.11 – Assessment of Cell Apoptosis and Cell Death.....	96
2.12 – Assessment of Cell Viability.....	97
2.13 – MTT Assay for Determination of Cellular Viability.....	98
2.14 – Cell Survival Analyses.....	99
2.15 – Assessment of Reactive Oxygen Species Generation.....	100
2.16 – Cell Cycle Analysis.....	100
2.17 – DNA Fragmentation.....	101

2.18 – Statistical Analyses.....	103
Chapter Three: Results.....	104
3.1.1 – Transfection of RCC lines to express MDA-7 resulted in cell death.....	104
3.1.2 – As ₂ O ₃ causes dose-dependent reduction in cell proliferation.....	110
3.1.3 – N-acetyl cysteine reduces cell killing.....	119
3.1.4 – Protein expression in response to GST-MDA-7 and As ₂ O ₃	122
3.1.5 – Alterations in nuclear DNA integrity in response to GST-MDA-7 and As ₂ O ₃	125
3.1.6 – Summary of findings in renal cell carcinoma (RCC).....	127
3.2.1 – Ad. <i>mda-7</i> enhances the radiosensitivity of glioma cells.....	128
3.2.2 – Ad. <i>mda-7</i> enhances ERK1/2 and p38 activity in RT2 cells.....	140
3.2.3 – Role of p38 and JNK1/2 signaling in glioma radiosensitization.....	146
3.2.4 – Ad. <i>mda-7</i> infected RT2 cells express a 23 kDa MDA-7 protein.....	148
3.2.5 – Summary of findings in glioblastoma multiforme (GBM).....	150
3.3.1 – 17-AAG interacts with bile acid to kill primary rat hepatocytes.....	151
3.3.2 – Hepatocyte cell death is ROS-dependent.....	154
3.3.3 – DCA and 17-AAG activate MAPK pathways.....	158
3.3.4 – Small molecule inhibitors and adenovirus effect 17-AAG and DCA lethality.....	162
3.3.5 – Role of ASK1 in hepatocyte cell death.....	167
3.3.6 – Role of acidic sphingomyelinase in 17-AAG and DCA toxicity.....	170
3.3.7 – Further ROS studies in hepatocytes and human HuH7 hepatoma cells.....	173
3.3.8 – 17-AAG and DCA toxicity, and the intrinsic/extrinsic pathways.....	177

3.3.9 – 17-AAG and DCA cause cell death in transformed mouse embryonic fibroblasts.....	179
3.3.10 – Summary of findings in hepatocellular carcinoma (HCC).....	183
Chapter Four: Discussion.....	185
4.1 – MDA-7 and Renal Cell Carcinoma.....	185
4.2 – MDA-7 and Glioblastoma Multiforme.....	191
4.3 – Geldanamycins and Liver Toxicity.....	194
4.4 – Conclusions.....	200
References.....	202
Vita.....	221

List of Tables

Table Page

1. Solutions required for preparing resolving and stacking gels
for SDS-PAGE.....95

List of Figures

Figure Page

1. Extrinsic and intrinsic pathway involved in the apoptotic response.....	13
2. Relationship between MAPK signaling pathways and apoptotic pathways.....	23
3. MAPK intracellular signaling pathways.....	25
4. ERK1/2 MAPK signaling pathway.....	26
5. SAPK/JNK MAPK signaling pathway.....	27
6. p38 MAPK signaling pathway.....	28
7. ERK5 MAPK signaling pathway.....	29
8. AKT signaling pathway.....	30
9. Cell cycle.....	48
10. G ₁ /S cell cycle checkpoint.....	52
11. G ₂ /M cell cycle checkpoint.....	55
12. GST-MDA-7 causes a dose-dependent reduction in the proliferation of the A498 renal carcinoma cell line.....	106
13. GST-MDA-7 causes a dose-dependent reduction in the proliferation of the UOK121N renal carcinoma cell line.....	107
14. GST-MDA-7 does not cause a dose-dependent reduction in the proliferation of primary renal epithelial cells.....	108
15. Medium obtained from primary rat hepatocytes infected with Ad. <i>cmv</i> or Ad. <i>mda-7</i> (m.o.i. = 50) causes a dose-dependent reduction in the proliferation of the A498 renal carcinoma cell line.....	109
16. Arsenic trioxide causes a dose-dependent reduction in the growth of A498 renal carcinoma cells, and in the primary renal epithelial cells.....	111

17. GST-MDA-7 and arsenic trioxide interact in a greater than additive fashion in the A498 renal carcinoma cell line to reduce cell growth.....	114
18. GST-MDA-7 and arsenic trioxide interact in a greater than additive fashion in the UOK121N renal carcinoma cell line to reduce cell growth.....	115
19. GST-MDA-7 and arsenic trioxide do not interact in a greater than additive fashion in the primary renal carcinoma cell line to reduce cell growth.....	116
20. GST-MDA-7 (0.5 nM) and arsenic trioxide (0.5 μ M) interact in a greater than additive fashion to reduce colony formation ability in the A498 renal carcinoma cell line.....	117
21. GST-MDA-7 (0.5nM) and arsenic trioxide (0.5 μ M) interact in a greater than additive fashion to reduce colony formation ability in the UOK121N renal carcinoma cell line.....	118
22. GST-MDA-7 and arsenic trioxide interact in a greater than additive fashion to enhance A498 renal carcinoma cell killing, which is blocked by N-acetyl-cysteine.....	120
23. GST-MDA-7 and arsenic trioxide interact in a greater than additive fashion to enhance UOK121N renal carcinoma cell killing, which is blocked by N-acetyl-cysteine.....	121
24. GST-MDA-7 and arsenic trioxide interact to enhance cleavage of pro-caspase 3 and PARP in renal carcinoma cells that coincided with reduced expression of Bcl-X _L	123
25. ERK1/2, JNK1/2, and p38 activity in renal cell carcinoma, in response to GST, GST-MDA-7, and arsenic trioxide.....	124
26. Nucleosomal DNA integrity in renal cell carcinoma.....	126
27. Ad. <i>mda-7</i> suppresses RT2 cell growth and enhances radiosensitivity.....	129
28. Ad. <i>mda-7</i> suppresses RT2 cell colony formation and enhances radiosensitivity.....	130
29. Ad. <i>mda-7</i> suppresses U251 cell growth and enhances radiosensitivity.....	131
30. Ad. <i>mda-7</i> suppresses U373 cell growth and enhances radiosensitivity.....	132

31. <i>Ad.mda-7</i> causes an increase in RT2 cell death that is enhanced in a greater than additive fashion by ionizing radiation.....	134
32. Expression of PARP and p32 pro-caspase 3 in RT2 cells, in response to <i>Ad.mda-7</i> and <i>Ad.cmv</i> in combination with ionizing radiation.....	135
33. Combination of <i>Ad.mda-7</i> and radiation enhance RT2 cell numbers in G ₁ phase and reduced numbers in S phase.....	137
34. Combination of <i>Ad.mda-7</i> and radiation enhance U251 cell numbers in G ₂ /M phase and reduced numbers in S phase.....	138
35. Expression of p21 and p53 in RT2 cells, in response to <i>Ad.mda-7</i> and <i>Ad.cmv</i> in combination with ionizing radiation.....	139
36. MAPK activity in response to multiple inhibitors, radiation, and <i>Ad.mda-7</i> , and <i>Ad.cmv</i>	142
37. Anti-proliferative effects of <i>Ad.mda-7</i> is enhanced by combined inhibition of MEK1/2 and PI3K, in RT2 cells.....	143
38. Toxicity of <i>Ad.mda-7</i> , as judged by Wright-Geimsa assay, is enhanced by combined inhibition of MEK1/2 and PI3K, in RT2 cells.....	144
39. Toxicity of <i>Ad.mda-7</i> , as judged by trypan blue-exclusion assay, is enhanced by combined inhibition of MEK1/2 and PI3K, in RT2 cells.....	145
40. Pretreatment with the JNK1/2 inhibitor, SP600125, abolished the radiosensitizing effect of <i>Ad.mda-7</i> in RT2 cells.....	147
41. Infection of RT2 cells with <i>Ad.mda-7</i> results in the expression of the 23 kDa MDA-7 protein.....	149
42. Combined exposure of primary rat hepatocytes to 17-AAG and DCA resulted in a significantly greater than additive induction of cell killing above that induced by either agent alone.....	153
43. ROS levels generated in hepatocytes.....	155
44. NAC and Trolox abolished lethality and induction of cell killing in Response to 17-AAG and DCA treatment.....	156
45. HeLa cervical carcinoma lines expressing active and mutated inactive thioredoxin reductase, in response to 17-AAG and DCA treatment.....	157

46. ERK1/2, AKT, and p38 MAPK activation levels in response to treatment with 17-AAG, DCA, and the combination.....	159
47. JNK1/2 and p38 MAPK activation levels in response to treatment with 17-AAG, DCA, and the combination.....	160
48. Treatment of hepatocytes with ROS quenching agents suppressed enhanced levels of p38 MAPK and JNK1/2 activation.....	161
49. Constitutively activated AKT, not MEK1, suppressed 17-AAG and DCA lethality, coinciding with suppressed JNK1/2 activation.....	163
50. PI3K inhibitor and dominant negative MEK1, not AKT, enhanced 17-AAG and DCA toxicity.....	164
51. Dominant negative p38 α MAPK, dominant negative JNK1, and inhibition of p38 α / β suppressed induction of cell death.....	165
52. Dominant negative TAM67 enhances DCA lethality.....	166
53. Dominant negative ASK1 abolished p38 MAPK activation.....	168
54. Dominant negative ASK1 abolished 17-AAG and DCA lethality.....	169
55. ROS generation in wild type and ASM $^{-/-}$ mouse hepatocytes.....	171
56. Loss of acidic sphingomyelinase reduces 17-AAG and DCA-induced hepatocyte cell death.....	172
57. Hepatocyte ROS generation suppressed by cyclosporine A and bongkreikic acid.....	174
58. ROS generation in HuH7 and HuH7 Rho(0) hepatoma cells.....	175
59. Loss of functional mitochondria suppressed 17-AAG and DCA lethality in HuH7 Rho(0) hepatoma cells.....	176
60. Inhibition of caspase 9, not caspase 8, significantly abolished 17-AAG and DCA toxicity.....	178
61. Loss of combined BAX and BAK expression abolished 17-AAG and DCA toxicity in transformed mouse embryonic fibroblasts.....	181

62. Loss of BAX and PERK expression abolished 17-AAG and DCA
toxicity in transformed mouse embryonic fibroblasts.....182

List of Abbreviations

Full Name	Abbreviation
17-allylamino-17-demethoxygeldanamycin	17-AAG
Adaptor Protein	AP
AKT8 Virus Oncogene Cellular Homolog	AKT
Apoptosis-inducing Factor	AIF
Apoptotic Protease-activating Factor	Apaf
Apoptotic Signaling Kinase-1	ASK1
Arsenic Trioxide	As ₂ O ₃
Adenosine Tri-phosphate	ATP
cAMP Response Element-binding Protein	CREB
Caspase Recruitment Domain	CARD
Cyclin-dependent Kinase	CDK
c-Jun NH ₂ -terminal Kinase	JNK
Coxsackievirus and Adenovirus Receptor	CAR
Cytomegalovirus	CMV
Death Domain	DD
Death Effector Domain	DED
Death-inducing Signaling Complex	DISC
Deoxycholic Acid	DCA
Dulbecco's Modified Eagle's Medium	DMEM
Dimethyl Sulfoxide	DMSO
Epidermal Growth Factor	EGF
Ethylenediaminetetraacetic Acid	EDTA
Extracellular Signal-Regulated Kinase	ERK
FADD-like ICE (Caspase 8) Inhibitory Protein	FLIP
Fatty Acid Synthase	Fas
Fas-ligand	Fas-L
Fas-receptor	Fas-R
Fas-associated Protein with Death Domain	FADD
Glutathione S-transferase	GST
Growth Arrest and DNA Damage Protein	GADD
Heat-shock Protein	Hsp
Hepatocellular Carcinoma	HCC
Horseradish Peroxidase	HRP
Inhibitors of Apoptosis	IAP
Interferon	IFN
Interleukin	IL
MAPK/ERK Kinase	MEK
MAP Kinase-activating Death Domain	MADD

Melanoma Differentiation-associated 7	MDA-7
Micro (10^{-6})	μ
Milli (10^{-3})	m
Mitogen-activated Protein Kinase	MAPK
Mitogen and Stress-activated Protein Kinase	MSK
Molar	M
(3-[4,5-Dimethylthiazol-2-yl]-2,5-diphenyltetrazolium bromide	MTT
N-acetyl Cysteine	NAC
Nano (10^{-9})	n
Phosphate-buffered Saline	PBS
Protein Kinase C	PKC
Poly-(ADP-ribose) Polymerase	PARP
p21-activated Kinase	PAK
Reactive Oxygen Species	ROS
Receptor Interacting Protein	RIP
Renal Cell Carcinoma	RCC
RIP-associated ICH-1/CED-3 Homologous Protein with Death Domain	RAIDD
Ribosomal S6 Kinases	RSK
Sodium Dodecyl Sulfate	SDS
Sodium Dodecyl Sulfate Polyacrylamide Gel Electrophoresis	SDS-PAGE
Stress-activated Protein Kinase	SAPK
Truncated Bid	tBid
TNF-related Apoptosis-inducing Ligand	TRAIL
TNF-receptor Associated Death Domain	TRADD
Transforming Growth Factor	TGF
Tris-buffered Saline plus Tween 20	TBST
Tumor Necrosis Factor Receptor	TNFR
X-chromosome Linked Inhibitor of Apoptosis	XIAP
3-phosphoinositide-dependent Protein Kinase	PDK
Phosphatidylinositol 3-kinase	PI3K

Abstract

NOVEL CANCER THERAPEUTICS, THE GENERATION OF ROS, AND CELL SURVIVAL.

By Clint Mitchell, MS

A dissertation submitted in partial fulfillment of the requirements for the degree of Doctor of Philosophy at Virginia Commonwealth University.

Virginia Commonwealth University, 2006.

Paul Dent, Ph.D., Professor, Department of Biochemistry

The impact of Ad.*mda-7* on the survival of renal cell carcinoma lines (RCC), primary renal epithelial cells, glioblastoma multiforme lines (GBM), and primary rodent astrocytes is unknown. The present studies examine whether the GST fusion protein, GST-MDA-7, and the adenovirus, Ad.*mda-7*, altered the growth and survival of the A498 and UOK121N RCC lines or radiosensitized GBM, respectively. Due to previous findings that the RCC lines, but not primary renal epithelial cells, were resistant to type 5 adenoviral infection, we used purified GST-MDA-7 protein to show that GST-MDA-7, but not GST, caused a dose-dependent reduction in A498 and UOK121N proliferation but not that of primary renal epithelial cells. Free radical species, generated by clinically relevant concentrations of arsenic trioxide, synergized with subnanomolar concentrations of GST-MDA-7 to inhibit the proliferation, viability, and long-term survival of RCC. We also found that MDA-7 (IL-24), when expressed via a recombinant replication defective adenovirus, Ad.*mda-7*, exerted anti-proliferative effects on GBM cells, an effect found to be enhanced in a greater than additive fashion when combined with ionizing radiation.

These findings argue that MDA-7, in combination with agents that generate free radicals, such as arsenic trioxide and ionizing radiation, may have potential in the treatment of RCC and GBM. Geldanamycins are currently being used in a number of clinical trials in different tumor cell types, such as hepatocellular carcinoma (HCC), targeting the inhibition of the heat shock protein and molecular chaperone Hsp90. Previous studies have demonstrated that geldanamycins have dose limiting toxicity *in vivo* due to their actions in promoting normal liver dysfunction. These studies show that the geldanamycin derivative, 17-allylamino-17-demethoxygeldanamycin (17-AAG), interacts with the secondary bile acid, deoxycholic acid (DCA), to kill primary rat hepatocytes and HuH7 human hepatoma cells. An effect abolished by the addition of the ROS-quenchers, NAC and Trolox. Collectively, these findings argue that geldanamycins may not be a viable therapy for HCC treatment and that 17-AAG toxicity in primary hepatocytes may be, at least upon initial drug exposure, due to ROS generation and mechanisms independent of Hsp90 inhibition and the down-regulation of “classical” Hsp90 client proteins.

CHAPTER ONE

INTRODUCTION

1.1.1 Background on Renal Cell Carcinoma

Renal cell carcinoma (RCC), also referred to as renal adenocarcinoma or hypernephroma, is the development of transformed cells in the renal tubules. As RCC proliferates, it may invade organs adjacent to the kidney such as the liver, colon, or pancreas. Kidney cancer cells may also spread (metastasize) to other areas such as the lymph nodes, brain, lungs or bone. Detection prior to metastasis greatly improves a patient's chance of survival (Godley et al. 2001, Vogelzang et al. 1998, Motzer et al. 1996).

The most common form of cancer found in the kidney is renal cell carcinoma (RCC). Approximately 40,000 new cases occur each year in the United States and slightly less than 10,000 deaths occur per year due to metastatic disease. A combination of treatments approach is currently being used to treat RCC, although surgery, including full or partial kidney removal, is the mainstay of RCC treatment. Other treatments, depending on the individual, include biological therapy to trigger an immune response, hormone therapy, radiotherapy, and chemotherapy (Godley et al. 2001, Vogelzang et al. 1998, Motzer et al. 1996). Metastatic RCC is highly resistant to the majority of conventional chemotherapies, with low response rates, and a 5-year survival of less than ten percent (Godley et al. 2001, Motzer et al. 1996, Vogelzang et al. 1998). More recent attempts at treating this

disease involve the use of growth inhibitory and pro-inflammatory cytokines, such as IL-2, a protein produced during the immune response, and interferon- α (IFN- α), a protein secreted by many cell types generally known for their anti-viral and anti-tumor properties, have also proved to be of marginal benefit (Glaspy et al. 2002, Milowsky et al. 2001). Thus, the development of new therapies that provide greater efficacy in controlling RCC growth and survival is warranted.

1.1.2 Gene Therapy and Melanoma Differentiation Associated Gene-7 (MDA-7)

Gene therapy is a novel approach in cancer treatment utilizing recombinant viruses containing tumor suppressor genes, or genes encoding toxic cytokines, that reduce tumor cell growth and survival (Ponnazhagan et al. 2001) while other approaches have used modified adenoviruses that are selectively replicative and lytic only in tumor cells, but not in non-transformed cells (Gomez-Navarro et al. 2000). In the majority of gene therapeutic approaches currently under investigation, the efficacy of the treatment with respect to cell killing depends on the rate of infection of the target tumor cells, or m.o.i (multiplicity of infection), in that a higher rate of infection results in an increase in cell killing (Curiel et al. 1999). The Curiel group recently demonstrated that RCC cells were resistant to infection by type 5 adenoviruses that recognize the coxsackievirus and adenovirus receptor (CAR), due to the fact RCC cells have low levels of CAR expression (Haviv et al. 2002). The lack of CAR expression not only results in a loss of adenoviral

infection, but has also been associated with enhanced tumor cell growth *in vivo* (Okegawa et al. 2001, Rauen et al. 2002).

Subtraction hybridization and microarray analyses are currently being utilized to define the spectrum of gene expression changes occurring as a consequence of induction of irreversible growth arrest and terminal differentiation in human melanoma cells (Lebedeva et al. 2003). The application of subtraction hybridization using human melanoma cells, induced to undergo terminal differentiation by IFN γ , and the protein kinase C activator, mezarin, resulted in the reversion of malignant melanoma cells to a phenotype indicative of a normal cell (terminal differentiation), and ultimately resulted in the cloning of the gene encoding *mda-7* (IL-24) (Jiang et al. 1995, Sarkar et al. 2002, Sauane et al. 2003). Interleukins are cellular proteins secreted by a variety of cells that function to stimulate the proliferation of only those T and B cells bearing the required interleukin receptors (Cox et al. 2000). Due to the fact that T and B cells produce interleukin receptors only when they are complexed with an antigen, the only immune system cells that proliferate are those few that can respond to the antigen. The stimulus of human melanoma cells by IFN γ and mezarin induced the secretion of MDA-7/IL-24. MDA-7/IL-24 is a member of the IL-10 family, which includes IL-10, IL-19, IL-20, IL-22, and AK155 (IL-26) family (Parrish-Novak et al. 2002, Sarkar et al. 2002, Sauane et al. 2003, Wang et al. 2002).

MDA-7 expression is decreased in advanced melanomas, with nearly undetectable levels in metastatic disease (Ekmekcioglu et al. 2001, Jiang et al. 1995, Sarkar et al. 2002, Sauane et al. 2003). Enforced expression of MDA-7, by use of a recombinant adenovirus *Ad.mda-7*, has been shown to inhibit the growth of a broad spectrum of cancer cells *in vitro*, including those derived from skin, prostate, breast, central nervous system, cervical, sarcoma, colorectal, and lung, without exerting deleterious effects in normal human epithelial or fibroblast cells (Jiang et al. 1996, Saeki et al. 2000, Sauane et al. 2003, Sarkar et al. 2002, Su et al. 2003, Madireddi et al. 2000). On the basis of the apparent selectivity of *mda-7* toward cancer cells *in vitro* and animal studies confirming anti-tumor properties *in vivo*, *Ad.mda-7* was recently evaluated in a Phase I/II clinical trial in patients with advanced carcinomas (Chada et al. 2001). These studies document that *Ad.mda-7* is safe, and a single intratumoral injection can result in >70% tumor apoptosis associated with an inhibition in disease progression. MDA-7 is also shown to secrete from infected cells *in vitro* and *in vivo*, which may in part explain its profound anti-tumor bystander effects *in vivo* (Su et al. 2001, Lebedeva et al. 2002).

1.1.3 Cellular Signaling Pathways Involved in Apoptosis

Signaling mechanisms and pathways in cancer cells are currently being investigated with the aim of developing more potent interventions to decrease tumor cell growth potential and increase apoptosis. Apoptosis, or programmed cell death, is a form of cellular suicide and is widely observed in nature (Janicke et al. 1998). The process is

biochemically and morphologically different from the cellular necrosis mode of cell death, in which the cell experiences a ruptured cell membrane and swollen nuclei. There are a variety of stimuli that can trigger an apoptotic response, such as cytokines, viruses, hormones, or toxic insults. Initial approaches to define apoptosis were aimed at describing apoptosis morphologically, with the knowledge that dying cells exhibit a characteristic pattern of changes, including cytoplasmic shrinkage, membrane blebbing, chromatin condensation, and most commonly, cellular fragmentation into membrane-enclosed vesicles. A large amount of biochemical processes occur leading up to and during a cell's transformation to apoptosis. Cell surface alterations include externalization of phosphatidylserine and other alterations that promote recognition by phagocytes. On the intracellular level, degradation of the chromosomal DNA into high-molecular weight and oligonucleosomal fragments occurs, as well as cleavage of a specific subset of cellular polypeptides. These polypeptide cleavages occur via a specialized family of cysteine-dependent aspartate-directed proteases commonly referred to as caspases (Earnshaw et al. 1999).

Caspases exist in normal cells as inactive zymogens (Clem et al. 1998). The structure of caspases includes an N-terminal pro-domain, followed by multiple sequences encoding a large and small subunit. In some pro-caspases, the large and small subunits are separated by a small spacer region. All cleavages involved in caspase maturation occur on the carboxyl side containing the aspartate residues. There are two cleavages that must occur

in order for a caspase to become activated and these cleavages always occur in an ordered sequence. The large subunit is first cleaved from the small subunit and the pro-domain is removed from the large subunit. These pro-domains range in length from 23 amino acids for caspases-6 and -7, to 219 amino acids for caspase-10. Large pro-domains are representative of caspases that are involved in the initiation of an apoptotic response and are referred to as initiator caspases. Short pro-domain caspases are activated by the initiator caspases and are referred to as effector caspases (Earnshaw et al. 1999).

The regulation of apoptosis requires the activation of pro-caspases, of which can occur via at least two mechanisms deemed the extrinsic and intrinsic pathways. The former involves death receptor signaling through caspase-8, while the latter stems from changes in mitochondrial permeability, resulting in cytochrome c release, activation of caspase-9, and ultimately cell death.

Initiator caspases are activated in response to death stimuli. Upon stimulation, a molecular platform is assembled, followed by the recruitment of pro-caspases (Budihardjo et al. 1999). Death receptors contained on the cell surface are transmembrane proteins that belong to the tumor necrosis factor and nerve growth factor receptor families. Fas receptor and TNFR1 have a cytosolic region of homology referred to as the death domain (DD). The Fas ligand binds to the Fas receptor, resulting in the trimerization of Fas. The DD of Fas recruits a DD-containing molecule referred to as the

Fas-associated protein with death domain (FADD) that binds to Fas through its death domain. Other molecules that contain this death domain include the TNF-receptor associated death domain (TRADD), the receptor interacting protein (RIP), RIP-associated ICH-1/CED-3 homologous protein with death domain (RAIDD), and the MAP kinase-activating death domain protein (MADD). The N-terminus of FADD contains a death effector domain (DED) crucial to the recruitment of initiator caspases including pro-caspase-8 and pro-caspase-10. Pro-caspase-8 contains two DED domains on the N-terminus that enable it to bind to FADD. This binding allows the initiator pro-caspases to become closer together and upon binding, the pro-caspase-8 then becomes proteolytically cleaved into its active form through the dimerization of the two pro-caspase-8 proteins, thus allowing autoproteolysis to occur (Earnshaw et al. 1999). There are also inhibitors of the receptor mediated apoptotic response (i.e. IETD). This process can be mediated by numerous mechanisms, with emphasis on the mechanisms regulated by a protein referred to as the FADD-like ICE inhibitory protein (FLIP). This protein is expressed in two forms, FLIP-short and FLIP-long. Each isoform contains a DED, which allows for competitive binding with pro-caspase-8 and -10 for binding sites on FADD. This competitive binding can prevent the formation of the activation platform and can thereby inhibit the activation of the pro-caspases, resulting in no further amplification of the signal (Earnshaw et al. 1999).

Once activated, caspase-8 initiates downstream events that include the cleavage of pro-caspase-3 and other effector caspases, as well as activating the induction of mitochondrial dysfunction. Previous studies have argued that the activated form of caspase-8 can directly proteolyse and activate pro-caspase-3. However, studies have also found that in certain cell types, cytochrome c must be released in order to permit the initiator caspases to activate the effector caspases (Yin et al. 1999). The activated caspase-8 initiates the cleavage of Bid, which can displace Bax and Bak from cytoprotective Bcl-2 family of proteins, i.e. Bcl-2, Bcl-XL, Mcl-1. The release of cytochrome c initiates the cleavage of other pro-caspases, resulting in further amplification of the signal. In contrast to cytochrome c, an apoptosis-inducing factor (AIF) is also simultaneously released from the mitochondrial intermembrane into the cytoplasm during cell death and acts in a caspase-independent manner (Lipton et al. 2002). AIF has further been characterized as having both a pro- and anti-apoptotic role in the cell during cell death. In the former, AIF relocates from the mitochondria to the nucleus where its DNA binding activity is thought to mediate chromatin condensation and large-scale DNA fragmentation. In contrast, recent findings have argued that AIF could play a protective role in mitochondrial respiratory function and electron transfer as a free radical scavenger in order to protect the cell (Klein et al. 2002).

A direct release of cytochrome c from the mitochondria, independent of death receptor interactions, can occur in a cell exposed to radiation therapy, numerous chemicals, and

growth factor deprivation (cell starvation). Each of these conditions can result in mitochondrial dysfunction and the subsequent release of cytochrome c (Yin et al. 2000). A protein found in the cytoplasm, referred to as Apaf-1, binds and hydrolyzes ATP in the presence of cytochrome c, thus forming a complex between Apaf-1 and cytochrome c. It is this complex that binds pro-caspase-9, which is auto-proteolytically cleaved into the activated form and released from the complex. This activated caspase-9 becomes involved in the activation of the effector caspases-3, -6, and -7, which can then trigger apoptosis by acting on the caspase activated DNase (CAD), also called the DNA fragmentation factor (DFF) (Daugas et al. 2000) or cleaving poly (ADP-ribose) polymerase (PARP), a key protein in maintaining cell viability, the cleavage of which facilitates cellular disassembly and is a marker for an apoptotic mode of cell death. This process can become more potent due to an amplification loop contained in the system, which will be further discussed below. The initial binding of pro-caspase-9 to the Apaf-1/cytochrome c complex occurs in 1:1 ratio, which is pivotal in modulating the levels of pro-caspase available for cleavage. This ratio, along with the formation of the complex, allows for an increase in the levels of pro-caspase available for cleavage, and thus an amplification of the signal. The opposite can also occur, in which there is a decrease in the levels of pro-caspase available for cleavage, and thus prevention of signal amplification results. The inhibition of pro-caspase levels is crucial in preventing a small release of cytochrome c from inducing apoptosis (Budihardjo et al. 1999).

The effector caspases contain large amounts of substrates ranging from structural components of the cytoskeleton and nucleus, proteins involved in DNA metabolism and repair, as well as numerous protein kinases involved in signal transduction (Earnshaw et al. 1999). The amplification loop is initiated once the activated form of caspase-3 initiates proteolysis of pro-caspase-8. The activated form of caspase-8 can initiate the proteolytic cleavage, and subsequent activation of Bid, a BH3 domain-only protein, resulting in the activation of the extrinsic pathway leading to cell death, or can further cleave additional pro-caspase-3 (McKinstry et al. 2002), shown below in Figure 1.

The Apaf-1/cytochrome c complex is regulated by the anti-apoptotic Bcl-2 family members. Bcl-2 family members all contain Bcl-2 homology domains, designated BH1-BH4 domains (Adams et al. 1998). It has been verified in previous studies that the members of the Bcl-2 family do not necessarily contain all of the BH-domains (Yin et al. 2000). The Bcl-2 family of proteins regulates apoptosis by controlling mitochondrial permeability and the release of cytochrome c and can be divided into three groups based on function and sequence homology. The survival (anti-apoptotic) group of Bcl-2 proteins consists of Bcl-2 and Bcl-x_L, which reside in the outer mitochondrial wall and inhibit cytochrome c release, as well as Bcl-w, Mcl-1, and A1. The multi-domain pro-apoptotic group of Bcl-2 proteins consists of Bax, Bak, and Bok, and the BH3 only domain protein group (also pro-apoptotic) consists of Bad, BID, Bik, Bim, Hrk/DP5, Bmf, Puma and Noxa. These pro-apoptotic proteins reside in the cytosol but translocate

to mitochondria following death signaling, where they promote the release of cytochrome c (Craxton et al. 2005). The translocation of Bad, for instance, is controlled by numerous survival factors, such as the ErbB receptors, which activate intracellular signaling pathways that result in the phosphorylation of Bad as Ser112 and Ser136. The phosphorylation of Bad results in the binding of Bad to 14-3-3 proteins, leading to its cytosolic sequestration, and subsequent inhibition of Bad binding to Bcl-2 and Bcl-X_L (Yang et al. 1995). This protects the cell from apoptosis by inhibiting the inactivation of the pro-survival proteins. Cytosolic Bid is cleaved by caspase-8 following death signaling through Fas, and the resulting cleaved fragment (tBid) translocates to the mitochondria. Upon apoptotic stimulation, tBid induces a conformational change in Bak to form oligomer channels on the mitochondrial membrane, thus enabling cytochrome c and Smac/Diablo release. Bax, Bak, and Bik translocate to the mitochondria in response to death stimuli including survival factor withdrawal, or cell starvation. Bim activity is critical in regulating apoptosis in hematopoietic cells and can be stimulated in response to growth factor withdrawal and blockage of the phosphatidylinositol 3-kinase-AKT pathway. This phosphorylation of Bim is also mediated by either extracellular signal-regulated kinase (ERK) or c-Jun NH₂-terminal protein kinase (JNK) and it has been reported that ERK-induced phosphorylation of Bim promotes its ubiquitination and subsequent degradation via the S26 proteasome (Craxton et al. 2005). Thus, anti-apoptotic Bcl-2 family members function to promote cell survival by binding to and antagonizing death-promoting members, while the BH3 only domain family members

promote apoptosis by binding survival groups of proteins (Bouillet et al. 2002). Although the mechanisms regulating mitochondrial permeability and the release of cytochrome c during apoptosis are not fully understood, the accepted paradigm consists of the pro-apoptotic Bcl-2 proteins residing in the cytosol and upon death signaling, translocating to the mitochondria, where they promote the release of cytochrome c by binding to anti-apoptotic members located on the outer mitochondrial membrane. The presented evidence thus suggests that both the extrinsic pathway, involving death receptor signaling through caspase-8, as well as the intrinsic pathway, from the mitochondria via cytochrome c, can lead to cell death, as shown in Figure 1.

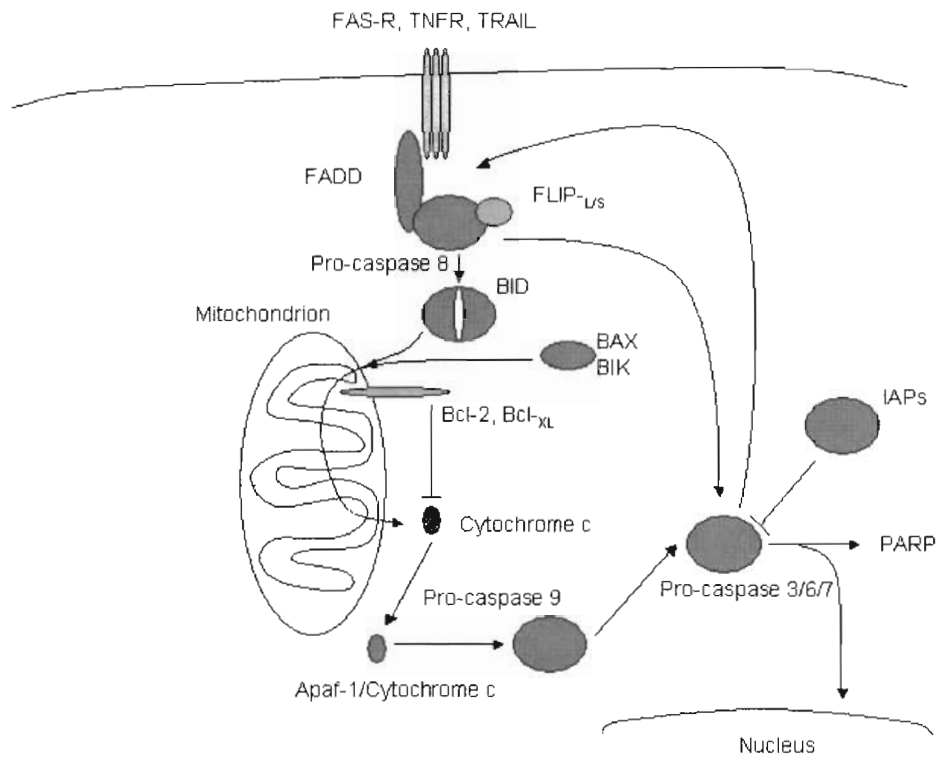


Figure 1. Extrinsic/intrinsic pathway involved in the apoptotic response

(Modified version of Dent et al. 2002).

Studies initially performed in the context of human breast carcinoma cells documented that *Ad.mda-7* up-regulates expression of the pro-apoptotic protein Bax and decreases expression of the anti-apoptotic protein Bcl-2, thereby shifting the balance from survival to death (Lebedeva et al. 2003). The fact that these changes in the levels of Bcl-2-family proteins and mitochondrial function were due to *mda-7/IL-24* were verified by studies showing that the over-expression of Bcl-2 was able to protect the breast cancer cells from loss of survival after infection with *Ad.mda-7* (Su et al. 1998). The apoptotic response of the cell is frequently modulated by the ratio of the anti-apoptotic proteins, such as Bcl-2 and/or Bcl-X_L to the pro-apoptotic proteins, such as Bad, Bid, Bax, Bak, and Bik. A shift in favor of the anti-apoptotic proteins results in cell survival, while a shift towards the pro-apoptotic proteins results in an apoptotic form of cell death (Chao et al. 1998, Ackermann et al. 1999). Bcl-X_L has also been found to inhibit the formation of the Apaf-1/pro-caspase 9 complex and subsequent activation of pro-caspases (Kluck et al. 1999). These findings could explain how the over-expression of Bcl-2 or Bcl-X_L inhibits the triggering of apoptosis even after cytochrome c has been released into the cytosol. This also suggests a more general model in which anti-apoptotic Bcl-2 family members regulate caspase activation by modulation of the scaffolding proteins ability to recruit pro-caspases (Earnshaw et al. 1999).

A family of intracellular apoptosis caspase inhibitor proteins, referred to as IAPs (inhibitors of apoptosis), also exist, and the overexpression of which, particularly survivin

and livin, has been found in numerous cancer cell lines and primary tumors (Altieri 2003, Tamm et al. 2000, Kasof et al. 2001). A total of six IAPs have been discovered in humans, c-IAP-1, c-IAP-2, XIAP, survivin, livin and NAIP. These proteins contain two to three copies of a common motif consisting of approximately 70 amino acids in length and function through direct interactions to inhibit caspase activity. The binding of Smac/Diablo to IAP family members, such as XIAP and survivin, blocks IAP interaction with caspase 9, allowing for the processing and activation of the caspases. Smac/Diablo is a mammalian mitochondrial protein that is released along with cytochrome c during apoptosis and promotes cytochrome c-dependent caspase activation by neutralizing inhibitor of apoptosis proteins (Srinivasula et al. 2000). It has been hypothesized that c-IAP-1 and c-IAP-2 have a caspase recruitment domain, or CARD, that functions to interfere with the activation of pro-caspase-9 via the Apaf-1/cytochrome c complex. XIAP functions to inhibit the active site of caspase-3, thus inhibiting the downstream signaling caused by caspase-8 or caspase-9. Survivin is an anti-apoptotic protein that, when activated by phosphorylation by cdc2, is responsible for the control of the G₂/M checkpoint, inhibition of apoptosis, and promotion of cell division. Other IAP proteins can bind to domain proteins such as FADD and pro-caspase-3, inhibiting their function (Altieri 2000).

In transformed cancer cells, anti-apoptotic proteins are up-regulated as a mechanism to protect the cell from programmed cell death, or cell apoptosis. Numerous therapies are

currently targeting these proteins in an effort to manipulate cancer cells towards an apoptotic form of cell death. Gene therapy utilizing Ad.*mda-7* is one method currently under investigation whereby apoptosis is induced by promoting mitochondrial dysfunction, as described above, and/or by the production of reactive oxygen species (ROS) (Lebedeva et al. 2003).

As discussed above, the over-expression of Bcl-2 or Bcl-_{XL} has been shown to inhibit mitochondrial dysfunction and apoptosis. It has also been found to inhibit ROS production (Lebedeva et al. 2003). The fact that *mda-7*/IL-24 induces changes in mitochondrial function and the production of reactive oxygen species, lends to the selective killing effects of *mda-7*/IL-24 on numerous type of cancer cells (Lebedeva et al. 2003, Yacoub et al. 2003).

The pathways by which MDA-7 enhances apoptosis in tumor cells are not fully characterized, although published results show the involvement of multiple genes important for the onset of growth inhibition and apoptosis, including p21, p53, GADD genes, Bcl-_{XL}, Bcl-2, Bax, and APO2/tumor necrosis factor-related apoptosis-inducing ligand. However, previous studies clearly reveal that MDA-7 suppresses growth in cancer cells independently of p53 status, and the retinoblastoma protein (Sauane et al. 2003, Sarkar et al. 2002, Saeki et al. 2000, Jiang et al. 1996, Su et al. 2003, Lebedeva et al. 2002). It was also found that in melanoma cell lines infected by Ad.*mda-7*, both anti-

apoptotic proteins, Bcl-2 and Bcl-X_L, experienced significant decreases in expression levels, but pro-apoptotic proteins Bax and Bak, experienced slight increases in expression (Lebedeva et al. 2002). In addition, recent studies demonstrate that over-expression of Bcl-2 and Bcl-X_L can differentially protect specific prostate cancer cell lines from Ad.*mda-7* induced apoptosis (Lebedeva et al. 2003). Previous investigations also show the ability of Ad.*mda-7* to induce apoptosis in the prostate cancer cell line, DU145, which is Bax null. These findings indicate that Ad.*mda-7* can modulate apoptosis through a Bax-independent pathway (Sauane et al. 2003, Sarkar et al. 2002, Mhashilkar et al. 2001).

1.1.4 Background on Reactive Oxygen Species (ROS)

In living cells, there is a steady formation of DNA lesions. A substantial number of these lesions that damage DNA occur naturally and on a continual basis. These include species such as superoxide anion (O₂⁻), hydrogen peroxide, and hydroxyl radical (·OH) derived from oxidative respiration. Free radicals generate a large number of affects within DNA, including modified DNA bases. The hydroxyl radical causes the formation of a large number of pyrimidine and purine derived lesions in DNA. Many of these modified DNA bases have great potential to damage the integrity of the genome. 8-Hydroxyguanine (8-OH-Gua) is one of the most widely studied lesions and the presence of which leads to transversions in the DNA, ultimately leading to mutagenesis. Due to the importance of DNA damage in carcinogenesis, it is probable that any agent capable of reacting with

DNA and chemically modifying it could be considered carcinogenic. Reactive oxygen species fall into this category. There is strong evidence that ROS play a role in the etiology of atherosclerosis, as well as influencing the progression of human immunodeficiency virus (HIV) and cancer research. Research has shown that the number of modified bases is increased in adenocarcinomas and that a further increase in levels of modified DNA bases can contribute to the genetic instability of tumor cells in fully developed cancer (Olinski et al. 2002).

Many of the agents utilized in anticancer therapies are also responsible for the induction of secondary malignancies by the generation of free radicals. Free radical-induced DNA damage may also possess premutagenic properties and may play a role in carcinogenesis. Ionizing radiation is one of the most commonly utilized therapeutic agents in cancer, with approximately half of all cancer patients receiving radiation therapy as part of their treatment (Olinski et al. 2002). Anthracycline derivatives and arsenic trioxide have also been utilized in the treatment of several types of human malignancies. The cytotoxicity of these drugs, as well as radiation therapy, has been attributed to the intracellular production of free radicals. These anticancer therapies have caused a significant increase in the amount of DNA base modifications, although the extent of these modifications differed in individuals due to individual differences in exposure, metabolism, repair capacity and genetic predisposition among patients. There is a risk associated with developing secondary cancers after chemotherapy and radiation therapy. However, the

benefits of utilizing therapies responsible for causing ROS generation, such as ionizing radiation and arsenic trioxide, have had positive results in anticancer therapy (Olinski et al. 2002). Research has shown that ROS are critically involved in As_2O_3 -induced apoptosis. Although arsenic trioxide induces apoptosis in a relatively wide spectrum of tumors, the sensitivity of different cell types to this treatment varies to a great extent (Jing et al. 2004). The true efficacy of arsenic trioxide in the treatment of cancer has yet to be characterized.

Radical oxygen species (ROS) are generated in multiple compartments and by multiple enzymes within the cell. The vast majority, approximately 90%, of cellular ROS generation lies within the mitochondria. Other key contributors to ROS generation include proteins within the plasma membrane, such as NADPH oxidases, lipid metabolism within the peroxisomes, as well as the activity of various cytosolic enzymes such as cyclooxygenases. The generation of mitochondrial ROS is a consequence of oxidative phosphorylation, a process that utilizes the controlled oxidation of NADH or FADH to generate a potential energy for protons across the mitochondrial inner membrane. This potential energy is in turn used to phosphorylate ADP and, at several sites along the cytochrome chain, electrons derived from NADH or FADH can directly react with oxygen or other electron acceptors and generate free radicals. ROS generated within the mitochondria can potentially feed back on the organelle and directly damage mitochondrial DNA and other components in a cyclic manner. Mitochondrial oxidants

can also damage nuclear DNA leading to the activation of p53 and other DNA damage pathways described below. Cytosolic elements including the stress-activated kinases such as SAPK/JNK and p38 MAPK may be potential targets. Finally, mitochondrial ROS production may also alter protein structure, resulting in carbonyl derivative formation, oxidation of amino acid side chains, and protein fragmentation, potentially eliciting the ER stress response (to be discussed below) and subsequent cellular apoptosis or death (Balaban et al. 2005).

1.1.5 Erb-B Receptors Interact with the Intrinsic/Extrinsic Pathways

The Erb-B family of receptor tyrosine kinases consists of ErbB1-ErbB4. ErbB1 is most commonly known as the epidermal growth factor (EGF) receptor and these molecules are also referred to as the EGFR and HER2-HER4 (Stern et al. 2000). ErbB1 and its autocrine ligands epidermal growth factor and transforming growth factor alpha (TGF α) were characterized over 20 years ago (Stern et al. 2000). The EGF receptor was found to have a tyrosine kinase within its intracellular domain whose activity was stimulated upon ligand binding. Studies have found that the EGF receptor is frequently over-expressed in a wide range of carcinomas (Zhang et al. 1989). ErbB1 modulation has become a focus for research in that there are numerous truncated forms of the EGF receptor that play a pivotal role in tumorigenic processes include tumor cell growth (Grant et al. 2002).

ErbB1 has been shown to homo- and hetero-dimerize with other ErbB family molecules and for the tyrosine kinase domain of each ErbB1 molecule to trans-phosphorylate each other Erb element. Therefore, ErbB1 can mediate the activation of ErbB1 as well as ErbB2-4. ErbB2 is similar to ErbB1 in that it contains a tyrosine kinase motif within its intracellular domain (Hsuan et al. 1989). ErbB2, although it has no ligand, is thought to facilitate the activation of all ErbB family members via heterodimerization (Huang et al. 1998). ErbB2 is also over-expressed in solid tumors (15-25%), including mammary carcinoma, and in combination with ErbB1, is thought to play a protective role against cytotoxic insults (Paik et al. 2001).

Unlike ErbB1 and ErbB2, ErbB3 does not have an active tyrosine kinase domain within the molecule. Erb3 is also capable of binding to ligands of the NDF/heregulin family and does not bind to ligands of the EGF/TGF α family, again, in contrast to ErbB1 and ErbB2 (Tzahar et al. 1994). Thus, signaling by ErbB3 is mediated by interactions with the heterodimeric ErbB complexes utilizing ErbB receptors that contain an active tyrosine kinase domain to mediate signals, mainly ErbB1 and ErbB2 (Waterman et al. 1999). ErbB4 is similar to ErbB3 in that it can also bind ligands of the NDF/heregulin family. However, the kinase domain of ErbB4 is functional and it has been proposed that ErbB4 can play roles in pathological processes including cancer and heart disease (Carraway et al. 1996). Similar to ErbB1, there are numerous truncated forms of ErbB4, however, the roles of these in the process of cellular transformation are less clear. Downstream of the

ErbB family of receptors are intracellular signal transduction cascades that mediate receptor signaling into the cell. Figure 2 below, shows a simplified version of the relationship between the ErbB receptors and the apoptotic pathways.

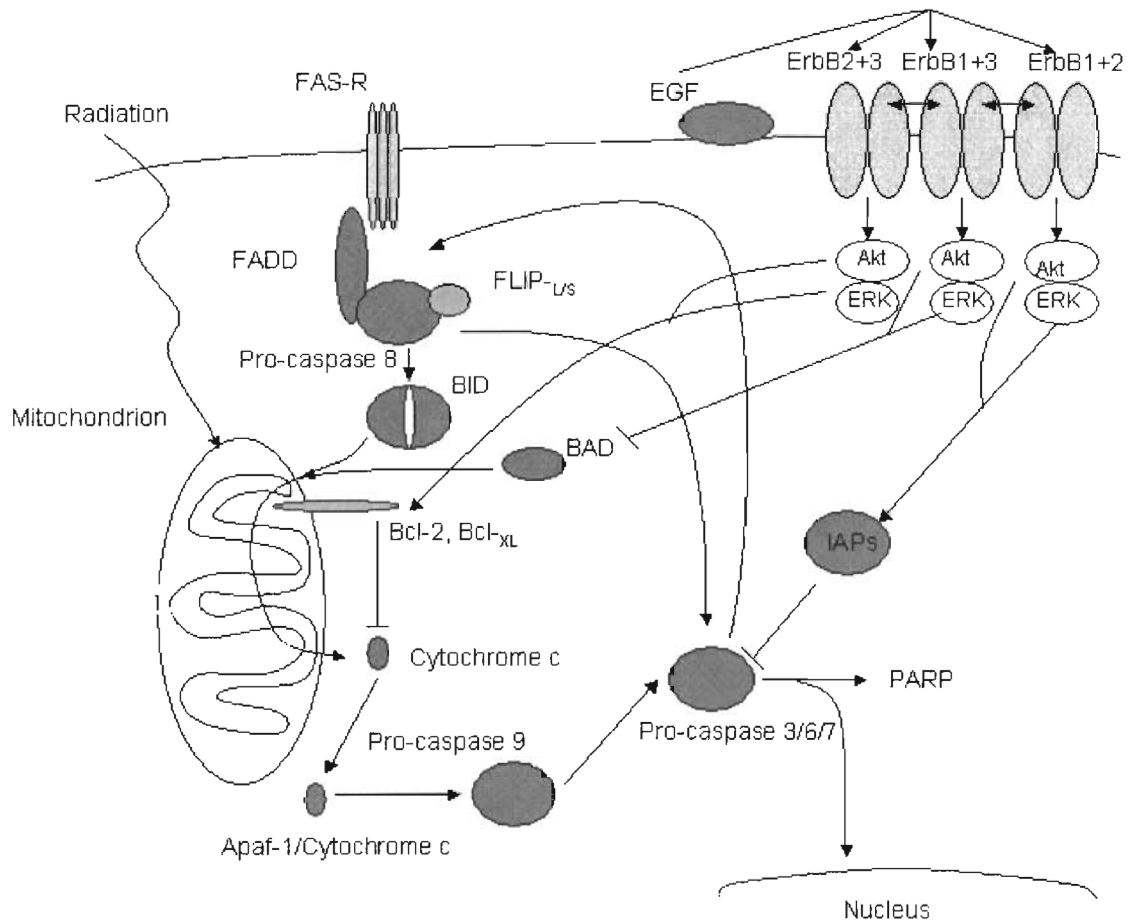


Figure 2. Relationship between MAPK signaling pathways and apoptotic pathways

(Modified version Dent et al. 2002).

1.1.6 Background on Mitogen-activated Protein Kinase (MAPK) Pathways

The MAPK (mitogen-activated protein kinase) pathways are an area being intensely studied in cancer research. Intracellular signaling pathways are pivotal in the regulation of cellular proliferation, via growth factors and/or growth inhibitors. The signals are mediated via cascades of protein kinases that sequentially bind and phosphorylate each other leading to consecutive activations of each protein kinase. These cascades facilitate the signal from the plasma membrane into the cytoplasm, and ultimately into the nucleus. The MAPK super family is made up of multiple kinases; the “classic” MAPK pathway ERK1 (extracellular signal-regulated kinase) and ERK2, which are often referred to as p44 and p42 MAP kinases; the JNK/SAPK (c-Jun N-terminal kinase/stress-activated protein kinases); p38 MAP kinase, which has 4 isoforms: α , β , γ , and δ ; and finally the less investigated ERK3, ERK4, ERK5 and ERK7 pathways (English et al. 1999). The PI3K/AKT signaling pathway also plays a pivotal role in multiple carcinoma cell lines, and is shown below in Figure 3, along with the MAPK signaling pathways, with more detailed descriptions found in Figures 4-8.

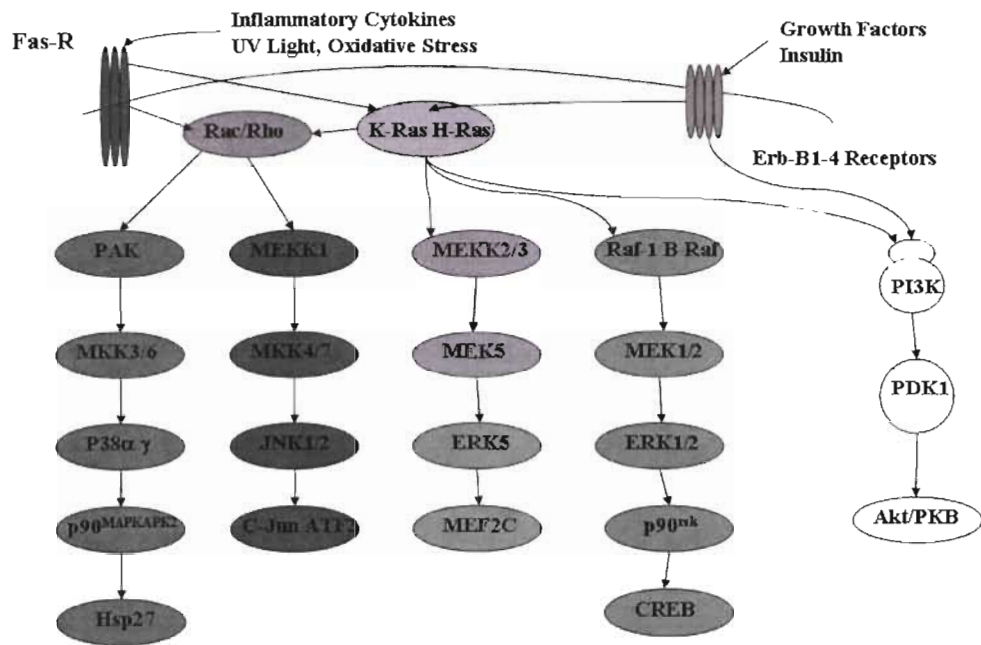


Figure 3. MAPK intracellular signaling pathways

(Modified version of Dent et al. 2002).

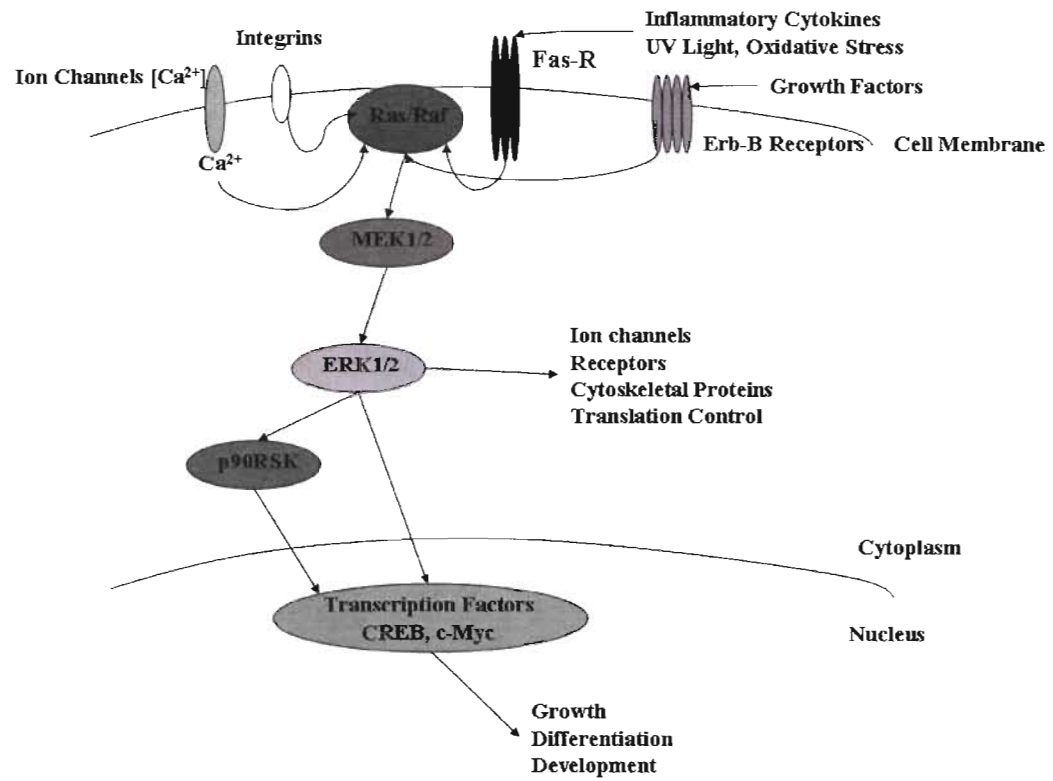


Figure 4. ERK1/2 MAPK Signaling Pathway.

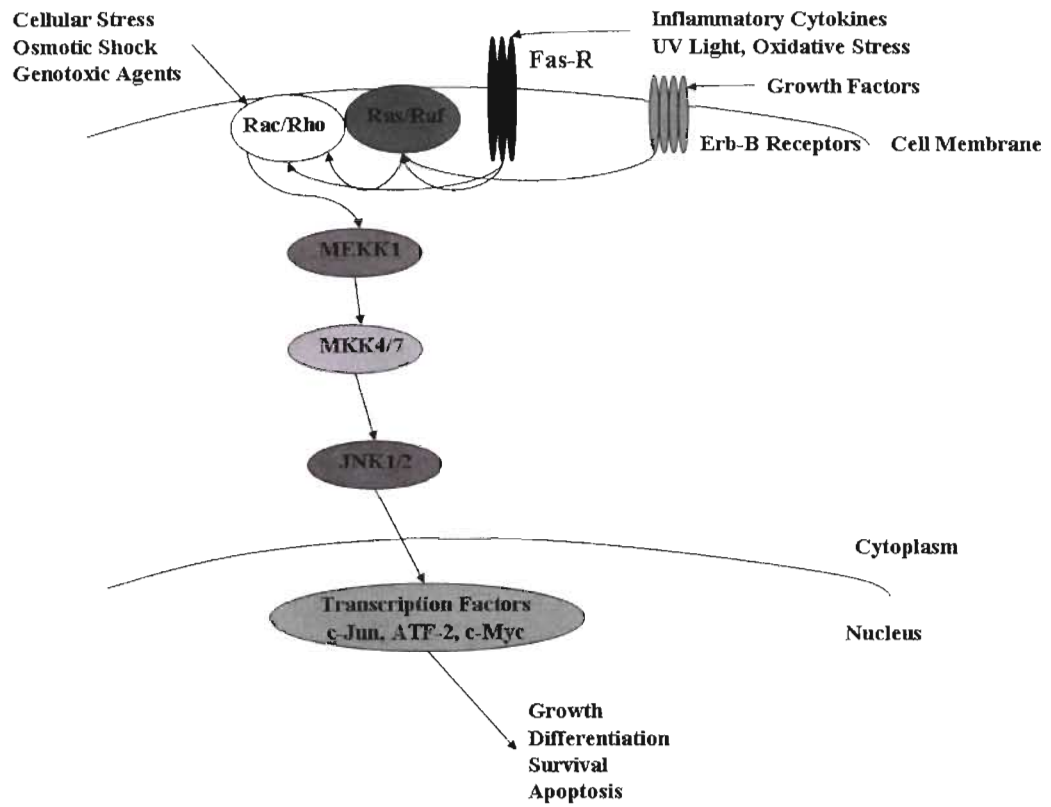


Figure 5. SAPK/JNK MAPK Signaling Pathway.

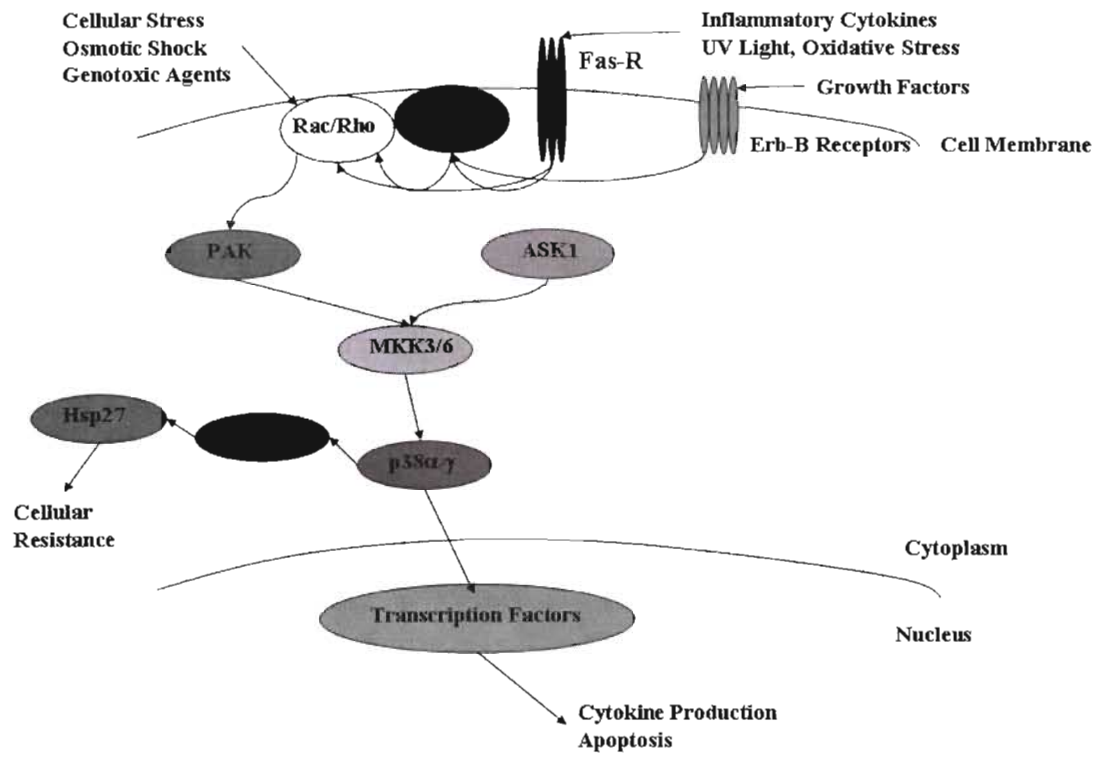


Figure 6. p38 MAPK Signaling Pathway.

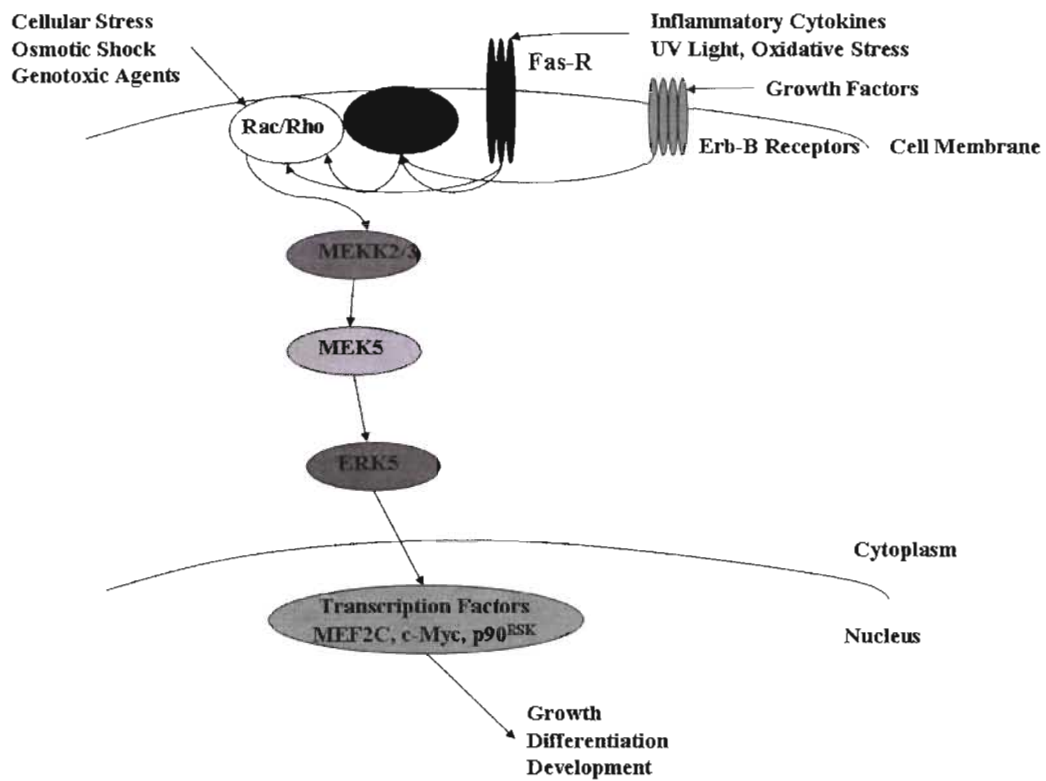


Figure 7. ERK5 MAPK Signaling Pathway.

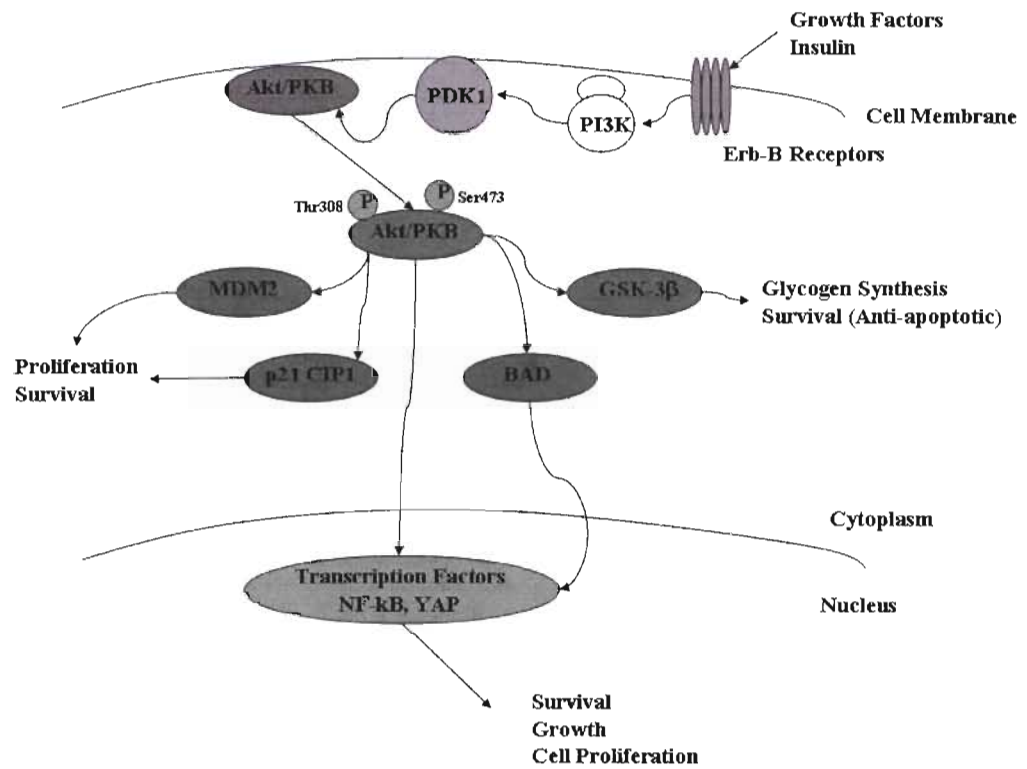


Figure 8. AKT Signaling Pathway.

The first MAPK was originally described as a 42-kDa insulin-stimulated protein kinase, whose tyrosine phosphorylation activity increased after insulin exposure, and phosphorylated the cytoskeletal protein MAP-2 (Sturgill et al. 1986). Further investigations identified another 44-kDa isoform of MAPK, ERK1 (Extracellular-signal Regulated Kinase) (Boulton et al. 1991). Numerous growth factors and mitogens are capable of activating MAPK. Additional studies have demonstrated that the p42/p44 MAPKs regulate another protein kinase activity, p90^{rsk} (Sturgill et al. 1988), and that these MAPKs were regulated by protein kinase activities designated MKK1/2 (MAPK kinase) or MEK1/2. Raf-1 is a protein kinase responsible for catalyzing MKK1/2 activation (Kyriakis et al. 1992). Studies have also revealed that other enzymes at the level of MKK1/2 are capable of activating p42/44 MAPK by phosphorylation (Navas et al. 1999). Signaling by the ErbB family of receptors is thought to be pro-proliferative and cytoprotective. Further studies have revealed that in some cell types, EGF and EGF receptor signaling is shown to promote growth arrest and apoptosis. In carcinoma cells, both receptor expression and autocrine growth factor levels are increased when compared to normal tissue. This has led to the discovery that when signaling from ErbB family receptors is blocked, by a number of methods, tumor cell growth can be reduced and the sensitivity of these cells to various therapies is increased (Grant et al. 2002).

Raf-1 is a member of a family of serine-threonine protein kinases referred to as Raf-1, B-Raf, and A-Raf (Morrison et al. 1997). All Raf family members can phosphorylate and

activate MKK1/2, although the ability of each member to catalyze this reaction is variable in that B-Raf exhibits a large amount of MKK1/2 activation, followed by Raf-1, and then A-Raf. Therefore, Raf kinases act at the level of a MAPK kinase kinase (MAPKKK). The NH₂ domain of Raf-1 reversibly interacts with Ras in the plasma membrane. The ability of Raf-1 to associate with Ras is dependent upon the Ras molecule being bound to GTP (Moodie et al. 1993). Other findings have found that the ability of Raf-1 to undergo activation depends on Raf-1 translocating to the plasma membrane (Leevers et al. 1994). The regulation of Raf-1 activity involves numerous mechanisms that coordinate with one another when in the plasma membrane environment, with studies revealing that the association of Raf-1 with Ras accounts for only partial stimulation of Raf-1 activity (Stokoe et al. 1997). These mechanisms involve numerous proteins such as 14-3-3 and PKC (protein kinase C), phosphorylation of Ser338 by PAK enzymes, and the inhibition of Raf-1 and its upstream activity by phosphorylation at Ser259 by AKT (Grant et al. 2002).

ErbB-dependent activation of downstream signaling pathways eventually leads to a cytoprotective response that is mediated by multiple anti-apoptotic proteins involved in the control of apoptosis by caspase enzymes. ErbB family receptors initiate signaling through numerous downstream modules, including the MAPK/ERK pathway. Inhibition of this pathway can cause a reduction in the expression of anti-apoptotic mitochondrial proteins such as Bcl-X_L, and caspase inhibitor proteins such as the FLIP isoforms and

XIAP. A loss in MAPK/ERK signaling can reduce phosphorylation of the pro-apoptotic proteins Bad and Bim, leading to a functional activation of the molecule. Therefore, a loss of MAPK/ERK signaling will promote enhanced basal levels of apoptosis and will further potentiate cell killing induced by death receptors and other toxic agents that disrupt mitochondrial function (Grant et al. 2002).

Signaling by the ErbB family of receptors in response to growth factors is believed to play a critical role in an anti-apoptotic response in both normal and tumor cells.

Downstream of these receptors are signaling modules that have been shown to be anti-apoptotic effector pathways in a variety of cell types. These include the MAPK super family pathways, including the ERK1/2 and ERK5 pathways discussed above, as well as the JNK1/2 and p38 pathways discussed below.

The c-Jun NH₂ terminal kinase (JNK) pathway was recently discovered and described in the 1990's (Hibi et al. 1993). JNK1/2 were initially biochemically described to be a stress-induced protein kinase activity that phosphorylated the NH₂-terminus of the transcription factor c-Jun; hence the pathway is also referred to as the stress activated protein kinase (SAPK) pathway. JNK1/2 activity can be induced by a number of stresses, including UV- and γ -radiation, cytotoxic drugs, and of note with respect to this study, reactive oxygen species. Phosphorylation of the NH₂-terminal sites Ser63 and Ser73 in c-Jun results in an increase in the ability of the cell to transactivate AP-1 enhancer elements

in the promoters of many genes. More importantly for this study, JNK1/2 has also been found to phosphorylate c-Myc, a transcription factor that is a short-lived nuclear phospho-protein involved in cell proliferation and differentiation and may also be phosphorylated by p44/42 MAPK, thus potentially exhibiting a role in both proliferative and apoptotic signaling (Noguchi et al. 1999). Similar to the MAPK pathway described above, JNK1/2 activities are regulated by dual threonine and tyrosine phosphorylations, which are catalyzed by a protein similar to MKK1/2, referred to as stress-activated extracellular regulated kinase 1 (SEK1), also called MKK4 (Derijard et al. 1995). Another isoform of MKK4, referred to as MKK7, has also been discovered (Tournier et al. 1999). As described above in the case of MKK1/2, MKK4/7 are also regulated by dual serine phosphorylation and in contrast to the MAPK pathway described above, which appears to primarily utilize the three protein kinases of the Raf family to activate MKK1/2, at least 10 protein kinases have been found to phosphorylate and activate MKK4/7, including MKKK1-4, Tak-1, and Tpl-2 (Schlesinger et al. 1998). Another family of JNK pathway protein kinases exist upstream of the MAPKKK enzymes and include low molecular weight GTP-binding proteins of the Rho family, such as Cdc42 and Rac1 (Yustein et al. 2000). It remains unclear how these kinases function to modulate downstream proteins, but the agonist and cell type specificity of each JNK pathway MAPKKK enzyme involved in the activation of this pathway is currently under investigation.

The p38 MAPK pathway is activated by numerous cellular stresses in a similar manner to that of the JNK1/2 pathway (Lin et al. 1995). The Rho family of GTPases appears to play an important role as upstream activators of the p38 MAPK pathway by activating several MAPKKK enzymes such as MKK3 and MKK6 (Lee et al. 2001). There are at least four isoforms, as described above, and there are several protein kinases downstream of p38 MAPK enzymes including p90^{RSK} and MSK1/2 (Deak et al. 1998, Maizels et al. 2001). The former is responsible for the phosphorylation and thus, activation of heat-shock protein-27 (Hsp27), which functions to confer cellular resistance to an unfavorable environmental change, while MSK1/2 can phosphorylate and activate transcription factors involved in cell growth and proliferation, such as CREB (cAMP Response Element-binding protein) (Kato et al. 2001, Wiggin et al. 2002).

The p38 MAPK pathway has a diverse role in the signaling of cellular responses that varies with cell type and stimulus. An example being that p38 MAPK signaling has been shown to promote cell death as well as enhance cell growth and survival (Liu et al. 2001, Juretic et al., 2001, Yosimichi et al. 2001). The ability of ionizing radiation, which causes the generation of free radical species, similar to the effect of arsenic trioxide, to modulate p38 MAPK activity appears to be highly variable with different groups reporting either no activation (Kim et al. 2002), weak activation (Taher et al. 2000) or strong activation (Lee et al. 2002) in response to this stimuli. This is opposite to the classical MAPK and JNK pathways where radiation-induced activation has been

observed in numerous cell types. In studies where p38 MAPK activation has been observed following ionizing radiation therapy, the p38 γ -isoform has been shown to signal growth arrest, specifically in the G2/M phase.

The AKT signaling pathway exists in three isoforms in mammals, AKT1/2/3, and is responsible for the regulation cell survival, proliferation, cell growth and glycogen metabolism. AKT is activated by insulin and other growth and survival factors through a pathway requiring a PI3K-dependent generation of phosphatidylinositol-3,4,5-triphosphate (Franke et al. 1997, Vivanco et al. 2002, Hajdich et al. 2001). Inositol phospholipids have an important role in intracellular signaling in response to hormones, growth factors, and neurotransmitters. Phosphoinositide 3-kinase (PI3K) catalyzes the production of phosphatidylinositol-3,4,5-triphosphate by phosphorylating phosphatidylinositol (PI), phosphatidylinositol-4-phosphate (PIP) and phosphatidylinositol-4,5-biphosphate (PIP₂) (Cantley et al. 2002). PTEN reverses this process, and the PI3K signaling pathway is constitutively activated in human cancers that have loss PTEN functionality (Simpson et al. 2001).

PI3Ks are composed of a catalytic subunit, p110, and a regulatory subunit, p85. Various isoforms of the catalytic subunit have been isolated (p110 α , p110 β , p110 δ , and p110 γ), as well as two forms of their associating regulatory subunits, p85 α and p85 β (Neri et al. 2002). In contrast, p110 γ associates with a p101 regulatory subunit that is unrelated to

p85. Furthermore, p110 γ is activated by $\beta\gamma$ subunits of heterotrimeric G proteins (Stoyanov et al. 1995). Phosphoinositide-dependent protein kinase 1 (PDK1) plays a central role in activating AKT, PKC isoenzymes, p70 S6 kinase and p90^{rsk} (Williams et al. 2000). Through its effects on these kinases, PDK1 is involved in regulation of cell proliferation, differentiation, and apoptosis. PDK1 becomes phosphorylated at the Tyr373 and Tyr376 residues and translocates to the plasma membrane in response to pervanadate or insulin treatment. These sites are critical in terms of regulating PDK1 catalytic activity (Park et al. 2001). Several other serine sites (Ser25, Ser241, Ser393/396 and Ser410) of PDK1 are also phosphorylated in numerous cell lines, while autophosphorylation of Ser241 is required for PDK1 activity (Casamayor et al. 1999). Glycogen synthase kinase 3 (GSK-3) is an enzyme that functions to regulate glycogen synthesis in response to insulin and is expressed as a serine/threonine protein kinase that phosphorylates and inactivates glycogen synthase (Welsh et al. 1996). GSK-3 is a critical downstream element of the PI3 kinase/AKT cell survival pathway, and its activity can be inhibited by AKT-mediated phosphorylation of GSK-3 α at Ser21 and GSK-3 β at Ser9 (Cross et al. 1995, Srivastava et al. 1998). GSK-3 has been implicated in cell fate and cellular development and also regulates cyclin D1 proteolysis and subcellular localization (Diehl et al. 1998). Phosphatase and tensin homologue deleted on chromosome ten (PTEN), or mutated in multiple advanced cancers (MMAC), is a tumor suppressing phosphatase found in numerous human cancers (Cantley et al. 1999). PTEN encodes the 403 amino acid polypeptide originally described as a dual-specificity protein phosphatase

(Myers et al. 1997). The main substrates of PTEN are inositol phospholipids generated by the activation of PI3K. PTEN is a major negative regulator of the PI3K/AKT signaling pathway and possesses a carboxy-terminal noncatalytic regulatory domain that contains three phosphorylation sites (Ser380, Thr382, and Thr383), which function to regulate its stability and has a crucial role in controlling its own biological activity (Torres et al. 2001, Vazques et al. 2000). PTEN also regulates p53 protein levels and activity and is involved in G protein coupled signaling during chemotaxis (Funamoto et al. 2002, Iijima et al. 2002).

AKT activation requires the binding of phosphatidylinositol-3,4,5-triphosphate via the pleckstrin homology domain, activation at Thr308 by PDK1 and also the phosphorylation within the carboxy-terminus at Ser473 (Alessi et al. 1996, Stephens et al. 1998, Stokoe et al. 1997). Tyrosine phosphorylation of AKT by Src at the Tyr315 and Tyr326 residues is thought to occur prior to phosphorylation at Thr308 and Ser473 (Jiang et al. 2003). Carboxy-terminal modulator protein (CTMP) binds to the regulatory domain of AKT at the carboxy terminus and functions to inhibit the phosphorylation on the Thr308 and Ser473 residues.

An essential function of AKT is the regulation of glycogen synthesis through phosphorylation and inactivation of glycogen synthase kinase-3 α and β (Hajduch et al. 2001, Cross et al. 1995). Evidence has also shown that AKT may also play a role in

insulin stimulation of glucose transport (Hajduch et al. 2001). AKT also directly promotes cell survival via its ability to phosphorylate and inactivate several pro-apoptotic targets such as Bad and other transcription factors (Downward et al. 1999, Brunet et al. 1999). AKT may also indirectly promote cell survival by exerting a positive effect on NF- κ B function by the phosphorylation and activation of I κ B kinase, and subsequent phosphorylation and degradation of I κ B (Romashkova et al. 1999). Cell survival can also be indirectly enhanced via p53 in that phosphorylation by AKT enhances MDM2 activity, leading to the degradation of p53 (Mayo et al. 2001). In addition to its role in survival, AKT is involved in cell cycle regulation by preventing GSK-3 β -mediated phosphorylation and degradation of cyclin D1 (Diehl et al. 1998), and by negatively regulating the cyclin-dependent kinase inhibitors p27 and p21 (Gesbert et al. 2000, Zhou et al. 2001).

1.2.1 Background on Glioblastoma Multiforme and MDA-7 Review

Glioblastoma multiforme is annually diagnosed in approximately 20,000 patients in the United States. High grade tumors such as anaplastic astrocytoma and glioblastoma multiforme account for the majority of astrocytic tumors (Levin et al. 1993, Greenlee et al. 2000). Radiation therapy is currently the most common form of treatment for gliomas after surgical tumor removal or as a primary therapy in patients not eligible for surgical tumor removal. Even under the best of circumstances, in which virtually the entire tumor has been surgically removed and the patients have been fully treated with radiation and

chemotherapy, the mean survival of this disease ranges from a few months to one year. As therapeutic strategies utilizing both chemotherapy and radiation have failed to produce the additive or synergistic effects observed in other tumor types, novel approaches that enhance the effectiveness of standard treatments in gliomas are in high demand.

Enforced expression of MDA-7, by use of a recombinant adenovirus *Ad.mda-7*, as mentioned above, inhibits the growth of a broad spectrum of cancer cells, without exerting deleterious effects in normal human epithelial or fibroblast cells (Ellerhorst et al. 2002, Huang et al. 2001, Mhashilkar et al. 2001, Sauane et al. 2003). Previously obtained data supports the hypothesis that *Ad.mda-7* enhances the ratio of pro-apoptotic to anti-apoptotic proteins in cancer cells, thereby facilitating induction of apoptosis (Lebedeva et al. 2002, Madireddi et al. 2000, Pestka et al. 2003, Su et al. 2001, Saeki et al. 2000). MDA-7 has also been found to have anti-proliferative and cytotoxic effects in a variety of tumor cells, but not in non-transformed cells. This has provided a basis for the treatment of glioma cells with MDA-7 in the hopes of inhibiting growth and enhancing radiosensitivity.

Ionizing radiation induced cell killing has been linked to the activation of the c-Jun NH₂-terminal kinase (JNK) and in certain cell types the p38 mitogen activated protein kinase (MAPK) pathway (Cartee et al. 2000, Dent et al. 1999, Xia et al. 1995). In melanoma

cells, recent evidence has shown that p38 signaling to growth arrest and DNA damage (GADD) family transcription factors plays an important role in MDA-7 mediated cell killing (Sarkar et al. 2002). Blocking of the “classical” MAPK/ERK pathway has been shown to radiosensitize several carcinoma cells lines (Dent et al. 1999, Hagan et al. 2000, Yacoub et al. 2001). The expression of mutant H-RAS can lead to constitutive activation of phosphatidylinositol 3-kinase (PI3K) signaling in cells, which has also been linked to enhanced radiation resistance (Gupta et al. 2002, Vlahos et al. 1994).

The ability of Ad.*mda-7* to alter radiosensitivity has recently been investigated by a number of groups. Kawabe et al. demonstrated that lung cancer cells were radiosensitized by Ad.*mda-7* and JNK signaling and Su et al. demonstrated that Ad.*mda-7* radiosensitized human glioma cells *in vitro* (Kawabe et al. 2002, Su et al. 2003). In order to extend these *in vitro* observations in glioma, the ability of and mechanisms by which Ad.*mda-7* radiosensitizes RT2 glioma cells *in vitro* was investigated. These studies have revealed Ad.*mda-7* synergizes with radiation to enhance radiosensitivity *in vitro*. Inhibition of JNK1/2 signaling abolished the radiosensitizing properties of MDA-7 and combined inhibition of ERK and PI3K signaling enhanced cell killing, suggesting that MAPK and PI3K signaling can be protective against MDA-7 lethality.

1.2.2 Mechanisms Involved in Cell Cycle Control

Our group has previously established that the activation of ERK1/2 and ERK5 are required for the completion of the complex mechanisms involved in normal cell cycle

progression. Cancer cells experience rapid proliferation and oftentimes unchecked cell cycle progression, making these cells equally, if not more so, reliant on MAPK function in terms of survival and growth proliferation (McKinstry et al. 2002). The mechanisms involved in cell cycle progression are often a point of interest in cancer research in terms of inducing growth arrest or combining DNA damaging agents with cell cycle checkpoint abrogators to allow a damaged cancer cell to continue through the cell cycle unrepaired. Thus a brief explanation of the cell cycle is warranted.

When a eukaryotic cell divides into two, each daughter or progeny cell must receive a complete set of genes (for diploid cells, this is two complete genomes), a pair of centrioles, mitochondria, ribosomes, a portion of the endoplasmic reticulum, and other various organelles. However, the process of ensuring that each daughter cell receives two of every gene contained on the forty-six chromosomes in a human diploid cell is quite complicated and is accomplished by a tightly controlled series of events: 1) Duplicate each chromosome during the S phase of the cell cycle, producing dyads, each containing two identical sister chromatids held together by a ring of proteins, cohesins. 2) Condense the chromosomes into a compact form, which requires ATP and a protein complex, condensin. 3) Separate the sister chromatids. 4) Distribute sister chromatids equally between the two daughter cells. The process of mitosis completes events 2 – 4 described above and occurs in five phases: prophase, prometaphase, metaphase, anaphase, and telophase.

During prophase, the two centrosomes of the cell, each with a pair of centrioles, migrate to opposite poles of the cell. An array of spindle fibers referred to as the mitotic spindle, forms, each containing approximately twenty microtubules, synthesized from tubulin monomers in the cytoplasm, and extend from each centrosome. The chromosomes also become shorter and more compact. Prometaphase involves the disintegration of the nuclear envelope due to the dissolution of laminins that stabilize the inner membrane. A protein structure, referred to as the kinetochore, appears at the centromere of each chromatid. Upon the breakdown of the nuclear envelope, spindle fibers attach to the kinetochores as well as to the arms of the chromosomes. For each dyad, as mentioned in event 1 above, one of the kinetochores is attached to one pole, the sister chromatid to the opposite pole. The failure of a kinetochore to become attached to a spindle fiber interrupts the process and arrests the cell in metaphase and is the site for a cell cycle checkpoint to be discussed below. At metaphase, all the dyads have reached an equilibrium position midway between the poles, the metaphase plate, and the chromosomes are in the most compact form. Anaphase involves the separation of the sister kinetochores and their movement to their respective poles while bringing its attached chromatid behind. This separation of the sister chromatids is dependent on the breakdown of cohesins, caused by the protease separase or separin. Separase is stored in an inactive state until late metaphase by an inhibitory chaperone, securin. Anaphase begins when the anaphase promoting complex (APC) destroys securin via tagging for deposit in a proteasome, thus ending its inhibition of separase and allowing it to break

down the cohesins. During telophase, a nuclear envelope reforms around each cluster of chromosomes and the chromosomes return to a more extended form, thus completing the process of mitosis.

A eukaryotic cell cannot divide into two unless the alternating of the doubling of its genome (DNA) in S phase (synthesis phase) of the cell cycle, and halving of that genome during mitosis (M phase) continually occur. The period between M-phase and S-phase is referred to as G_1 ; that between S-phase and M-phase is G_2 . The process of growth and preparation of the chromosomes for replication occurs in the G_1 stage of the cell cycle. The synthesis of DNA and centrosomes occurs during the S-phase, preparation for mitosis occurs in G_2 , and mitosis occurs in the M-phase of the cell cycle. When a cell is in any phase of the cell cycle other than mitosis, it is often said to be in interphase. The passage of a cell through the cell cycle is controlled by proteins in the cytoplasm, with each phase containing its own set of regulators. Cyclin levels in the cell rise and fall with the stages of the cell cycle and are keys in signaling the initiation and termination of each phase. A G_1 cyclin, cyclin D, is present in the G_1 phase, S-phase cyclins E (also in G_1) and cyclin A in the S-phase, and mitotic cyclins B and A in the M-phase. CDKs, or cyclin-dependent kinases, remain at fairly stable levels, must bind to the appropriate cyclin in order to be activated, and function to add phosphate groups to a variety of protein substrates that control processes in the cell cycle. A G_1 CDK, CDK4, is present in the G_1 phase of the cell cycle, an S-phase CDK, CDK2 (also present in G_1), is present

in S-phase, and an M-phase CDK, CDK1, is present in the M-phase of the cell cycle. The anaphase-promoting complex (APC), or cyclosome (APC/C), triggers the events leading to the destruction of cohesins, as described above, allowing the sister chromatids to separate, and is responsible for the degradation of mitotic cyclin B.

The cell cycle contains a number of steps in its completion, beginning with a rising level of G₁-cyclins binding to their corresponding CDKs (cyclin D to CDK4), signaling the cell to prepare the chromosomes for replication. A rising level of S-phase promoting factor (SPF), which includes cyclin E bound to CDK2, enters the nucleus and prepares the cell to duplicate its DNA and centrosomes. As the DNA replication continues, cyclin E is destroyed and the level of mitotic cyclins B and A begins to rise (in G₂). The M-phase promoting factor (MPF), consisting of a complex of mitotic cyclins B and A with the M-phase CDK1, initiates the assembly of the mitotic spindle, breakdown of the nuclear envelope, and condensation of the chromosomes. These events take the cell to the metaphase stage of mitosis. It is at this point that the M-phase promoting factor activates the anaphase-promoting complex (APC/C), which allows the sister chromatids at the metaphase plate to separate and move to the poles (completing mitosis), and destroys cyclin B by attaching it to the protein ubiquitin, thereby targeting it for destruction by proteasomes. This turns on synthesis of the G₁ cyclin, cyclin D, for the next turn of the cycle and degrades geminin, a protein that has kept the newly-synthesized DNA in S phase from being re-replicated before mitosis.

The cell has several systems for interrupting the cell cycle, commonly referred to as checkpoints. A cell cycle checkpoint monitors the stages necessary for the completion of S phase, in which the cell monitors the presence of Okazaki fragments on the lagging strand during DNA replication, thus not permitting the cell to proceed in the cell cycle until these fragments have disappeared. There are DNA damage checkpoints capable of halting replication if damage is incurred before the cell enters S phase (a G_1 checkpoint), during S phase, or after DNA replication (a G_2 checkpoint). There are also spindle checkpoints capable of detecting any failure of spindle fibers attached to kinetochores, which would arrest the cell in metaphase (an M checkpoint). These spindle checkpoints are also capable of triggering apoptosis if the damage is irreparable, and detecting improper alignment of the spindle itself and blocking the separation of the cell into two, also deemed cytokinesis. These checkpoints all require the services of a complex of proteins. Mutations in the genes encoding these checkpoints have been associated with cancer, are referred to as oncogenes, and result in checkpoint failures, allowing the cell to continue dividing despite damage to its integrity.

Cells commonly exit the cell cycle, both temporarily and permanently, at G_1 and enter a stage designated G zero (G_0). A G_0 cell is oftentimes deemed quiescent, in that it is still functioning but not dividing. G_0 cells are often terminally differentiated in that they will never reenter the cell cycle, but will continue to serve their purpose in the organism until cell death. Other cells, for example lymphocytes in human blood, can reenter the cell

cycle at G_1 and proceed on to new rounds of alternating S phases and mitosis, in response to the appropriate antigen. G_0 not only represents the absence of signals for mitosis, but an active repression of the genes needed for mitosis. Transformed cancer cells cannot enter G_0 and are destined to repeat the cell cycle indefinitely, further building their resistance to death.

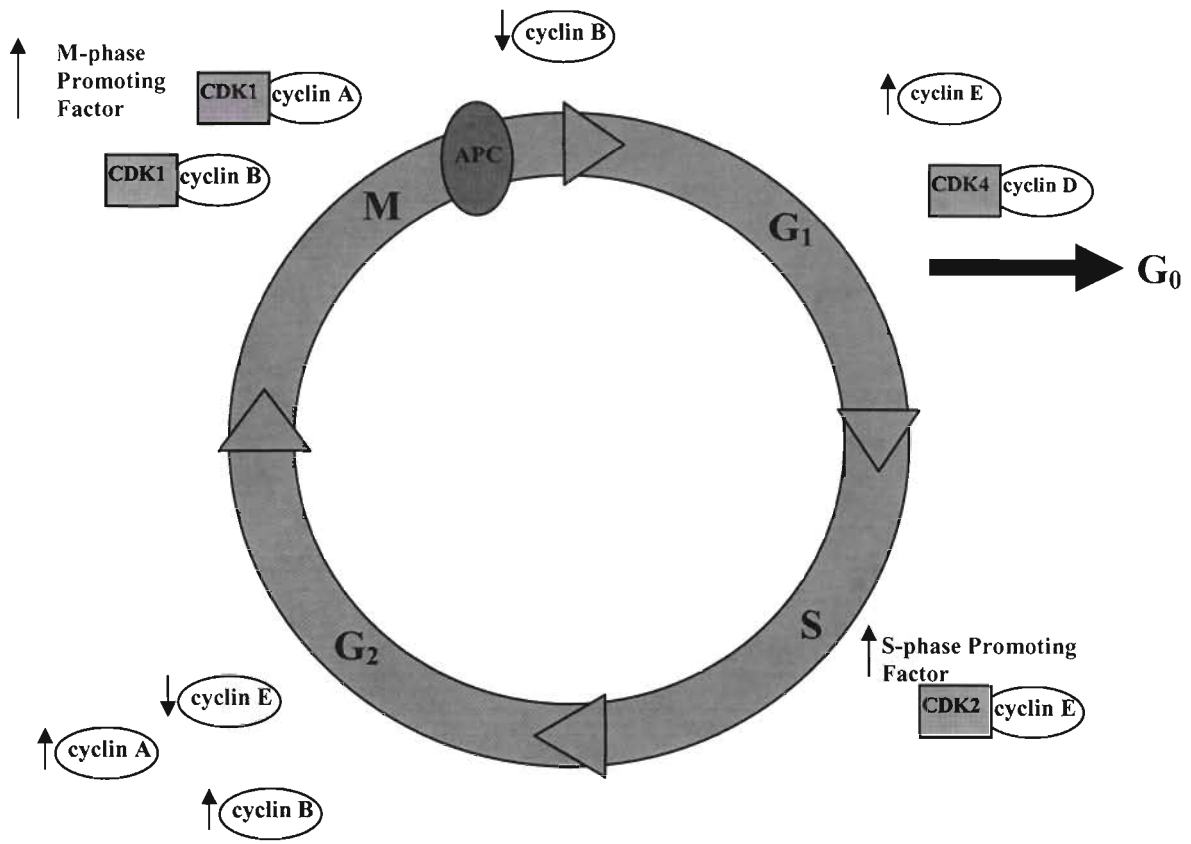


Figure 9. Cell Cycle

The p53 protein plays a pivotal role in the above stated G₁ checkpoint in that it senses DNA damage and is capable of halting the progression of the cell cycle in G₁. The product of the p53 gene, a 53 kilo-dalton protein, is also crucial in apoptosis, or pre-programmed cell death. As an important G₁ checkpoint regulator, p53 is involved in controlling the G₁ to S phase transition in response to DNA damage, caused by radiation and other DNA damaging agents (i.e. ROS). p53 evaluates the extent of damage to the DNA, typically in the form of double-strand breaks (DSBs), and at repairable damage levels triggers arrest of the cell cycle until the damage is repaired. At high levels of damage in which the cell produces irreversibly damaged DNA, p53 triggers an apoptotic response via a linker histone (H1) released from the chromatin, which leaves the nucleus and enters the cytosol where it triggers the release of cytochrome c from the mitochondria, which forms a complex with Apaf-1, cleaving caspase-9 and caspase-3, ultimately sending a signal to the nucleus, causing apoptosis. These functions make p53 a key player in protecting against cancer, hence its classification as a tumor suppressor gene. A cell containing only mutant versions of the protein is still capable of functioning and potentially developing into cancer, as greater than fifty-percent of all human cancers do contain p53 mutations and have no functioning p53 protein. Therefore, alterations in p53 are linked to poor prognosis, tumor progression, and decreased sensitivity to chemotherapeutic agents.

The ATM gene (ataxia telangiectasia mutated) produces the ATM protein involved in detecting DNA damage (especially DSBs), interrupting, with the aid of p53, the cell cycle when damage is found, and maintaining normal telomere length. Patients suffering from ataxia telangiectasia (AT), show signs of premature aging due to a lack of functioning gene product needed to detect DNA damage and initiate a repair response. The MAD (mitotic arrest deficient) genes encode proteins that bind to each kinetochore until a spindle fiber attaches. Upon failure to attach, MAD remains and blocks entry into anaphase. Mutations in MAD produce a defective protein and failure of the checkpoint. The cell finishes mitosis but produces daughter cells with too many or too few chromosomes, a term referred to as aneuploidy, a common characteristic of cancer cells, suggesting that failure of the spindle checkpoint is a major step in the conversion of a normal cell into a transformed cancer cell.

1.2.3 Cell Cycle Regulation

As mentioned above, the cell cycle is regulated by a family of serine/threonine protein kinases known as CDKs (cyclin dependent kinase). These kinases bind to partner cyclins and are phosphorylated by a CAK (cyclin-dependent kinase activating kinase) to become active. Progression of cells to mid G₁ phase is dependent on CDK4 and/or CDK6, with the association of cyclin D. Movement from mid G₁ into S is due to the activation of CDK2 and cyclin E. These CDK/cyclin complexes target a protein known as retinoblastoma protein (pRb), which is the protein product of the retinoblastoma tumor

suppressor gene and similar in function to the p53 gene discussed above. This protein becomes phosphorylated in mid to late G₁, is catalyzed by CDK2 and CDK4, and is necessary for the cell to progress from G₁ into S phase. Phosphorylation of Rb inactivates its ability to inhibit transcription driven by E2F. E2F can then transcribe genes necessary to proceed into S phase. Multiple mechanisms come into play during the inhibition of this checkpoint, including DNA damage and contact inhibition. These stimuli can cause the cell to up-regulate its expression of cyclin kinase inhibitor proteins p21 and p27, in a p53 dependent and independent manner. These proteins inhibit the kinase activity of CDK2/cyclin E and CDK4/cyclin D, which causes pRb to remain in a hypo-phosphorylated state. While in this form, pRb will remain associated with E2F and prevent the progression of the cell into S phase.

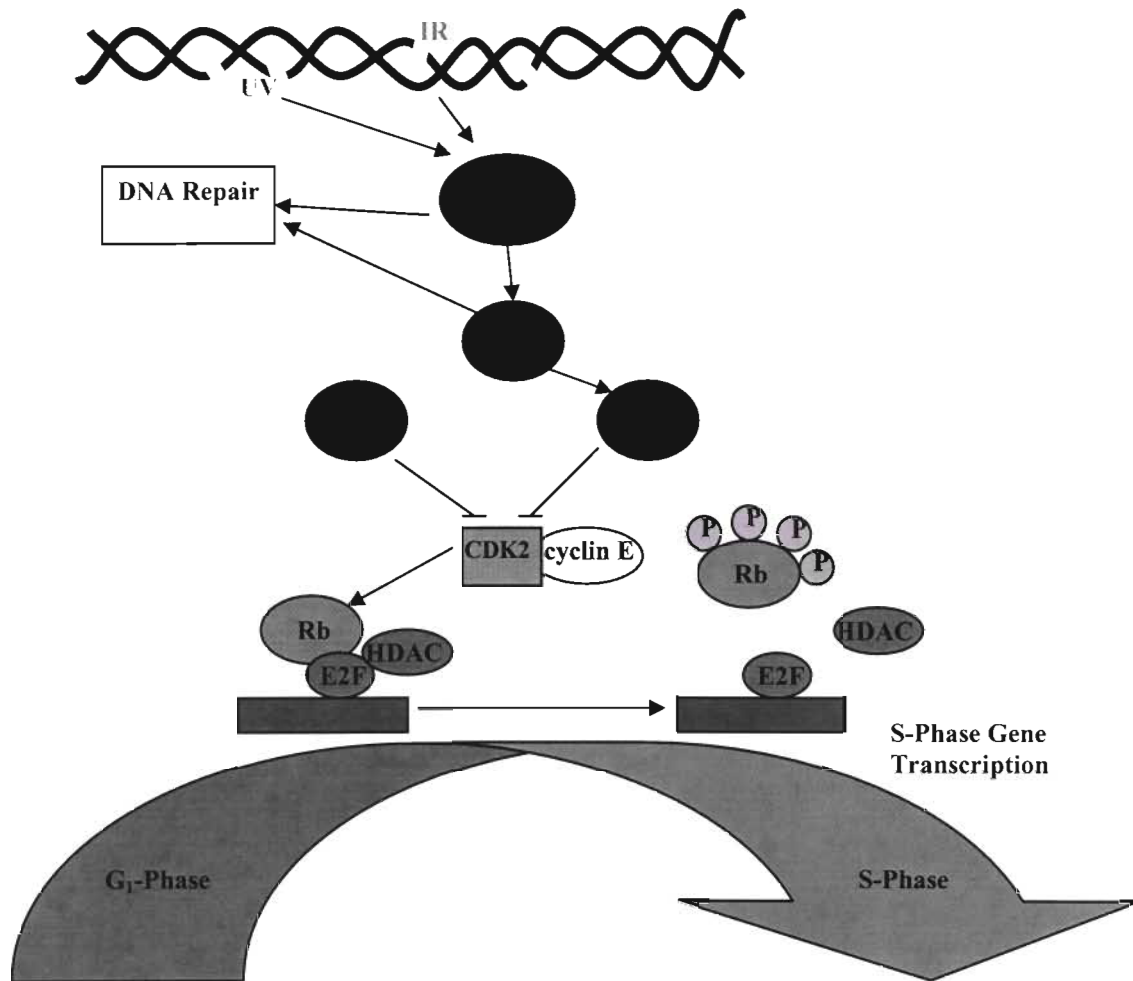


Figure 10. G₁/S Cell Cycle Checkpoint.

The G₂/M cell cycle checkpoint is controlled by another signaling pathway that can be activated by DNA damage. In this cascade, DNA damage causes the activation of the kinases ATM (ataxia telangiectasia mutated) and ATR (ATM and Rad3 related). These kinases phosphorylate and activate the cell cycle regulatory kinases Chk1/2. Chk1/2 in turn phosphorylates the protein tyrosine phosphatase Cdc25C on Ser216, rendering the protein catalytically inactive. Once Cdc25C is phosphorylated, 14-3-3 proteins are able to bind to the protein and export it from the nucleus. During normal cell cycle progression through G₂/M, this phosphatase remains in the nucleus and recognizes the downstream kinase Cdc2 (CDK1). Cdc25C removes the phosphates from Thr14 and Tyr15 of Cdc2, rendering it active. Cdc2 is maintained in an inactive state throughout the S and G₂ phases of the cell cycle by being phosphorylated on these sites. This control is rendered by the kinase Wee1 that phosphorylates Cdc2 on Tyr15 and Myt1, another kinase that phosphorylates both Thr14 and Tyr15.

In cells with wild type p53, genotoxic stresses can cause the accumulation of p21 and 14-3-3 σ ; the latter protein can bind to cyclin B1/Cdc2 complexes and remove them from the nucleus. This mechanism will prevent Cdc25C from coming in contact with cyclin B1/Cdc2 complex and activating it. It should be noted that p21 is a CDK inhibitor and will therefore also inhibit Cdc2 (CDK1). Another mechanism has been proposed that will exclude cyclin B1/Cdc2 from the nucleus. During interphase, cyclin B1/Cdc2 is shuttled back and forth between the nucleus and the cytoplasm. The cytoplasmic

localization is believed to be occurring through a nuclear export signal (NES) in cyclin B1, which causes the complex to be exported out of the nucleus. This signal can be phosphorylated in late prophase, and as a result will no longer recognize the nuclear export receptor, causing the accumulation of cyclin B1/Cdc2 in the nucleus.

Compartmentalization of the proteins involved in this cascade thus appears to play an important role as a regulatory mechanism. Once cyclin B1/Cdc2 complex is active, it allows the cell to progress into mitosis.

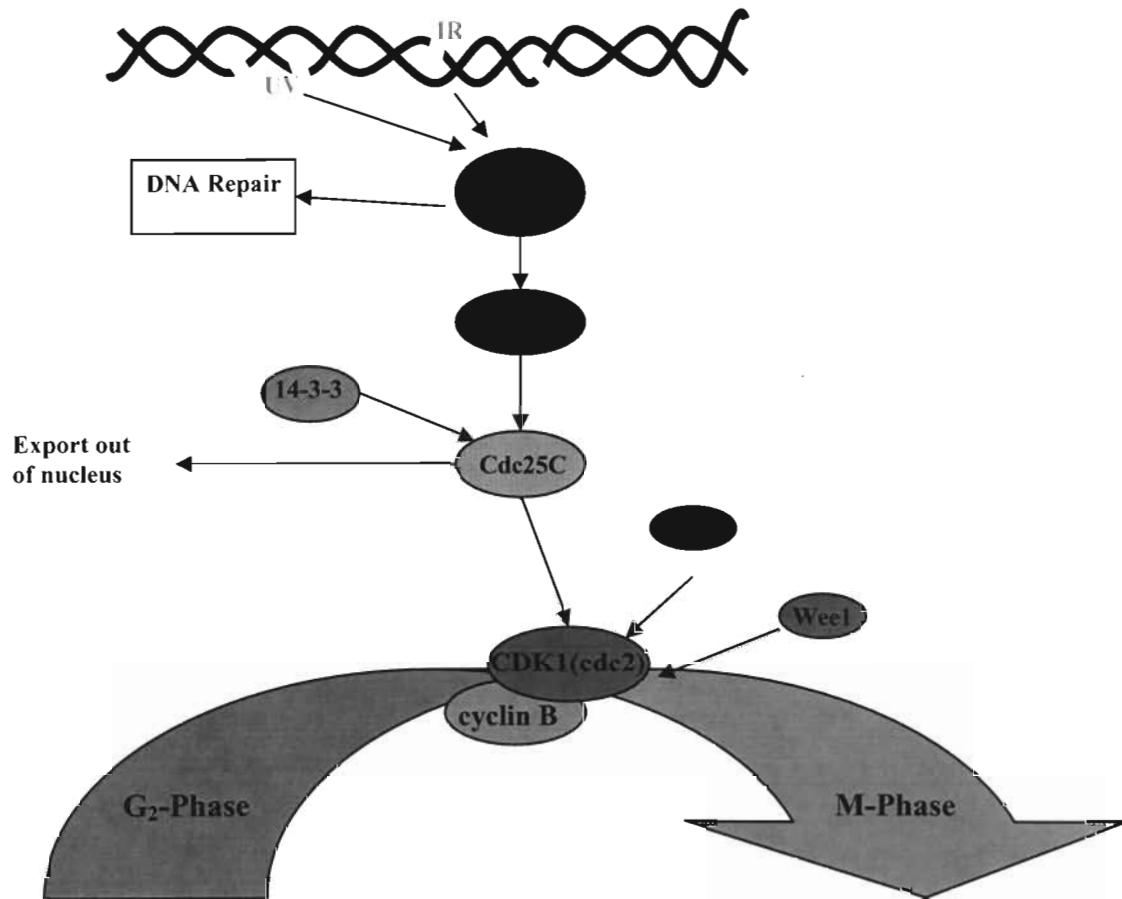


Figure 11. G₂/M Cell Cycle Checkpoint.

1.3.1 Background on Hepatocellular Carcinoma

The National Cancer Institute has estimated that there were 18,920 new cases of hepatocellular carcinoma (HCC) in the United States and 14,400 deaths due to HCC in the year 2004. The International Agency for Research on Cancer estimates that each year there are approximately 626,000 new cases of HCC and 598,000 deaths as a result of HCC worldwide. HCC accounts for approximately 84% of all liver cancers and is the fourth most common type of cancer. HCC is the third largest cause of cancer deaths in the world and approximately 1 in every 5,000 humans will contract HCC in their lifetime. The five-year survival for an HCC patient averages between 2 and 6% and approximately 52% of HCC patients that go into remission will experience a reoccurrence of HCC. It occurs more often in men than women, and largely affects the population 50-60 years of age.

Hepatocellular carcinoma is cancer that arises from hepatocytes, the major cell type of the liver. HCC, as statistically mentioned above, is relatively rare in the United States. Worldwide, however, it is abundantly more rampant and is one of the most common forms of cancer mortality. It is especially prevalent in parts of Asia and Africa.

Aflatoxins, which are produced by a contaminant mold most commonly found in peanuts, is also found in grains and beans, and has been implicated as a major risk factor for causing HCC. Although virtually non-existent in the United States, aflatoxins, are common in other parts of the world and often contaminate food supplies. Approximately

80% of humans with HCC also have cirrhosis, or scarring of the liver. Cirrhosis may be caused by viral hepatitis, primarily hepatitis B and C, alcohol abuse, hemochromatosis, certain autoimmune diseases of the liver and a number of other diseases that result in chronic inflammation of the liver leading to scarring. Of those patients diagnosed with HCC, between 70% and 95% also have Hepatitis B or C, and between 60% and 80% also have cirrhosis. The most common cause for cirrhosis in the United States is alcohol abuse (National Cancer Institute Home Page 2006).

Most HCCs are first suspected based on the results of CAT scans or ultrasound scans. Blood alpha-fetoprotein is a useful marker for the diagnosis of HCC in that approximately 70% of patients with HCC have elevated blood alpha-fetoprotein concentrations. It is often measured as a part of the screening in patients with chronic hepatitis B, hepatitis C, and cirrhosis, but is not specific for HCC. The definitive diagnosis of HCC is made by biopsy via a fiber optic instrument inserted into the abdomen, called a laproscope, or occasionally, open surgical biopsy is required. HCC is only curable by surgery if the tumor is of minimal size. Liver transplantation is also an option and may be curative for relatively small tumors. Surgery or liver transplantation is not typically possible in most cases as early diagnosis is somewhat rare, thus allowing tumors to be subsequently large, or the cancer having metastasized beyond the liver. In these instances, chemotherapy, ligating, or embolization of the hepatic artery, alcohol

injection into the tumor, or radiation may relieve symptoms and prolong life, but these procedures are not curative, as evidenced in the poor survival rate described above.

1.3.2 Role of Bile Acids in the Liver

Bile acids, or bile salts, are synthesized from cholesterol in the liver, stored in the gallbladder, secreted into the bile, and delivered into the lumen of the small intestine where they serve as detergents for the absorption of dietary lipids, cholesterol, and fat-soluble vitamins. In humans, conversion of cholesterol produces the primary bile acids, chenodeoxycholic (CDCA) and cholic (CA) acids. In the intestine, bile acids are absorbed with nutrients and transported back to the liver via portal circulation. However, primary bile acids escaping reabsorption are converted by intestinal bacteria to secondary deoxycholic (DCA) and lithocholic (LCA) acids, a portion of which are also absorbed. Enterohepatic recirculation allows for the recovery of 95% of the bile acids secreted in the intestine. The lost 5% is replaced by neosynthesis in the liver. The conversion into bile acids represents 90% of the amount of cholesterol that is metabolized daily in the human body (Trottier et al. 2006).

Bile acids are cytotoxic when their concentrations reach high levels (2 – 10 μ M), with deoxycholic acid concentrations found in human and rodent bile ducts ranging from 10 to 100 μ M. This toxicity increases with the hydrophobicity of the bile acid. Cholestasis, a condition in which bile excretion from the liver is blocked, is one of the most common

and devastating effects of liver disease, and is associated with intracellular accumulation of toxic bile acids and consecutive cellular damage. The causes of intrahepatic cholestasis range from inflammatory disorders, to pregnancy, alcohol and drug use, and tumor presence. Cholestasis is clinically characterized by elevated plasma concentrations of biliary constituents, such as bile acids and their sulfate and glucuronide conjugates. Under normal conditions, accumulation of bile acids in hepatocytes is avoided through stringent control mechanisms involving bile acid synthesis, transport, and metabolism (Sirica et al. 2005).

During enterohepatic recirculation, as mentioned above, bile acids undergo several metabolic alterations, such as amidation, hydroxylation, glucuronidation, or sulfonation. It should be noted that both neosynthesized primary or reabsorbed primary and secondary bile acids undergo conjugation and deconjugation reactions in the liver. With these mechanisms, taurine- and glycine-conjugated bile acids can be deconjugated and then hydroxylated and reconstituted with glucuronide or sulfate groups, promoting the detoxification and subsequent excretion of bile acids into the blood for subsequent urinary elimination. Amidation involves the addition of an amino acid, usually glycine or taurine, is experienced by 98% of the bile acids excreted from the liver, and promotes the excretion of bile acids into the bile (Trottier et al. 2006). In addition to being efficiently excreted, glycine and taurine conjugates of bile acids also exhibit higher hydrophobicity and stronger detergent properties to facilitate lipid and vitamin absorption in the intestine.

This increase in hydrophobicity, as mentioned above, also makes these bile acids more cytotoxic, DCA being of the more common toxic secondary bile acids. Bile acids, besides being well-established in dietary lipid absorption and cholesterol homeostasis, have recently emerged as key signaling molecules with systemic endocrine functionality. Bile acids activate mitogen-activated protein kinase pathways, more specifically, the p38 MAPK pathway mentioned above, are ligands for the G-protein-coupled receptor TGR5, and activate nuclear hormone receptors such as farnesoid X receptor alpha. Through the activation of these diverse pathways, bile acids are capable of regulating not only their own enterohepatic circulation, but also triglyceride, cholesterol, energy, and glucose homeostasis (Trottier et al. 2006). The cytotoxic effects of bile acids have been linked to ROS generation, causing mitochondrial electron transport chain dysfunction, and the elevation of the p38 MAPK stress response pathway described above (Hsieh et al. 2006). It has been shown that the reduced form of thioredoxin (Trx) interacts with the N-terminal portion of the apoptosis stimulating kinase 1 (ASK1) *in vitro* and *in vivo*, forming a Trx-ASK1 complex, and thereby inhibiting the kinase. This Trx-ASK1 complex formation is specific to reduced Trx. Oxidation of the ASK1 bound Trx by certain oxidants, such as ROS, disrupts the complex, thus enabling ASK1 activation. It has been proposed, therefore, that reduced Trx is an inhibitor of ASK1, and that the oxidation of which, releases Trx from the complex, allowing ASK1 to activate the p38 MAPK and SAPK/JNK stress response pathways described above (Hsieh et al. 2006).

1.3.3 Fas Receptor Review and Endoplasmic Reticulum Functionality

As mentioned above, ligation of Fas engages a potent and rapid signaling mechanism that can result in apoptosis in a variety of cell types. This signaling, again, generally involves the recruitment of an adapter protein, FADD, to the cytoplasmic domain of Fas. FADD then recruits pro-caspase-8, which processes and activates further downstream caspases (i.e. caspase-3), leading to apoptosis. Another function of Fas ligation, is to induce the production of ceramide, a known trigger of apoptosis. Research has indicated that, following Fas ligation, ASMase is the enzyme responsible for hydrolyzing sphingomyelin to produce ceramide, thus contributing to Fas-mediated cell death. The exact process by which this occurs remains to be recognized, although recent reports have shown that ASMase activation following Fas ligation is dependent on caspase activity, more specifically through the action of caspase-8 (Lin et al. 2000).

1.3.4 Endoplasmic Reticulum (ER) Stress Response

The endoplasmic reticulum (ER) is a central organelle of each eukaryotic cell and is the site of lipid synthesis, protein folding, and protein maturation. Plasma membrane proteins, secreted proteins, proteins from the Golgi apparatus, as well as lysosomes, fold into tertiary and quaternary structures within the ER. The ER is also the major signal transducing organelle, responsible for sensing and responding to changes in cellular homeostasis. ER stress is caused by the accumulation of unfolded proteins in the ER, which occurs under a variety of conditions (i.e. mutation in secretory proteins or

disruption of calcium homeostasis). This type of cellular stress is quickly becoming a focal point of research in that it is considered a cause of pathologically relevant apoptosis and is highly implicated in neurodegenerative disorders. ER stress can also be induced by the accumulation of unfolded protein aggregates (unfolded protein response, UPR) or by excessive protein trafficking, typically caused by viral infection (ER overload response, EOR). The unfolded protein response (UPR) utilizes a signaling pathway during which the signal of unfolded proteins activates a set of ER-located sensors. The first being the PK-R like ER kinase (PERK), or eIF2 kinase, responsible for the phosphorylation of the α subunit of eukaryotic initiation factor 2 (eIF2), leading to the attenuation of general protein synthesis. Another sensor molecule, Ire1 α and β , is also activated and, in mammals, initiates gene expressional changes by processing the mRNA of the transcription factor XBP1. XBP1 then translocates to the nucleus, inducing a wide range of ER located chaperones involving the glucose regulated protein (Grp) family members, such as Grp78 and Grp94. These chaperones play a pivotal role in protecting the cell by maintaining unfolded proteins in a folding-competent state, thereby preventing protein aggregation, and by binding and sequestering Ca^{2+} in the ER lumen, the release of which could alter mitochondrial membrane permeability, resulting in cytochrome c release, subsequent caspase activation, DNA fragmentation, and cell death. Notably, mitochondrial membrane integrity is regulated by the Bcl-2 family of proteins mentioned above, and evidence suggests a possible crosstalk between the ER stress response and this family of proteins in an effort to protect the cell from death (Hacki et al. 2000). Another

ER-stress sensor molecule, ATF6, is a transcription factor essential for XBP1 mRNA expression and chaperone induction upon ER stress (Nakanishi et al. 2005). During cellular duress, the rate of protein translation is decreased in order to prevent further accumulation of unfolded proteins. Simultaneously, transcription factors responsible for inducing the expression of ER-resident chaperones capable of handling the accumulated protein aggregates are activated. This counter-balancing of responses halts the accumulation of proteins, and allows time for the elimination of the unfolded proteins, thus restoring cellular homeostasis. Failure of the cell to activate either of these mechanisms can result in cellular apoptosis (Szegezdi et al. 2003).

The exact signaling mechanism underlying ER stress-induced apoptosis has yet to be clearly understood. However, two main pathways have been recognized, a transcription factor-dependent and a caspase-dependent pathway. Ire1, which alters XBP1, as mentioned above, is thought to provide a pro-apoptotic action through the upregulation of the ER-stress responsive proteins, GADD153, CHOP, and Bip, which amplify the pro-apoptotic signal by altering the balance between Bcl-2, an anti-apoptotic protein, and Bax, a pro-apoptotic protein (Nakanishi et al. 2005). ER stress-induced cell death can also be initiated through the activation of caspases, initiating with the activation of caspase-12. ER stress activates caspase-12 by a largely unknown mechanism. Caspase-12 then translocates from the ER to the cytosol, where it directly cleaves pro-caspase-9, which then activates the effector caspase, caspase-3, which signals apoptosis (Morishima et al. 2004). Research has shown that caspase-12-deficient cells are resistant to ER stress

inducers, indicating that caspase-12 is significant in ER stress-induced apoptosis.

Although it has been thought that cytochrome c released from mitochondria is required for caspase-9 activation, recent findings have shown that caspase-12 can activate caspase-9 directly without cytochrome c release in certain cell lines (Miroshima et al. 2004), which then activates the downstream effector caspase, caspase-3. Some groups have proposed the existence of an ER stress-specific caspase cascade consisting of caspase-12, -9, and -3, while others have shown that caspase-9 activation can occur in an Apaf-1-independent, and thus cytochrome c-independent, manner, and yet in some cell lines, ER stress induces cytochrome c release by an unknown pathway (Hacki et al. 2000). It is therefore likely that the activation of caspase-9 and its downstream effector caspases can be achieved in ER stress-induced apoptosis either by caspase-12 or by the Apaf-1/cytochrome c complex described above (Morishima et al. 2004).

1.3.5 Heat Shock Protein Background

Cells are equipped with several classes of structurally unrelated molecular chaperones that function to ensure both the proper folding of proteins upon synthesis and their refolding under conditions of denaturing stress. Different chaperones follow distinct strategies to achieve the general goal of preventing protein misfolding and aggregation in the highly crowded intracellular environment. Chaperone proteins often cooperate in folding. An example being a polypeptide bound by Hsp70 at an early stage of folding can be transferred to a chaperonin in order to achieve its final native state. Other research

argues that an alternate pathway exists in which certain polypeptides in the cytosol bind to Hsp70, which then interacts with the dimeric chaperone protein Hsp90, to achieve the same resulting native state. Recent advances in the areas of structure and function of Hsp90 indicate a unique mechanism, unlike other heat shock proteins, by which Hsp90 handles its substrate polypeptides. In order to further investigate Hsp90, the primary target anti-tumor agents such as geldanamycin and the roles and functionality of heat shock proteins must be discussed.

Heat shock proteins are some of the most prolific proteins in cells of all species. Heat shock proteins respond to a cell becoming stressed by any number of stimuli and account for 1-2 percent of total protein in unstressed cells. When heated or stressed, Hsp90, the most common heat related protein, increases to 4-6 percent of total cellular proteins. Hsp90 belongs to the structural protein family of GHKL ATPases. This abundant protein aids in the regulation of activity, turnover, and trafficking of various critical proteins. It facilitates in the folding and regulation of proteins in cellular signaling, such as transcription factors, steroid receptors, and protein kinases. Heat shock proteins in general serve vital intracellular roles including intracellular signaling, protein folding and tumor repression. This multi-functionality has allowed these proteins to remain under constant study since its discovery in the 1980s.

The molecular chaperone Hsp90 is an ubiquitous molecular chaperone found in eubacteria and all branches of eukarya. In mammalian cells, there are two genes encoding cytosolic Hsp90 homologues, with the human Hsp90 α showing 85% sequence identity to Hsp90 β . There is also high homology to Hsp90 from lower eukaryotes and prokaryotes: yeast Hsp90 is 60% identical to human Hsp90 α and the bacterial Hsp90 equivalent, HtpG, is still 34% identical to human Hsp90 α . Unlike Hsp70, eukaryotic cytosolic Hsp90 does not act generally in nascent protein folding. Hsp90 is distinguished from other chaperones in that most of its known substrates are signal transduction proteins, such as steroid hormone receptors and signaling kinases. Hsp90 plays a key role in cellular signal transduction networks in that it is essential for maintaining the activity of numerous signaling proteins. At a molecular level, Hsp90 binds to substrate proteins during a late stage of folding in which the protein is near readiness for activation by ligand binding or interaction with other factors. Hsp90 operates as part of a multichaperone mechanism in the cytosol, which includes the above mentioned Hsp70, but also peptidyl-prolyl isomerases and other cochaperones. This functional complexity has limited the knowledge base of Hsp90 in comparison to Hsp70 or other chaperonin proteins (Young et al. 2001). The following sections will discuss the structure and mechanism of the Hsp90 protein, its regulation by cochaperones, and the biological contribution of Hsp90 to cellular processes such as signal transduction, protein management, and morphological adaptations.

The highly conserved Hsp90 chaperone family includes Hsp90 (90 kD heat shock protein) of the eukaryotic cytosol, also described as Hsp90 α and β in humans, Hsp86 and Hsp84 in mice, Hsp83 in *Drosophila*, and Hsc82 and Hsp82 in yeast. Other family members are HtpG in the bacterial cytosol, Grp94/grp96 in the endoplasmic reticulum of eukaryotes, and Hsp75/TRAP1 in the mitochondrial matrix. All of these proteins share a common structural schematic and are therefore expected to have a similar mechanism of action. Hsp90 is a constitutive homodimer in which its main intersubunit makes contact within the COOH-terminal's 190 residues. The highly conserved 25 kD NH₂-terminal domain of Hsp90 is the binding site for ATP and for geldanamycin, a representative of the ansamycin drugs, which specifically targets Hsp90. Geldanamycin inhibits the Hsp90 ATPase with nanomolar affinity and occupies the nucleotide-binding cleft within the NH₂-terminal domain. A divergent charged sequence separates the NH₂-terminal domain from a flexible 35 kD middle domain and the 12 kD COOH-terminal domain required for dimerization. Both the NH₂- and COOH-terminal domains of Hsp90 have been found to bind substrate polypeptides. Substrate binding at the NH₂-terminal site are affected by nucleotides, geldanamycin, and the adjacent charged sequence of Hsp90 (Young et al. 2001).

The structure of Hsp90 is similar to all proteins in that it is a composite of alpha helices, beta pleated sheets, and random coils. The protein is globular in structure and is largely non-polar on the inside and polar on the outside, allowing it to be readily dissolved in

water. Hsp90 contains nine helices and eight anti-parallel beta pleated sheets that fold into various alpha/beta complexes. The 310 helices comprise 11% of the proteins amino sequences, as opposed to 4% in most proteins, and contain three highly important areas: the ATP binding, protein binding, and dimerizing regions. All of which will be discussed in further detail below (Young et al. 2001).

The ATP-binding domain of Hsp90 is structurally related to a superfamily of homodimeric ATPases, comprising in addition to Hsp90, DNA gyrase and topoisomerase II, the DNA mismatch repair protein MutL, and the histidine kinases CheA and EnvZ. The ATPase binding region of Hsp90 is near the N-terminus and exhibits a high affinity to bind ATP at an uncharacteristically bent manner, in comparison to other proteins, and is a focal point for numerous areas of research due to its role in cancer and protein maintenance. More specifically, the antibacterial agent geldanamycin, and its role in tumor suppression. The ATPase binding region is substantial in size (approximately 15 Angstroms in depth), and when provided with a suitable substrate, cleaves the ATP into ADP and a phosphate. Protein folding and regulation are ATP dependent. Thus these processes cease when the ATP site is blocked, potentially by an allosteric inhibitor. This ATP-binding region also undergoes a conformational change during ATP cleavage. The two conformational states in which Hsp90 appear are called the ATP-bound state and the ADP-bound state, and are responsible for the formation of a pincher type active site, in which the conformational change is between open and closed. While in the open

conformation, Hsp90 leaves some hydrophobic residues exposed, to which unfolded and misfolded proteins that have unusual hydrophobic regions exposed are recruited with high affinity. Upon binding of an appropriate substrate, the ATPase function near the N-terminal forces the shape changes that clamps the protein down on the substrate, allowing the protein to complete several functions such as protein maintenance and protein transport. Discrepancies exist as to the exact manner in which Hsp90 binds with its substrate. Evidence suggests that Hsp90 does not enclose its substrate but instead presents a substrate-binding face when in the ATP clamp state. Still other arguments persist that multiple substrate-binding sites exist along the length of the Hsp90 protein. Upon determining the exact mode of Hsp90 substrate-binding, further investigation into exactly how it aids in folding can be further pursued (Young et al. 2001).

Unlike the bacterial and endoplasmic reticulum forms of Hsp90, which function independently, Hsp90 in the eukaryotic cytosol interacts with a variety of cochaperone proteins that assemble into a multichaperone complex and regulate the function of Hsp90 and Hsp70. The largest class of cochaperones bind to Hsp90 via a modular domain containing typically three 34 amino acid, helix-turn-helix tetratricopeptide repeat (TPR) motifs. These TPR domains are found fused to a series of different functional domains, such as peptidyl-prolyl isomerase domains or a protein phosphatase. Hsp90-binding TPR domains have also been identified fused to other TPR domains, which recognize Hsp70 and then connect Hsp70 to Hsp90 or can recruit Hsp90 to the mitochondria. Recent

studies by Connell et al. have shown the ability of the TPR cofactor CHIP to link Hsp90 with the ubiquitination apparatus, thus controlling protein degradation by the proteasome (Connell et al. 2001). TPR domain cochaperones also compete with each other for a binding site at the COOH terminus of Hsp90. In the cochaperone Hop, for example, the TPR domain containing the main Hsp90-binding site recognizes the five COOH-terminal residues of Hsp90 and binds to this pentapeptide with specificity and affinity in comparison to its interaction with the full-length proteins. In addition to linking Hsp90 with the Hsc70 chaperone system, Hop acts as an inhibitor of the Hsp90 ATPase by preventing access to the nucleotide-binding site of Hsp90. This inhibitory activity of Hop serves as a sort of substrate-loading system for Hsp90, where an Hsp90-Hop-Hsc70 complex permits the transfer of a substrate polypeptide from Hsc70 to the nucleotide-free state of Hsp90. The binding of ATP onto Hsp90 should then displace the Hop-Hsc70 loading system and simultaneously close the substrate binding clamp of Hsp90 (Connell et al. 2001). Another cochaperone, p23, which is unrelated to the TPR domain proteins mentioned above, can itself act as a chaperone in binding unfolded polypeptides, and recognizes specifically the ATP-bound state of Hsp90, implying a more specialized function of p23 in regulating the Hsp90 ATPase cycle. Although p23 does not affect the ATPase activity of Hsp90, the cochaperone significantly stimulates the ATP hydrolysis-dependent dissociation of Hsp90-substrate complexes. The cochaperone protein p50/Cdc37 also interacts with Hsp90 and certain protein kinases, and has been proposed

to direct Hsp90 to kinases that are dependent on the chaperone for maturation (Senju et al. 2005).

A majority of the known Hsp90 substrates are signal transduction proteins. These proteins are critically dependent on Hsp90 for their maturation and conformational maintenance. Treatment with inhibitors, such as geldanamycin, can lead to multiple physiologic defects. In the regulation of cellular division, disruption of Hsp90 affects multiple stages of the mitogenic signal cascade, cyclin-dependent progression through G₁ and G₂, as well as centrosome function during mitosis, as earlier described. Hsp90 has proven vital for steroid hormone receptors, several tyrosine and serine/threonine kinases such as pp60/v-src, Wee-1, Cdk4, and Raf, as well as proteins including nitric oxide synthase and calcineurin. Although the exact structural features recognized by Hsp90 are not yet fully recognized, research has shown that interactions of substrate proteins with Hsp90 arise from structural properties at the molecular level rather than biological function. The best characterized example of an Hsp90-dependent signaling pathway is that of the steroid hormone receptors. Interaction of the glucocorticoid receptor with Hsp90 is essential for its activity and the unstable ligand-binding domain of the receptor is sufficient for this interaction. Monomeric glucocorticoid receptor and the closely related progesterone receptor are loaded onto Hsp90 via the Hsc70/Hop-dependent complex mentioned above and achieve their hormone-binding conformation after binding Hsp90 (Young et al. 2001). Once the folded monomeric receptor is released from the

chaperones, it can either bind the appropriate steroid hormone, resulting in dimerization and activation, or remain unstable, only to be recognized again by the chaperone complex.

The progesterone and glucocorticoid receptor have been utilized in exhibiting the multichaperone complexes containing Hsp90, Hsc70, Hop, and p23, and has further solidified the paradigm of ATP-dependent Hsp90 functionality. With respect to v-src and other kinases, Hsp90 is presumed to stabilize the exposed catalytic domains before final assembly into the signaling kinase complexes in a similar manner to the steroid receptor pathway. Hsp90 is also capable of regulating its own expression by sequestering the monomeric inactive form of heat shock transcription factor 1 (HSF1) under non-stressful conditions. Misfolded proteins produced by stress oftentimes compete with HSF1 for binding to Hsp90, thus liberating the transcription factor for trimerization and initiating the heat shock response. Hsp90-bound polypeptides are targets for degradation by the TPR cochaperone CHIP, which recognizes both Hsp90 and Hsc70, and contains domains similar to those of the E1 ubiquitination factors, thus perhaps presenting chaperone-bound misfolded proteins for ubiquitination. This is confirmed in cultured cells containing an overexpression of CHIP experiencing increased ubiquitination and degradation of the glucocorticoid receptor and cystic fibrosis transmembrane regulator, both known substrates of Hsp90 and Hsc70. The activity of CHIP suggests that substrates that reside longer on Hsp90, caused by ATPase inhibition by geldanamycin,

are more prone to ubiquitination. The existence of CHIP also suggests that like protein folding, protein targeting mechanisms responsible for degradation are regulated by multiple factors (Connell et al. 2001).

Tumor cancer cells allow massive overproduction of products, such as Her-2 (ErbB2), that serve as signals for apoptosis. Hsp90's function in the regulation and correct folding of at least one hundred proteins allows it to refold and/or degrade these products before they trigger cell death. In this manner, tumor cells commonly have elevated basal levels of Hsp90 and are thus allowed to grow relatively unchecked for longer periods of time before the body begins to combat the cancerous cells. Geldanamycins, originally thought to be kinase inhibitors, are currently being used as anti-tumor agents with great success as Hsp90 ATP binding site inhibitors. Geldanamycin and 17-allylamino-17-demethoxygeldanamycin (17-AAG) derivatives are part of the ansamycin family of agents, best known for their ability to bind to the ATP-binding site of the amino-terminal domain region of Hsp90, thus inhibiting its function. It is the blockage of Hsp90 function that has been ascribed to the antitumor effect of 17-AAG, a drug now used in many *in vitro* and *in vivo* research studies, as well as clinical trials (Beliakoff et al. 2004, Senju et al. 2005, Shen et al. 2005). The ansamycin family of agents greatly affects live cells by inducing the degradation of Hsp90 substrate proteins by the ubiquitin-dependent proteasome pathway and the compact conformation of the agent itself allows it to be inserted into the ATP-binding site, thus greatly reducing the Hsp90 function in cells.

Ansamycins can also inhibit the chaperone-mediated folding of Hsp90 substrates by blocking their ATP-dependent dissociation from Hsp90, or, can be responsible for the release of certain substrate proteins from Hsp90 (Young et al. 2001). Hsp90's role of chaperonin and transporter can also be described by its interaction with transforming cellular signal molecules and the proteasomes that may or may not degrade them. The S26 proteasome and all of its subsequent subunits are an integral part of proteolysis and regulation in the cell. Without the constant supply of functional Hsp90 that is required to maintain its tertiary structure, this proteasome will disassociate into its constituent subunits and cease functioning. Hsp90 significantly aids in the assembly and subsequent ATP-dependent folding of the S26 proteasome. The significance of this is that the S26 proteasome targets virtually all eukaryotic proteins for degradation and is usually marked for destruction through the polyubiquination pathway. Further research utilizing heat sensitive Hsp90 mutants and the S26 proteasome have shown that Hsp90 is responsible for the majority of the ATPase activity of the proteasome. This is also relevant in that the S26 proteasome performs proteolysis on virtually all ubiquinated proteins, including some tyrosine kinases, such as Her-2 (ErbB2), which, as mentioned above, are commonly overproduced in cancerous tumors. Studies using benzoquinone ansamycin antibiotics have indicated that Hsp90's ATPase active binding site is blocked in a manner similar to geldanamycins, rendering the chaperonin unable to adequately complex the tyrosine kinases. This inability of Hsp90 to bind to the kinases prevents their ubiquitination and subsequent tagging and degradation by proteasomes (Adams et al. 2004).

The ubiquitin proteasome pathway is required for the targeted degradation of most short-lived proteins in the eukaryotic cell. Targets include cell cycle regulatory proteins, whose timely destruction is vital for controlled cell division, as well as proteins unable to fold properly at the endoplasmic reticulum. Ubiquitin modification is an ATP-dependent process carried out by three classes of enzymes. An “ubiquitin activating enzyme” (E1) forms a thio-ester bond with ubiquitin, a highly conserved 76 amino acid protein. This reaction allows subsequent binding of ubiquitin to an “ubiquitin conjugating enzyme” (E2), followed by the formation of an isopeptide bond between the carboxy-terminus of ubiquitin and a lysine residue on the substrate protein. The latter reaction requires an “ubiquitin ligase,” (E3) that can be single or multisubunit enzymes. In some cases, the ubiquitin-binding and substrate-binding domains reside on separate polypeptides brought together by adaptor proteins or cullins. Numerous E3s provide specificity in that each can modify only a subset of substrate proteins. Further specificity is achieved by post-translational modification of substrate proteins, oftentimes by phosphorylation. Effects of monoubiquitination include changes in subcellular localization. However, multiple ubiquitination cycles resulting in a polyubiquitin chain are required for targeting a protein to the protease for degradation. The multisubunit S26 proteasome recognizes, unfolds and degrades polyubiquitinated substrates into small peptides. The reaction occurs within the cylindrical core of the proteasome complex, and peptide bond hydrolysis employs a core threonine residue as the catalytic nucleophile. Recent research has indicated that an

additional layer of complexity, in the form of multiubiquitin chain receptors, may lie between the polyubiquitination and degradation steps (Pickart et al. 2004). These receptors react with a subset of polyubiquitinated substrates, aiding in their recognition by the S26 proteasome and thereby promoting their degradation. This is not only important in cellular homeostasis, but also in human disease. Because ubiquitin/proteasome-dependent degradation is often employed in control of normal biological processes and pathologies, cell cycle progression, differentiation, cell stress response, and apoptosis, proteasome inhibitors are currently under investigation as cancer therapeutic agents. Furthermore, the accumulation of misfolded proteins may contribute to some neurodegenerative diseases such as Alzheimer's disease. The ability of the chaperonin Hsp90 to illicit S26 proteasome stability *in vivo*, allowing the cell to degrade the unwanted or harmful proteins, and allow tumor causing kinases to persist in the cytoplasm that, under normal conditions, would normally be degraded by the same proteasome, confirms the functional diversity of Hsp90. The critical and ever-changing role of chaperonin Hsp90 in multiple cellular processes has made the protein a major focal point in cancer research (Young et al. 2001).

1.3.6 Geldanamycin Background

As mentioned above, Hsp90 is known to be a molecular chaperone involved in the folding, assembly, maturation, and stabilization of the client proteins which regulate survival of cancer cells. The client proteins include hormone receptors and various signal

transducers, HER2, epidermal growth factor receptor (EGFR), AKT, Raf-1, hypoxia-inducible factor (HIF)-1 α , mutated p53, and Bcr-Abl. The antitumor activity of various Hsp90 inhibitors, such as the geldanamycin derivative 17-AAG, has been demonstrated in numerous cell types, including resultant inhibition of prostate tumor growth in nude mice, associated with degradation of HER2 and the androgen receptor. Exposure to 17-AAG in breast cancer xenografts resulted in the downregulation of AKT, a downstream target of PI3 Kinase and an important factor in tumor proliferation and cell survival. In prostate cancer lines, an oxygen-regulated transcriptional activator, HIF-1 α , responsible for contributing to the promotion of angiogenesis and adaptation to hypoxia, was found to be degraded by treatment with geldanamycin. This activator is also, subsequently, mediated by the proteasome pathway in prostate cancer cells. In addition, 17-AAG has enhanced the radiosensitivity of tumor cell lines, associated with reduction of levels of proteins such as Raf-1, HER2, and AKT, which are known to be client proteins of Hsp90 as well as key factors in radioresistance. More recently, 17-AAG has been shown to cause G2/M cell cycle arrest via a reduction of Cdc25C and Cdc2 in lung cancer cell lines. Based on these cumulative findings, 17-AAG was ushered into and has completed a multi-institution Phase I clinical trial, while a Phase II trial is currently underway (Senju et al. 2006).

Preliminary reports of clinical trials have indicated that the agent has efficacy as an anticancer therapeutic. However, it has also been reported that hepatic toxicity is dose-

limiting. Non-dose-limiting toxicities have been reported to include anemia, anorexia, nausea, emesis, and diarrhea (Shen et al. 2005). This dose limiting toxicity, and the relative lack of information regarding the effects of 17-allylamino, 17-demethoxygeldanamycin (17-AAG) on primary rat hepatocyte cultures (HPC), in terms of 17-AAG interactions with bile acids produced in the liver, and intracellular signaling cascades, in particular the MAPK pathways, presents reason for further investigation.

1.4.1 Objective: Renal Cell Carcinoma and MDA-7

The impact of Ad.*mda-7* on the survival of RCC lines and primary renal epithelial cells is unknown, and the present studies examined whether Ad.*mda-7* altered the growth and survival of the A498 and UOK121N RCC lines. Due to previous findings (Haviv et al. 2002, Yacoub et al. 2003) that the RCC lines, but not primary renal epithelial cells, were resistant to type 5 adenoviral infection, purified GST-MDA-7 protein was used to treat the RCC lines. Null hypothesis: GST or GST-MDA-7 will have no effect on RCC proliferation and cell death. We used purified GST-MDA-7 protein to show that GST-MDA-7, but not GST, caused a dose-dependent reduction in A498 and UOK121N proliferation but not that of primary renal epithelial cells. Free radical species, generated by clinically relevant concentrations of arsenic trioxide, synergized with subnanomolar concentrations of GST-MDA-7 to inhibit the proliferation, viability, and long-term survival of renal cell carcinoma. These findings argue that MDA-7, in combination with

agents that generate free radicals, may have potential in the treatment of renal cell carcinoma (RCC).

1.4.2 Objective: Glioblastoma Multiforme and MDA-7

Despite therapeutic interventions including surgery, chemotherapy and radiotherapy, glioblastoma multiforme (GBM) has a very poor prognosis and novel therapies are therefore required. MDA-7 (IL-24), when expressed via a recombinant replication defective adenovirus, *Ad.mda-7*, has profound anti-proliferative and cytotoxic effects in a variety of tumor cells, but not in non-transformed cells. Null hypothesis: infection with *Ad.cmv* or *Ad.mda-7* will have no effect on GBM proliferation and cell death. We showed that *Ad.mda-7* exerted anti-proliferative effects on GBM cells and when utilized in combination with ionizing radiation, the anti-proliferative effects of *Ad.mda-7* were enhanced by radiation in a greater than additive fashion. These findings correlated with an *in vitro* cellular change of enhanced cell numbers in the G₁/G₀ and G₂/M phases of the cell cycle, implying *Ad.mda-7* radiosensitizes tumor cells in a cell cycle-independent manner, and that these effects were not observed in cultures of non-transformed primary astrocytes. These findings argue that *Ad.mda-7*, in combination with ionizing radiation, may have potential in the treatment of glioblastoma multiforme (GBM).

1.4.3 Objective: Hepatocellular Carcinoma, Bile Acid, and 17-AAG

There are relatively few effective therapies available, outside of tumor excision or liver transplantation, for patients suffering from hepatocellular carcinoma (HCC). HCC has a very poor prognosis and therefore novel therapies are required. The antibiotic geldanamycin is currently being used in a number of clinical trials in different tumor cell types, such as HCC, targeting the inhibition of the heat shock protein and molecular chaperone Hsp90. Previous studies have demonstrated that geldanamycins have dose limiting toxicity *in vivo* due to their actions in promoting normal liver dysfunction. The present studies were initiated to determine the molecular mechanisms by which geldanamycins and bile acids altered hepatocyte viability *in vitro*. Null hypothesis: treatment with geldanamycin (17-AAG), bile acid (DCA), or the combination will not effect the survival of primary rat hepatocytes and human hepatoma cell lines. We have showed that the geldanamycin derivative 17-allylamino, 17-demethoxygeldanamycin (17-AAG) interacts with the secondary bile acid, deoxycholic acid (DCA), to kill primary rat hepatocytes. This finding correlated with prolonged increases in levels of mitochondria generated ROS, phosphorylated levels of p38 and SAPK/JNK MAPK pathways, classical morphological apoptosis, and cell death. These effects were eliminated by the addition of the free radical quenchers, N-acetyl cysteine and Trolox. Collectively, these findings argue that geldanamycins may not be a viable therapy for HCC treatment and that 17-AAG toxicity in primary hepatocytes may be, at least upon

initial drug exposure, due to mechanisms independent of Hsp90 inhibition and down-regulation of “classical” Hsp90 client proteins.

CHAPTER TWO

MATERIALS AND METHODS

2.1 Materials

Dulbecco's Modified Eagle's Medium (DMEM), Minimum Essential Medium Alpha (MEM α), RPMI 1640 medium, William's Medium, and penicillin-streptomycin were purchased from Invitrogen Life Technologies, Inc. (Carlsbad, CA). Minimum Essential Medium (MEM), Non-essential amino acids (NEAA) and sodium pyruvate were from Cellgro (Herndon, VA). Insulin, dexamethasone, and thyroxine were obtained from Novo Nordisk Pharmaceuticals (Princeton, NJ). MTT reagent and Giemsa Stain were obtained from Sigma-Aldrich Biotechnology LP (St. Louis, MO). Anti-caspase 3 (17/32 kDa cleaved/full, 1:500, mouse monoclonal), phospho-/total ERK1/2 (42, 44 kDa, 1:1000, mouse monoclonal), phospho-/total-p38 α / β (38 kDa, 1:1000, rabbit polyclonal), phospho-/total-JNK1/2 (46, 54 kDa, 1:1000, mouse monoclonal), phospho-/total-AKT (60 kDa, 1:1000, mouse monoclonal), anti-Bcl-2 (26 kDa, 1:500, mouse monoclonal), anti-Bcl-XL (30 kDa, 1:1000, mouse monoclonal), anti-FAS receptor (48 kDa, 1:1000, rabbit polyclonal), anti-FAS ligand (40 kDa, 1:1000, rabbit polyclonal), anti-Bax (20 kDa, 1:1000, rabbit polyclonal), β -Actin (42 kDa, 1:1000, mouse monoclonal), and all of the secondary antibodies (anti-rabbit-HRP, anti-mouse-HRP, and anti-goat-HRP) were obtained from Santa Cruz Biotechnology (Santa Cruz, CA). Anti-PARP (85/118 kDa cleaved/full, 1:2500, rabbit polyclonal) was obtained from Calbiochem-Novabiochem Ltd. (La Jolla, CA). Arsenic trioxide (As₂O₃) was generously provided by Dr. Steve

Grant. It was dissolved in RPMI 1640 medium, aliquoted in light-protective tubes, and stored at -20 degrees C. N-acetyl-cysteine (NAC) was purchased from Sigma-Aldrich, dissolved in sterile water, aliquoted, and stored at -20 degrees C. The selective MEK 1/2 inhibitor (PD98059), and the PI3K inhibitor (LY294002) were obtained from Calbiochem-Novabiochem Ltd. (La Jolla, CA), dissolved in DMSO, and added 60 minutes prior to radiation treatment. Western immunoblotting was performed using the Perkin-Elmer Life Sciences Chemiluminescence System (Boston, MA).

2.2 Cell Culture

Cells were originally purchased from American Type Culture Collection (Rockville, MD). Human U373 glioma cells, and primary human renal epithelial cells were cultured in DMEM supplemented with 10% (v/v) fetal calf serum (Hyclone, Logan, UT) and 100 $\mu\text{g}/\text{mL}$ (1% v/v) penicillin-streptomycin according to the supplier instructions. The renal cell carcinoma A498 and UOK121N cell lines, were cultured in RPMI 1640 supplemented in 10% (v/v) fetal calf serum and 1% (v/v) penicillin-streptomycin according to the supplier instructions. Fischer rat RT2 glioblastoma cells (University of Alabama, Birmingham), primary rodent astrocytes (kindly provided by Dr. E. Ellis, Dept. Pharmacology, VCU), HeLa cells, and mouse embryonic fibroblasts were cultured in DMEM supplemented with 10% (v/v) fetal calf serum and 1% (v/v) penicillin-streptomycin according to the supplier instructions. U251 and U373 human astrocytoma cells were grown in MEM supplemented with 10% (v/v) fetal calf serum, (1X) NEAA,

and (1X) Sodium Pyruvate. Cells were incubated in a humidified atmosphere of 5% (v/v) CO₂ at 37 degrees C. Cells were plated at a density of 3.2×10^4 cells per cm² plate area.

2.3 Primary Culture of Rodent Hepatocytes

Hepatocytes were isolated from adult male Sprague Dawley rats or athymic nude mice by the two-step collagenase perfusion technique (Yacoub et al. 2003). The isolated hepatocytes were plated on rat-tail collagen (Invitrogen) coated at a density of 2.5×10^5 cells per well and cultured in Williams E Medium supplemented with 250 nM insulin (Novo Nordisk), 0.1 nM dexamethasone, 1 nM thyroxine, and 100 µg/mL penicillin-streptomycin, and incubated in a humidified atmosphere of 5% CO₂ at 37 degrees C. Culture medium was changed 4 hours after cell seeding and at the time of viral infection, with the purpose of removing any dead or mechanically damaged cells.

2.4 Generation of Rho-zero HuH7 Cells

HuH7 human hepatoma cells (kindly provided by Dr. Youwen Fang, Dept. of Hepatology, VCU) were cultured in Dulbecco's Modified Eagle Medium supplemented with 10% (v/v) fetal calf serum and 1% (v/v) penicillin-streptomycin according to the suppliers instructions. To generate HuH7 Rho-zero cells, HuH7 cells were cultured in Dulbecco's Modified Eagle Medium supplemented with 10% (v/v) fetal calf serum, 50 µg/mL uridine, 1 mmol/L Na pyruvate, and the growth medium was supplemented (for Rho-zero cell generation) with 10 µg/mL ethidium bromide. Ethidium bromide serves to intercalate with the mitochondrial DNA, thereby halting synthesis and eventually

eliminating the majority of mitochondria within the cell. The growth medium must be supplemented with uridine, and sodium pyruvate, due to the lack of functional mitochondria typically responsible for their production within the cell. Cells were cultured in this medium or in parallel in growth media without ethidium bromide for 8 weeks prior to any further experimentation. Removal of uridine and sodium pyruvate from the growth media of established HuH7 Rho-zero cells resulted in rapid (~24-48 h) growth arrest and cell death.

2.5 Generation of Adenovirus Ad.mda-7 and Synthesis of GST-MDA-7

Recombinant type 5 adenovirus expressing MDA-7 (*Ad.mda-7*), and control vector (*Ad.cmv*) were generated using recombination in HEK293 cells. A bacterial expression vector containing the open reading frame 3' end was fused to the glutathione S-transferase (GST) open reading frame in a GST-4T2 vector (Amersham / Pharmacia) by introducing BamHI and NotI sites into the *mda-7* gene via polymerase chain reaction (PCR). In order for the expression of the MDA-7 protein to be verified, a culture was subjected to an overnight inoculation of a 1:100 dilution followed by incubation at 25 degrees C until an A_{600nm} of 0.4-0.6 was obtained. The culture was then exposed to 0.1 μ M isopropyl-1-thio- β -D-galactopyranoside for two hours. The cells were collected by centrifugation and sonicated in phosphate-buffered solution (PBS) (Invitrogen). The solution was then centrifuged to obtain the soluble protein. The lysate was then bound to a glutathione-agarose column (Amersham Pharmacia) for two hours at 4 degrees C. The

column was then washed with 50 volumes of PBS and 10 volumes of PBS containing 500 mM sodium chloride. The bound protein was then eluted by passing 20 mM of reduced glutathione through the column, while collecting 1 ml fractions. These fractions were then analyzed by gel electrophoresis to determine the presence of bound GST-MDA-7, and positive samples were dialyzed in the presence of 1000 volumes of PBS for four hours, the PBS replaced, and the dialysis repeated for another four hours. The samples were then dialyzed against 500 volumes of DMEM for four hours. The protein concentration was determined by Coomassie blue staining, as well as gel electrophoresis using an anti-GST-MDA-7 antibody (50 kDa, 1:3000, rabbit polyclonal) generated in Rabbits using gel-purified fragments of GST-MDA-7.

2.6 Recombinant Adenovirus Vectors: generation, titering, *in vitro* infection

The viral titers and infection efficiencies for each cell type was determined by plaque formation assays using the crude stock virus of the *Ad.mda-7* and *Ad.cmv* (cytomegalovirus) adenoviruses. In order to amplify the crude virus, 293N cells were cultured in DMEM, in 15 cm dishes until confluent in a humidified atmosphere of 5% (v/v) CO₂ and 37 degrees C. The crude virus was then thawed at 37 degrees C and placed on ice. The medium was removed from each dish and replaced with 3 ml DMEM. Approximately 50-100 µl of crude virus was added to each 15 cm dish in order to obtain an m.o.i. (multiplicity of infection) of 1 (m.o.i. = cell # * desired moi / titer of virus). The plates were then placed on a rocker, in the same humidified atmosphere for 4 hours.

The plates were then removed from the rocker and 10 ml of fresh DMEM was added to each 15 cm dish. The cells were incubated in 5% (v/v) CO₂ at 37 degrees C until all of the cells detached from the dish surface, approximately 4-7 days. When all the cells detached, the medium was removed and placed in 50 ml conical tubes. The tubes were then frozen on dry ice and then thawed at 37 degrees C. This process was repeated two more times (3 freeze/thaw cycles). The tubes were then centrifuged at 5000 RPM for 5 minutes at room temperature in a bench centrifuge (~10,000 x g). A total of 1 ml of the supernatant containing the crude virus was removed and placed in 2 ml dolphin-nosed Eppendorf tubes. The pellet was then discarded and the crude virus frozen on dry ice. A total of four 6 cm dishes containing 293B cells were used to titer each virus. The 293B cells were incubated in 5% (v/v) CO₂ and 37 degrees C until confluent. The following serial dilutions using DMEM supplemented with 10% (v/v) fetal calf serum, 1% (v/v) penicillin-streptomycin, and 1 mM L-glutamine were performed in Eppendorf tubes up to a dilution of 10⁻⁸, with a 1:100 dilution containing 5 µl of crude virus in 495 µl DMEM, and added to each dish of 293B cells. A total of 200 µl of each dilution was added to the confluent 293B cells containing 1 ml DMEM. The plates were then placed on a rocker, in a humidified atmosphere at 37 degrees C, for two hours. A Noble Agar/DMEM overlay is prepared thirty minutes prior to removing the dishes from the rocker. This involves the melting of 25 ml of 1.8% (w/v) Noble Agar. This solution must then be kept at 42 degrees C. A total of 25 ml of DMEM was placed in a sterile 50 ml conical tube and heated to 37 degrees C. The 293B dishes were then removed from the rocker, the

Noble Agar and DMEM solutions mixed, and the medium removed from each plate in descending order of virus dilution. A total of 5 ml of the Noble Agar/DMEM mixture was then gently added as not to disturb the cell monolayer. The plates were allowed to cool at room temperature for 15 minutes before returning them to 5% (v/v) CO₂ at 37 degrees C. After 13 days, post-infection, the existing overlay was covered with 3 ml of a Neutral Red overlay containing the Noble Agar/DMEM solution described above, containing 1% (v/v) 100x Neutral Red. Twenty-four hours later the number of plaques on each plate were observed and the titer determined by multiplying the number of plaques by the appropriate dilution factor. *In vitro* adenoviral infections were performed 24 hours and 4 hours after plating in glioma cells and hepatocytes, respectively. Monolayer cultures were washed in PBS prior to infection and purified Ad.*mda-7* or Ad.*cmv* virus was added to the monolayer cultures in serum-free growth medium. The dishes were then placed on a rocker for 4 hours in a humidified atmosphere of 5% (v/v) CO₂ at 37 degrees C. The growth medium was removed after 4 hours and the appropriate medium was added back to the glioma and hepatocyte cells and allowed to incubate overnight in the same humidified atmosphere.

2.7 Poly-L-lysine Adenoviral Vectors: Infection *In Vitro*

Hepatocytes were isolated from adult male Sprague Dawley rats by the two-step collagenase perfusion technique (Yacoub et al. 2003). The isolated hepatocytes were plated on rat-tail collagen (Invitrogen) coated 12-well plates at a density of 2.5×10^5 cells

per well and cultured in Williams E Medium supplemented with 250 nM insulin (Novo Nordisk), 0.1 nM dexamethasone, 1 nM thyroxine, and 100 µg/mL penicillin-streptomycin, and incubated in a humidified atmosphere of 5% CO₂ at 37 degrees C. Culture medium was changed 4 hours after cell seeding, prior to infection, with the purpose of removing any dead or mechanically damaged cells. In separate polystyrene tubes, 1X HBS (20 mM Hepes, 150 mM NaCl, pH 7.3), was mixed with 0.1 mg/ml poly-L-lysine in 1X HBS (Sigma), at the ratio of 13 µl of 1X HBS to 2 µl of stock poly-L-lysine (15 µl per corresponding well), and allowed to incubate at room temperature for 30 minutes. In another polystyrene tube, plasmid DNA (0.5 µg per well), adenovirus (~100 moi), and 1X HBS were mixed so as to achieve a total volume of 30 µl per well. The solutions were then allowed to incubate in the dark, at room temperature, for 30 minutes. Both solutions were then mixed together and allowed to incubate in the dark at room temperature for 30 minutes. The virus-DNA-poly-L-lysine complex was then added to each well (45 µl per well) and the cells allowed to incubate for 4 hours in an environment of 5% (v/v) CO₂ at 37 degrees C on a rocker to ensure homogenous contact of virus particles with the cells. The cells were then washed with fresh culture medium to remove virus that were not taken-up by the cells, replenished with fresh medium and allowed to incubate in the same humidified atmosphere for 24 hours to ensure adequate expression of the transduced gene products (dnASK1 and CMV). Cells were then treated with 17-AAG (Calbiochem), DCA (Sigma), or the combination as described below.

2.8 Ionizing Radiation Exposure

Cells were cultured in 10 cm dishes or 12-well plates for 24 hours. Cells were then subjected to the above described infection with adenovirus and incubated at 37 degrees C and 5% (v/v) CO₂ for an additional 24 hours, and subjected to a pretreatment of the appropriate inhibitors or ROS-quenchers, followed by exposure to a Cobalt-60 ionizing radiation source for the appropriate length of time corresponding to the prescribed radiation dosage (Gy). Cells were then allowed to incubate for the appropriate time interval in the same humidified environment.

2.9 Cell Homogenization and Protein Assay Analysis

Cells were cultured in 10 cm dishes for 24 hours. Cells were then subjected to 30 minutes pretreatment with GST or GST-MDA-7 (0-30 nM), and where indicated NAC. Cells were then exposed to As₂O₃, and were incubated at 37 degrees C and 5% (v/v) CO₂ for the specified times (typically 96 hours). At the specific time point, the medium was aspirated from the dishes and the cells rinsed with ice-cold phosphate-buffered saline (PBS). The PBS solution was then completely aspirated and the plates were snap frozen at -70 degrees C on dry ice. The frozen cells were lysed in 150 µl of 2x SDS-PAGE blue sample buffer containing 125 mM Tris-Cl, 20% (v/v) glycerol, 4% (v/v) sodium dodecyl sulfate, 10% (v/v) β-mercaptoethanol (BME), 0.04% (v/v) bromophenol blue, pH 6.8. The plates were scraped and the lysate collected and placed in 2 ml dolphin eppendorf

tubes. Lysate samples were boiled at 100 degrees C for 10 minutes prior to performing a protein assay to normalize protein levels and loading of the sample for SDS PAGE.

For protein concentration assays, a 1:1 dilution of Coomassie Protein Assay Reagent, purchased from Pierce (Rockford, IL), and milli-Q water was prepared and 500 μ l placed in 2 ml dolphin tubes, corresponding to the number of lysate protein samples to be determined, plus an extra tube for a blank sample. The protein lysates were removed from the hot plate and 3 μ l of lysate was added to the corresponding tube containing the Coomassie dilution, 3 μ l of blank 2X SDS-PAGE blue sample buffer was added to one dolphin tube to act as a blank for the protein assay. The lysate/Coomassie mixtures were thoroughly shaken and allowed to sit at room temperature for five minutes. A total of 200 μ l of each sample, including the blank, was loaded into two separate wells on a 96-well plate (100 μ l per well). The 96-well plate was then read on a Dynatech MR600 Microplate Reader at 540 nm, in order to determine the mean optical density of each well. The samples were then normalized to the blank mean OD and the amount of protein in each sample determined.

2.10 SDS Poly-Acrylamide Gel Electrophoresis and Western Blot Analysis

The BioRad Protean II xi gel apparatus, purchased from Bio-Rad Laboratories (Hercules, CA), was assembled in the following manner. The glass plates were thoroughly cleaned

with 70% (v/v) ethanol and allowed to dry. The appropriate size spacers were placed in-between the glass plates and secured with single screw clamps, making sure to evenly align the bottom of the glass plates and the bottom of the spacers. The apparatus was then secured in the BioRad casting stand. The resolving gel was then prepared according to the values in Table 1, with the concentration of acrylamide varying in accordance with the molecular weight of the protein under investigation (a high mw protein, use low % acrylamide). The resolving gel was prepared by adding the appropriate amount of milli-Q water, 1.5 M Tris (pH 8.8), 40% (w/v) acrylamide (Biorad), 10% (w/v) ammonium persulphate, and TEMED (Fisher Scientific, Suwanee, GA), in that order, and allowing the TEMED to mix with the solution for 30 seconds before pouring. Directly after pouring the resolving gel, a layer of deionized water was placed on top of the separating gel and the gel was allowed to sit for 1 hour. The deionized water was then removed and the residual water removed with 3M paper. The appropriate combs (15 or 20 well) were then placed in the apparatus and the stacking gel solution prepared according to Table 1. The reagents were added in the same manner as described above and the stacking gel was slowly poured on top of the resolving gel without allowing air bubbles to form around the wells formed by the comb. The stacking gel was allowed to sit for 1 hour and the combs removed. The gel apparatus was assembled and each well underlined in pen to more easily identify the wells during sample loading. A 1X SDS running buffer was then prepared (3.02g Tris-base, 14.40g glycine, 1.0g SDS, QS to 1 L deionized water) and poured in-between the glass plates, and outside of the glass plates until the gel case was

one-fourth full. The appropriate volume of each sample lysate to obtain 40 μg of protein was added to each well, and 25 μl of dual color precision protein marker, purchased from BioRad, was loaded into one well to determine the migration of the proteins according to molecular weight. The gel apparatus was then connected to a 200 V power supply, purchased from BioRad, and electrophoresis was performed at 40 mA per gel until the bromophenol blue dye front reached the bottom of the resolving gel. The gel was then removed and the proteins transferred to a 0.2 μm nitrocellulose membrane, purchased from BioRad. The transfer consisted of the gel being placed in an immunoblot transfer cassette containing in order: one Scotch-Brite pad, two pieces of Whatman 3M filter paper, acrylamide gel, 0.2 μm nitrocellulose paper, two pieces of Whatman 3M filter paper, and one Scotch-Brite pad. The transfer cassette was then placed in a transfer box, with the nitrocellulose side oriented to the anode for proper protein transfer, containing 1X transfer buffer (5.8g Tris-base, 2.9g glycine, milli-Q water to 800ml, 1.8ml 20% (w/v) SDS, 200ml methanol). The transfer box was connected to a 200 V power source and allowed to transfer overnight at 15 Volts. The nitrocellulose was then removed from the transfer cassette and rinsed in 1X Tris Buffered Saline (TBST) buffer (1L 10X TBS: 24.2g Tris-base (Fisher Scientific), 292.2g NaCl (Fisher Scientific), 1ml Tween (BioRad), pH 7.5) for five minutes, then placed in blocking buffer, 5% (w/v) nonfat milk (BioRad) in 1X TBST, for 4 hours at 4 degrees C on a shaker. The blocking buffer was then removed and the desired primary antibody, diluted in 5% (w/v) nonfat milk in 1X TBST as described in Section 2.1, for 4 hours or overnight at 4 degrees C (depending on

the antibody specifications). The nitrocellulose was then washed with blocking buffer 3 times for 15 minutes each. The secondary antibody specific to the primary antibody conjugated with horse-radish peroxidase (HRP) was diluted 1:2000 in blocking buffer, and placed on the nitrocellulose for one hour. The nitrocellulose was then washed 3 times in TBST for 15 minutes each. The nitrocellulose was removed from the TBST and taken to a dark room to obtain the immunoblot. A 1:1 solution of Enhanced Luminol Reagent and Oxidizing Reagent was prepared using the Renaissance Western Blot Chemiluminescence kit from Life Sciences, and placed on the nitrocellulose for 2 minutes. The nitrocellulose was then taken out of the solution, covered in clear polyvinyl plastic, and placed in a developing cassette. Kodak X-Ray film was placed in the cassette and left for exposure times ranging from 10 seconds to 20 minutes, depending on the intensity of the signal obtained. The film was then developed using a Konica Medical Film Processor SRX-501A, and the images scanned into Adobe Photoshop.

Resolving Gel			
		One Side	Two Sides
Gel	Components	50 mL	100 mL
10%	40% Acrylamide	12.5	25.5
	1.5M Tris (pH 8.8)	12.5	25
	10% AP	0.5	1
	TEMED	0.02	0.04
	Milli-Q Water	24.5	49
12%	40% Acrylamide	15	30
	1.5M Tris (pH 8.8)	12.5	25
	10% AP	0.5	1
	TEMED	0.02	0.04
	Milli-Q Water	22	44

Stacking Gel			
		One Side	Two Sides
Gel	Components	10 mL	20 mL
5%	40% Acrylamide	1.25	2.5
	0.5M Tris (pH 6.8)	2.5	5
	10% AP	0.1	0.2
	TEMED	0.01	0.02
	Milli-Q Water	6.2	12.4

Table 1. Solutions required for Resolving and Stacking Gels for SDS-PAGE

To work out the volume required for a particular gel, use the formula: Volume of stock acrylamide (ml) = [Total Volume (ml) x % of gel] / concentration of stock; ex: to make 50 ml of 12% gel, requiring 40% acrylamide: $[50 \text{ ml} \times 12\%] / 40\% = 15 \text{ ml}$. The difference in total volume is the amount of milli-Q water required.

2.11 Assessment of Cell Apoptosis and Cell Death

The level of apoptosis and necrosis was determined using Wright-Giemsa-stained cytopsin slides under light microscopy and scoring the number of cells exhibiting the classic morphological features of apoptosis. In each of the conditions, 10 randomly selected fields per slide were evaluated, thus encompassing approximately 15,000 cells per condition. RCC cells were plated in 6-well plates at a concentration of approximately 5×10^4 cells per well, and 24 h later treated with 0.5 nM GST, 0.5 nM GST-MDA-7, 0.5 μM As_2O_3 , or pre-treated 1 h before the addition of As_2O_3 with 10 mM N-acetyl cysteine. The medium was removed 96 h after treatment, the cells washed in 1X PBS, trypsinized and harvested with appropriate serum-free medium supplemented 1% (v/v) penicillin-streptomycin, and placed in individual 15 ml conical tubes. The samples were then centrifuged at 1,000 RPM for 5 minutes at 25 degrees C in an Eppendorf 5804 R centrifuge. The supernatant was then aspirated and the cells re-suspended in PBS. The cells were then counted and approximately 4×10^4 cells were loaded into each cytopsin cartridge. Each cytopsin cartridge contained one appropriately labeled slide, purchased from Fisher Scientific (Pittsburgh, PA) and one filter card, purchased from Shandon Inc (Pittsburgh, PA). The cytopsin cartridges were then centrifuged at 800 RPM for 10 minutes at room temperature in a Shandon Cytospin 3 centrifuge. Slides were then placed in a fixation solution containing a 3:1 mixture of methanol (Fisher Scientific) and glacier acetic acid (Fisher Scientific) for 10 minutes. The slides were then removed and placed in a staining solution containing a 1:10 mixture of Giemsa (Sigma-Aldrich) and

milli-Q water for 10 minutes. The slides were then removed, gently washed with milli-Q water, and allowed to dry overnight.

2.12 Assessment of Cell Viability

A method used for evaluating cell viability involves the trypan blue inclusion/exclusion of isolated cells under light microscopy and scoring the percentage of cells exhibiting blue staining. RCC cells were plated in 6-well plates at a concentration of approximately 5×10^4 cells per well, and 24 hours later treated with 0.5 nM GST, 0.5 nM GST-MDA-7, 0.5 μM As_2O_3 , or pre-treated 1 hour before the addition of As_2O_3 with 10 mM N-acetyl cysteine. Glioma cells were plated in 6-well plates at a concentration of approximately 5×10^4 cells per well, and 24 hours later either infected with Ad.*mda-7* or control virus at the indicated multiplicity of infection (MOI). Twenty-four hours after infection, cells were treated with kinase inhibitor drugs and then irradiated. The medium was removed 96 h after treatment, the cells washed in 1X PBS, trypsinized and harvested with the appropriate serum-free medium supplemented with 1% (v/v) penicillin-streptomycin, and placed in individual 15 ml conical tubes. The samples were then centrifuged at 1000 RPM for 5 minutes at 25 degrees C in an Eppendorf 5804 R centrifuge. The supernatant was then aspirated and the cells re-suspended in a trypan blue solution containing a 1:10 mixture of 0.4 % (v/v) trypan blue (Sigma-Aldrich) and phosphate buffered solution (PBS). Cells in the four 1 mm^2 corner areas of a Neuhauser cell cartridge were counted and the percentage of cells exhibiting blue staining determined. The trypan blue inclusion/exclusion represents the integrity of the cellular membrane in that healthy,

viable cells contain intact cell membranes and thus reject the trypan blue stain, while damaged cells exhibit a blue color due to a compromised cellular membrane that allows the trypan blue stain to be incorporated into the cell.

2.13 MTT Assay for Determination of Cellular Viability

Cell viability was also evaluated using the MTT assay. This test is based on the enzymatic reduction of tetrazolium salt MTT (3-[4,5-Dimethylthiazol-2-yl]-2,5-diphenyl-tetrazolium bromide) in living, metabolically active cells, but not in dead cells. RCC cells were plated in 12-well plates at a concentration of 1×10^4 cells per well, and 24 h later treated with GST, GST-MDA-7, arsenic trioxide, or N-acetyl cysteine at the indicated concentrations. The cytotoxicity of the various treatments was assessed 96 h after protein treatment using the MTT assay. Glioma cells were plated in 12-well plates at a concentration of 1×10^4 cells per well, and 24 h after plating infected with either *Ad.mda-7* or control virus at the indicated multiplicity of infection (MOI). Twenty-four hours after infection, cells were treated with kinase inhibitor drugs and then irradiated. The cytotoxicity of the various treatments was assessed 96 h after irradiation using the MTT assay. Stock MTT reagent (Sigma-Aldrich) was diluted in the universal solvent dimethyl sulfoxide (DMSO) (Fisher Scientific) to obtain a 100 mg/ml solution, aliquoted into 500 μ l aliquots and stored at -20 degrees C in light protective tubes. The MTT reagent was thawed and the cells treated 96 h after protein exposure or radiation treatment with 1 μ g/ml of the reagent. The cells were then incubated in a humidified atmosphere of 5% (v/v) CO₂ at 37 degrees C for 90 minutes. The medium was then

removed and 500 μ l of DMSO added to each well. A total of three 100 μ l samples from each well was then removed and placed in a 96-well plate. This was done for each of the wells in the 12-well plate. The 96-well plate was then read on a Dynatech MR600 Microplate Reader at 540 nm, in order to determine the mean optical density of each well. All data was then normalized to the control sample receiving treatment with either vehicle (DMSO) or infection with *Ad.cmv*.

2.14 Cell Survival Analyses

RCC cells were assayed for the effect(s) of GST-MDA-7 and arsenic trioxide on long-term cell survival. Cells were plated on 60 mm dishes at a concentration of 1×10^4 cells per dish and 24 h later treated with GST, or GST-MDA-7, and thirty minutes later treated with As_2O_3 at the indicated concentrations. Glioma cells were assayed for the effect(s) of *Ad.mda-7* and radiation on cell survival. Cells were plated on 60 mm dishes at a concentration of 1×10^4 cells per dish and 24 h later infected with either *Ad.mda-7* or control virus at the indicated MOI. Twenty-four hours after infection cells were irradiated. The trypan blue inclusion/exclusion assay was then performed 96 h after protein treatment, as described above in section 2.12. The viable trypan blue-negative cells were then re-plated in 60 mm dishes at 250-1,000 cells per dish. The dishes were then incubated in a humidified atmosphere of 5% (v/v) CO_2 at 37 degrees C and RCC colonies were allowed to form from the surviving cells for 10-14 days, while glioma colonies were allowed to form from the surviving cells for 7-9 days. Upon colony formation, the medium was removed and the cells washed in 1X PBS. The cells were

then fixed on the dish by adding methanol for 10 minutes. The methanol was then removed and the cells were placed in a 0.1% (v/v) crystal violet (Sigma-Aldrich) staining solution for 1 h. Colonies containing more than 50 cells were then counted and normalized to the control cell survival sample. The survival data shown includes individual assays performed at multiple dilutions with a total of six plates per data point, repeated for a total of three experiments.

2.15 Assessment of Reactive Oxygen Species Generation

Hepatocytes were plated in 96-well plates. Cells were preincubated with dihydro-dichlorofluorescein (H₂DCF) (5 μ mol/L for 30 minutes) in phenol red-free culture medium, which is nonfluorescent in its dihydro form but upon reaction with ROS becomes highly fluorescent. Dihydro-DCF is sensitive to oxidation by hydroxyl radicals and hydrogen peroxide in the presence of peroxidase. Fluorescence measurements were obtained by invoking excitation at a 495 nm wavelength, resulting in emission readings at 520 nm 0-20 minutes after 17-AAG and DCA addition with a Packard Fluorocount plate reader (Albertville, MN).

2.16 Cell Cycle Analysis

Glioma cells were treated as described for the MTT assay above (150,000 cells per 60 mm dish). At the time of irradiation and 24 h after irradiation, cells were isolated to determine their cell cycle profiles. Cells were washed once with 1X PBS, fixed in 80%

ice-cold ethanol, centrifuged, washed in 1X PBS, and approximately 10^6 cells per condition were stained with propidium iodide (50 $\mu\text{g}/\text{mL}$) in 1X PBS containing 100 $\mu\text{g}/\text{mL}$ Rnase A. The cells were then subject to flow cytometric analysis of DNA content using a Becton Dickinson FACScalibur cytometer and analysed using Verity Winlist software.

2.17 DNA Fragmentation

Nucleosomal DNA degradation is suggestive of a necrotic form of cell death and is used as an indicator of the extent of cellular damage experienced by cells treated with numerous cytotoxins. Cells were plated in 100 mm dishes at a concentration of 2×10^5 cells per dish and 24 h later treated with 0.5 nM GST, 0.5 GST-MDA-7, and 0.5 μM As_2O_3 . The medium was removed 96 h after protein treatment and the cells washed in PBS, trypsinized, centrifuged, and counted as previously described above. A total of 1×10^6 cells were homogenized with 1 ml of lysis buffer (10 mM Tris (Fisher Scientific), 5 mM EDTA (Fisher Scientific), and 1 % (v/v) Triton (Fisher Scientific)). RNase A (Sigma-Aldrich) was then added to each sample at 100 $\mu\text{g}/\text{ml}$ and the samples incubated at 50 degrees C for 1 h. Proteinase K (Roche Diagnostics Corp., Indianapolis, IN) was then added at a concentration of 100 $\mu\text{g}/\text{ml}$ and the samples were incubated overnight at 50 degrees C. Each of these digestive enzymes function to eliminate contaminants in the DNA sample attributed to RNA and proteins still present in the samples. The DNA was extracted using phenol and chloroform and was centrifuged at 10,000 x g for 5 minutes at

4 degrees C in an Eppendorf 5804 R centrifuge. The aqueous phase was mixed with two volumes of ice-cold ethanol (Aaper Alcohol and Chemical Co., Shelbyville, KY) and then precipitated by centrifugation at 15,000 x g for 10 minutes. The supernatants were then aspirated and the DNA pellets washed with 80% (w/v) ethanol and centrifuged at 15,000 x g for 15 minutes. The supernatant was then removed and the samples allowed to air-dry overnight. The DNA pellet was then dissolved in TE buffer (Gibco Life Technologies, Grand Island, NY). The DNA concentration was then determined by creating a 1:100 dilution of the DNA containing TE buffer and milli-Q water. The sample was then analyzed on a Beckman DU-64 Spectrophotometer at 260 nm and 280 nm wavelengths and the DNA concentration (ng/ μ l) determined.

In order to verify the DNA fragmentation, the DNA samples were electrophoresed on a 1.5% (w/v) agarose gel and analyzed for the presence of a laddering pattern. The agarose gel was prepared by mixing 1.5 g of agarose (Fisher Scientific) and 100 ml of milli-Q water. The mixture was then heated while on a stir-plate and 10 μ l of ethidium bromide (BioRad) was added to the mixture to act as a fluorescent dye. The ThermoEC minicell primo EC320 electrophoretic gel system (Fisher Scientific) was then assembled and the 10-well comb securely fastened to the apparatus. The heated agar mixture was then poured into the apparatus and allowed to sit for 1 h. The ThermoEC apparatus was then filled with TBE buffer (1L 5x TBE buffer: 54g Tris-base, 27.5g boric acid, 20 ml 0.5 M EDTA (pH 8.0), QS to 1L with milli-Q water). The first lane of the agarose gel was

loaded with 10 μ l of lambda DNA HindIII marker (Invitrogen). Prior to loading in the agarose gel, 5 μ g of each DNA sample was mixed with the appropriate volume of 1X TBE buffer and marker to obtain a 20 μ l total volume. This DNA sample mixture was then loaded into the appropriate wells. The gel apparatus was then connected to a power supply (BioRad), set to a constant voltage of 50 V or constant amperage of 100 mA, and allowed to electrophorese for 2 to 3 h. When the blue dye front was observed to be at the bottom of the gel, the power supply was turned off, disconnected, and the gel removed from the apparatus. The gel was then placed in a BioRad Transluminator and the presence of a DNA laddering pattern observed using the BioRad Quantity One application.

2.18 Statistical Analyses

The effects of various treatments were analyzed using one-way ANOVA and a two-tailed t test. Differences containing a p-value less than 0.05 were considered statistically significant. The experiments shown are the means of multiple individual points (+/- SEM).

CHAPTER THREE

RESULTS

3.1.1 Transfection of RCC lines to express MDA-7 resulted in cell death.

Tumor cells, but not untransformed cells, infected with the type 5 recombinant adenovirus, *Ad.mda-7*, undergo growth arrest and apoptosis (Lebedeva et al. 2002, Mhashilkar et al. 2001, Sarkar et al. 2002, Sauane et al. 2003, Su et al. 2003, Su et al. 2001, Su et al. 1998). The reproduction of these results, obtained by using *Ad.mda-7* in other tumor cell types, was attempted in the A498 and UOK121N renal carcinoma cell lines (RCC). We were unable to observe any effect of *Ad.mda-7* on the growth of the A498 or UOK121N cell line. In contrast, the transfection of the both cell lines with a plasmid expressing MDA-7 resulted in the reduction of cell growth and colony formation (Yacoub et al. 2003).

Due to the fact that transfection, and not infection, of the RCC line to express MDA-7 resulted in reduced cell growth and colony formation, the expression of coxsackievirus and adenovirus receptors (CARs), which are essential for adenovirus entry into cells, was investigated. CAR levels in the A498 and UOK121N cell lines were found to be very low in contrast to those of the U373 glioma cell line (Yacoub et al. 2003), known to readily infect with adenovirus, and primary human renal epithelial cells, which have been previously established in other studies (Haviv et al. 2002).

Since the RCC lines were resistant to adenoviral infection, MDA-7 was synthesized as a GST fusion protein in *Escherichia coli* to determine whether purified MDA-7 protein could alter RCC growth and survival. It was found via MTT assay, that GST-MDA-7, but not GST, caused a dose-dependent reduction in both A498 and UOK121N RCC cell proliferation, as shown in Figure 12 and 13. It was also found that this effect was not observed in primary renal epithelial cells, as shown in Figure 14. In order to determine that the effect of GST-MDA-7 was due to MDA-7 and not a contaminating bacterial protein, we made use of the MDA-7 protein synthesized in primary rodent hepatocytes. Cultures of primary rodent hepatocytes were infected with *Ad.mda-7* or an *Ad.cmv* control virus as described in Materials and Methods. Ninety-six hours after infection, the culture media from the hepatocytes was transferred to the culture media of the RCC lines. It was observed that A498 and UOK121N cells incubated with either fresh media or media from the control virus-infected hepatocytes experienced similar growth rates. Alternatively, renal cancer cells incubated with media from *Ad.mda-7*-infected hepatocytes experienced a significantly reduced growth rate (Figure 15).

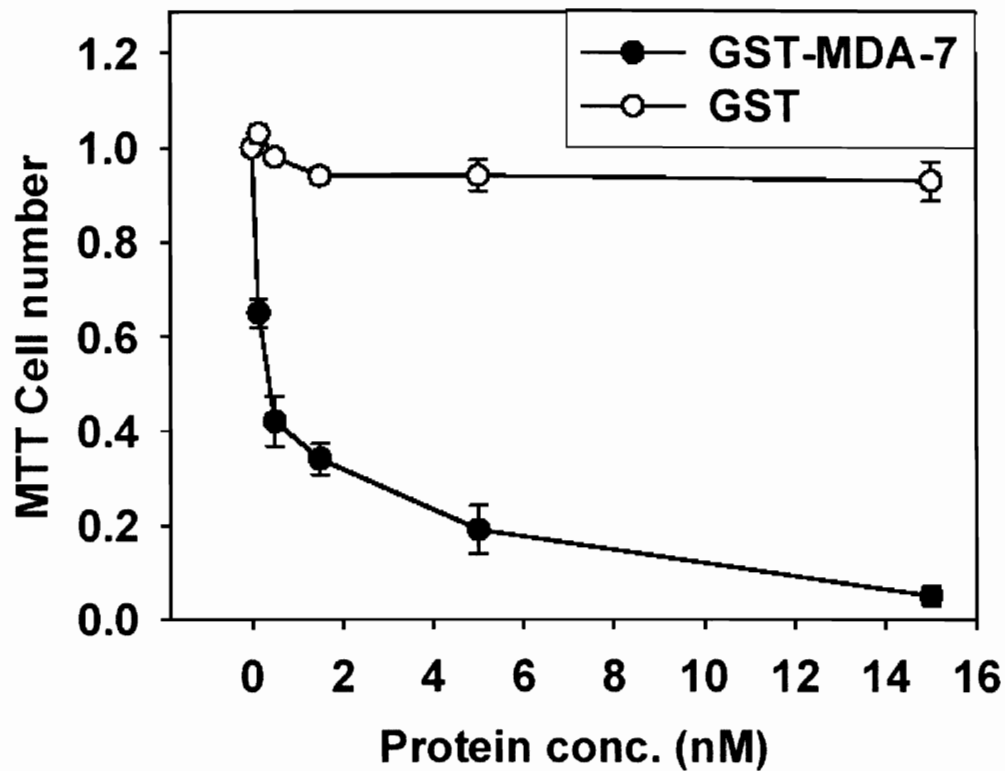


Figure 12. GST-MDA-7 causes a dose-dependent reduction in the proliferation of the A498 renal carcinoma cell line. MTT assay data are the means of 12 wells (one plate per condition, +/- SEM) from a representative experiment using different preparations of GST-MDA-7 (n = 3).

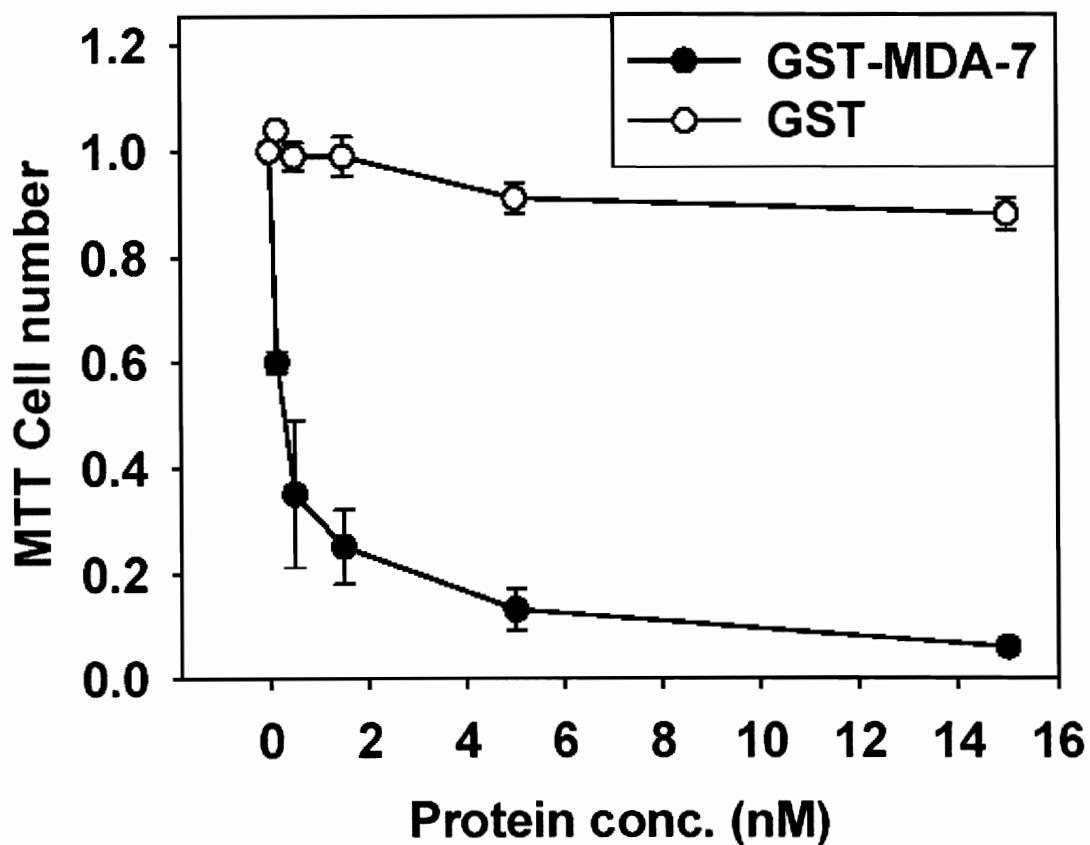


Figure 13. GST-MDA-7 causes a dose-dependent reduction in the proliferation of the UOK121N renal carcinoma cell line. MTT assay data are the means of 12 wells (one plate per condition, +/- SEM) from a representative experiment using different preparations of GST-MDA-7 (n = 3).

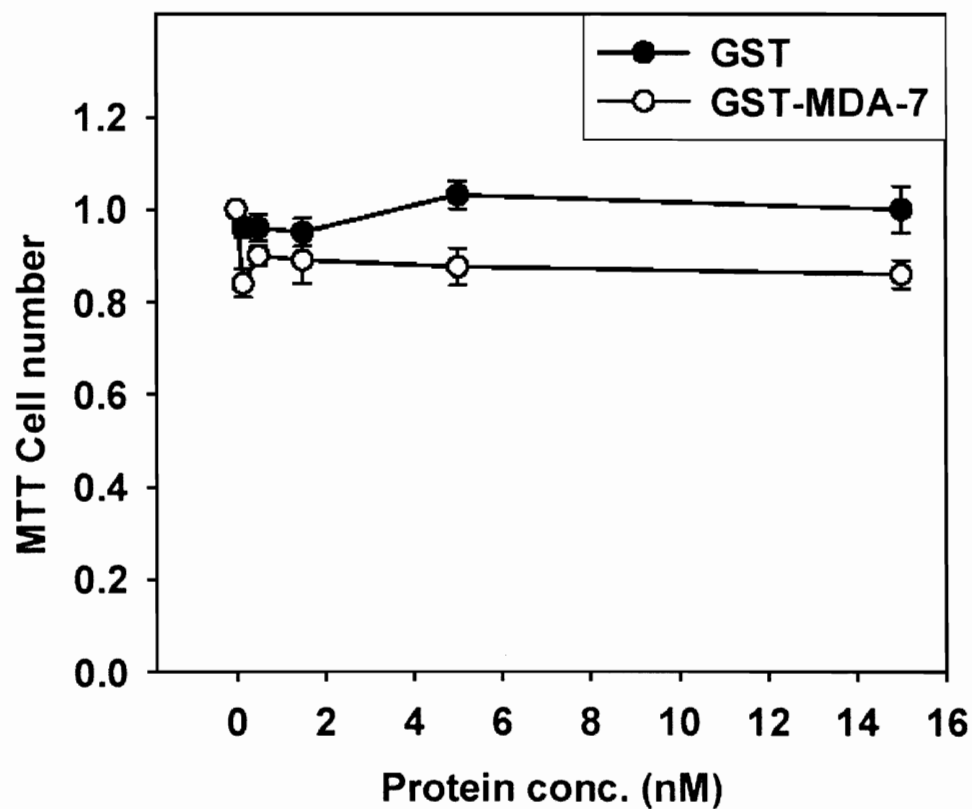


Figure 14. GST-MDA-7 does not cause a dose-dependent reduction in the proliferation of primary renal epithelial cells. MTT assay data are the means of 12 wells (one plate per condition, +/- SEM) from a representative experiment using different preparations of GST-MDA-7 (n = 3).

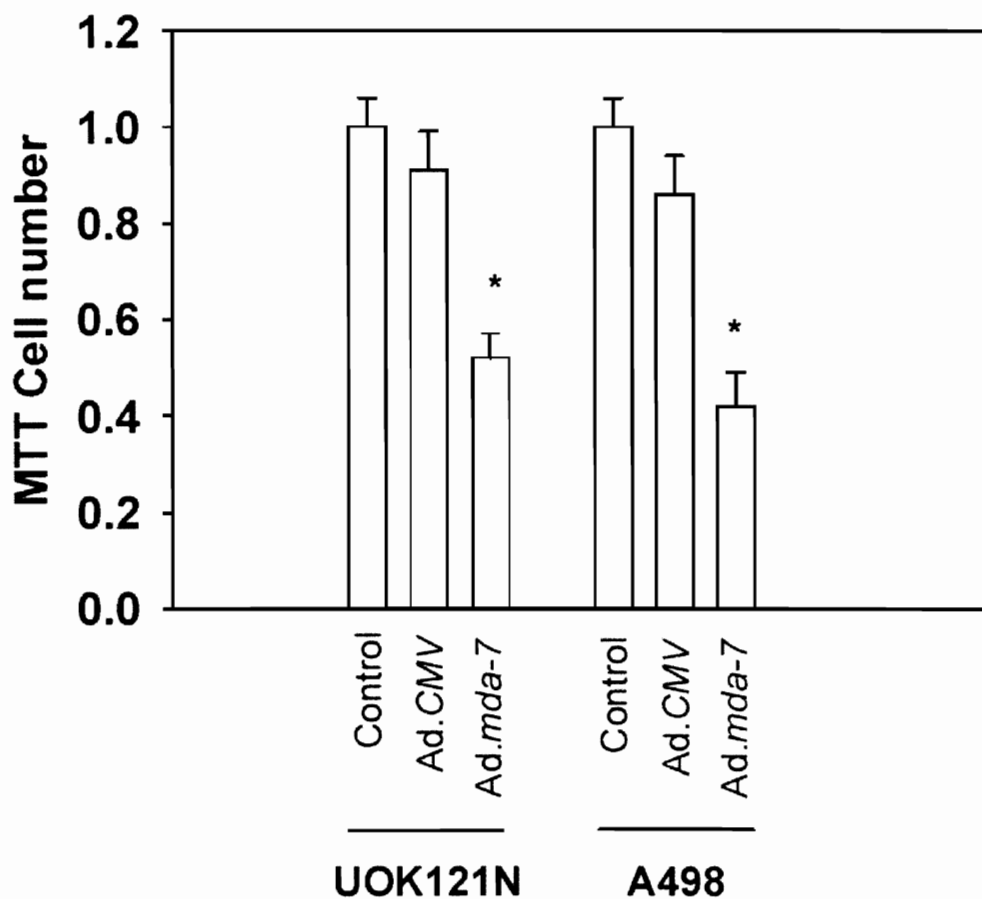


Figure 15. Medium obtained from primary rat hepatocytes infected with *Ad.cmv* or *Ad.mda-7* (u.o.i. = 50) causes a dose-dependent reduction in the proliferation of the A498 and UOK121N renal carcinoma cell line. MTT assay data are the means of 12 wells (one plate per condition, \pm SEM, * $p < 0.05$ less than control CMV media or fresh media) from a representative experiment using different hepatocyte infections ($n = 2$).

3.1.2 Arsenic Trioxide (As₂O₃) causes dose-dependent reduction in cell proliferation.

Arsenic trioxide is known to magnify the toxicity of certain established chemotherapeutic drugs (Dai et al. 2002, Miller et al. 2002) through the generation of free radical species in cells (Grad et al. 2001). The effect of arsenic trioxide as an individual agent was investigated using MTT assays to evaluate cell growth 96 hours after arsenic trioxide exposure, as described above in Materials and Methods. We discovered that arsenic trioxide did not significantly alter cell growth at concentrations less than 1 μ M (Figure 16). However, at concentrations above 1 μ M, arsenic trioxide caused a dose-dependent reduction in RCC and primary renal epithelial cell proliferative potential.

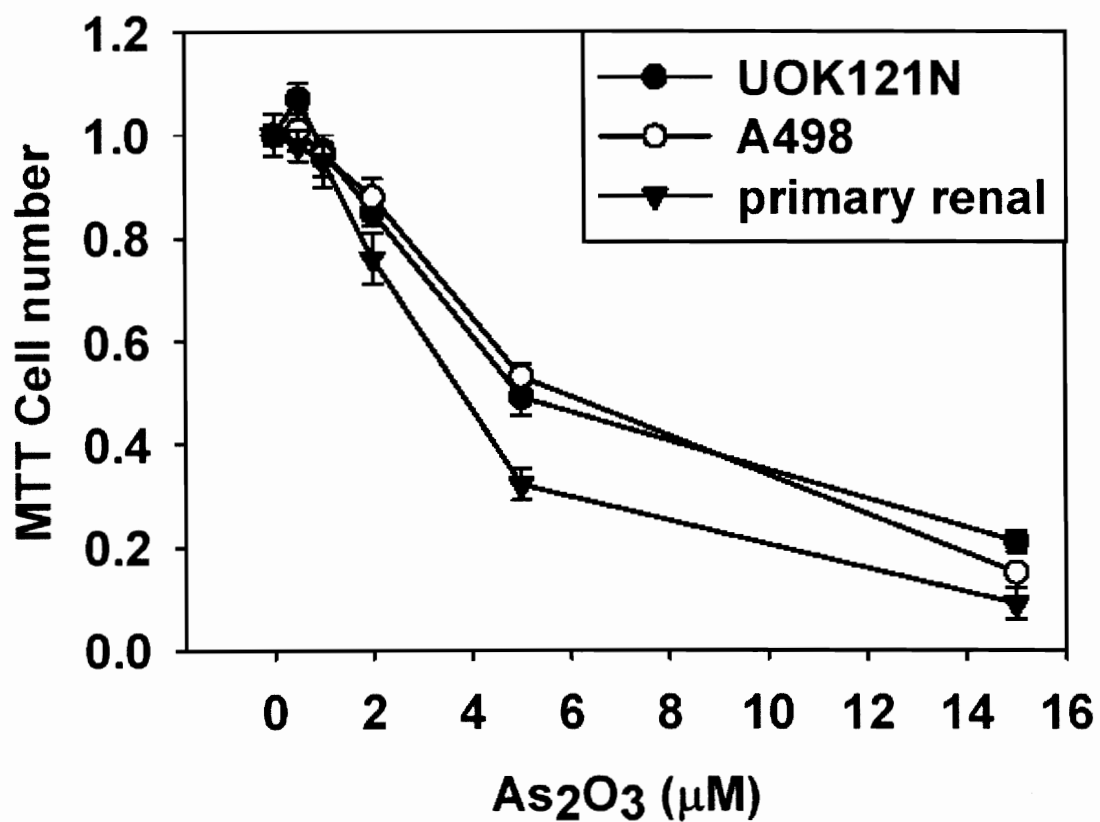


Figure 16. Arsenic trioxide causes a dose-dependent reduction in the A498, UOK121N, and the primary renal epithelial cell line. MTT assay data are the means of 12 wells (one plate per condition, \pm SEM) from a representative experiment using different preparations of arsenic trioxide ($n = 3$).

The effects of combining arsenic trioxide with GST-MDA-7 and GST were then investigated using the MTT assay to evaluate the overall amount of cell death 96 hours after treatments. The anti-proliferative and killing effects of the individual agents were found to be enhanced in a greater than additive fashion when arsenic trioxide was combined with GST-MDA-7, but not when arsenic trioxide was combined with GST alone, in the RCC lines but not in primary renal epithelial cells (Figure 17, 18, and 19). In parallel to the assays shown in Figures 17, 18, and 19, the viability of cells was determined 96 hour after treatments by Wright Giemsa staining of fixed cells, followed by microscopic examination of the nuclear morphology of the cells. It was observed that GST-MDA-7, arsenic trioxide, or the combination of agents did not enhance “classical” nuclear apoptosis. The cell nuclei appeared to be degraded in a necrotic fashion, not in a “classical” nuclear apoptotic manner. This finding also correlates with trypan blue staining assays performed in parallel. These assays resulted in more trypan blue-positive cells present in the combined GST-MDA-7 and arsenic trioxide treatment conditions than under any other single treatment condition (data not shown).

Due to the fact that GST-MDA-7 and arsenic trioxide significantly enhanced tumor cell death, as evident in the data obtained from the Wright Giemsa assays, MTT assays, and presence of enhanced trypan blue inclusion in treated cells, the long-term proliferative effects of the combination was investigated by performing clonogenic survival assays, as described in Materials and Methods. It was found that treatment of the RCC lines with

low concentrations of GST or GST-MDA-7 (0.5 μM) did not significantly alter long-term proliferation or cell survival. However, the combination of GST-MDA-7 with arsenic trioxide (0.5 μM) did cause a greater than additive (synergistic) reduction in cell survival, as shown in Figures 20 and 21.

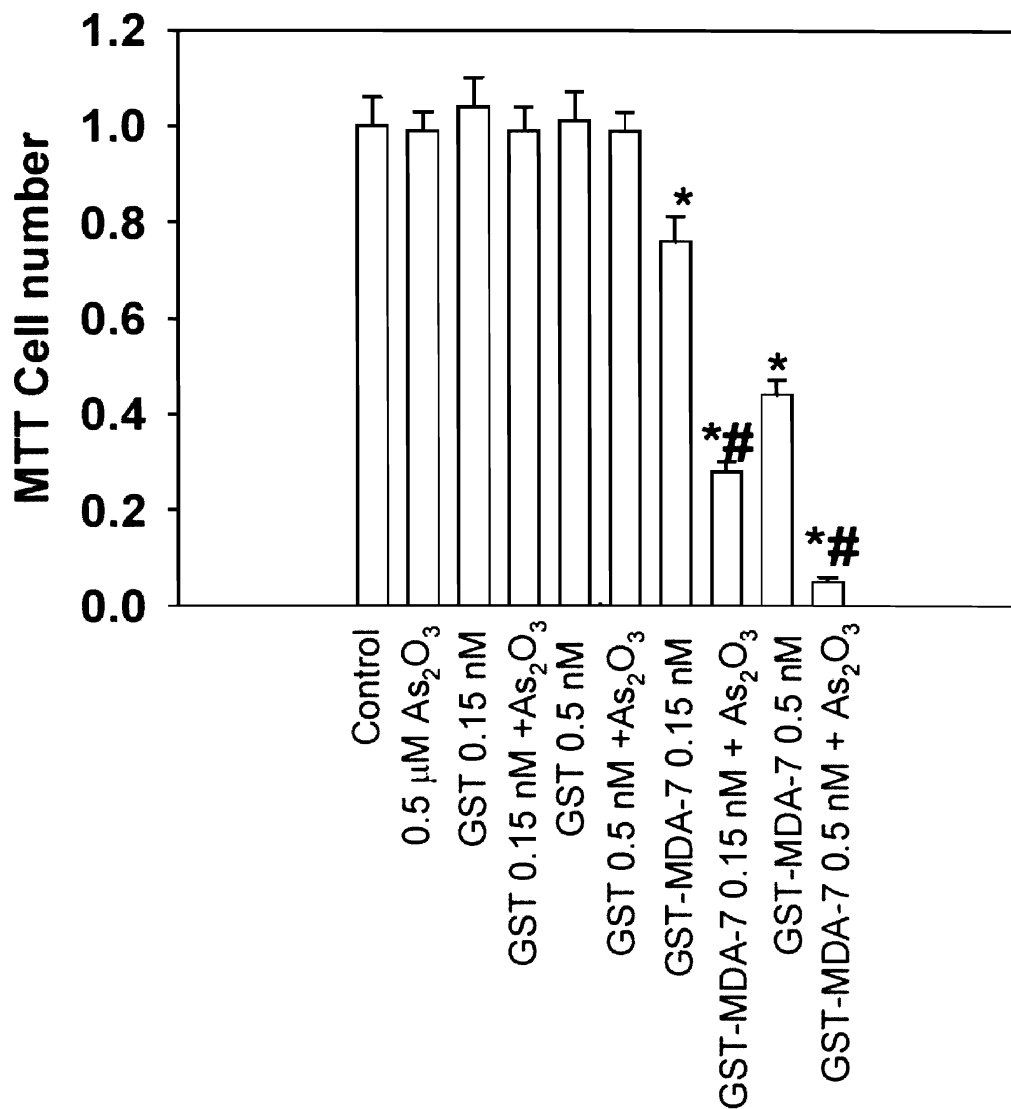


Figure 17. GST-MDA-7 and arsenic trioxide interact in a greater than additive fashion in the A498 renal carcinoma cell line. MTT assay data are the means of 12 wells (one plate per condition, +/- SEM) from a representative experiment using different preparations of GST-MDA-7 and GST (n = 3). * p < 0.05 less than GST value cells; # p < 0.05 less than corresponding GST-MDA-7 value without As₂O₃ co-treatment.

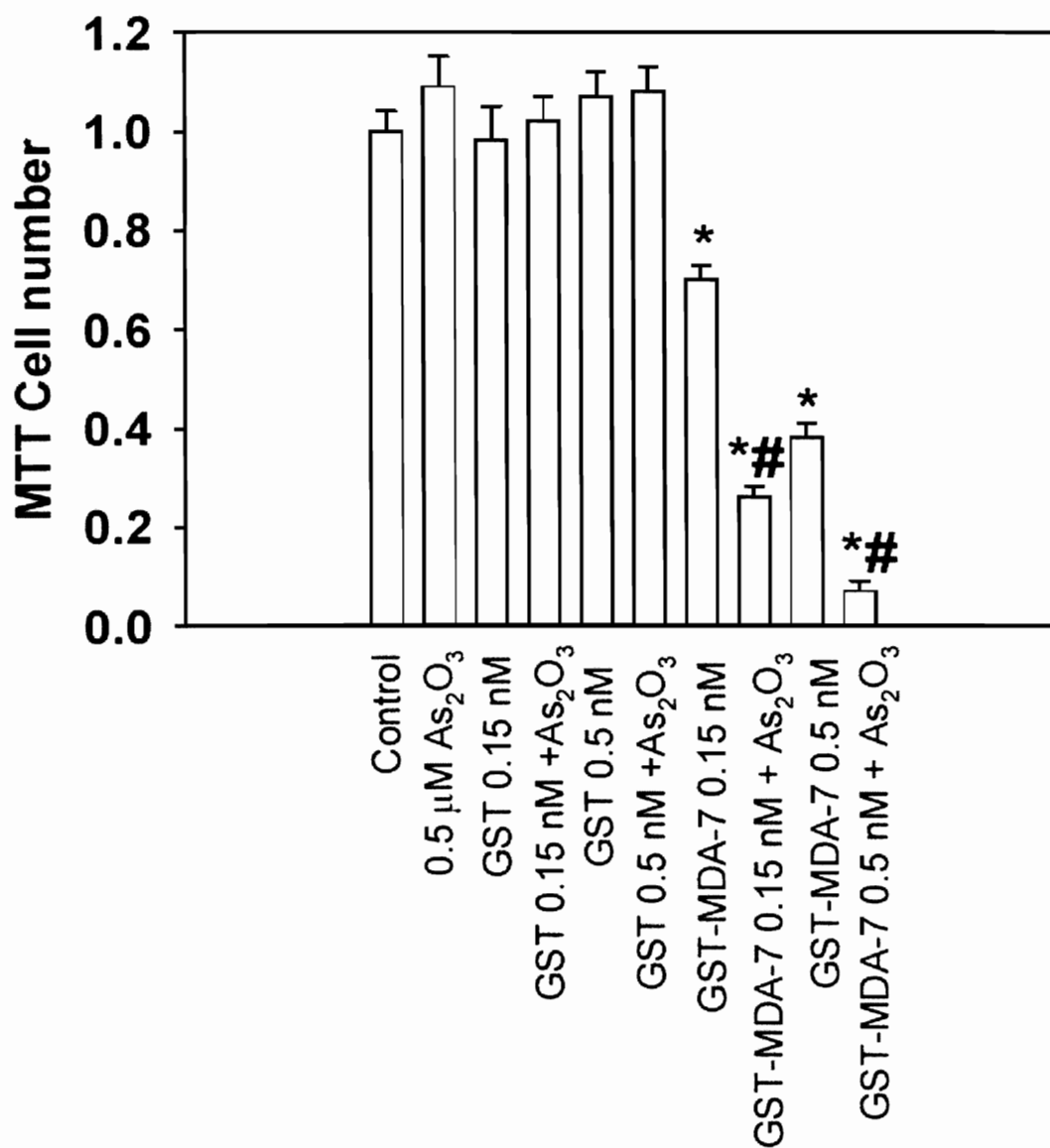


Figure 18. GST-MDA-7 and arsenic trioxide interact in a greater than additive fashion in the UOK121N renal carcinoma cell line. MTT assay data are the means of 12 wells (one plate per condition, +/- SEM) from a representative experiment using different preparations of GST-MDA-7 and GST (n = 3). * p < 0.05 less than GST value cells; # p < 0.05 less than corresponding GST-MDA-7 value without As₂O₃ co-treatment.

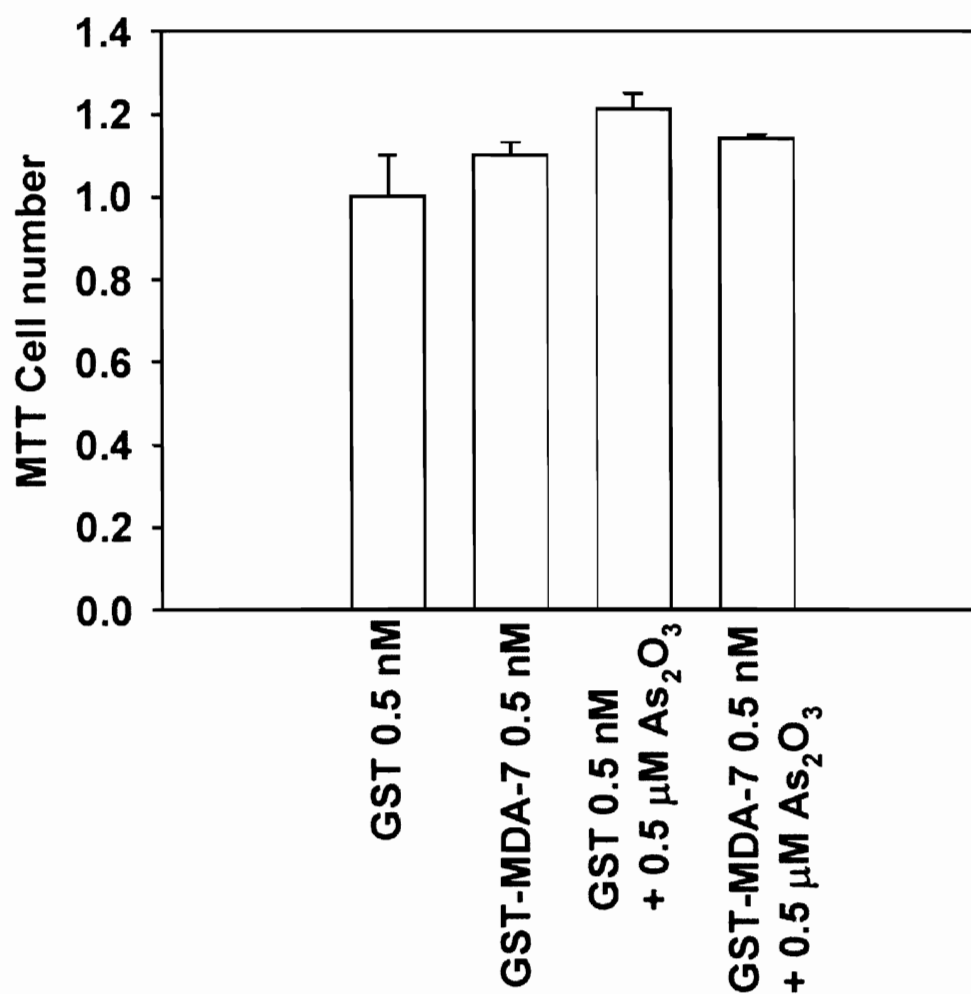


Figure 19. GST-MDA-7 and arsenic trioxide do not interact in a greater than additive fashion in the primary renal cell line. MTT assay data are the means of 12 wells (one plate per condition, +/- SEM) from a representative experiment using different preparations of GST-MDA-7 and GST (n = 3).

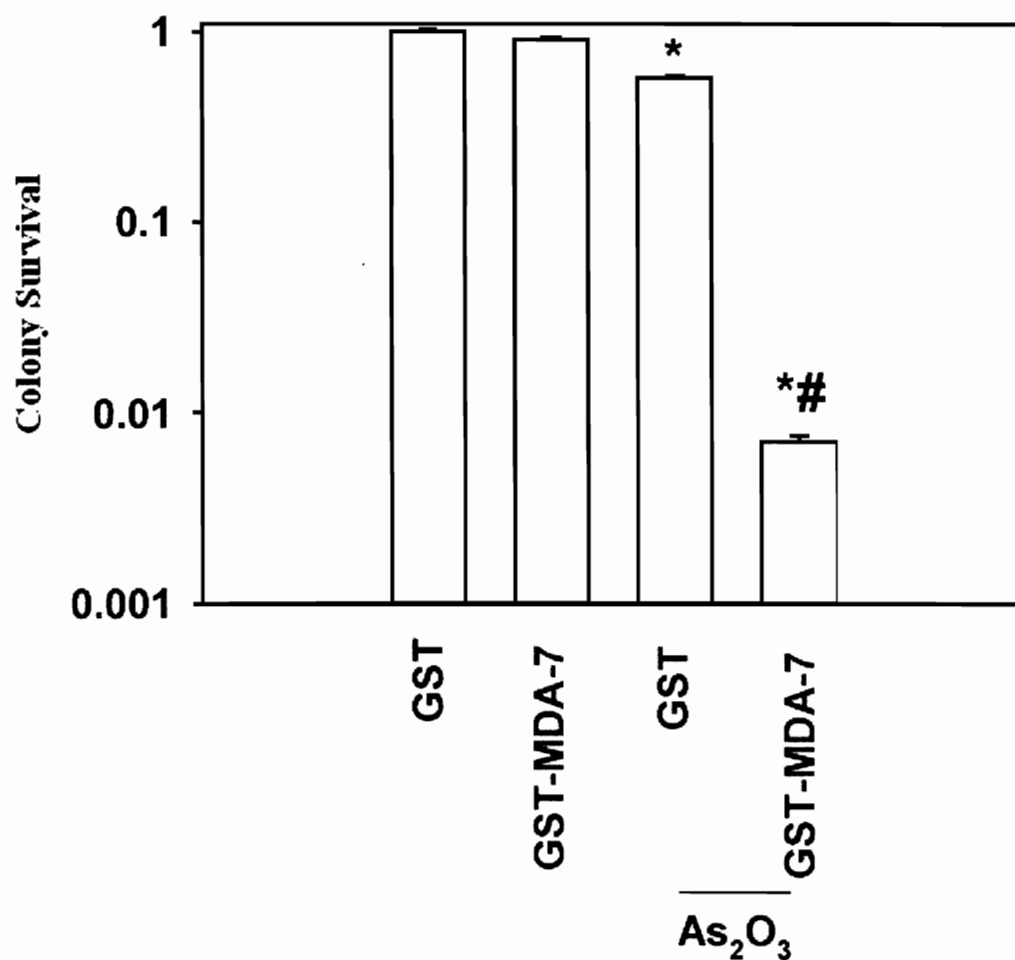


Figure 20. GST-MDA-7 (0.5 nM) and arsenic trioxide (0.5 μ M) interact in a greater than additive fashion to reduce colony formation ability in the A498 renal carcinoma cell line. Colony formation assay data values are the means of 3 separate experiments (\pm SEM). * $p < 0.05$ less than control cells; # $p < 0.05$ less than As₂O₃ or GST-MDA-7 treated cells.

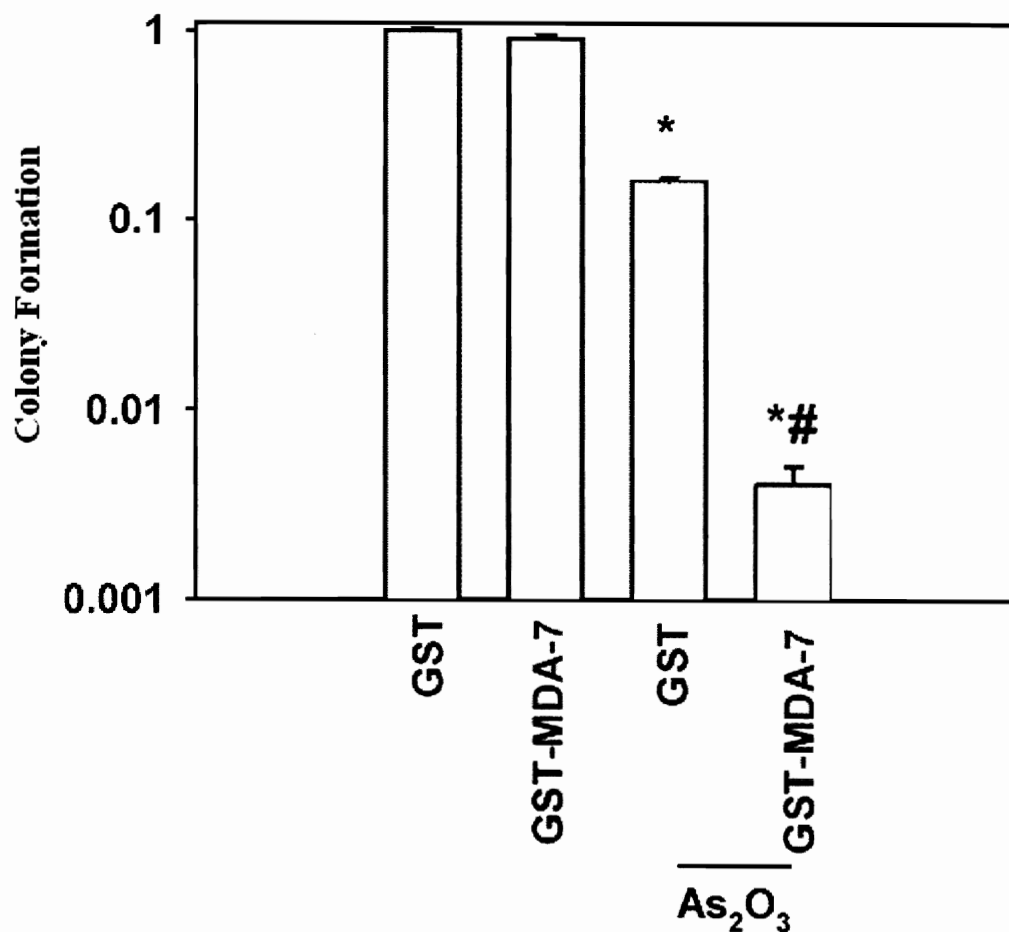


Figure 21. GST-MDA-7 (0.5 nM) and arsenic trioxide (0.5 μ M) interact in a greater than additive fashion to reduce colony formation ability in the UOK121N renal carcinoma cell line. Colony formation assay data values are the means of 3 separate experiments (\pm SEM). * $p < 0.05$ less than control cells; # $p < 0.05$ less than As₂O₃ or GST-MDA-7 treated cells.

3.1.3 N-acetyl cysteine reduces cell killing.

As previously stated above, arsenic trioxide in other cell systems can enhance cell killing by the generation of free radicals. The effects of N-acetyl cysteine, a free radical scavenger, were therefore investigated in our system. Wright Giemsa staining assays revealed that a 1 hour pre-treatment with 10 mM N-acetyl cysteine significantly reduced cell killing in both RCC lines treated with GST-MDA-7 (0.5 nM), arsenic trioxide (0.5 μ M), or the combination, as shown in Figure 22 and 23.

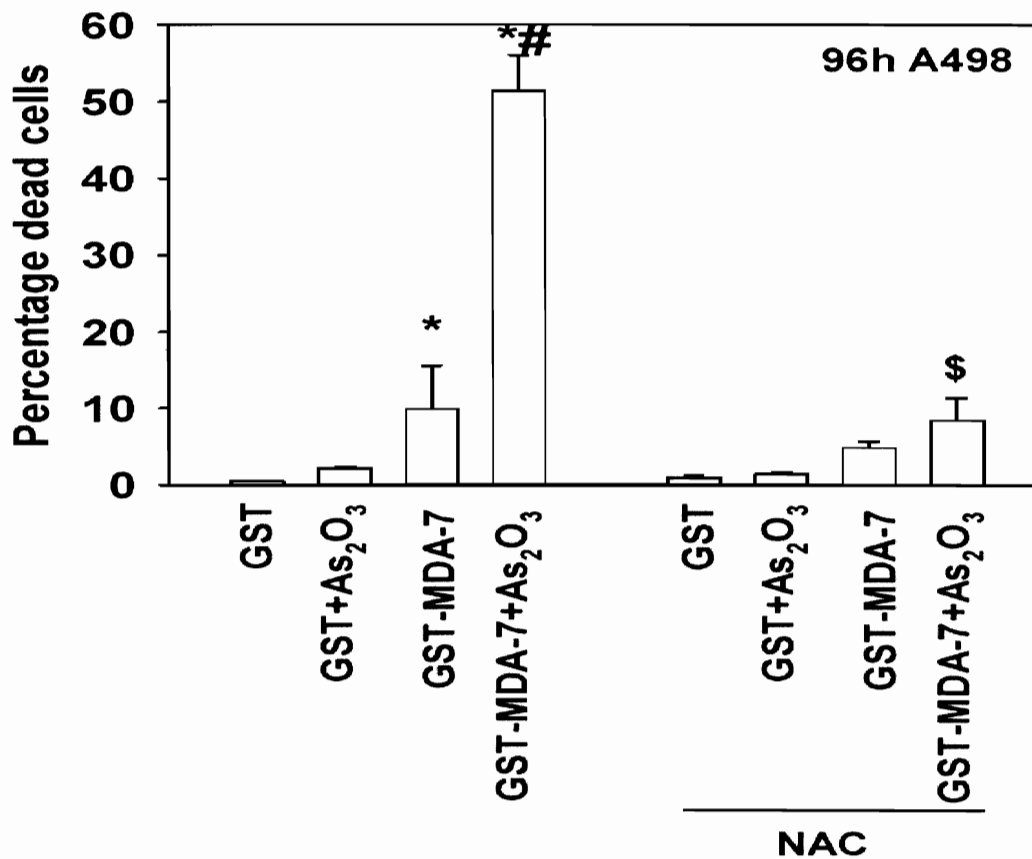


Figure 22. GST-MDA-7 and arsenic trioxide interact in a greater than additive fashion to enhance A498 renal carcinoma cell killing. The effect of arsenic trioxide was blocked by 1 hour pretreatment with the 10 mM N-acetyl cysteine (NAC), a known free radical scavenger. Wright Giemsa assay data are the means of 6 wells (one plate per condition, \pm SEM) from a representative experiment using different preparations of GST and GST-MDA-7 (n = 3). * p < 0.05 greater than GST value cells; # p < 0.05 greater than corresponding GST-MDA-7 value without As₂O₃ co-treatment; \$ p < 0.05 less than value in cells not incubated with NAC.

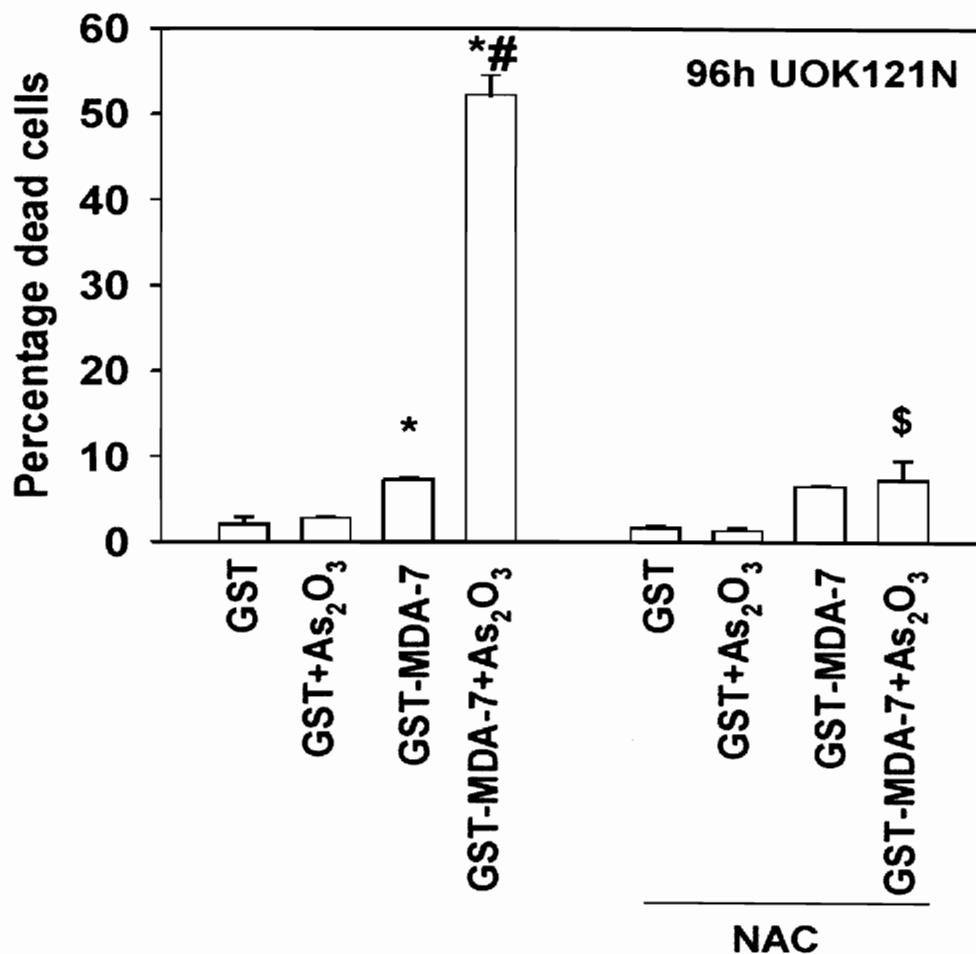


Figure 23. GST-MDA-7 and arsenic trioxide interact in a greater than additive fashion to enhance UOK121N renal carcinoma cell killing. The effect of arsenic trioxide was blocked by 1 hour pretreatment with the 10 mM N-acetyl cysteine (NAC), a known free radical scavenger. Wright Giemsa assay data are the means of 6 wells (one plate per condition, \pm SEM) from a representative experiment using different preparations of GST and GST-MDA-7 (n = 3). * p < 0.05 greater than GST value cells; # p < 0.05 greater than corresponding GST-MDA-7 value without As₂O₃ co-treatment; § p < 0.05 less than value in cells not incubated with NAC.

3.1.4 Protein expression in response to GST-MDA-7 and As₂O₃

Although treatment with GST-MDA-7 and arsenic trioxide induced minimal levels of “classical” apoptosis, western blot analysis revealed the cleavage of both p32 pro-caspase 3 and PARP (Poly (ADP-ribose) polymerase), as well as a reduced level in Bcl-X_L expression, as shown in Figure 24. It has been previously established that MDA-7 radiosensitizes lung cancer cells by the activation of the JNK1/2 pathway (c-Jun NH₂-terminal kinase), and it has also been found to kill melanoma cell lines by the activation of the p38 pathway (Kawabe et al. 2002, Sarker et al. 2002). In the RCC lines, it was found that GST-MDA-7 induced growth arrest correlated with the activation of ERK1/2 and p38 pathways. Cell death induced by the combination of GST-MDA-7 and arsenic trioxide correlated with the activation of JNK1/2 and p38, and with the reduction of ERK1/2 phosphorylation, as shown in Figure 25. In all figures, β-Actin serves as the loading control, and total ERK2 provides a basal ERK2 level.

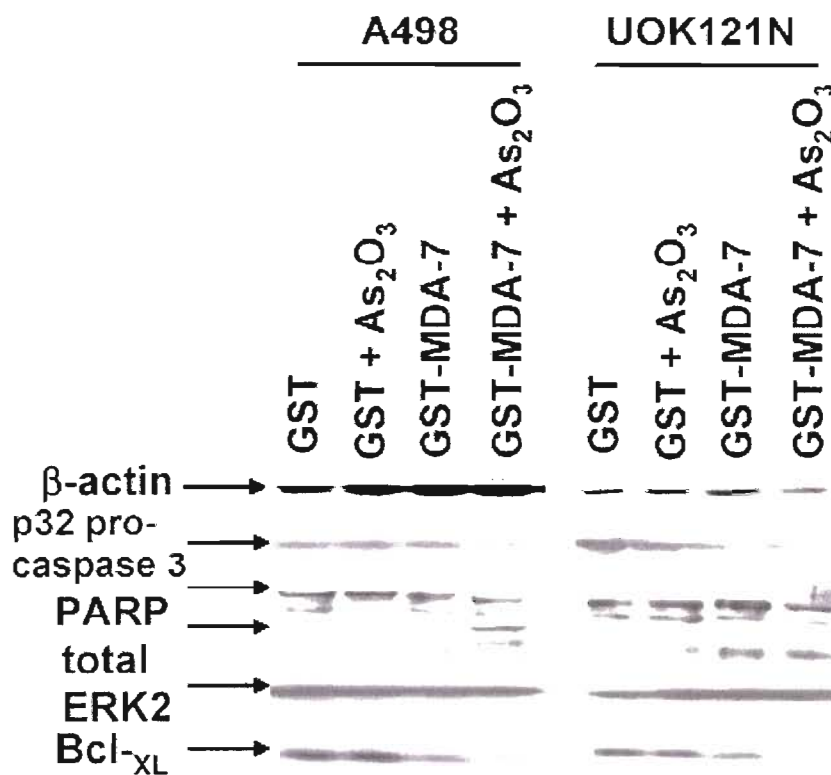


Figure 24. GST-MDA-7 and arsenic trioxide interact to enhance cleavage of pro-caspase 3 and PARP in renal carcinoma cells that correlates with reduced expression of Bcl-_{XL} and enhanced activity of p38 and JNK1/2. Cells were plated in 100 mm plates ($\sim 2 \times 10^5$ cells / well) and 24 hours later treated with GST, GST-MDA-7 (both 0.5 nM) and As₂O₃ (0.5 μ M) as indicated. Cells were isolated 96h after GST-MDA-7 treatment. Data are from a representative experiment (n = 3).

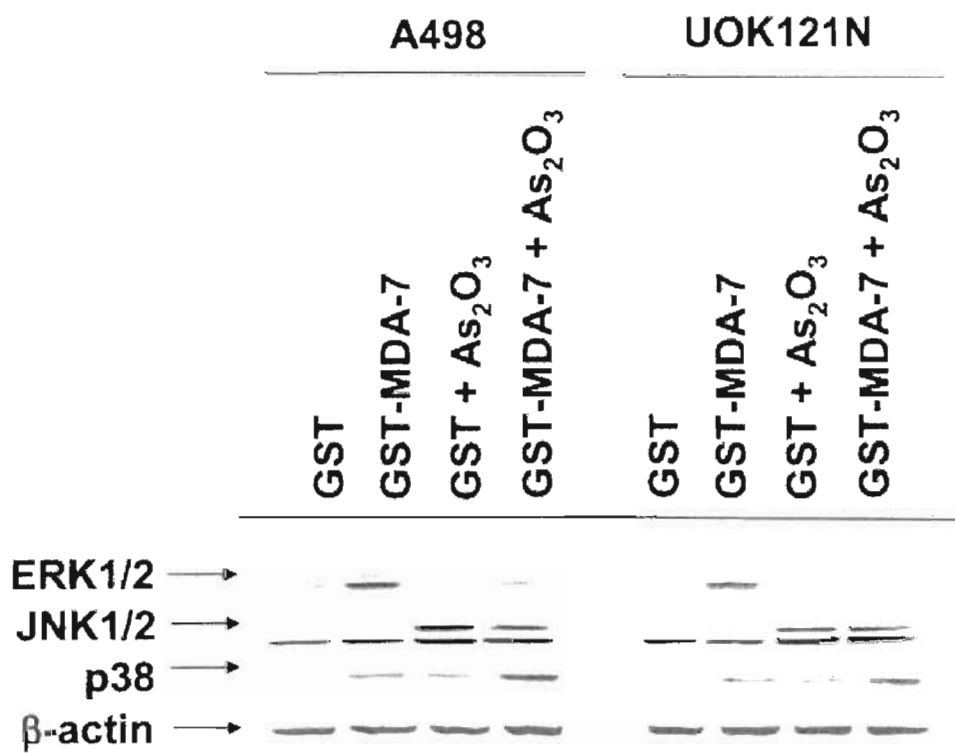


Figure 25. ERK1/2, JNK1/2 and p38 activity in both the A498 and UOK121N RCC lines. Cells were plated in 100 mm plates ($\sim 2 \times 10^5$ cells / well) and 24 hours later treated with GST, GST-MDA-7 (both 0.5 nM) and As₂O₃ (0.5 μ M) as indicated. Cells were isolated 96h after GST-MDA-7 treatment. Data are from a representative experiment (n = 3).

3.1.5 Alterations in nuclear DNA integrity in response to GST-MDA-7 and As₂O₃

A near complete nucleosomal DNA degradation was observed after combined treatment with both GST-MDA-7 and arsenic trioxide for 96 hours, as shown in Figure 26. This degradation, as well as the minute presence of “classical” apoptotic morphology, suggests the RCC lines experienced a necrotic form of cell death in response to the combination of these two agents.

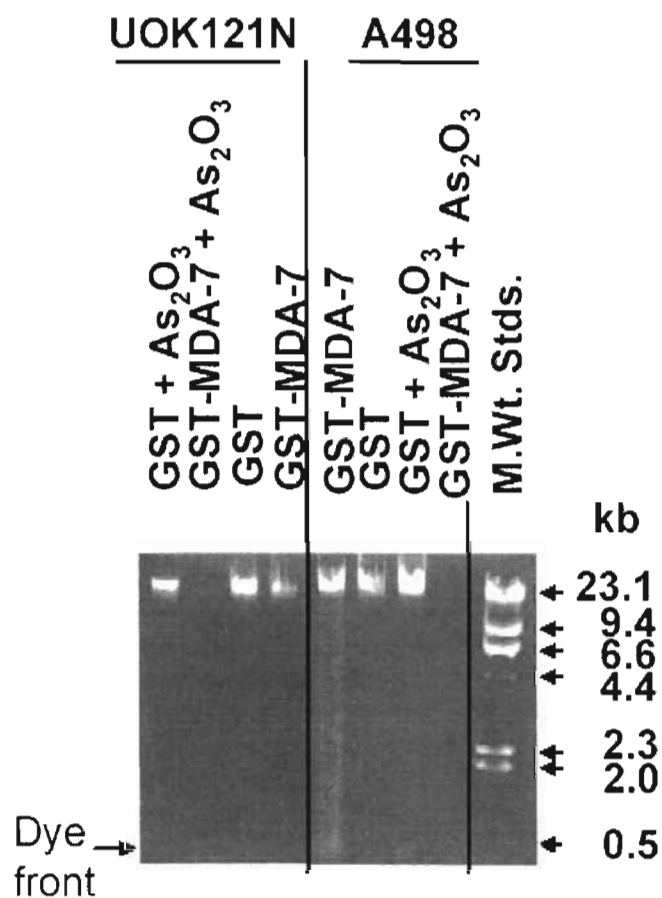


Figure 26. Nucleosomal DNA integrity in the RCC lines. Cells were plated in 100 mm plates ($\sim 2 \times 10^5$ cells / well) and 24 hours later treated with GST, GST-MDA-7 (both 0.5 nM) and As₂O₃ (0.5 μ M) as indicated. Agarose gel analysis performed as described in Materials and Methods. Data are from a representative experiment (n = 3).

3.1.6 Summary of findings in renal cell carcinoma (RCC)

These findings indicate that MDA-7 has a significant impact on RCC proliferation and survival. The RCC lines A498 and UOK121N, but not primary renal epithelial cells, were found to be resistant to adenoviral infection due to a lack of coxsackievirus and adenovirus receptor expression that correlated with previous findings (Haviv et al. 2002). These studies were therefore performed using purified preparations of bacterially synthesized GST-MDA-7 protein. GST-MDA-7, but not GST, was found to cause a dose-dependent inhibition of RCC proliferation, but had no effect on primary renal epithelial cells. Clinically achievable concentrations of the novel therapeutic agent arsenic trioxide (0.5 – 1.0 μ M) were found to have little effect on RCC growth. The combination of GST-MDA-7 and arsenic trioxide, however, resulted in a greater than additive reduction in cell growth that correlated with a large increase in tumor cell death. Also, the free radical scavenger N-acetyl cysteine abolished the effect of arsenic trioxide. Despite the fact that Bcl-X_L, pro-caspase 3, PARP and nucleosomal DNA integrity were reduced by the combined treatment, cell death was predominantly non-apoptotic. The combined treatment of GST-MDA-7 and arsenic trioxide also resulted in a substantial reduction in clonogenic survival when compared to either treatment individually. These above said findings support the conclusion that the MDA-7 protein, in combination with agents that generate free radicals, may have a potential in the treatment of renal cell carcinoma.

3.2.1 Ad.*mda-7* enhances the radiosensitivity of glioma cells.

As mentioned above, numerous studies have shown that infection of tumor cells, but not non-transformed cells, with Ad.*mda-7* inhibits tumor cell growth. In order to assess the effect of Ad.*mda-7* (25 m.o.i.) and radiation exposure on the growth and survival of RT2, U251, and U373 glioma cells, MTT assays were utilized to examine cell proliferation, colony formation assays to examine cell survival (5 m.o.i.), and trypan blue staining to assess cell viability. Cells were plated, infected, irradiated 24 hours after infection with increasing radiation doses, and examined utilizing the methods mentioned above. The results of which are shown below in Figures 27-30. It was found that radiation reduced proliferation and interacted with Ad.*mda-7*, but not Ad.*cmv*, to further reduce cell growth. These effects were not observed in either primary rodent or human astrocytes, as shown previously (Yacoub et al. 2003).

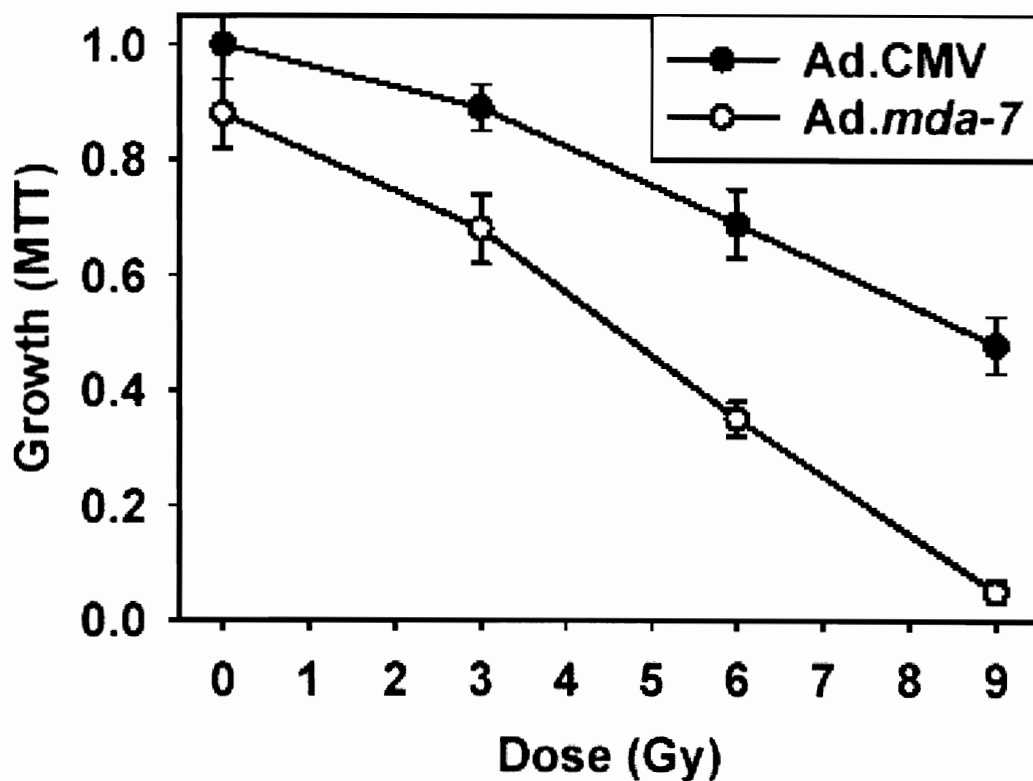


Figure 27. *Ad.mda-7* suppresses RT2 cell growth and enhances radiosensitivity. Glioma cells were cultured for 24 hours after plating then infected with *Ad.mda-7* or *Ad.cmv* at 25 m.o.i. The cells were irradiated, as indicated, 24 hours after infection. The values were normalized to the control nonirradiated cells, which is defined as 1.00. MTT assays were performed as described in Materials and Methods. MTT data are the means of 12 data points +/- SEM from a representative experiment (n = 3).

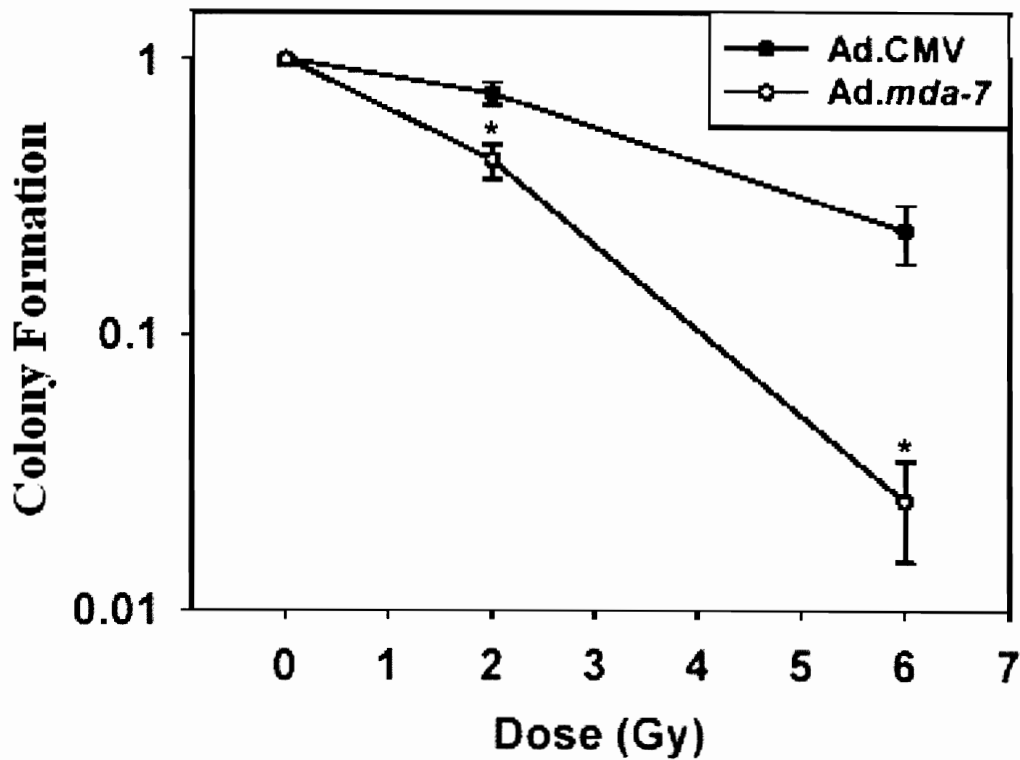


Figure 28. *Ad.mda-7* suppresses RT2 colony formation and enhances radiosensitivity.

Glioma cells were cultured for 24 hours after plating then infected with *Ad.mda-7* or *Ad.cmv* at 5 m.o.i. The cells were irradiated, as indicated, 24 hours after infection. The values were normalized to the control unirradiated cells, which is defined as 1.00.

Colony formation assays were performed as described in Materials and Methods. Colony data are the means of 12 data points \pm SEM from a representative experiment ($n = 3$), * $p < 0.05$ less than corresponding CMV value.

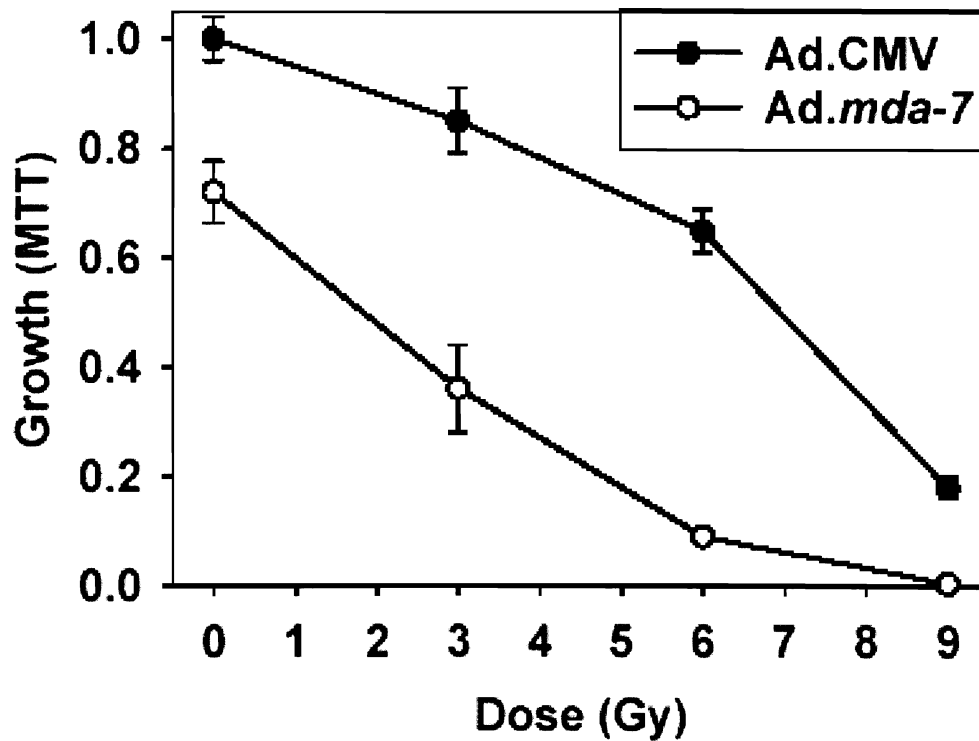


Figure 29. *Ad.mda-7* suppresses U251 cell growth and enhances radiosensitivity.

Glioma cells were cultured for 24 hours after plating then infected with *Ad.mda-7* or *Ad.cmv* at 25 m.o.i. The cells were irradiated, as indicated, 24 hours after infection. The values were normalized to the control unirradiated cells, which is defined as 1.00. MTT assays were performed as described in Materials and Methods. MTT data are the means of 12 data points +/- SEM from a representative experiment (n = 3).

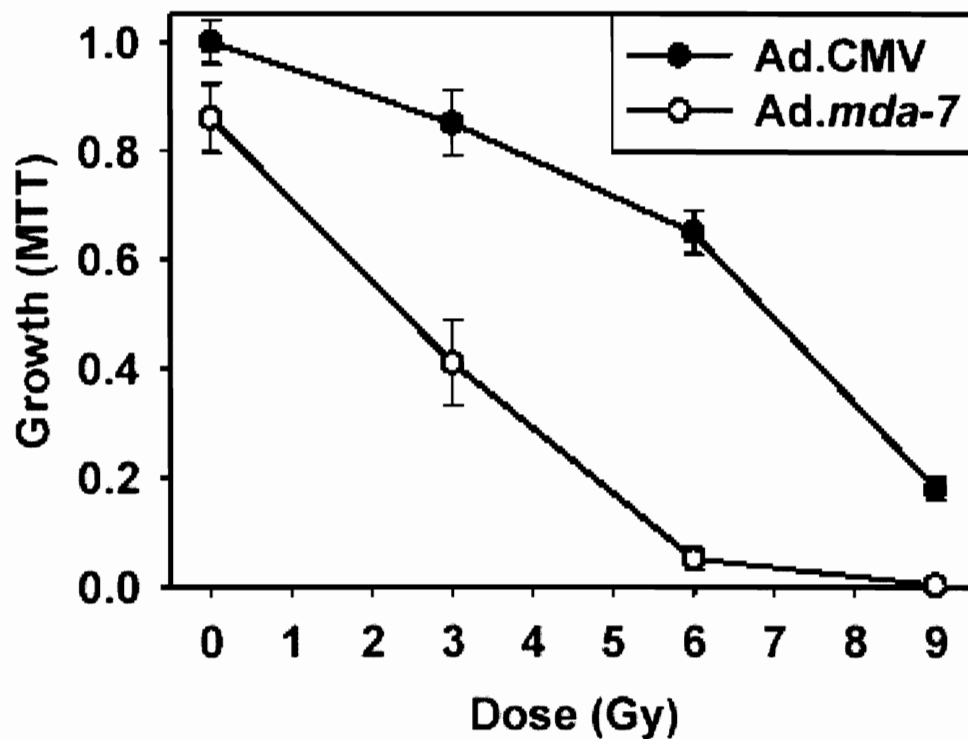


Figure 30. *Ad.mda-7* suppresses U373 cell growth and enhances radiosensitivity.

Glioma cells were cultured for 24 hours after plating then infected with *Ad.mda-7* or *Ad.cmv* at 25 m.o.i. The cells were irradiated, as indicated, 24 hours after infection. The values were normalized to the control unirradiated cells, which is defined as 1.00. MTT assays were performed as described in Materials and Methods. MTT data are the means of 12 data points +/- SEM from a representative experiment (n = 3).

In agreement with the findings presented above, *Ad.mda-7* enhanced cell death, as judged by trypan blue staining, that was significantly increased following radiation exposure, as shown below in Figure 31. This effect was not observed in primary rodent astrocytes (Yacoub et al. 2003). As an additional separate measure of cell survival, the integrity of poly-ADP ribosyl polymerase (PARP), p32 pro-caspase 3, and nuclear DNA, 96 hours after irradiation / 120 hours after viral infection was investigated. Irradiation and/or infection of cells with control virus did not significantly alter PARP, pro-caspase 3, and DNA integrity, as shown below in Figure 32. However, infection of cells with *Ad.mda-7* caused cleavage of PARP and pro-caspase 3 and the appearance of a smear of lower molecular weight DNA, suggestive of a necrotic mode of cell death (Yacoub et al. 2003).

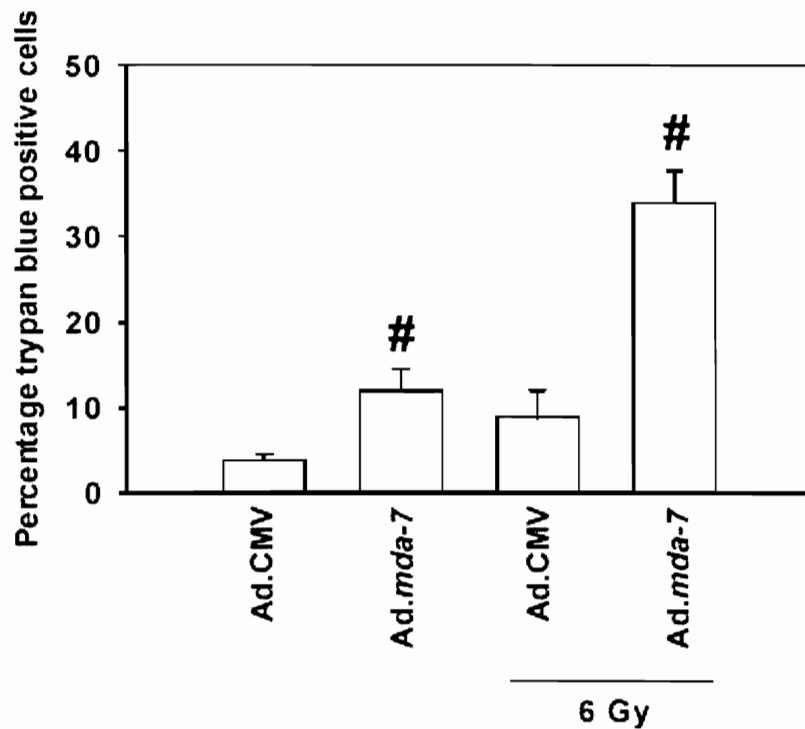


Figure 31. *Ad.mda-7* causes an increase in RT2 cell death that is enhanced in a greater than additive fashion by ionizing radiation. Cells were cultured for 24 hours then infected with *Ad.mda-7* or *Ad.cmv* (25 m.o.i.) as described in Materials and Methods. The cells were irradiated (6 Gy) 24 hours after infection. Cells were isolated 96 hours after irradiation and cell viability determined by trypan blue exclusion staining and by Wright Giemsa staining of fixed cells. Data are the means of \pm SEM from a representative experiment ($n = 3$), # $p < 0.05$ greater than corresponding *Ad.cmv* infected cells.



Figure 32. Expression and integrity of PARP and p32 pro-caspase 3 in RT2 cells (25 m.o.i.). Cells were cultured for 24 hours then infected with *Ad.mda-7* or *Ad.cmv* (25 m.o.i.) as described in Materials and Methods. The cells were irradiated (6 Gy) 24 hours after infection. Cells were isolated 96 hours after irradiation and protein samples obtained as described in Materials and Methods. Data are from a representative experiment (n = 3).

The reduction in proliferation caused by *Ad.mda-7* was further examined in RT2 and U251 cells. In RT2 cells, *Ad.mda-7* enhanced cell numbers in G₁ phase that was further increased after irradiation, as shown below in Figure 33. This correlated with enhanced p21 and p53 expression as shown in Figure 34. In contrast however, U251 cells exposed to *Ad.mda-7* experienced enhanced cell numbers in G₂/M phase of the cell cycle that was further increased following radiation exposure (Figure 35) and experienced no alteration in the expression of p53 and p21. It was also found that cell numbers in S phase significantly decreased in both cell types following combined *Ad.mda-7* and radiation treatment.

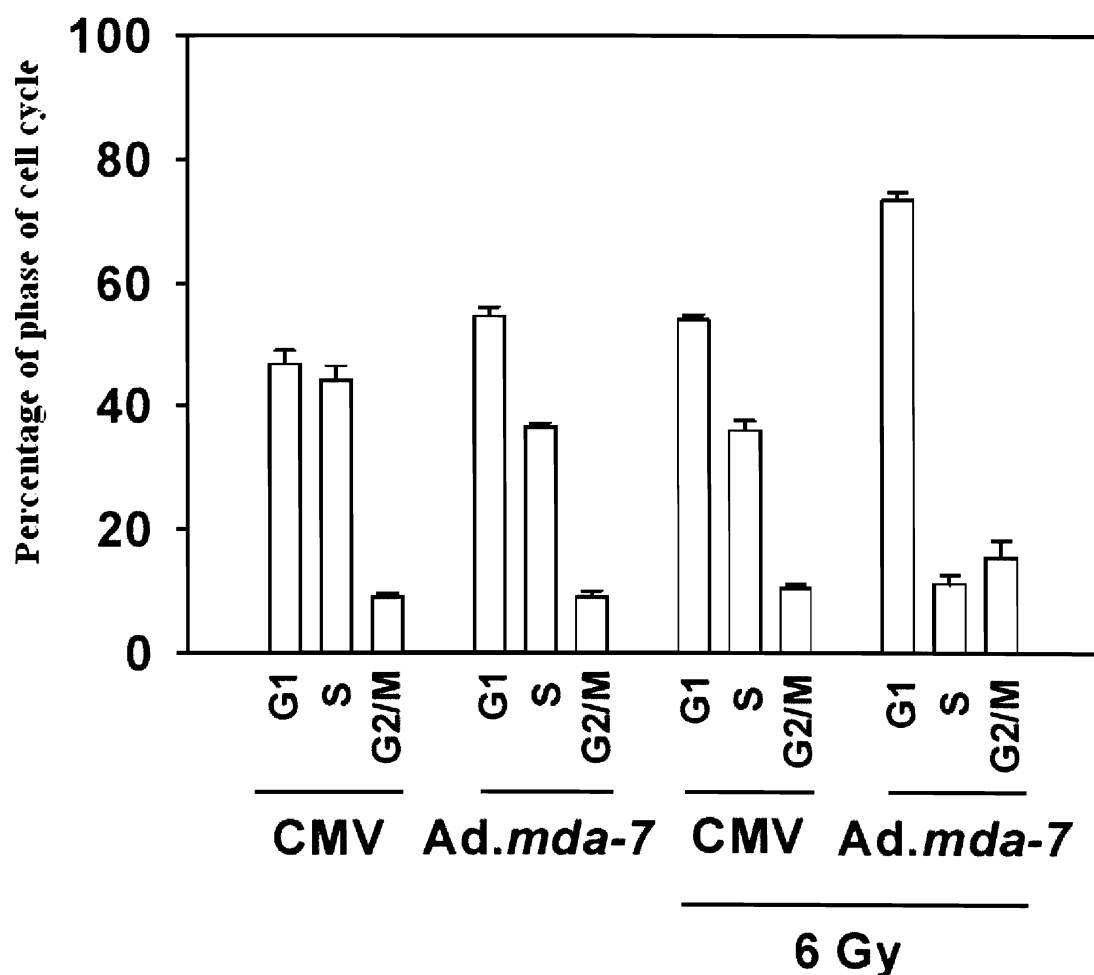


Figure 33. The combination of *Ad.mda-7* and radiation enhance RT2 cell numbers in G₁ phase and reduced numbers in S phase. Cells were cultured for 24 hours, then infected with *Ad.mda-7* or *Ad.cmv* at 25 m.o.i. The cells were irradiated (6 Gy) 24 hours after infection. Cells were isolated 24 hours after irradiation and the cell cycle distribution under each condition determined as described in Materials and Methods. Data are the means + / - SEM of three separate experiments.

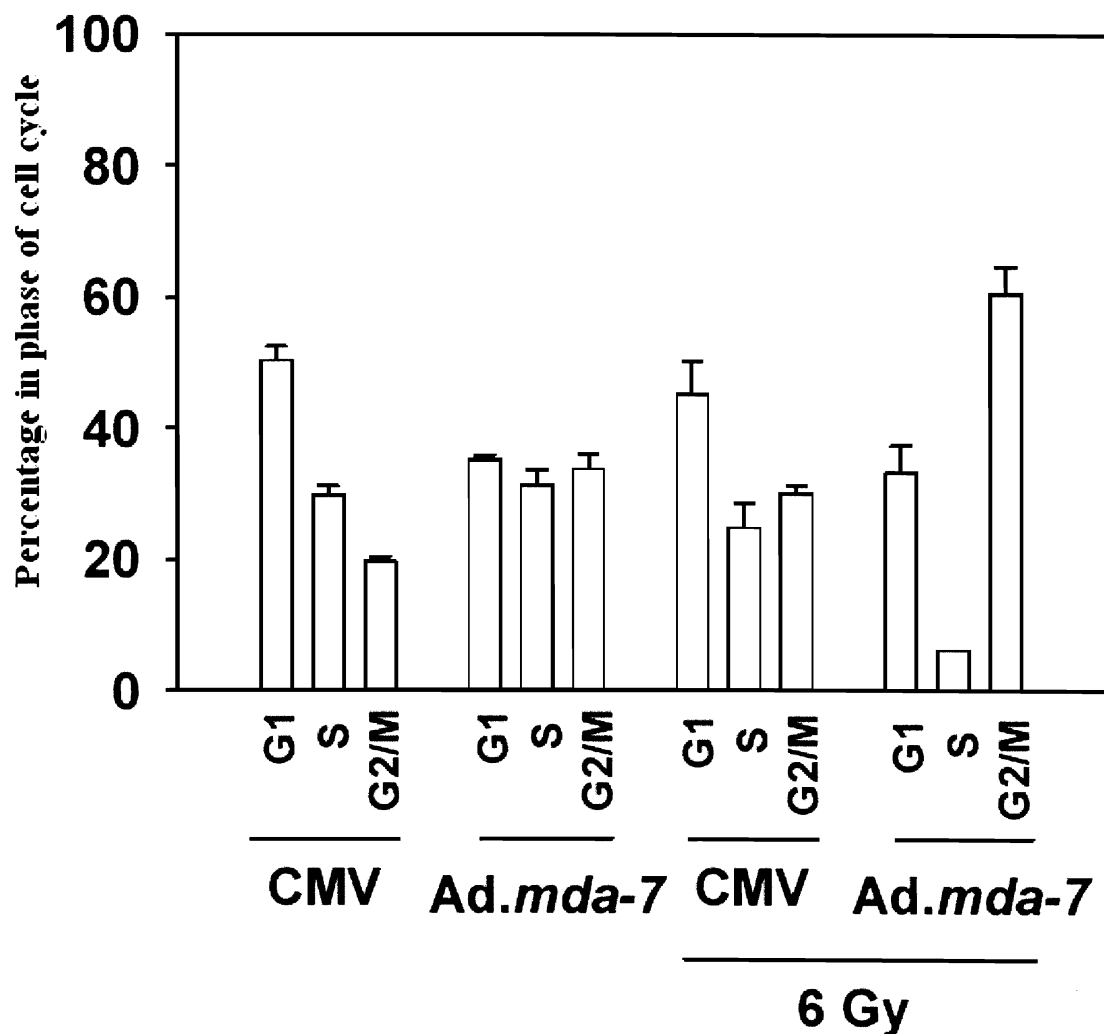


Figure 34. The combination of *Ad.mda-7* and radiation enhance U251 cell numbers in G₂/M phase and reduced cell numbers in S phase. Cells were cultured for 24 hours, then infected with *Ad.mda-7* or *Ad.cmv* at 25 m.o.i. The cells were irradiated (6 Gy) 24 hours after infection. Cells were isolated 24 hours after irradiation and the cell cycle distribution under each condition determined as described in Materials and Methods. Data are the means + / - SEM of three separate experiments.

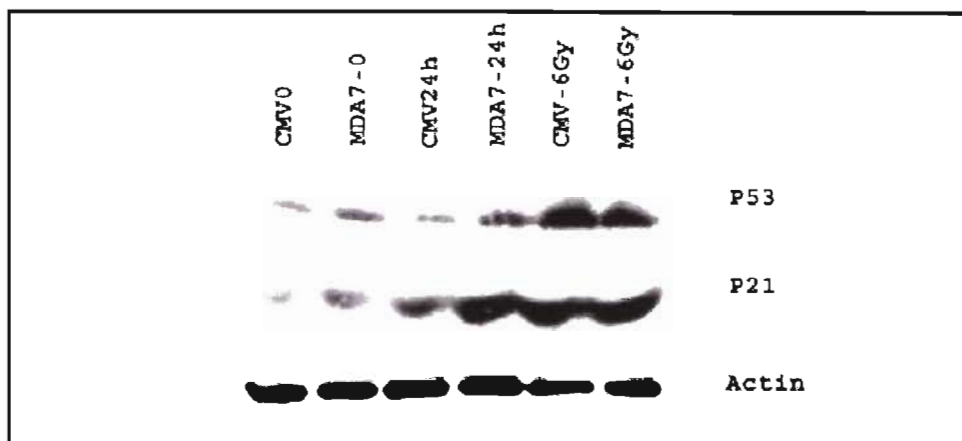


Figure 35. Expression of p21 and p53 in RT2 cells under each treatment condition. The combination of *Ad.mda-7* and radiation enhance RT2 cell numbers in G₁ phase. Cells were cultured for 24 hours, then infected with *Ad.mda-7* or *Ad.cmv* at 25 m.o.i. The cells were irradiated (6 Gy) 24 hours after infection. Protein samples were obtained 24 hours after irradiation as described in Materials and Methods. Data shown is from a representative experiment (n = 3).

3.2.2 *Ad.mda-7* enhances ERK1/2 and p38 activity, not JNK1/2 and AKT, in RT2

Recent studies have linked MDA-7-induced cell killing to activation of the p38 and JNK1/2 pathways (Kawabe et al. 2002, Sarkar et al. 2002). JNK1/2 signaling has also been proposed as the mechanism by which *Ad.mda-7* radiosensitizes lung carcinoma cells (Kawabe et al. 2002). Based on these findings, further studies investigated whether *Ad.mda-7* and radiation interacted to alter the activities of ERK1/2, JNK1/2, p38 and AKT in RT2 cells. Infection with *Ad.mda-7* enhanced the activity of p38 and ERK1/2, but not of JNK1/2 or AKT (Figure 36). In contrast with previous research, radiation reduced *Ad.mda-7*-induced ERK1/2 activity 96 hours after exposure, but had no effect on either p38 or AKT activity. However, while *Ad.mda-7* did not alter basal JNK1/2 activity, JNK1/2 phosphorylation was significantly enhanced following irradiation after *Ad.mda-7* infection.

Signaling by the PI3K/AKT and ERK1/2 MAPK pathways have been linked to enhanced radioresistance and survival to chemotherapy (Cartee et al. 2000, Xia et al. 1995, Dent et al. 1999, Sarkar et al. 2002, Hagan et al. 2000, Yacoub et al. 2001, Gupta et al. 2002, and Vlahos et al. 1994). To investigate the roles of these pathways in resistance to MDA-7-induced cell killing, cells were infected with *Ad.mda-7* and then incubated with the MEK1/2 inhibitor PD98059 and/or the PI3K inhibitor LY294002. Neither the inhibition MEK1/2 or PI3K enhanced the anti-proliferative effects of *Ad.mda-7*, as shown below in

Figure 36. The combined inhibition of both pathways, however, resulted in a significant additional reduction in proliferation (Figure 37) and cell survival (Figures 38 and 39).

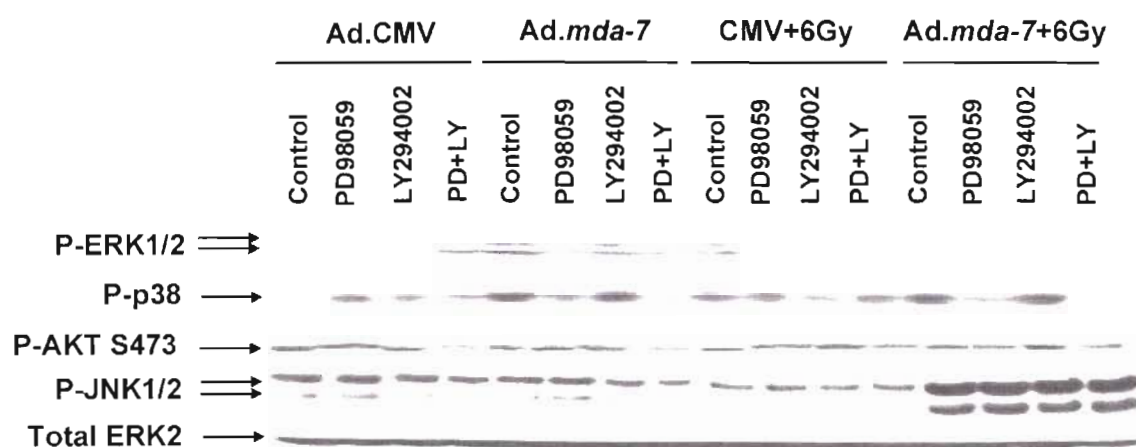


Figure 36. *Ad.mda-7* enhances p38 and ERK1/2 activity, but not that of AKT or JNK1/2, in RT2 cells: radiation abolishes *Ad.mda-7*-induced ERK1/2 activity and enhances *Ad.mda-7*-dependent JNK1/2 activity. Cells were cultured for 24 hours, then infected with *Ad.mda-7* or *Ad.cmv* (25 m.o.i.) as described in Materials and Methods. Cells were incubated for an additional 24 hours then treated with either 10 μ m PD98059, 5 μ m LY294002, or both drugs in combination: 30 min later the cells were irradiated (6 Gy). After irradiation (96 hours), the cells were harvested and protein samples obtained as described in Material and Methods. Immunoblotting data are from a representative experiment (n = 3).

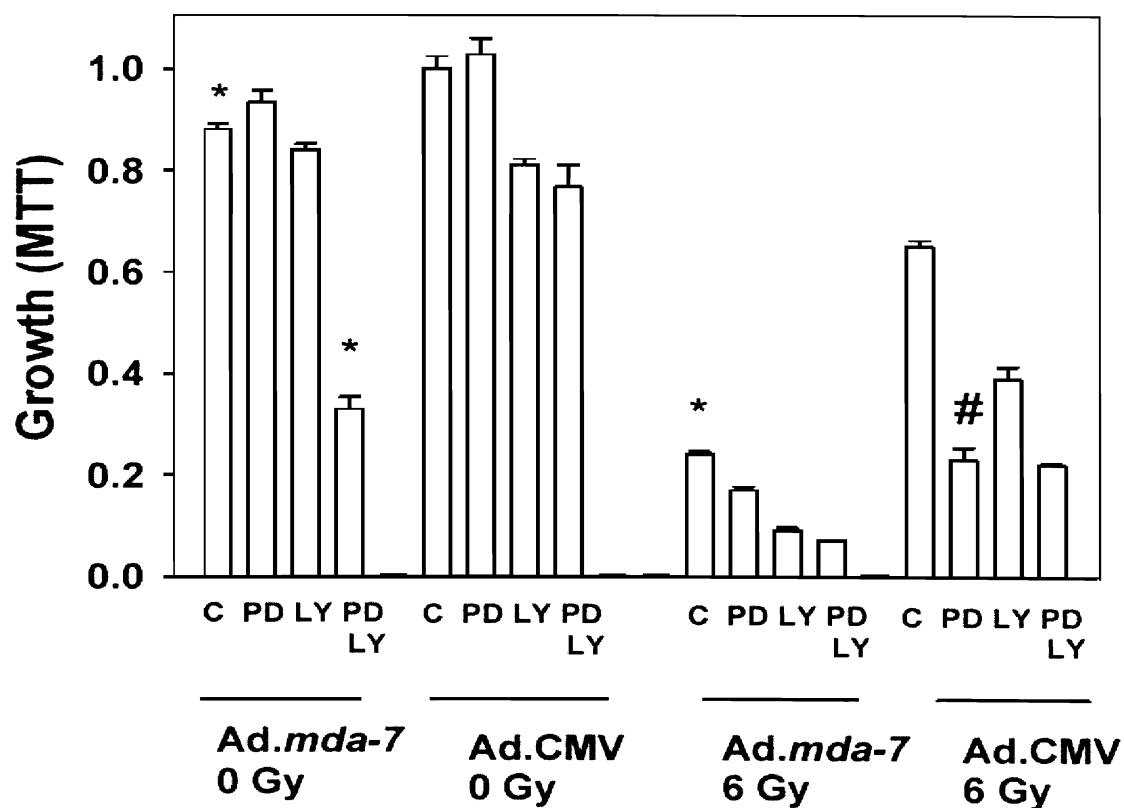


Figure 37. The anti-proliferative effect of *Ad.mda-7* is enhanced by combined inhibition of MEK1/2 and PI3K, in RT2 cells. Cells were cultured for 24 hours, then infected with *Ad.mda-7* or *Ad.cmv* (25 m.o.i.) as described in Materials and Methods. Cells were incubated for an additional 24 hours, then treated with either 10 μ m PD98059, 5 μ m LY294002, or both drugs in combination: 30 min later the cells were irradiated (6 Gy). MTT assays were performed 96 hours after irradiation as described in Material and Methods. MTT data are the means \pm SEM of three experiments, # $p < 0.05$ less than control treated cells, * $p < 0.05$ less than corresponding value in cells not infected with *Ad.mda-7*.

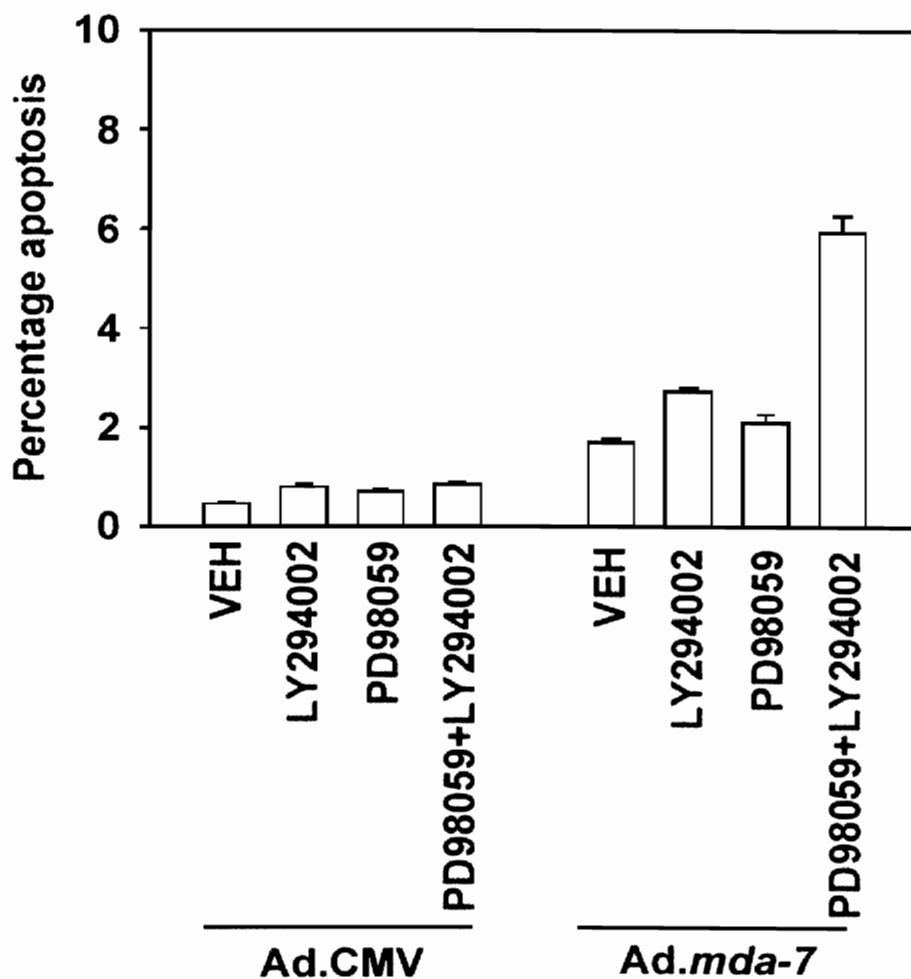


Figure 38. The toxicity of *Ad.mda-7*, as determined by Wright-Giemsa staining of fixed cells, is enhanced by the combined inhibition of MEK1/2 and PI3K, in RT2 cells. Cells were cultured for 24 hours, then infected with *Ad.mda-7* or *Ad.cmv* (25 m.o.i.) as described in Materials and Methods. Cells were incubated for an additional 24 hours then treated with either 10 μ m PD98059, 5 μ m LY294002, or both drugs in combination, and analyzed via Wright-Giemsa staining as described above in Materials and Methods. Data are the means \pm SEM of three separate experiments.

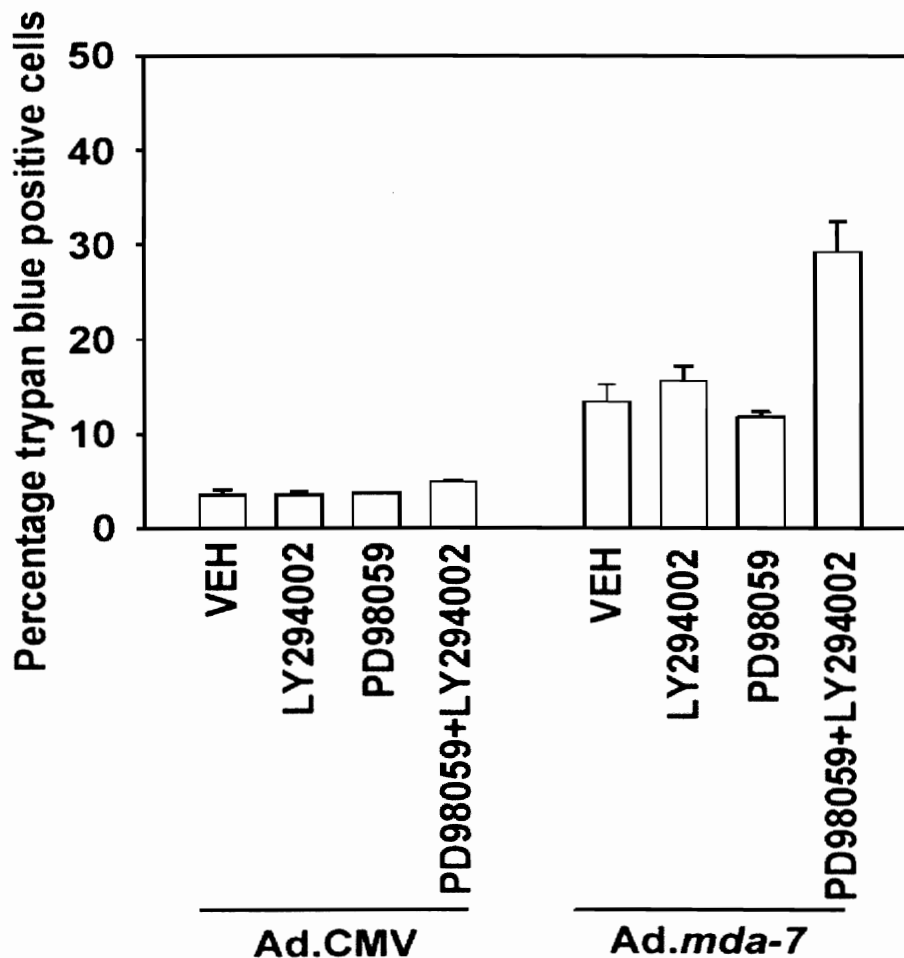


Figure 39. The toxicity of Ad.*mda-7*, as judged by trypan blue exclusion staining of fixed cells, is enhanced by combined inhibition of MEK1/2 and PI3K, in RT2 cells. Cells were cultured for 24 hours, then infected with Ad.*mda-7* or Ad.*cmv* (25 m.o.i.) as described in Materials and Methods. Cells were incubated for an additional 24 hours then treated with either 10 μ m PD98059, 5 μ m LY294002, or both drugs in combination, and counted for trypan blue exclusion as described Materials and Methods. Data are the means + / - SEM of three separate experiments.

3.2.3 Role of p38 and JNK1/2 signaling in glioma radiosensitization

Due to the fact that infection of cells with *Ad.mda-7* activated p38 as well as promoted radiation-induced activation of JNK1/2 in RT2 cells, the role of p38 and JNK1/2 signaling in the radiosensitization effect was investigated. Based on previous studies, it was expected that p38 would play an active role in enhancing the cell killing induced by *Ad.mda-7* and radiation. However, inhibition of p38 signaling via SB203580 (2 μ M) did not alter the radiosensitizing properties of *Ad.mda-7*. In contrast, and in general agreement with the findings of Kawabe et al., use of a relatively specific JNK1/2 inhibitor, SP600125 (10 μ M), abolished the radiosensitizing properties of *Ad.mda-7*, as shown below in Figure 40.

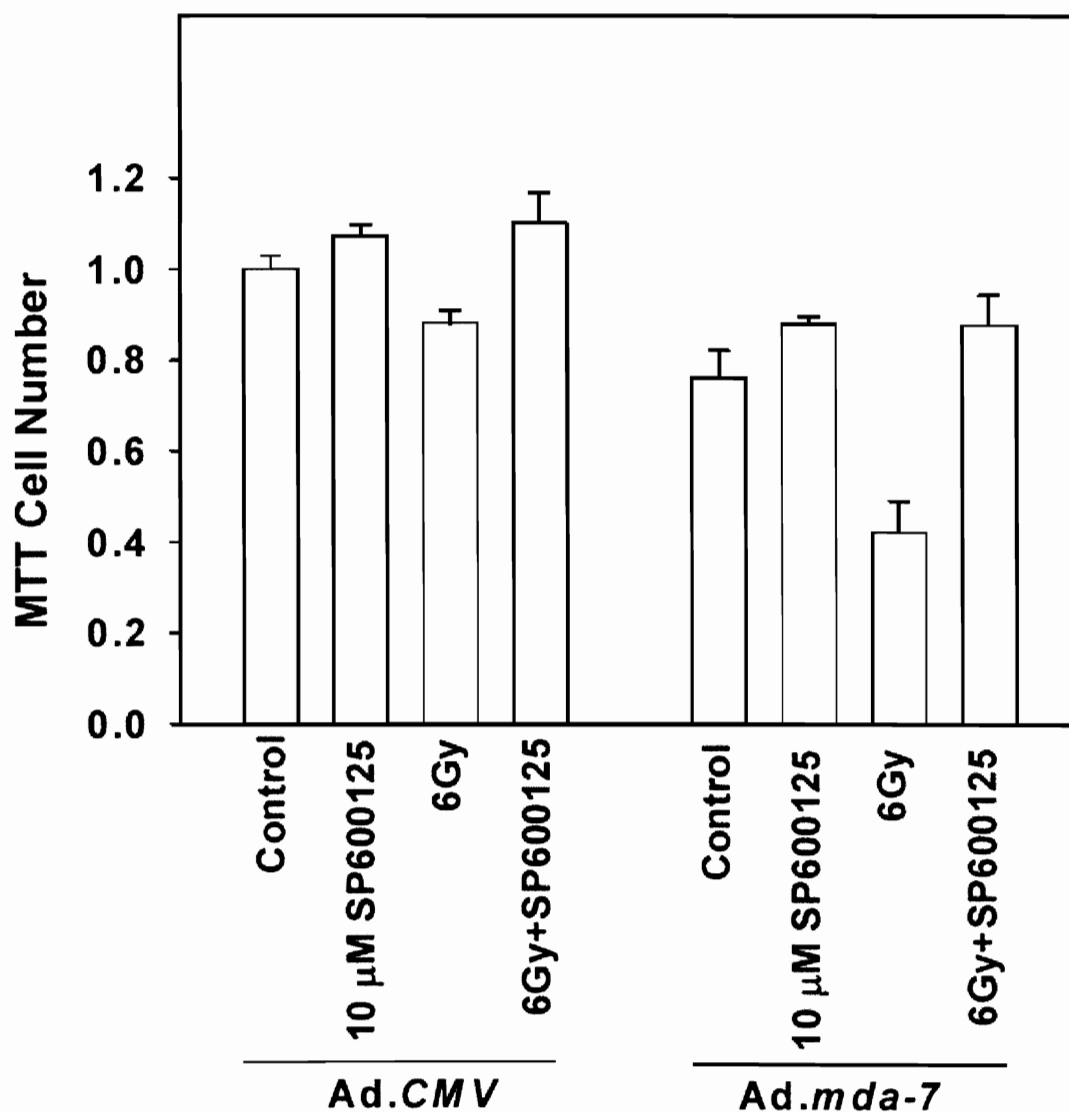


Figure 40. The JNK1/2 inhibitor SP600125 abolished the radiosensitizing effect of *Ad.mda-7*. Cells were cultured for 24 hours, then infected with *Ad.mda-7* or *Ad.cmv* (25 m.o.i.) as described in Materials and Methods. Cells were incubated for an additional 24 hours then treated with either vehicle or 10 μM SP600125 30 minutes prior to irradiation. Growth was determined via MTT assay 96 hours after irradiation as described Materials and Methods. MTT data are the means +/- SEM of four separate experiments.

3.2.4 Ad.*mda-7* infected RT2 cells express a ~23 kDa MDA-7 protein.

It should be mentioned that prior to performing the experiments described above, RT2 cells were infected with increasing amounts of Ad.*mda-7* or Ad.*cmv* control virus and the expression of MDA-7 determined 48 hours after infection as shown in Figure 41. These findings, as well as previously generated data (Su et al. 2003), support the idea that increasing the viral particle multiplicity of infection (m.o.i.) enhances the amount of MDA-7 protein produced in each cell. It was then determined, through western blot analysis, that an m.o.i. of 25 was appropriate to achieve our desired MDA-7 protein expression. Also, previous studies utilizing a recombinant adenovirus to express β -galactosidase were performed to determine the percentage of cells infected at each m.o.i. These findings revealed that infection at an m.o.i. of 25 with a virus to express β -galactosidase caused approximately 20% of RT2 and 5% of U251 cells to stain blue when incubated with X-gal (Yacoub et al. 2003).

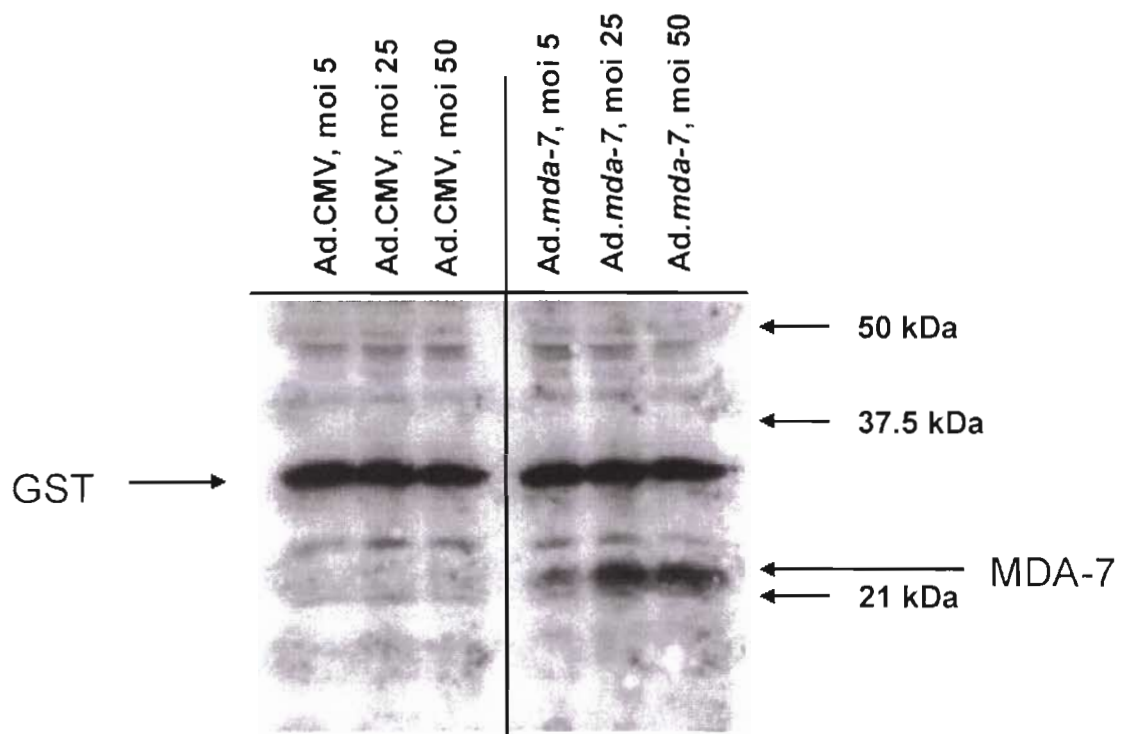


Figure 41. Infection of RT2 cells with *Ad.mda-7* results in the expression of the 23 kDa MDA-7 protein. RT2 cells were cultured for 24 hours, then infected with *Ad.mda-7* or *Ad.cmv* at the indicated m.o.i. as described in Materials and Methods. Cells were harvested 48 hours after infection and protein samples were separated using SDS PAGE. Data shown are from a representative experiment (n = 3).

3.2.5 Summary of findings in glioblastoma multiforme (GBM)

These studies examined the impact of Ad.*mda-7* and ionizing radiation on the proliferation and survival of GBM cells. The findings suggest that Ad.*mda-7* reduced the proliferation of rodent (RT2) and human glioma cells in MTT assays and in colony formation assays. The anti-proliferative effects of Ad.*mda-7* were found to be enhanced by radiation in a greater than additive fashion (synergy). It was also discovered that, *in vitro*, these anti-proliferative effects correlated with an increase in cell numbers in G₁/G₀ and G₂/M phases of the cell cycle, implicating a cell cycle-independent manner of radiosensitization, and that cultures of non-transformed primary astrocytes were immune to these effects. It was also found that Ad.*mda-7* alone did not alter JNK1/2 or AKT activity, but enhanced both p38 and ERK1/2 activity. It was then found that the irradiation of cells expressing the MDA-7 protein did not alter AKT or p38 activity, but caused suppression of ERK1/2 activity and dramatically enhanced JNK1/2 activity. These findings led to experiments involving inhibitors of each MAPK signaling pathway in which it was discovered that inhibition of JNK1/2 (SP600125), but not p38 (SB203580), signaling abolished the deleterious radiosensitizing properties of MDA-7. It was also found that inhibition of neither ERK1/2 (PD98059) nor PI3K (LY294002) signaling enhanced the anti-proliferative effects of Ad.*mda-7*, but the combined inhibition of both pathways significantly enhanced glioma cell killing, suggesting that ERK and PI3K signaling can be protective against MDA-7 lethality. These findings further establish MDA-7 as a potential therapeutic agent in the treatment of GBM.

3.3.1 17-AAG synergizes with bile acid (DCA) to kill primary rat hepatocytes

Geldanamycins are best known for their ability to bind to the ATP-binding site of the amino-terminal domain region of heat shock protein 90 (Hsp90). This abundant protein aids in the folding, assembly, maturation, and stabilization of the client proteins which regulate survival of cancer cells, thus making Hsp90 inhibitors potential molecular targeting agents for cancer therapy (Senju et al. 2006). Bile acids are detergent molecules synthesized from cholesterol in the liver and delivered to the small intestine where they serve as detergents for the absorption of dietary lipids, cholesterol, and fat-soluble vitamins. During intrahepatic cholestasis, which is a common occurrence in patients with hepatocellular carcinoma, bile excretion from the liver is blocked, causing an accumulation of intracellular toxic bile acids, resulting in consecutive cellular damage. This cytotoxic effect has been linked to ROS generation and subsequent mitochondrial dysfunction. This, in combination with the fact that geldanamycins have dose-limiting toxicity due to their actions in promoting liver dysfunction, and that there is little information regarding the effects of 17-AAG on primary rat hepatocyte cultures, is the basis for our investigation into the interactions between 17-AAG and the common secondary bile acid, deoxycholic acid (DCA), typically found at elevated levels in circulation.

Initial studies examined the killing of primary rat hepatocytes exposed for 4h to DCA (50 μ M) and 17-AAG (0.03 – 3.0 μ M) as single agents and in combination. Treatment of

hepatocytes with DCA very weakly promoted cell killing, whereas treatment with 17-AAG at all concentrations promoted a modest to strong induction of cell death (Figure 42). Combined exposure of hepatocytes to 17-AAG and DCA resulted in a significantly greater than additive induction of cell killing above that induced by either agent alone, as judged by Wright-Giemsa assay.

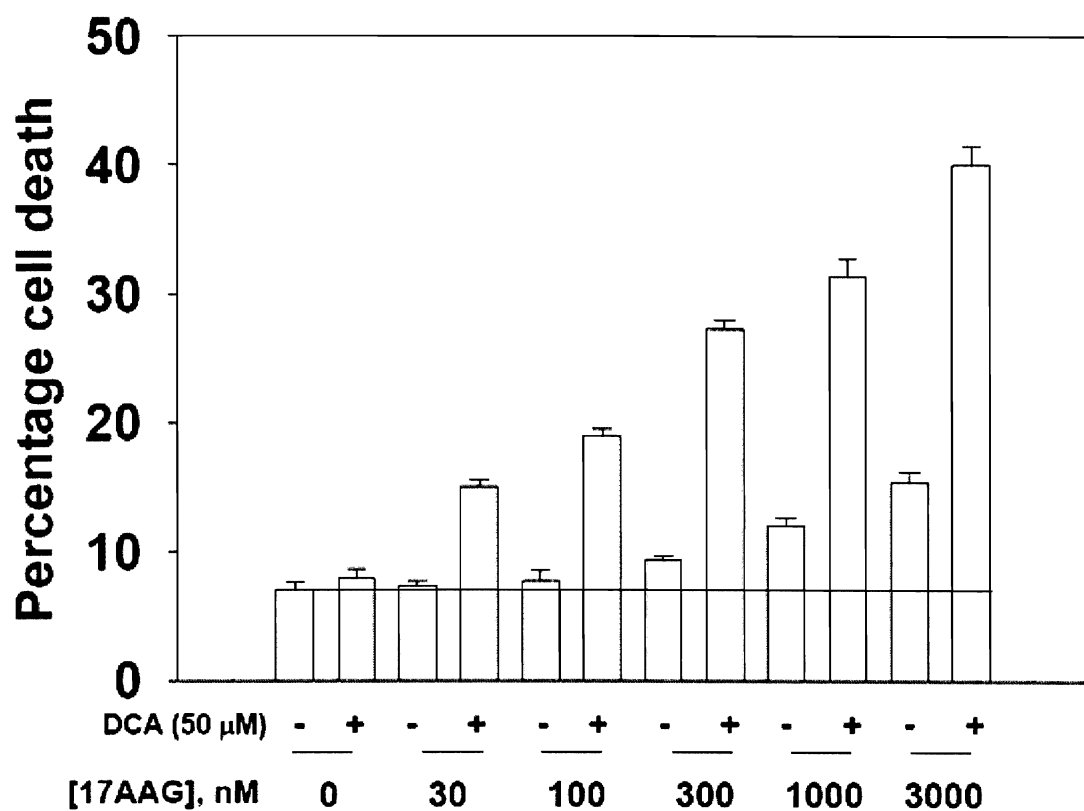


Figure 42. Combined exposure of hepatocytes to 17-AAG and DCA resulted in a greater than additive induction of cell killing above that induced by either agent alone. Cells were cultured in 12-well plates ($\sim 1.5 \times 10^5$ cells per well) for 24 hours as described above in Material and Methods. Cells were then treated with the corresponding concentration of 17-AAG, DCA, or the combination. Cell death was determined 4 h after exposure. Wright-Giemsa assay data are the means \pm SEM of four separate experiments.

3.3.2 Hepatocyte cell death is ROS-dependent

Both DCA and geldanamycins have been shown to induce production of reactive oxygen species (ROS) in primary hepatocytes and in other established cell types (Lai et al. 2003), respectively, and we next examined whether DCA and 17-AAG interacted to modulate ROS levels in hepatocytes. Both DCA and 17-AAG significantly enhanced ROS levels in hepatocytes (Figure 43). Combined DCA and 17-AAG exposure enhanced ROS production above that generated by each agent individually, and in addition, combined treatment with both agents prolonged the duration of ROS production. The production of ROS was suppressed by inclusion of the free radical quenching agents N-acetyl cysteine (NAC) and Trolox. Based on these observations, we then determined whether the elevated levels of ROS production were responsible for the enhanced levels of cell killing. Incubation of hepatocytes with either NAC or Trolox abolished 17-AAG lethality and also the greater than additive induction of cell killing caused by combined DCA and 17-AAG treatment (Figure 44). Of note, and in agreement with these findings, parallel cell survival data were obtained when active and mutated inactive forms of thioredoxin reductase were stably over-expressed in cervical carcinoma (HeLa) cells treated with DCA and 17-AAG (Figure 45).

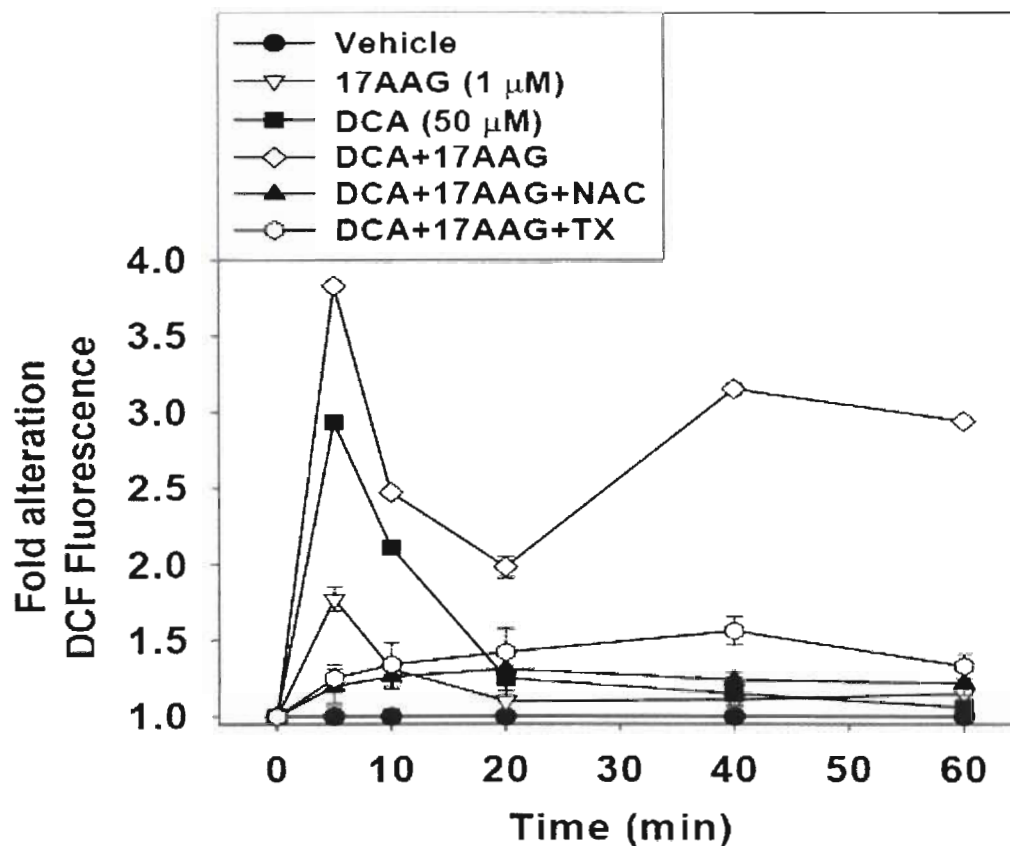


Figure 43. ROS levels generated in hepatocytes. The production of ROS was suppressed by the inclusion of free radical quenching agents N-acetyl cysteine (NAC) and Trolox (TX). Hepatocytes were cultured in 96-well plates (10,000 cells per well) for 24 hours as described above in Material and Methods. Cells were then pre-treated with NAC (20mM) or Trolox (1mM) or vehicle, followed by treatment with the corresponding concentration of 17-AAG (3μM), DCA (50μM), or the combination. ROS generation was determined at the appropriate time intervals. Data are the means \pm SEM of three separate experiments.

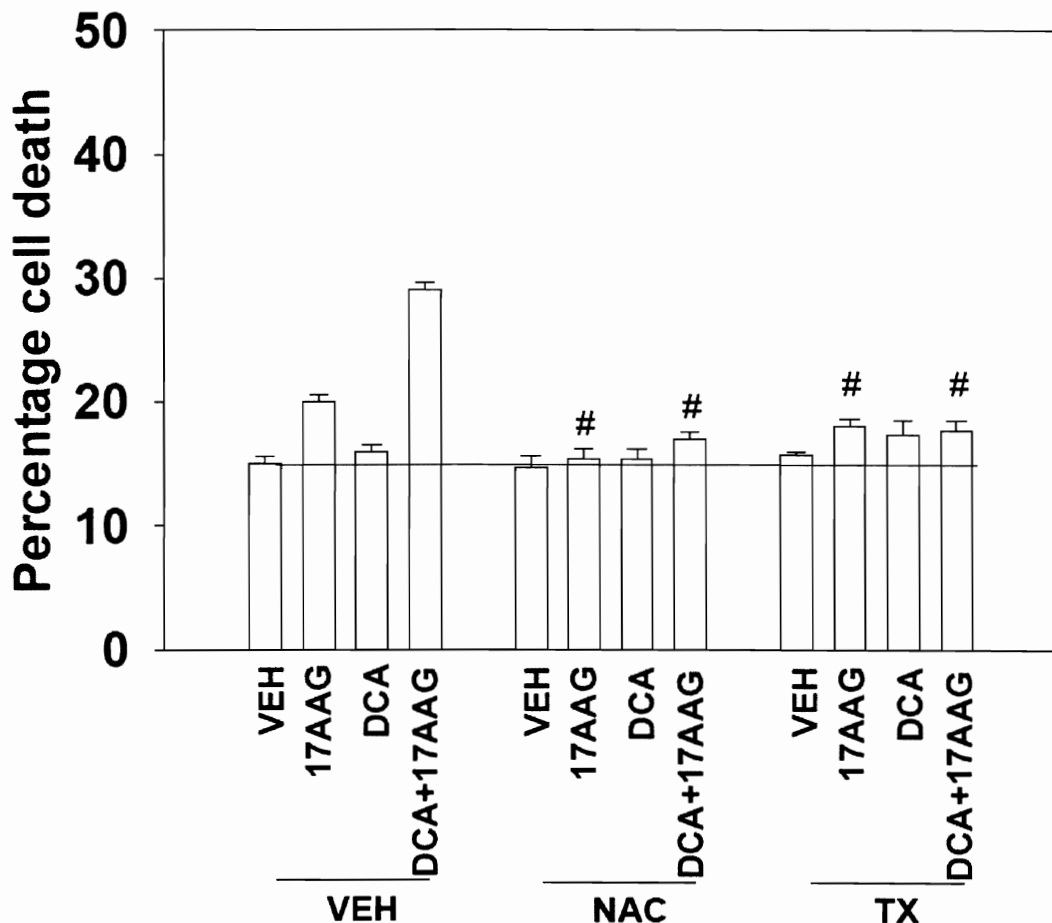


Figure 44. Incubation of hepatocytes with either NAC or Trolox abolished the lethality and also the greater than additive induction of cell killing caused by combined DCA and 17-AAG treatment. Hepatocytes were cultured in 12-well plates ($\sim 1.5 \times 10^5$ cells per well) for 24 hours as described above in Material and Methods. Cells were then pre-treated for 1 hour with NAC (20mM) or Trolox (1mM) or vehicle, followed by treatment with 17-AAG (3 μ M), DCA (50 μ M), or the combination. Cell death was determined 4 hours after exposure. Wright-Giemsa assay data are the means \pm SEM of four separate experiments. # $p < 0.05$ less than corresponding vehicle treatment value.

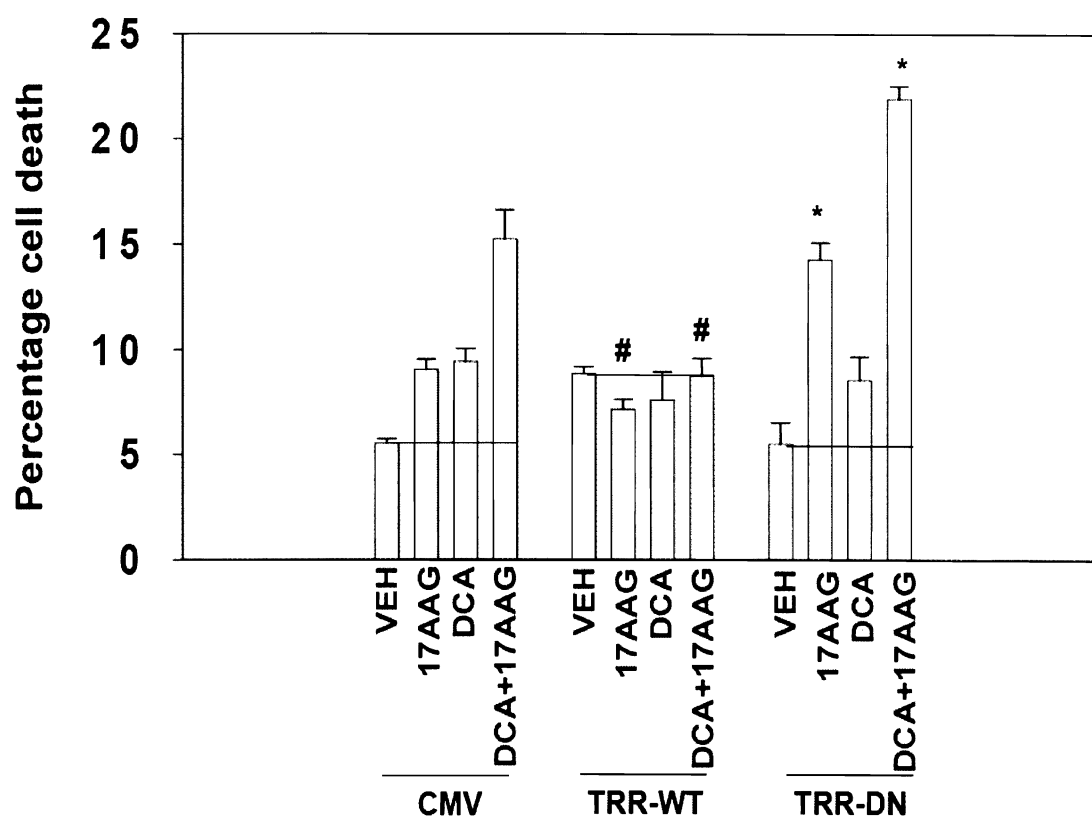


Figure 45. Cell survival data obtained when active and mutated inactive forms of thioredoxin reductase were stably expressed in cervical carcinoma (HeLa) cells and treated with DCA and 17-AAG. HeLa cells were cultured in 12-well plates (25,000 cells per well) for 24 h as described above in Material and Methods. Cells were then exposed to vehicle, DCA (50 μ M), 17-AAG (3 μ M), or the combination. Cell death was determined 4 hours after exposure via Wright-Giemsa assay. Data are the means \pm SEM of three separate experiments. # $p < 0.05$ less than corresponding CMV infected cells; * $p < 0.05$ greater than corresponding CMV infected cells.

3.3.3 DCA and 17-AAG activate MAPK pathways

Prolonged exposure of tumor cell lines to 17-AAG (12-24 hours) has been shown to inhibit Hsp90 function, leading to reduced expression of pro-survival signal transduction proteins, several of which are expressed in primary hepatocytes and that have previously shown to be activated by DCA, including ERBB1, ERBB2, Raf-1 and AKT. Inhibition of all four noted kinases has also been shown to promote bile acid toxicity. As such, we determined whether ERK1/2 and AKT, as well as the stress activated MAPK pathways, JNK1/2 and p38 MAPK, were activated following DCA and 17-AAG exposure.

Treatment of hepatocytes with DCA activated ERK1/2, AKT, JNK1/2 and to a lesser extent p38 MAPK (Figures 46-47). Treatment of cells with 17-AAG as a single agent did not significantly alter kinase phosphorylation within the 6 hour time frame of our study.

To our surprise, short term exposure of hepatocytes to DCA and 17-AAG promoted further activation of JNK1/2 and p38 MAPK 2-6 hours after exposure and of ERK1/2 and AKT 2 h after exposure, without altering activation of ERK1/2, while activity of AKT dissipated 4-6 hours after treatment. DCA-induced activation of ERK1/2 remained elevated for up to 6 hours; the activity of AKT dissipated 4-6 hours after exposure.

Treatment of hepatocytes with ROS quenching agents did not alter DCA-induced activation of either p38 α MAPK or JNK1/2, but suppressed the enhanced levels of p38 α MAPK and JNK1/2 activation observed in cells treated with DCA and 17-AAG (Figure 48).

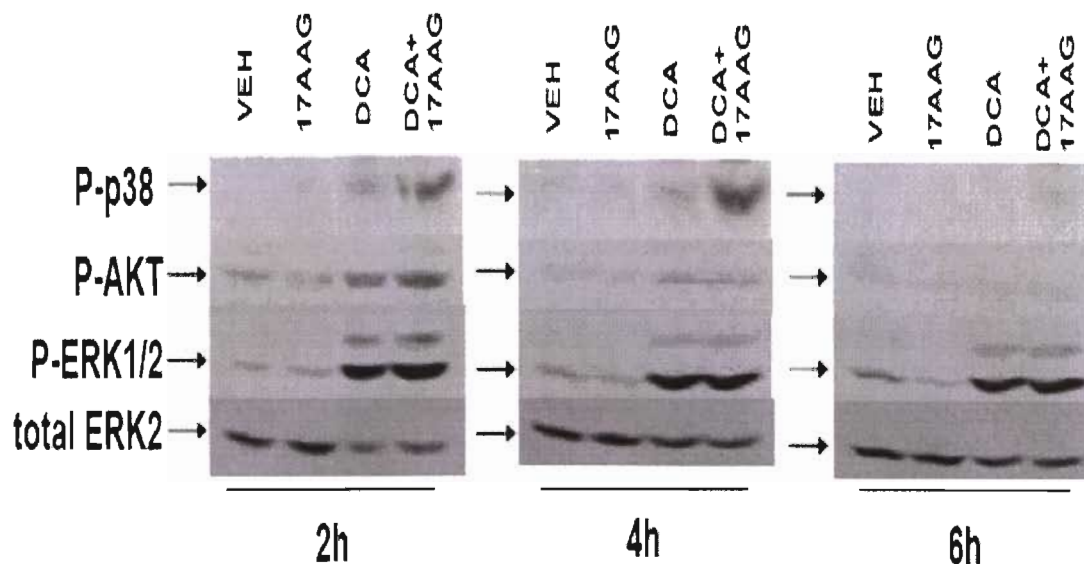


Figure 46. ERK1/2, AKT, and p38 MAPK activation levels in response to treatment with 17-AAG, DCA, and the combination. Hepatocytes were plated in 12-well plates ($\sim 1.5 \times 10^5$ cells per well) for 24 hours as described above in Materials and Methods. Cells were then exposed to vehicle, 17-AAG ($3\mu\text{M}$), DCA ($50\mu\text{M}$), or the combination. After 2, 4, and 6 hours, the cells were harvested and protein samples obtained as described in Material and Methods. Immunoblotting data are from a representative experiment ($n = 3$).

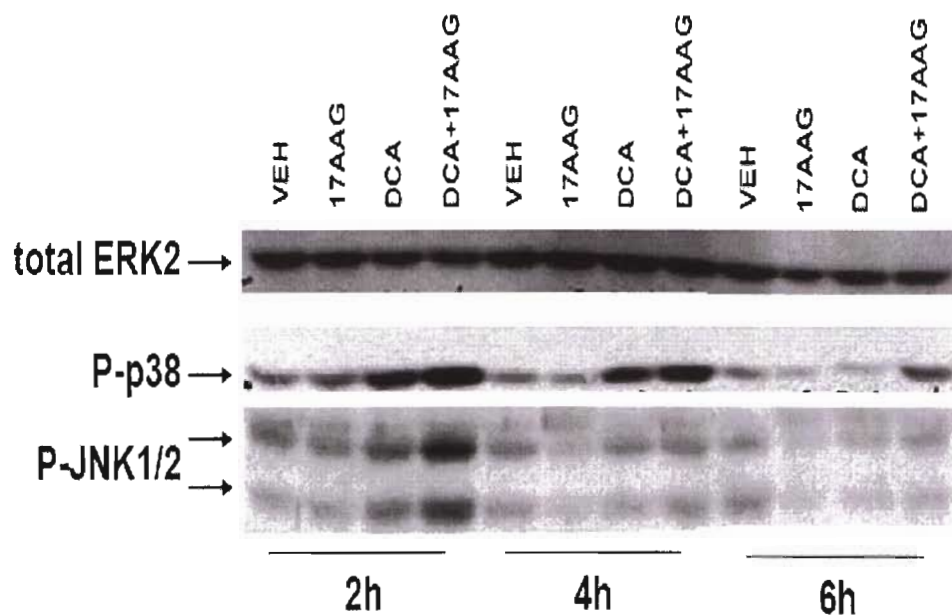


Figure 47. JNK1/2 and p38 MAPK activation levels in response to treatment with 17-AAG, DCA, and the combination. Hepatocytes were plated in 12-well plates ($\sim 1.5 \times 10^5$ cells per well) for 24 hours as described above in Materials and Methods. Cells were then exposed to vehicle, 17-AAG (3 μ M), DCA (50 μ M), or the combination. After 2, 4, and 6 hours, the cells were harvested and protein samples obtained as described in Material and Methods. Immunoblotting data are from a representative experiment (n = 3).

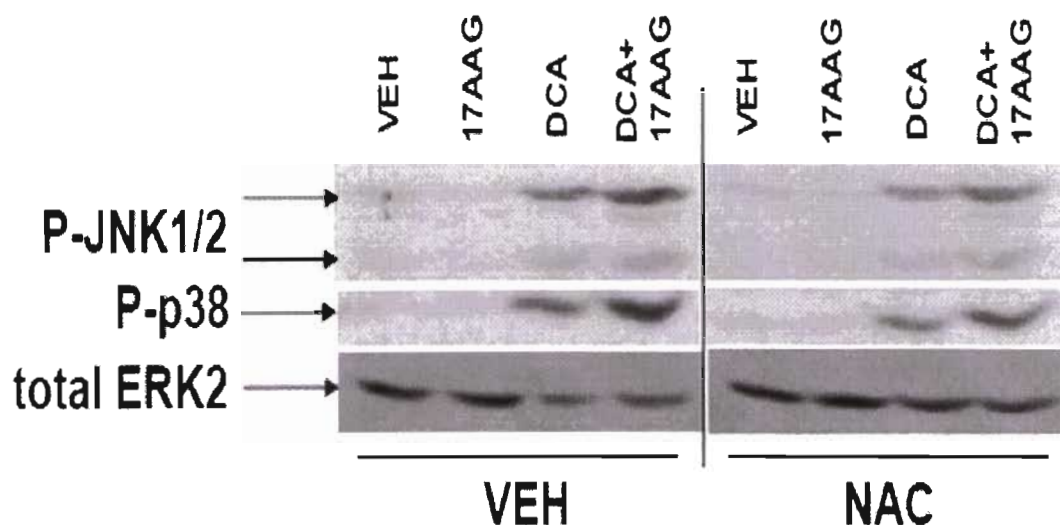


Figure 48. Treatment of hepatocytes with ROS quenching agents did not alter DCA-induced activation of either p38 α MAPK or JNK1/2, but suppressed the enhanced levels of p38 α MAPK and JNK1/2 activation observed in cells treated with DCA and 17-AAG. Hepatocytes were plated in 12-well plates ($\sim 1.5 \times 10^5$ cells per well) for 24 hours as described above in Materials and Methods. Cells were pre-treated with vehicle or 20mM NAC for 1 hour, followed by exposure to vehicle, 17-AAG (3 μ M), DCA (50 μ M), or the combination. After 2 hours, the cells were harvested and protein samples obtained as described in Material and Methods. Immunoblotting data are from a representative experiment (n = 3).

3.3.4 Small molecule inhibitors and adenovirus effect DCA and 17-AAG lethality

Expression of constitutively activated AKT, but not MEK1, suppressed the lethality of 17-AAG and DCA (Figure 49). However, while expression of dominant negative AKT did not further enhance the toxicity of 17-AAG and DCA exposure, expression of dominant negative MEK1 or treatment with the PI3K inhibitor LY294002 promoted 17-AAG and DCA toxicity (Figure 50).

Activation of the JNK1/2 and p38 MAPK pathways in many cell types has been linked to the promotion of cell death. In hepatocytes, we and others have shown that JNK1, but not JNK2, is linked to death signaling by ROS generating agents. Expression of dominant negative p38 α MAPK or expression of dominant negative JNK1 suppressed the induction of cell death by 17-AAG and by combined DCA and 17-AAG exposure (Figure 51). Expression of constitutively active AKT modestly suppressed the activation of JNK1/2, but not p38 α MAPK, by DCA and by the DCA/17-AAG combination (Figure 49, inset panel), which coincided with enhanced survival. Loss of TAM67 in hepatocytes significantly enhanced the lethality of DCA treatment, but did little to enhance that of 17-AAG or the combination (Figure 52). Arguing that the activation of activating protein (AP-1) transcription factor is not involved in inducing cell death, but that signaling through the kinases, not transcription factors, are primarily responsible for cellular mortality (Wu et al. 2003).

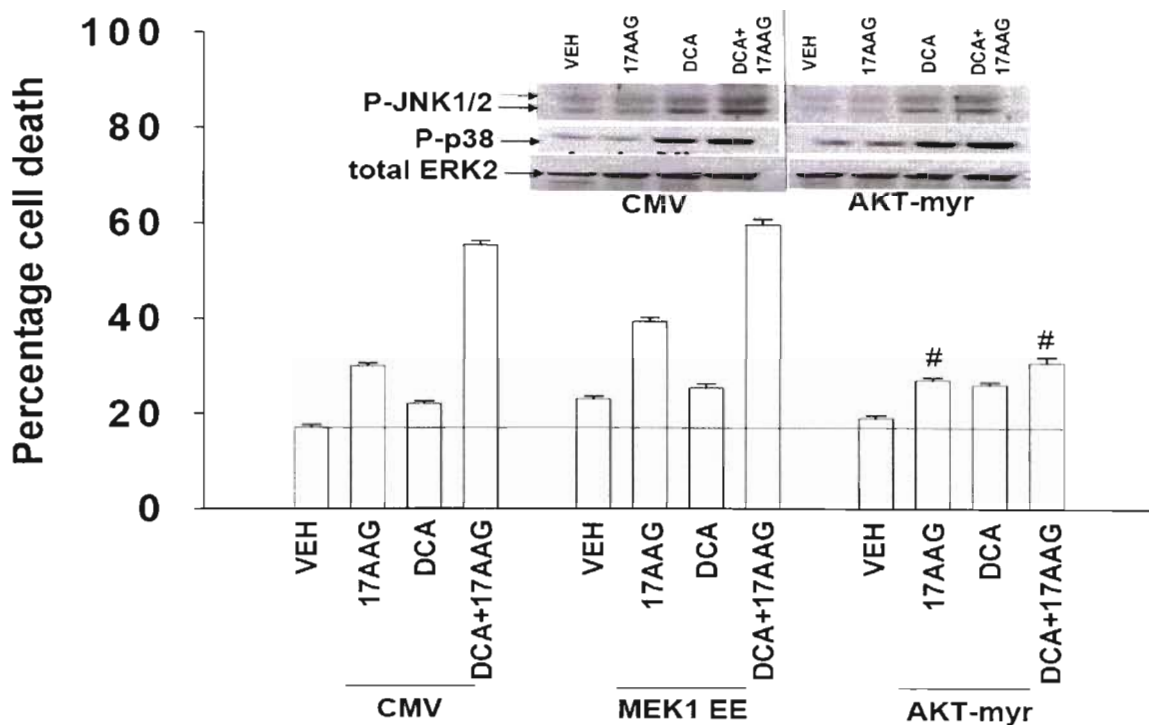


Figure 49. Expression of constitutively activated AKT, but not MEK1, suppressed the lethality of 17-AAG and DCA. Expression of constitutively active AKT modestly suppressed the activation of JNK1/2, but not p38 α MAPK, by DCA and by the DCA/17-AAG combination, which correlated with enhanced survival. Hepatocytes were plated in 12-well plates ($\sim 1.5 \times 10^5$ cells per well) for 6 hours and infected with the corresponding adenovirus (m.o.i. of 50) as described in Materials and Methods. Cells were then exposed to vehicle, 17-AAG (3 μ M), DCA (50 μ M), or the combination. After 4 hours, the cells were harvested and protein samples obtained, or observed via Wright-Giemsa assay, respectively, as described in Material and Methods. Immunoblotting and Wright-Giemsa data are from a representative experiment (n = 3). [#] p < 0.05 less than corresponding CMV value.

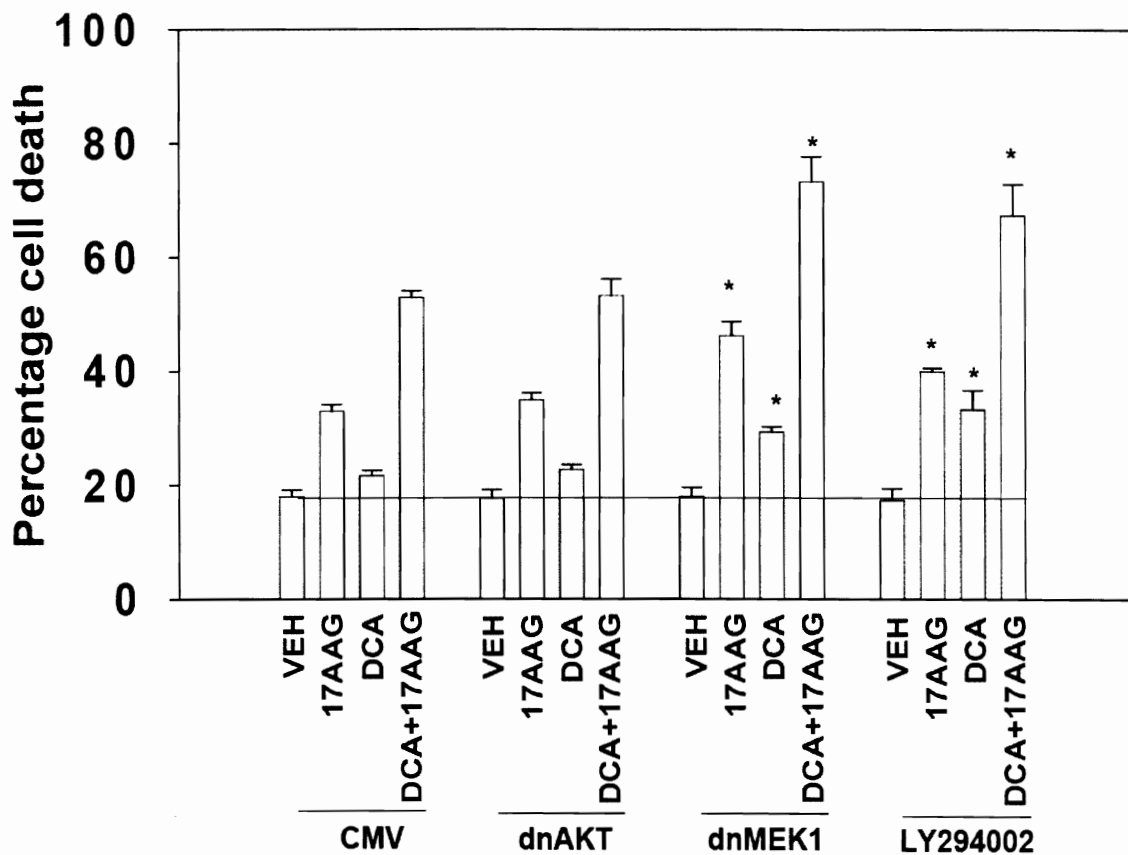


Figure 50. Expression of dominant negative AKT did not further enhance the toxicity of 17-AAG and DCA exposure. Expression of dominant negative MEK1 or treatment with the PI3K inhibitor LY294002 promoted 17-AAG and DCA toxicity. Hepatocytes were plated in 12-well plates ($\sim 1.5 \times 10^5$ cells per well) for 6 hours, infected with the corresponding adenovirus (m.o.i. = 50), and allowed to incubate overnight as described in Materials and Methods. Cells were then pre-treated with vehicle or LY294002 ($5\mu\text{M}$) for 30 minutes, then exposed to vehicle, 17-AAG ($3\mu\text{M}$), DCA ($50\mu\text{M}$), or the combination. After 4 hours, the cells were observed via Wright-Giemsa assay. Wright-Giemsa data are from a representative experiment ($n = 3$). * $p < 0.05$ greater than CMV value cells.

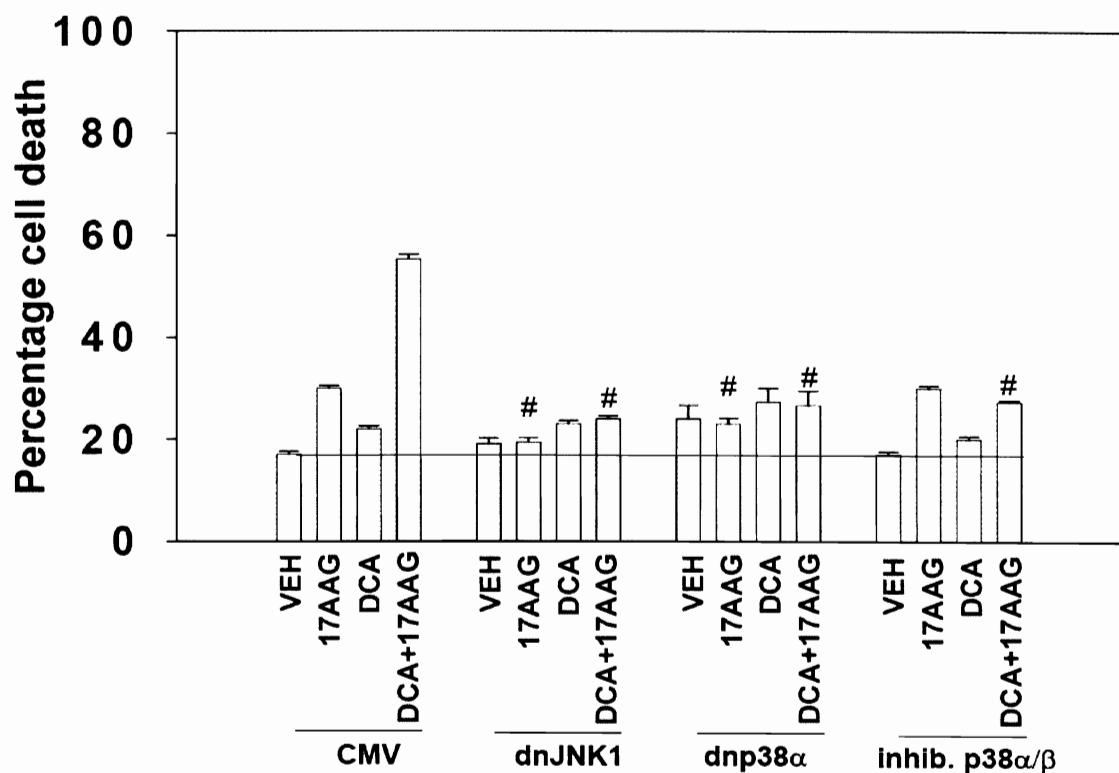


Figure 51. Expression of dominant negative p38 α MAPK, expression of dominant negative JNK1, and inhibition of p38 α/β suppressed the induction of cell death by 17-AAG and by combined DCA and 17-AAG exposure. Hepatocytes were plated in 12-well plates ($\sim 1.5 \times 10^5$ cells per well) for 6 hours, infected with the corresponding adenovirus (m.o.i. = 50), and allowed to incubate overnight as described in Materials and Methods. Cells were then pre-treated with vehicle or SB203580 (1 μ M) for 30 minutes, then exposed to vehicle, 17-AAG (3 μ M), DCA (50 μ M), or the combination. After 4 hours, the cells were observed via Wright-Giemsa assay. Wright-Giemsa data are from a representative experiment (n = 3). [#] p < 0.05 less than corresponding CMV value.

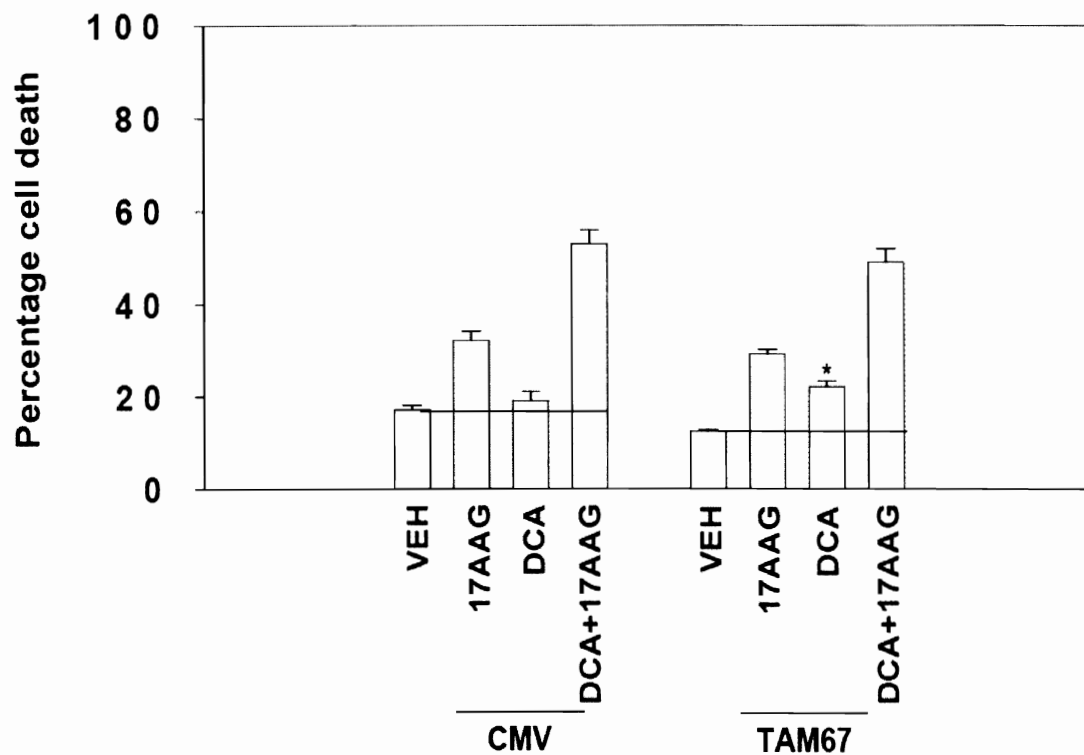


Figure 52. Loss of TAM67 in hepatocytes significantly enhanced the lethality of DCA treatment, but did little to enhance that of 17-AAG or the combination. Hepatocytes were plated in 12-well plates ($\sim 1.5 \times 10^5$ cells per well) for 6 hours, infected with the corresponding adenovirus (m.o.i. = 50), and allowed to incubate overnight as described in Materials and Methods. Cells were treated with vehicle, 17-AAG (3 μ M), DCA (50 μ M), or the combination. After 4 hours, the cells were observed via Wright-Giemsa assay as described in Material and Methods. Wright-Giemsa data are from a representative experiment (n = 3). * p < 0.05 greater than corresponding CMV value.

3.3.5 Role of ASK1 in hepatocyte cell death

As cell killing was ROS-dependent, and required activation of both the JNK1 and p38 MAPK pathways, we next investigated whether the ROS-sensitive kinase, previously determined in other cell types to be an ROS-dependent upstream p38 MAPK and JNK1/2 activator, apoptosis signaling kinase 1 (ASK1), was involved in promoting p38 MAPK activation and altering the survival response to DCA and 17-AAG exposure. Expression of dominant negative ASK1 did not reduce the activation of JNK1/2 induced by DCA but suppressed the enhanced level of JNK1/2 activation induced by combined DCA and 17-AAG exposure (Figure 53). Expression of dominant negative ASK1 also abolished the activation of p38 MAPK induced by DCA or by combined DCA and 17AAG exposure (Figure 53). Expression of dominant negative ASK1 modestly reduced the lethality of 17-AAG as a single agent, but abolished the enhancement of 17-AAG lethality caused by DCA (Figure 54).

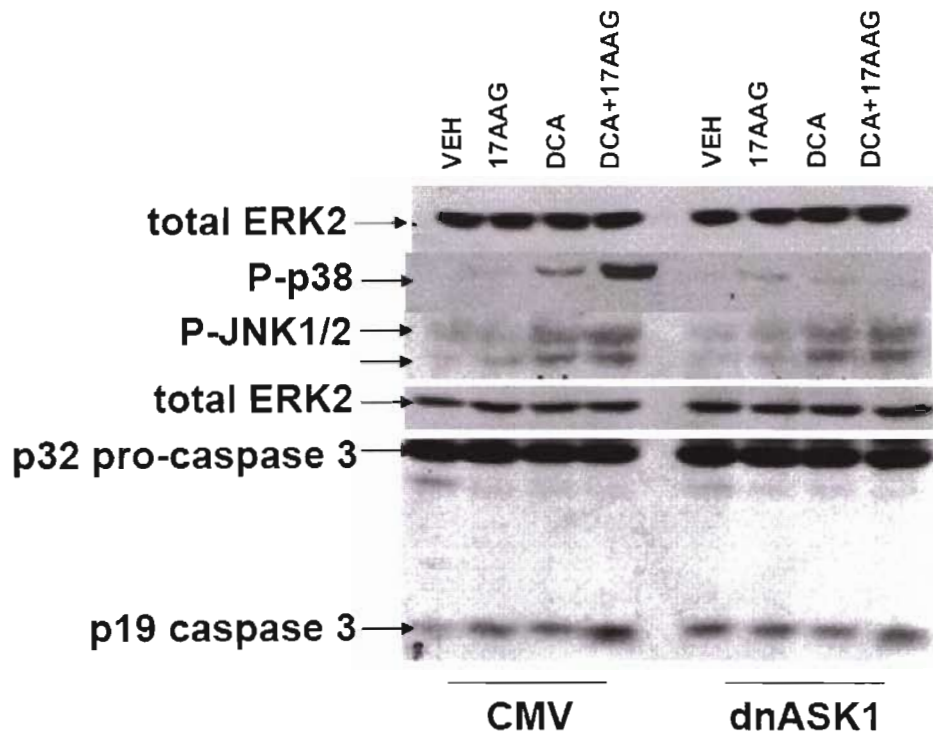


Figure 53. Expression of dominant negative ASK1 abolished p38 MAPK activation, lowered JNK1/2 activation and caspase 3 cleavage in response to the combination. ERK1/2 activity remained unaltered. Hepatocytes were plated in 12-well plates ($\sim 1.5 \times 10^5$ cells per well) for 6 hours, infected with the corresponding poly-lysine virus (m.o.i. = 100), and allowed to incubate overnight as described in Materials and Methods. Cells were then exposed to vehicle, 17-AAG ($3\mu\text{M}$), DCA ($50\mu\text{M}$), or the combination. After 4 hours, the cells were harvested and protein samples obtained for immunoblotting. Immunoblotting data are from a representative experiment ($n = 3$).

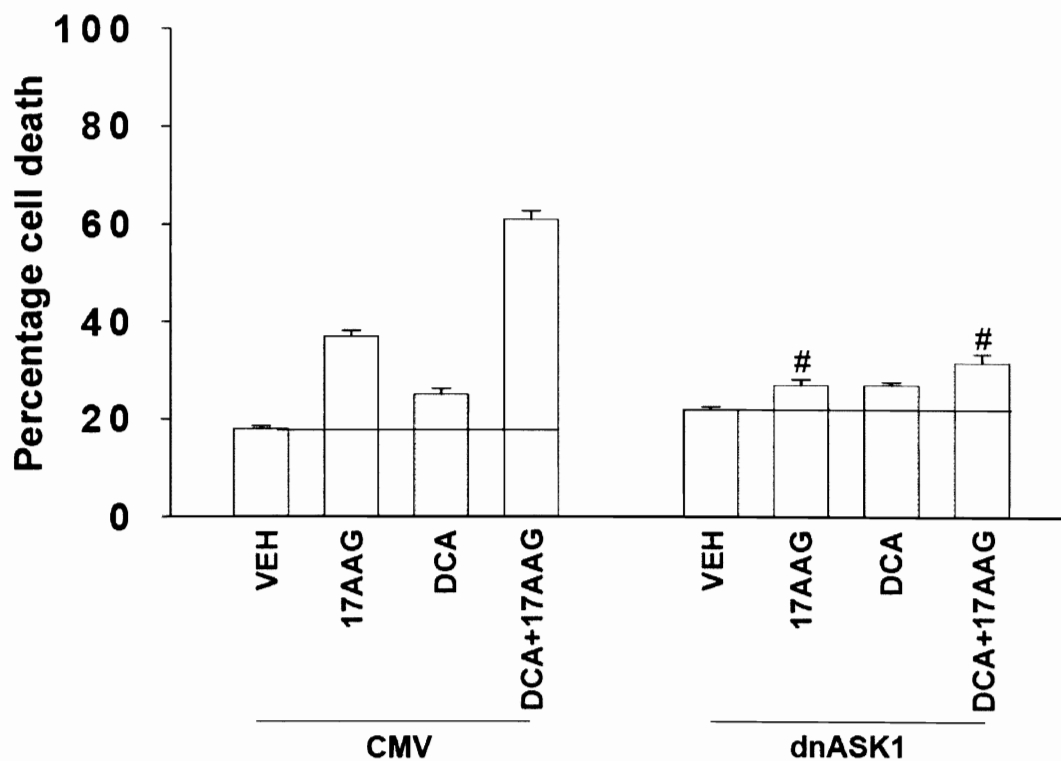


Figure 54. Expression of dominant negative ASK1 modestly reduced the lethality of 17-AAG as a single agent, but abolished the enhancement of 17-AAG lethality caused by DCA. Hepatocytes were plated in 12-well plates ($\sim 1.5 \times 10^5$ cells per well) for 6 hours and infected with the corresponding poly-lysine virus (m.o.i. of 100) as described in Materials and Methods. Cells were then exposed to vehicle, 17-AAG (3 μ M), DCA (50 μ M), or the combination. After 4 hours, the cells were observed via Wright-Giemsa assay, as described in Material and Methods. Wright-Giemsa data are from a representative experiment (n = 3). [#] p < 0.05 less than corresponding CMV value.

3.3.6 Role of acidic sphingomyelinase in DCA and 17-AAG toxicity

In prior studies we have shown in hepatocytes lacking acidic sphingomyelinase (ASMase) expression that bile acids no longer enhance the production of ceramide and cannot activate JNK1/2. Treatment with 17-AAG did not alter ceramide production after DCA exposure. ROS generation induced by DCA and 17-AAG was abolished in ASMase $-/-$ mice (Figures 55-56) which was associated with lower or no activation of JNK1/2 and of p38 MAPK (data not shown), and reduced hepatocyte cell killing. Collectively, our findings demonstrate that: (i) activation of p38 MAPK and JNK1/2 by DCA may be ceramide dependent; (ii) that the elevated activation of p38 MAPK and JNK1/2 caused by combined DCA and 17-AAG exposure is ROS-dependent; and (iii) that loss of ROS / ASK1 signaling into the p38 MAPK and JNK1/2 pathways after DCA and 17-AAG exposure results in the suppression of pathway activation and reduced cell killing.

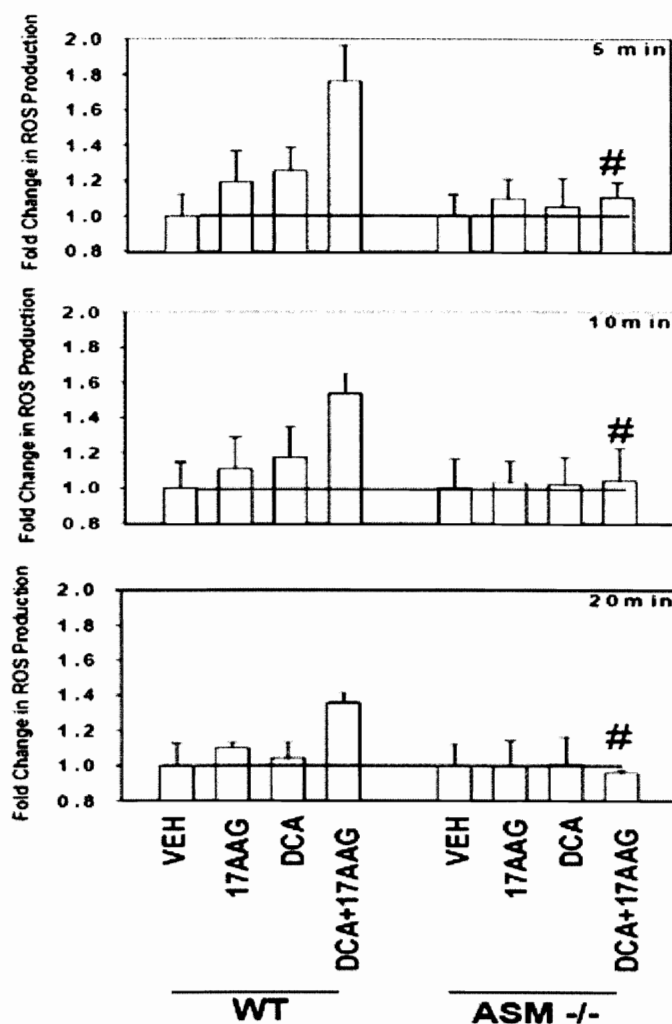


Figure 55. ROS generation in wild type mouse hepatocytes and hepatocytes lacking acidic sphingomyelinase (ASM^{-/-}). Hepatocytes were cultured in 96-well plates (10,000 cells per well) for 24 hours as described in Material and Methods. Cells were then treated with the corresponding concentration of 17-AAG (3 μ M), DCA (50 μ M), or the combination. ROS generation was determined at the appropriate time intervals. Data are the means \pm SEM of three separate experiments. # $p < 0.05$ less than corresponding wild-type value.

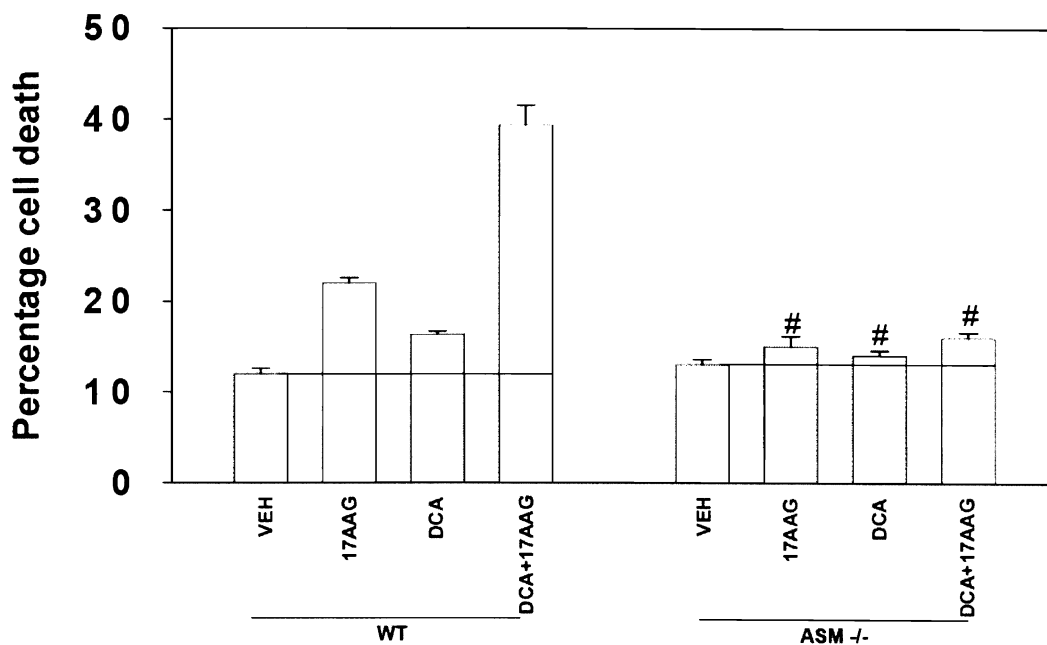


Figure 56. The loss of acidic sphingomyelinase reduced hepatocyte cell death in response to treatment with DCA, 17-AAG, and the combination. Hepatocytes were plated in 12-well plates ($\sim 1.5 \times 10^5$ cells per well) for 24 hours as described in Materials and Methods. Cells were then exposed to vehicle, 17-AAG (3 μ M), DCA (50 μ M), or the combination. After 4 hours, the cells were observed via Wright-Giemsa assay, as described in Material and Methods. Wright-Giemsa data are the means \pm SEM of three separate experiments. # $p < 0.05$ less than corresponding wild type value.

3.3.7 Further ROS studies in hepatocytes and human HuH7 hepatoma cells

Our present studies have argued that ROS generation by DCA and 17-AAG is a primary causal event in the hyper-activation of p38 α MAPK and JNK1/2 and subsequent activation of the intrinsic apoptosis pathway. Previous analyses from our group have shown that DCA promotes ROS generation in hepatocytes that is dependent on the presence of functional mitochondria. ROS generation induced by DCA and 17-AAG was suppressed in hepatocytes incubated with inhibitors of mitochondrial respiration, cyclosporin A (CsA) and bongkreikic acid (BA) (Figure 57), both of which bind to the cyclophilin peptide groups on the outer mitochondrial membrane, preventing alterations in mitochondrial permeability that would normally cause cytochrome c release, thus protecting the cell from death. ROS generation was also suppressed in human HuH7 hepatoma cells lacking functional mitochondria (Figure 58). Loss of mitochondrial ROS production suppressed the lethality of DCA and 17-AAG in HuH7 cells lacking functional mitochondria (Figure 59). Collectively, our findings argue that DCA and 17-AAG interact to promote ROS, although no significant ceramide production was found to occur. This leads to profound activation of the p38 α MAPK and JNK1/2 pathways that trigger the association of pro-apoptotic proteins i.e. Bax with mitochondria, leading to the release of cytochrome c and the activation of the intrinsic cell death pathway.

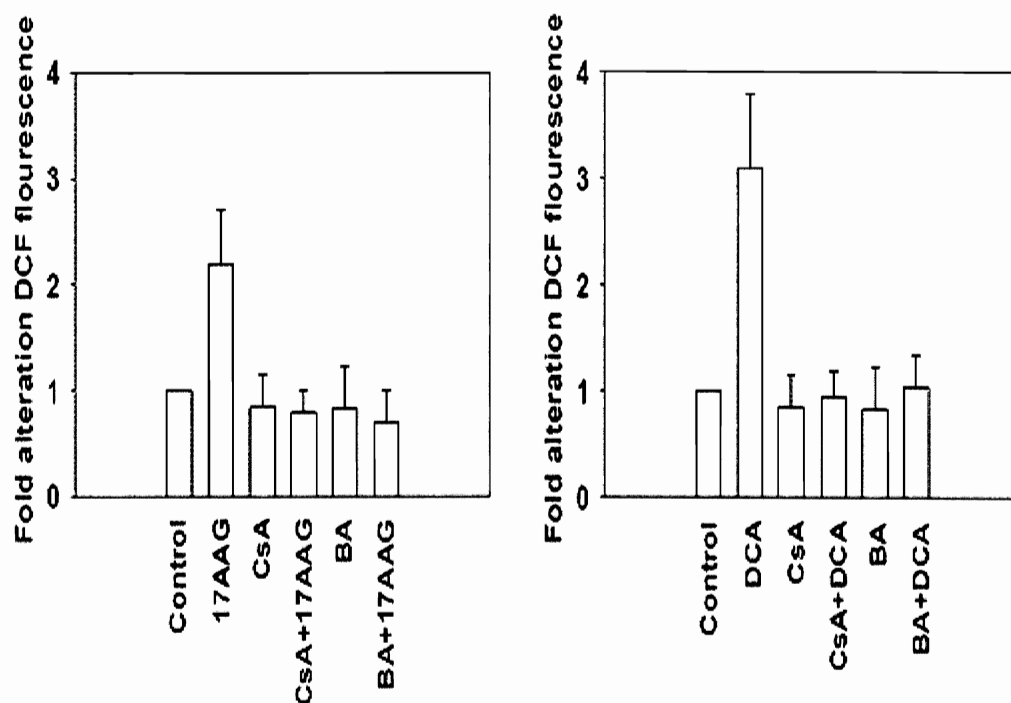


Figure 57. ROS generation induced by DCA and 17-AAG was suppressed in hepatocytes incubated with inhibitors of mitochondrial respiration: cyclosporin A (CsA) and bongkreic acid (BA). Hepatocytes were cultured in 96-well plates (10,000 cells per well) for 24 hours as described in Material and Methods. Cells were pre-treated with CsA (1 μ M) or BA (50 μ M) for 1 hour, followed by exposure to the corresponding concentrations of vehicle, 17-AAG (3 μ M), DCA (50 μ M), or the combination. ROS generation was determined 10 minutes after exposure to 17-AAG, DCA, or the combination. Data are the means \pm SEM of three separate experiments.

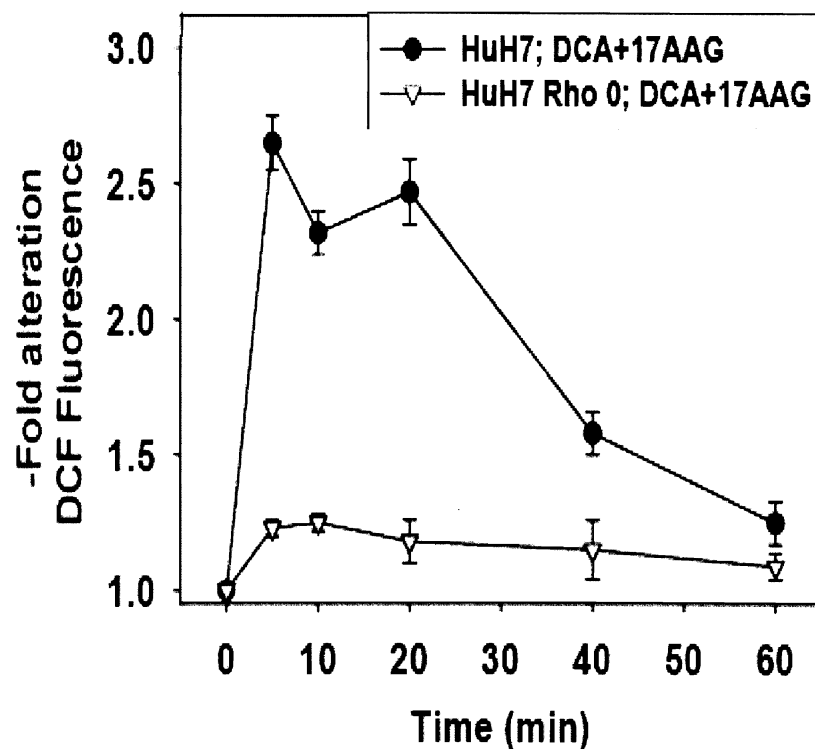


Figure 58. ROS generation was suppressed in human HuH7 hepatoma cells lacking functional mitochondria. Hepatoma cells were cultured in 96-well plates (10,000 cells per well) for 24 hours as described in Material and Methods. Cells were then treated with the 7-AAG (3 μ M) and DCA (50 μ M) combination. ROS generation was determined at the appropriate time intervals. Data are the means \pm SEM of three separate experiments.

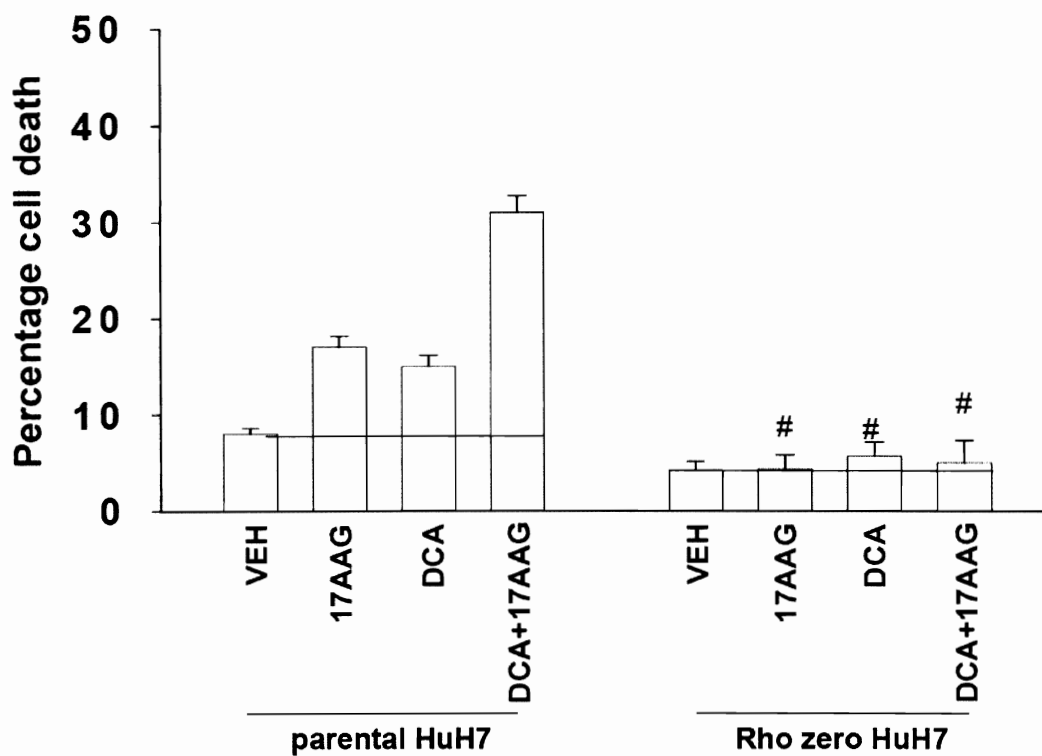


Figure 59. Loss of mitochondrial ROS production suppressed the lethality of DCA and 17-AAG in HuH7 cells lacking functional mitochondria. Hepatoma cells were plated in 12-well plates (25,000 cells per well) for 24 hours as described in Materials and Methods. Cells were then exposed to vehicle, 17-AAG (3 μ M), DCA (50 μ M), or the combination. After 12 hours, the cells were observed via Wright-Giemsa assay. Wright-Giemsa data are from a representative experiment (n = 3). [#] p < 0.05 less than corresponding parental value.

3.3.8 17-AAG and DCA toxicity, and the intrinsic/extrinsic pathways

Based on the above findings we next determined the molecular mechanisms by which DCA and 17-AAG interacted to cause cell death. Prior studies by our group have demonstrated that DCA lethality as a single agent, and DCA lethality enhanced in combination with ERBB1 / IFG1R / MEK1/2 / PI3K inhibitors, is dependent on ligand independent activation of FAS death receptor (CD95) leading to activation of caspase 8, BID cleavage, mitochondrial dysfunction and cell killing (Dent et al. 2005, Fang et al. 2004). Inhibition of caspase 8 function via IETD or expression of dominant negative FADD (data not shown) weakly suppressed the lethality of DCA and 17-AAG. In contrast, inhibition of caspase 9 function via LEHD and expression of dominant-negative caspase 9 abolished the lethal effects of DCA and 17-AAG (Figure 60). Also, over-expression of BCL-X_L abolished DCA and 17-AAG-induced cell killing (data not shown). Collectively, these findings demonstrate that combined DCA and 17-AAG exposure promotes hepatocyte cell killing via mitochondrial dysfunction and activation of the intrinsic apoptosis pathway.

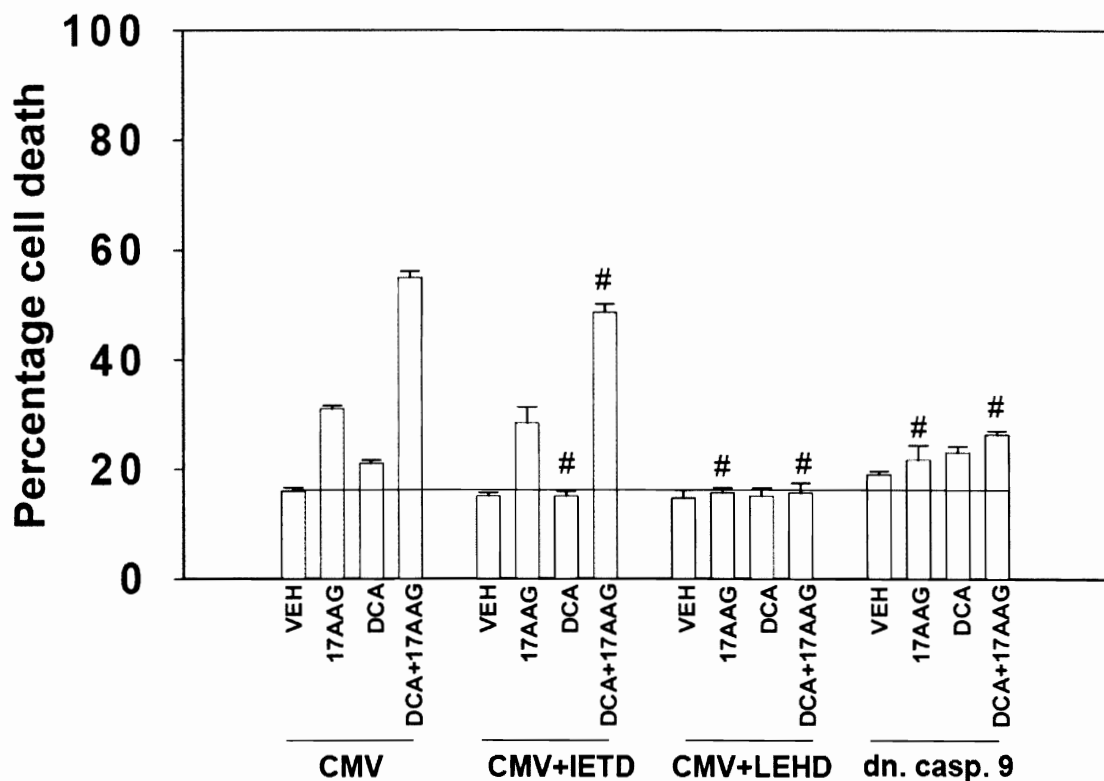


Figure 60. Inhibition of caspase 8 slightly lowered the toxic effects of DCA, while inhibition of caspase 9 significantly abolished the toxicity of 17-AAG and the 17-AAG / DCA combination. Hepatocytes were plated in 12-well plates ($\sim 1.5 \times 10^5$ cells per well) for 6 hours, infected with the corresponding adenovirus (m.o.i. = 50), and allowed to incubate overnight as described above in Materials and Methods. Cells were then pre-treated with vehicle, IETD (20 μ M), or LEHD (20 μ M) for 30 minutes, followed by exposure to vehicle, 17-AAG (3 μ M), DCA (50 μ M), or the combination. After 4 hours, the cells were observed via Wright-Giemsa assay. Wright-Giemsa data are from a representative experiment (n = 3). # p < 0.05 less than corresponding CMV value.

3.3.9 DCA and 17-AAG cause cell death in mouse embryonic fibroblasts

In general agreement with activation of the intrinsic apoptosis pathway, the ability of DCA and 17-AAG to promote rapid release of cytochrome c from mitochondria is currently being investigated. It is also hypothesized that this cytochrome c release can be blocked by ROS quenching agents, expression of dominant negative p38 α MAPK, expression of dominant negative JNK1, or expression of constitutively active AKT. The ability of DCA and 17-AAG to promote the association of BAX and BAK with hepatocyte mitochondria, as well as the effect of ROS quenching agents, expression of dominant negative p38 α MAPK, expression of dominant negative JNK1 or expression of constitutively active AKT, on this association is also under investigation, in part due to our findings with transformed mouse embryonic fibroblasts.

Treatment of transformed mouse embryonic fibroblasts with DCA and 17-AAG caused a significantly greater than additive increase in cell killing within 12 hours that was of a similar level to that observed in primary hepatocytes 4 hours after exposure; loss of combined BAX and BAK expression abolished the ability of DCA and 17-AAG to cause fibroblast cell death (Figure 61). In general agreement with our data showing that inhibition of caspase 8 function modestly suppressed DCA and 17-AAG lethality in primary hepatocytes, loss of BID function did not significantly alter the death response of DCA and 17-AAG treated cells (Figure 61). Further investigations utilizing mouse embryonic fibroblasts revealed that the sole loss of BAX expression, was responsible for

abolishing the ability of DCA and 17-AAG to cause cell death, while loss of BAK expression slightly hindered the interaction of DCA and 17-AAG (Figure 62). As 17-AAG could cause an unfolded protein response and endoplasmic reticulum stress, we determined whether the loss of PERK function altered 17-AAG lethality. As shown below in Figure 62, the loss of PK-R like kinase (PERK) expression significantly decreased the toxicity of 17-AAG and the combination of DCA and 17-AAG, while having little to no effect on DCA toxicity (Figure 62), indicating the involvement of ER stress signaling in the cellular response to 17-AAG and the interaction between 17-AAG and bile acids. PERK is a key protein in halting protein synthesis in response to an accumulation of misfolded proteins via phosphorylation of eIF2. It is this protein aggregation that stimulates the ER stress response (i.e. signaling to caspase-12). The fact that the loss of PERK in these fibroblasts protected the cells from 17-AAG and the 17-AAG / DCA combination suggests that the ER stress response was abrogated, or delayed, thus protecting the cells from death.

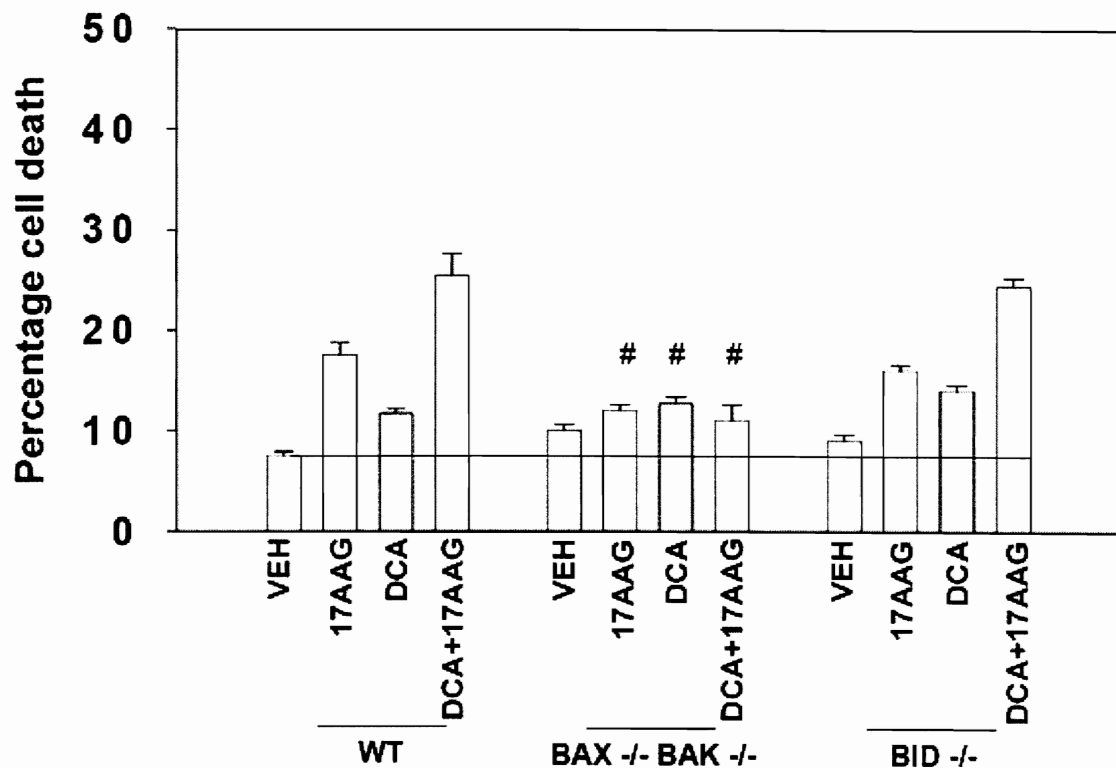


Figure 61. Treatment of transformed mouse embryonic fibroblasts with DCA and 17-AAG caused a greater than additive increase in cell killing within 12 hours that was of a similar level to that observed in primary hepatocytes 4 hours after exposure; loss of combined BAX and BAK expression abolished the ability of DCA and 17-AAG to cause fibroblast cell death, while loss of BID expression did not significantly alter fibroblast cell killing. Fibroblasts were plated in 12-well plates (25,000 cells per well) for 24 hours as described above in Materials and Methods. Cells were then exposed to vehicle, 17-AAG (3 μ M), DCA (50 μ M), or the combination. After 12 hours, the cells were observed via Wright-Giemsa assay. Wright-Giemsa data are from a representative experiment (n = 3). [#] p < 0.05 less than corresponding wild type value.

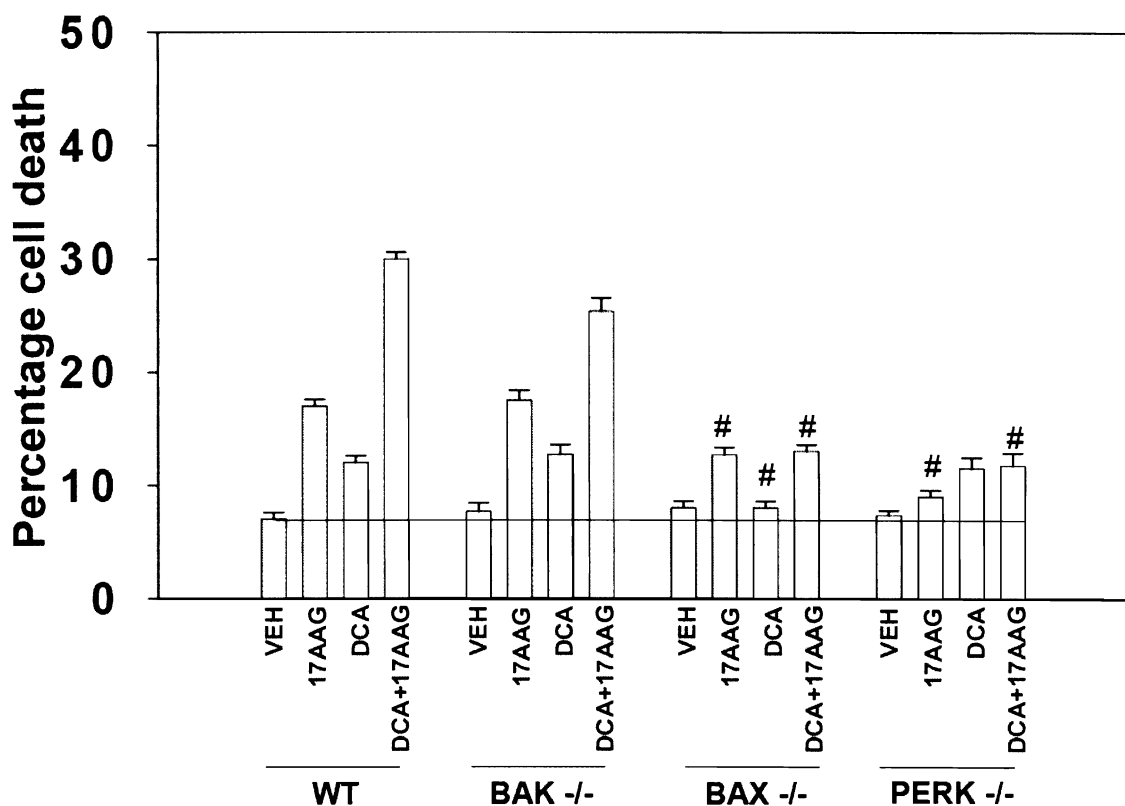


Figure 62. In mouse embryonic fibroblasts, loss of BAX expression was responsible for abolishing the ability of DCA and 17-AAG to cause cell death, while loss of BAK expression slightly hindered the interaction of DCA and 17-AAG. It was also noted that the loss of PERK expression significantly decreased the toxicity of 17-AAG and the combination of DCA and 17-AAG, while having little to no effect on DCA toxicity. Fibroblasts were plated in 12-well plates (25,000 cells per well) for 24 hours as described above in Materials and Methods. Cells were then exposed to vehicle, 17-AAG (3 μM), DCA (50 μM), or the combination. After 12 hours, the cells were observed via Wright-Giemsa assay. Wright-Giemsa data are from a representative experiment (n = 3). # p < 0.05 less than corresponding wild type value.

3.3.10 Summary of findings in hepatocellular carcinoma (HCC)

The present studies were initiated to determine the molecular mechanisms by which geldanamycins and bile acids altered hepatocyte viability *in vitro*. We have showed that the geldanamycin derivative 17-allylamino-17-demethoxygeldanamycin (17-AAG) interacts with the secondary bile acid, deoxycholic acid (DCA), to kill primary rat hepatocyte cultures. This finding coincided with prolonged increases in levels of mitochondria generated ROS, phosphorylated levels of p38 and SAPK/JNK MAPK pathways, classical morphological apoptosis, and cell death. These effects were eliminated by the addition of the free radical quenchers, N-acetyl cysteine and Trolox, as well as the loss of functional ASMAse. The loss of thioredoxin reductase activity resulted in an increase in cell mortality. Use of caspase inhibitors and dominant-negative adenovirus revealed the effects of 17-AAG and the combination did not correlate with death receptor signaling through caspase 8, but through mitochondrial dysfunction and caspase 9, as supported by data generated from experiments using mouse embryonic fibroblasts lacking several key Bcl-2 family proteins. It was found that the loss of Bax, not Bak or Bid, resulted in abrogation of the toxic effects of 17-AAG and the 17-AAG and DCA combination. The loss of PERK in these same cell lines also protected hepatocytes from cell death, suggesting the role of the ER stress response in the hepatotoxic interaction between geldanamycin and bile acids. Collectively, these findings argue that geldanamycins may not be a viable therapy for HCC treatment and that 17-AAG toxicity in primary hepatocytes may be, at least upon initial drug exposure,

due to mechanisms independent of Hsp90 inhibition and down-regulation of “classical”

Hsp90 client proteins.

CHAPTER FOUR

DISCUSSION

4.1 Discussion: MDA-7 and Renal Cell Carcinoma (RCC)

Renal cell carcinoma is known to be relatively resistant to a variety of conventional anticancer therapies such as the combination of chemotherapy and radiotherapy. The experiments conducted in this study were designed to examine the effect of the novel therapeutic cytokine MDA-7 (Suane et al. 2003, Sarkar et al. 2002) on the growth and survival of both the A498 and UOK121N renal cell carcinoma cell line.

The adenoviral vector *Ad.mda-7* did not alter RCC proliferation. This correlated with the weak infectivity and absence of CAR, common to RCC lines (Haviv et al. 2002). It was also found, in contrast to results in the RCC lines, that primary renal epithelial cells were more easily infected by type 5 adenovirus. This data collectively demonstrates that kidney cancer cells have reduced expression of CAR protein compared with non-transformed kidney epithelial cells, which also agrees with the concept that several cell types, among them bladder carcinomas and prostate carcinomas, experience a loss of CAR protein expression as they become transformed (Rauen et al. 2002, Okegawa et al. 2001).

Recent studies have shown that *Ad.mda-7* can act as a radiosensitizer in brain, lung, and mammary carcinoma cell lines (Rauen et al. 2002, Kawabe et al. 2002, Liu et al. 2002, Yacoub et al. 2003). It has also been found that *Ad.mda-7* and purified MDA-7 protein

enhanced the growth inhibitory and cytotoxic effects of ionizing radiation that were blocked by the free radical scavenger N-acetyl cysteine (Yacoub et al. 2003). These effects also correlated with the reduced expression of the anti-apoptotic protein, Bcl-X_L. It was also found that constitutive over-expression of Bcl-X_L abolished the toxic and growth inhibitory effects of Ad.*mda-7* (Yacoub et al. 2003). In the A498 and UOK121N RCC lines, GST-MDA-7, but not GST caused a dose-dependent reduction in proliferation without causing cell killing. As a single agent, high concentrations of GST-MDA-7 caused a further reduction in growth and modestly enhanced cell death. The fact that GST did not alter cell biology or morphology allows the argument that the effect is specific to MDA-7 and not because of bacterial endotoxins in our purified protein preparations, which was supported by the use of MDA-7 synthesized in primary hepatocytes. These effects also coincided with reduced expression of the anti-apoptotic protein Bcl-X_L.

Arsenic trioxide interacted with GST-MDA-7 in the RCC lines to cause a greater than additive reduction in cell growth, as well as a greater than additive increase in cell death which coincided with a further reduction in Bcl-X_L expression. The fact that the free radical scavenger, N-acetyl cysteine, blocked the effects of arsenic trioxide, suggests that the generation of free radicals enhances the effects of MDA-7. These findings demonstrate that tumor cell growth can be altered by low concentrations of MDA-7 and that free radical species can interact with MDA-7 to promote greater than additive growth suppression and cell killing.

Low concentrations of GST-MDA-7 resulted in approximately fifty percent growth arrest without a large increase in cell killing, whereas higher concentrations of GST-MDA-7 result in arrest and cell death. These results coincide with studies performed with A431 squamous carcinoma cells treated with epidermal growth factor (EGF) (Gulli et al. 1996). In A431 cells, low picomolar concentrations of EGF were found to promote cell growth, but growth arrest occurred at concentrations higher than 100 picomolar EGF. At EGF concentrations above 1 ng/ml, A431 cells undergo growth arrest, followed by apoptosis. It has also recently been insinuated that the ability of MDA-7 to promote growth arrest and cell death can be dissociated (Parrish-Novak et al. 2002).

Previous studies have implicated the involvement of the mitogen-activated protein kinase pathways in response to MDA-7, with signaling by p38 and JNK1/2 being implicated in MDA-7 induced cell death. Reduced ERK1/2 activity and enhanced p38 activity, as well as JNK1/2 acting as a protective signal (Iwama et al. 2001), are linked to arsenic trioxide induced cell death in response to high concentrations of arsenic trioxide (Su et al. 2003, Kawabe et al. 2002, Liu et al. 2002, Sarkar et al. 2002). This study shows that enhanced JNK1/2 signaling, but not p38 signaling, is the key contributor to the toxic interaction between MDA-7 and arsenic trioxide.

The novel therapeutic, arsenic trioxide, is currently being examined as an agent capable of enhancing the toxicity of established chemotherapeutic agents (Miller et al. 2002).

Arsenic trioxide is thought to generate primarily oxygen-derived free radical species (Barchowsky et al. 1999), thereby enhancing oxidative stress and DNA damage, which ultimately leads to the promotion of cell death in numerous cell types, including the A498 and UOK121N RCC lines (Hyun Park et al. 2003). Arsenic trioxide has consequently been linked to enhanced proliferation and to the promotion of cellular differentiation in certain cell types, and at certain concentrations (Barchowsky et al. 1999, Halicka et al. 2002). Previous studies also show the cytotoxic effects of arsenic trioxide to be lower in non-transformed cells (Barchowsky et al. 1999). Arsenic trioxide is also currently being investigated in differentiation therapies used in treating hematologic malignancies (Miller et al. 2002). With respect to these studies, MDA-7 has been linked to cell differentiation and the induction of growth arrest in undifferentiated tumor cells, but not non-differentiated non-transformed cells (Suane et al. 2003, Sarkar et al. 2002, Pestka 2003). Therefore, it is possible that MDA-7 and arsenic trioxide interact to cause growth arrest, abnormal differentiation, and cell death in RCC lines. The fact that non-transformed human kidney epithelial cells were found to be resistant to the combination of MDA-7 and arsenic trioxide implies that normal tissue toxicity may not be dose limiting.

The signaling pathways of cell death induced by GST-MDA-7 and arsenic trioxide were also investigated. Due to the results of previous findings (Suane et al. 2003, Sarkar et al. 2002), as well as Bcl-X_L data generated in these experiments, in which the expression levels of the anti-apoptotic protein significantly decreased, it was expected that GST-MDA-7 and arsenic trioxide would interact to primarily increase apoptosis. Although

GST-MDA-7 and arsenic trioxide did cause pro-caspase 3 and PARP cleavage, the increase did not correspond to a large induction of “classical” apoptotic nuclear morphology. In contrast, cell viability measured by trypan blue staining revealed that the combination of GST-MDA-7 and arsenic trioxide caused a large increase in cell morbidity. Agarose gel DNA fragmentation analyses also indicated that nuclear DNA was being degraded into small molecular weight fragments, rather than into a “classical” DNA ladder, normally associated with cellular apoptosis. This finding is also suggestive of a non-apoptotic mode of cell death. These results suggest that GST-MDA-7 and arsenic trioxide promote cell death through a necrotic mechanism.

The colony formation assay is arguably the best *in vitro* measurement of a particular therapeutic agents performance on impacting tumor cell growth *in vivo* (Haviv et al. 2002). MTT assays and manual cell counting reveals the growth of RCC lines were reduced by approximately fifty percent when treated with low concentrations of GST-MDA-7. However, colony formation assays revealed that cells treated with the GST-MDA-7 and then allowed to grow in the absence of the cytokine experienced very little alteration in colony-formation ability. This argues that low concentrations of GST-MDA-7 cause a reversible growth arrest in the RCC lines. It was also found in MTT assays that arsenic trioxide had a minimal effect on short-term cell growth, but significantly reduced colony formation ability, which is suggestive that the effects of free radical generation are evident many cell cycles after the initial exposure. This is similar to the findings of laboratories utilizing ionizing radiation to generate free radicals (Dewey

et al. 1995). MTT assays and trypan blue staining revealed the combination of GST-MDA-7 and arsenic trioxide caused a ten-fold increase in cell killing, when compared to either agent individually.

In conclusion, our data coincides with that of previous studies (Haviv et al. 2002), by showing the RCC cell lines, and not the primary renal epithelial cell line, to be resistant to type 5 adenoviral infections. This follows the paradigm previously established that RCC lines experience weak infectivity due to a lack of CAR expression (Yacoub et al. 2003). It was also found that purified GST-MDA-7 protein, but not GST, caused a dose-dependent reduction in the proliferation of the RCC lines, but not that of primary renal epithelial cells, via the reduction in Bcl-X_L expression, an anti-apoptotic protein.

However, our study revealed the mechanism of cell death to be largely necrotic, due to the lack of “classical” apoptotic nuclear morphology and DNA fragmentation. Free radical species, generated by clinically relevant concentrations of arsenic trioxide, interacted in a greater than additive fashion with subnanomolar concentrations of GST-MDA-7 to inhibit the proliferation, viability, and long-term survival of the A498 and UOK121N RCC lines. These findings argue that the use of MDA-7 in combination with agents that generate free radicals may have potential in the treatment of renal cell carcinoma.

4.2 Discussion: MDA-7 and Glioblastoma Multiforme (GBM)

These experiments were performed in order to examine the impact of the novel therapeutic cytokine, MDA-7 (IL-24), on the growth and radiosensitivity of glioma cell lines. Expression of MDA-7, mediated by an adenoviral vector *Ad.mda-7*, reduced cell proliferation and enhanced cell death in glioma cells but not in primary astrocytes.

Recent studies using lung carcinoma cells found that *Ad.mda-7* can act as a radiosensitizer, a finding supported in these studies using glioma cells (Kawabe et al. 2002). *Ad.mda-7* also enhanced the growth inhibitory and cytotoxic effects of radiation.

Ad.mda-7 and radiation caused pro-caspase 3 and PARP cleavage as well as significant enhancement of apoptosis in glioma cells. When cell viability was measured via trypan blue staining, a measure of necrosis and late apoptosis, the combination of *Ad.mda-7* and radiation resulted in a dramatic increase in cell morbidity. In concurrence with a non-apoptotic mode of cell death, agarose gel DNA fragmentation analyses indicated that nuclear DNA was being degraded into small molecular weight fragments, rather than into a “classical DNA ladder,” indicative of apoptosis. These findings suggest that the combination of *Ad.mda-7* and ionizing radiation primarily promote cell death through a necrotic mechanism.

The studies performed utilized recombinant adenoviral infections at m.o.i.'s of 5-25, which correspond to ~4% and ~20%, respectively, of the RT2 cells being infected. For

the U251 cell line, this corresponded with approximately 5% of the cells becoming infected. Based on these findings, our survival data suggests that MDA-7, secreted from infect tumor cells, may have a bystander effect on the radiosensitivity of cells that have not been infected. In general agreement with this paradigm, purified GST-MDA-7 protein has been shown to radiosensitize human glioma cells, as well as the RCC lines described above, *in vitro*.

Due to the fact that the activation of PI3K and ERK1/2 pathways have been found in other cell lines to enhance survival in response to a variety of toxic stimuli, including Ad.*mda-7* (Su et al. 2001), the inhibition of these pathways after exposure to radiation and/or Ad.*mda-7* and its effect on glioma cell growth and viability was analyzed.

Treatment of control infected RT2 cells (Ad.*cmv*) with the MEK1/2 inhibitor PD98059 in combination with the PI3K inhibitor LY294002 reduced RT2 cell growth, but weakly enhanced cell killing. In cells infected with Ad.*mda-7*, neither kinase inhibitor enhanced the anti-proliferative effects of this virus. However, combined inhibition of MEK1/2 and PI3K did significantly enhance the growth suppressive effects of Ad.*mda-7*, which also coincided with increased cell death. This finding demonstrates that multiple pathways signal to protect cells from MDA-7 toxicity and that inhibition of a single pathway may be insufficient in certain cell lines to enhance cell killing.

Ad.mda-7 activated the ERK1/2 and p38 pathways, which is concurrent with previously established data showing enhanced p38 signaling linked to *Ad.mda-7*-induced cell death (Sarkar et al. 2002). These experiments demonstrated that PD98059 and LY294002 enhanced *Ad.mda-7* toxicity, but abolished p38 activity. This suggests that while *Ad.mda-7*, as an individual agent, can promote cell killing potentially through the activation of the p38 pathway, the abilities of kinase inhibitors to further enhance morbidity is a p38-independent process. This idea is further supported by the fact that inhibition of p38 α/β via SB203580 (2 μ M) did not alter the toxic or radiosensitizing properties of *Ad.mda-7*.

These experiments also revealed that radiation abolished *Ad.mda-7*-induced ERK1/2 activity and enhanced JNK1/2 activity, with little or no effect on p38 or AKT activity. Previous data has shown that elevated levels of JNK1/2 and p38 signaling combined with loss of ERK1/2 signaling can enhance cell killing by ionizing radiation (Cartee et al. 2000, Xia et al. 1995). Kawabe et al. have argued that *Ad.mda-7* enhanced radiosensitivity in lung carcinoma cells via the JNK1/2 pathway, as judged by the abolished radiosensitization by curcumin, although in these studies, radiation did not enhance JNK1/2 activity beyond that already induced by *Ad.mda-7* (Kawabe et al. 2002). In RT2 cells, *Ad.mda-7* as a single agent did not cause activation of JNK1/2, but in general agreement with the findings of Kawabe et al., inhibition of JNK1/2 by the

relatively specific inhibitor SP600125 (10 μ M) abolished the radiosensitizing effect of *Ad.mda-7*.

Enhanced cell numbers in G₂/M phase of the cell cycle at the time of irradiation have been linked to increased radiosensitivity, as has abrogation of the radiation-induced G₂/M cell cycle checkpoint (Cartee et al. 2000, Dent et al. 1999, Biade et al. 1997). *Ad.mda-7* significantly enhanced cell numbers in G₂/M phase in U251 cells that were further enhanced following radiation exposure (Su et al. 2003). In contrast, *Ad.mda-7* enhanced cell numbers in G₁ phase in RT2 cells, which were further enhanced following radiation exposure. In both cell types, the percentage of cells residing in S phase was almost abolished in the *Ad.mda-7* and radiation combination treatment group. These findings demonstrate that *Ad.mda-7*-induced alterations in cell cycle distribution are not a key mechanism by which radiosensitization occurs. In addition, as cells are removed from the most radioresistant portion of the cell cycle by combined *Ad.mda-7* and radiation treatment (Biade et al. 1997), repeated radiation exposures may cause further radiosensitization and cell killing via the synchronization of cells in G₂/M and G₁ phases. Additional studies will be required to further support this hypothesis.

4.3 Discussion: Geldanamycins and Liver Toxicity

Previous studies have demonstrated that geldanamycins have dose limiting toxicity *in vivo* due to their actions in promoting liver dysfunction. The present studies were

initiated to determine the molecular mechanisms by which geldanamycins and bile acids altered hepatocyte viability *in vitro*.

The majority of published studies with regard to toxic geldanamycin actions are based on the fact that ansamycin antibiotics suppress the function of Hsp90, thereby promoting the degradation and ultimate inhibition of kinase signaling i.e. ErbB, B-Raf, and AKT, whose function in tumor cells is to promote growth and cell survival. In addition, it has also been noted that mutated active (oncogenic) forms of such kinases i.e. B-Raf, in tumor cells have a higher rate of degradation following Hsp90 inhibition than non-mutated forms of the same proteins (Behrsing et al. 2005, Senju et al. 2006, Shen et al. 2005, Webb et al. 2000). In primary hepatocytes however, that have low basal activities of kinases within all signaling pathways, we noted that co-administration of 17-AAG did not prevent the secondary bile acid DCA from activating ERK1/2 or AKT within a 6 hour time frame. In general agreement with these findings, within 6 hours of 17-AAG treatment, Raf-1 protein levels in hepatocytes remained constant, yet 17-AAG as a single agent and when combined with DCA caused significant amounts of hepatocyte cell killing. Furthermore, when combined with DCA, 17-AAG caused an enhanced and prolonged activation of both the p38 MAPK and JNK1/2 pathways. Activation of both the p38 MAPK and JNK1/2 pathways were then demonstrated to be required for manifestation of the cytotoxic effects of combined 17-AAG and DCA treatment. These effects occurred within approximately two hours of drug exposure as judged by caspase

activation and cellular morphology indicative of cell death. Collectively, these findings argue that 17-AAG toxicity in primary hepatocytes may be, at least upon initial drug exposure, due to mechanisms independent of Hsp90 inhibition and down-regulation of “classical” Hsp90 client proteins.

In one study using hematopoietic cells, geldanamycins have been argued to mediate their toxicity, in part, by causing the generation of reactive oxygen species (ROS) (Lai et al. 2003). In primary rat hepatocytes and HuH7 human hepatoma cells, 17-AAG modestly increased ROS levels within 30 minutes of exposure. In primary hepatocytes, DCA and 17-AAG interacted to promote significantly higher peak levels of ROS production. Production of ROS was dependent on functional mitochondria, based on a loss of ROS production in Rho-zero cells and by use of the drugs cyclosporine A and bongkreikic acid. Suppression of ROS levels using small molecule and molecular approaches following DCA and 17-AAG exposure blunted the enhanced and prolonged activation of both p38 MAPK and JNK1/2 signaling, as well as the induction of cell killing. These findings argue that the primary mode of 17-AAG toxicity in primary hepatocytes is in part based on the generation of ROS and that the toxic interaction of 17-AAG and DCA is dependent on prolonged generation of ROS by mitochondria. As hepatocytes are known to contain significantly more mitochondria per cell than many other cell types (Cox et al. 2000), these findings may explain why the liver is a site of dose limiting toxicity for geldanamycins.

Previous manuscripts from our group have demonstrated that bile acid-induced activation of JNK1/2 in hepatocytes is dependent upon increased ceramide levels and not upon ROS generation; ceramide generation being reliant on the activation of acidic sphingomyelinase (ASMase). As 17-AAG and DCA promoted JNK1/2 activation, we examined the impact of ASMase function on 17-AAG and DCA toxicity. Loss of ASMase function reduced JNK1/2 activation under all treatment conditions that correlated with lower levels of cell killing following 17-AAG and DCA alone, as well as the 17-AAG and DCA combination exposure. Loss of ASMase function also suppressed activation of p38 MAPK by DCA and by combined DCA and 17-AAG treatment. Thus in addition to confirming our prior findings with DCA, the present studies demonstrate that 17-AAG lethality as a single agent in hepatocytes requires ASMase function. The role of ASMase signaling with respect to ROS generation was also investigated: loss of ASMase function considerably reduced ROS generation by DCA and 17-AAG exposure, arguing that ceramide generation may also play a role in the ability of these agents to generate ROS, activate JNK1/2 and p38 MAPK, and promote cell killing.

Several studies have noted that bile acids generate ROS in hepatocytes, and that lower levels and more transient generation of ROS promoted activation of growth factor receptors and the ERK1/2 and AKT pathways (Fang et al. 2004, Dent et al. 2005). The higher and more prolonged generation of ROS induced by 17-AAG and DCA modestly enhanced ERK1/2 and AKT activation above that induced by DCA alone 2 hours after

exposure, whereas in contrast to the p38 MAPK and JNK1/2 pathways, no significant enhancement in the activation of ERK1/2 and AKT was observed at the 4 hour and 6 hour time points. Previous data from this group has argued that ERK1/2 and PI3K activation, following DCA exposure, is part of a compensatory survival response emanating from ErbB1 which counteracts DCA-induced, ceramide-dependent, activation of the FAS receptor and JNK1.

We then tested whether modulation of MEK1/2 and AKT signaling could alter activation of JNK1/2 and p38 MAPK, and cell survival. Expression of constitutively active AKT modestly reduced 17-AAG toxicity by approximately 50% and fully suppressed cell killing by DCA and 17-AAG, coinciding with a modest reduction in the total JNK1/2 activity under all treatment conditions as well as with suppression of the enhancement of JNK1/2 activation following DCA and 17-AAG exposure. Thus a portion of the protective effect of activated AKT may be due to a partial suppression of JNK1/2 signaling. Constitutively active AKT did not alter p38 MAPK activation. Activated MEK1, but not active AKT, suppressed the modest levels of DCA toxicity, but had no effect on survival after DCA and 17-AAG treatment. Thus, 17-AAG either inhibits protective MEK-ERK signaling at a downstream site, or 17-AAG recruits signaling pathways to kill hepatocytes whose pro-apoptotic functions cannot be suppressed by activated MEK1.

In contrast to data using activated constructs of AKT and MEK1, expression of dominant negative MEK1, treatment with the PI3K inhibitor LY294002, but not expression of dominant negative AKT significantly enhanced the lethality of both DCA and DCA and 17-AAG treatment. Prior manuscripts from this group have shown that inhibition of PI3K blocks bile acid-induced activation of both ERK1/2 and AKT. Collectively with our other findings, this data argues that DCA and DCA and 17-AAG-induced compensatory activation of the PI3K / MEK1/2 / ERK1/2 pathway plays a greater role in maintaining cell viability than activation of the PI3K / AKT pathway, i.e. MEK-ERK signaling represents the key initial endogenous compensatory protective signaling response for hepatocellular survival.

The protection of cells from 17-AAG and DCA exposure by activated AKT signaling could have been mediated by several previously reported mechanisms, including suppression of enhanced JNK1/2 activation, and inhibitory phosphorylation of ASK1 and Bax. In contrast to data using ROS quenching agents that only suppressed the enhanced activation of p38 MAPK and JNK1/2 following 17-AAG and DCA treatment, expression of dominant negative ASK1 nearly abolished activation of p38 MAPK by all agonists. Thus, inhibition of ASK1 function disrupts ROS-independent mechanisms by which p38 MAPK is activated in hepatocytes. Expression of dominant negative ASK1 did not alter JNK1/2 activation, but in a similar manner to active AKT, abolished the enhanced activation of JNK1/2 following combined 17-AAG and DCA exposure. In theory, these

findings may correlate with reduced Bax association with mitochondria, increased Bax inhibitory phosphorylation at an AKT-dependent site and demonstrate that DCA and 17-AAG-stimulated association of Bax with mitochondria is p38 MAPK and JNK1/2 dependent. Collectively, these findings would argue that activated AKT blocks DCA and 17-AAG-induced cell killing at multiple points within the chain of events leading to apoptosis.

4.4 Conclusions

We used purified GST-MDA-7 protein to show that GST-MDA-7, but not GST, caused a dose-dependent reduction in A498 and UOK121N proliferation but not that of primary renal epithelial cells. Free radical species, generated by clinically relevant concentrations of arsenic trioxide, synergized with subnanomolar concentrations of GST-MDA-7 to inhibit the proliferation, viability, and long-term survival of renal cell carcinoma. These findings resulted in the rejection of the null hypothesis and argue that MDA-7, in combination with agents that generate free radicals, may have potential in the treatment of renal cell carcinoma (RCC).

We showed that Ad.*mda-7* exerted anti-proliferative effects on GBM cells and when utilized in combination with ionizing radiation, the anti-proliferative effects of Ad.*mda-7* were enhanced by radiation in a greater than additive fashion. These findings correlated with an *in vitro* cellular change of enhanced cell numbers in the G₁/G₀ and G₂/M phases

of the cell cycle, implying Ad.*mda-7* radiosensitizes tumor cells in a cell cycle-independent manner, and that these effects were not observed in cultures of non-transformed primary astrocytes. These findings resulted in the rejection of the null hypothesis and also argue that Ad.*mda-7*, in combination with ionizing radiation, may have potential in the treatment of glioblastoma multiforme (GBM).

Our data also shows that the geldanamycin derivative 17-allylamino, 17-demethoxygeldanamycin (17-AAG) interacts with the secondary bile acid, deoxycholic acid (DCA), to kill primary rat hepatocytes and human hepatoma cells. An effect abolished by the addition of the free radical quenchers, N-acetyl cysteine and Trolox. These findings resulted in the rejection of the null hypothesis and, collectively, argue that geldanamycins may not be a viable therapy for HCC treatment and that 17-AAG toxicity in primary hepatocytes may be, at least upon initial drug exposure, due to mechanisms independent of Hsp90 inhibition and down-regulation of “classical” Hsp90 client proteins.

References

- Adams, J., and Cory, S. "The Bcl-2 protein family: Arbiters of cell survival." Science 281 (1998): 1322-1326.
- Adams, J. "The development of proteasome inhibitors as anticancer drugs." Cancer Cell 5 (2004): 417-421.
- Alessi, D., Anjelkovic, M., Caudwell, B., Cron, P., Morrice, N., Cohen, P., and Hemmings, B. "Mechanism of activation of protein kinase B by insulin and IGF-1." EMBO JOURNAL 15 (1996): 6541-6551.
- Altieri, D. "Survivin and apoptosis control." Advances in Cancer Research 88 (2003): 31-52.
- Balaban, R., Nemoto, S., and Finkel, T. "Mitochondria, oxidants, and aging." Cell 120 (2005): 483-495.
- Barchowsky, A., Klei, L., Dudek, E., Swartz, H., and James, P. "Stimulation of reactive oxygen, but not reactive nitrogen species, in vascular endothelial cells exposed to low levels of arsenite." Free Radical Biology in Medicine 27 (1999): 1405-1412.
- Barchowsky, A., Roussel, R., Klei, L., James, P., Ganju, N., Smith, K., and Dudek, E. "Low levels of arsenic trioxide stimulate proliferative signals in primary vascular cells without activating stress effector pathways." Toxicology and Applied Pharmacology 159 (1999): 65-75.
- Bedner, E., Li, X., Kucicki, J., and Darzynkiewicz, Z. "Translocation of Bax to mitochondria during apoptosis measured by laser scanning cytometry." Cytometry 41 (2000): 83-88.
- Behrsing, H., Amin, K., Ip, C., Jimenez, L., and Tyson, C. "In vitro detection of differential and cell-specific hepatobiliary toxicity induced by geldanamycin and 17-allylaminogeldanamycin in rats." Toxicology in Vitro 19 (2005): 1079-1088.
- Beliakoff, J., and Whitesell, L. "Hsp90: an emerging target for breast cancer therapy." Anticancer Drugs 7 (2004): 651-662.
- Biade, S., Stobbe, C., and Chapman, J. "The intrinsic radiosensitivity of some human tumor cells throughout their cell cycles." Radiation Research 147 (1997): 416-421.

- Bouillet, P., and Strasser, A. "BH3-only proteins – evolutionarily conserved proapoptotic Bcl-2 family members essential for initiating programmed cell death." Journal of Cell Science 115 (2002): 1567-1574.
- Boulton, T., and Cobb, M. "Identification of multiple extracellular signal-regulated kinases (ERKs) with antipeptide antibodies." Cell Regulation 2 (1991): 357-371.
- Brunet, A., Bonni, A., Zigmond, M., Lin, M., Juo, P., Hu, L., Anderson, M., Arden, K., Blenis, J., and Greenberg, M. "AKT promotes cell survival by phosphorylating and inhibiting a Forkhead transcription factor." Cell 96 (1999): 857-868.
- Budihardjo I, Oliver H, Lutter M, Luo X, and Wang X. "Biochemical pathways of caspase activation during apoptosis." Annual Review of Cell Developmental Biology 15 (1999): 269-290.
- Cantley, L., and Neel, B. " " Proceedings of the National Academy of Science of the United States of America 96 (1999): 4240-4245.
- Cantley, L., "The phosphoinositide 3-kinase pathway." Science 296 (2002): 1655-1657.
- Carraway, K. "Involvement of the neuregulins and their receptors in cardiac and neural development." Bioessays 18 (1996): 263-266.
- Cartee, L., Vrana, J., Wang, Z., Park, J., Birrer, M., and Fisher, P. "Inhibition of the mitogen activated protein kinase pathway potentiates radiation-induced cell killing via cell cycle arrest at the G2/M transition and independently of increased signaling by the JNK/c-Jun pathway." International Journal of Oncology 16 (2000): 413-422.
- Casamayor, A., Morrice, N., and Alessi, D. "Phosphorylation of Ser-241 is essential for the activity of 3-phosphoinositide-dependent protein kinase-2: identification of five sites of phosphorylation in vivo." Biochemical Journal 342 (1999): 287-292.
- Chada, S., Neumanaitis, J., Tong, A., Zhang, Y., Su, D., Mhashilkar, A., Zhou-Yang, H., Parker, K., Wilson, D., Merritt, J., and Coffee, K. "A Phase I dose-escalation study of Ad.*mda-7* in patients with advanced carcinoma." Cancer Gene Therapy 8(Supplement 2) (2001): S3.
- Clem R, Cheng E, Karp C, Kirsch D, Ueno K, Takahashi A, Kastan M, Griffin D, Earnshaw W, Veluona M, Hardwick J. "Modulation of death by Bcl-X_L through caspase interaction." Proceedings of the National Academy of Science 95 (1998): 554-559.

- Connell, P., Ballinger, C., Jiang, J., Wu, Y., Thompson, L., Hohfeld, J., and Patterson, C. "The co-chaperone CHIP regulates protein triage decisions mediated by heat-shock proteins." Nature and Cell Biology 3 (2001): 93-96.
- Cox, M., and Nelson, D. Lehninger Principles of Biochemistry. 3rd ed. New York: Worth Publishers, 2000.
- Craxton, A., Draves, K., Gruppi, A., and Clark, E. "BAFF regulates B cell survival by downregulating the BH3-only family member Bim via the ERK pathway." The Journal of Experimental Medicine 202 (2005): 1363-1374.
- Cross, D., Alessi, D., Cohen, P., Andjelkovich, M., and Hemmings, B. "Inhibition of glycogen synthase kinase-3 by insulin mediated by protein kinase B." Nature 378 (1995): 785-789.
- Curiel, D.T. "Strategies to adapt adenoviral vectors for targeted delivery." Annals of the New York Academy of Science 886 (1999): 158-171.
- Dai, Y., Landowski, T.H., Rosen, S.T., Dent, P., and Grant, S. "Combined treatment with the checkpoint abrogator UCN-01 and MEK1/2 inhibitors potently induces apoptosis in drug-sensitive and -resistant myeloma cells through an IL-6-independent mechanism." Blood 100 (2002): 3333-3343.
- Daugas, E., Nochy, D., Ravagnan, L., Loeffler, M., Susin, S., Zamzami, N., and Kroemer, G. "Apoptosis-inducing factor (AIF): a ubiquitous mitochondrial oxidoreductase involved in apoptosis." FEBS Letters 476 (2000): 118-123.
- Deak, M., Clifton, A., Lucocq, L., Alessi, D. "Mitogen- and stress-activated protein kinase-1 (MSK1) is directly activated by MAPK and SAPK2/p38, and may mediate activation of CREB." EMBO JOURNAL 17 (1998): 4426-4441.
- Dent, P., Reardon, D., Park, J., Bowers, G., Logsdon, C., and Valerie, K. "Radiation-induced release of transforming growth factor activates the epidermal growth factor receptor and mitogen-activated protein kinase pathway in carcinoma cells, leading to increased proliferation and protection from radiation-induced cell death." Molecular Biology of the Cell 10 (1999): 2493-2506.
- Dent, P., Fang, Y., Gupta, S., Studer, E., Mitchell, C., Spiegel, S., and Hylemon, P. "Conjugated bile acids promote ERK1/2 and AKT activation via a pertussis toxin-sensitive mechanism in murine and human hepatocytes." Hepatology 42 (2005): 1291-1299.

- Dent, P., Yacoub, A., Contessa, J., Caron, R., Amorino, G., Valerie, K., Hagan, M., Grant, S., and Schmidt-Ullrich, R. "Stress and radiation-induced activation of multiple intracellular signaling pathways." Radiation Research Society Annual Meeting April (2002): 1-40.
- Derijard, B., Raingeaud, J., Barret, T., Wu, I., Han, J., Ulevitch, R., and Davis, R. "Independent human MAP-kinase signal transduction pathways defined by MEK and MKK isoforms." Science 267 (1995): 682-685.
- Dewey, W., Ling, C., and Meyn, R. "Radiation-induced apoptosis: relevance to radiotherapy." International Journal of Radiation Oncology*Biophysics 33 (1995): 781-796.
- Diehl, J., Cheng, M., Roussel, M., and Sherr, C. "Glycogen synthase kinase-3beta regulates cyclin D1 proteolysis and subcellular localization." Genes & Development 12 (1998): 3499-3511.
- Downward, J. "How BAD phosphorylation is good for survival." Nature Cell Biology 1 (1999): E33-35.
- Du, C., Fang, M., Li, Y., Li, L., and Wang, X. "Smac, a mitochondrial protein that promotes cytochrome c-dependent caspase activation by eliminating IAP inhibition." Cell 102 (2000): 33-42.
- Dumoutier, L., Leemans, C., Lejeune, D., Kotenko, S., and Renauld, J. "Cutting edge: STAT activation by IL-19, IL-20 and mda-7 through IL-20 receptor complexes of two types." Journal of Immunology 167 (2001): 3545-3549.
- Earnshaw W, Martins L, and Kaufmann S. "Mammalian caspases: structure, activation, substrates, and functions during apoptosis." Annual Review in Biochemistry 68 (1999): 383-424.
- Ekmekcioglu, S., Ellerhorst, J., Mhashilkar, A.M., Sahin, A.A., Read, C.M., Prieto, V.G., Chada, S., and Grimm, E.A. "Down-regulated melanoma differentiation associated gene (mda-7) expression in human melanomas." International Journal of Cancer 94 (2001): 54-59.
- Ellerhorst, J., Prieto, V., Ekmekcioglu, S., Broemeling, I., Yekell, S., and Chada, S. Loss of MDA-7 expression with progression of melanoma." Journal of Clinical Oncology 20 (2002): 1069-1074.

- Franke, T., Kaplan, D., and Cantley, L. "PI3K: downstream AKTion blocks apoptosis." Cell 88 (1997): 435-437.
- Funamoto, S., Meili, R., Lee, S., Parry, L, and Firtel, R. "Spatial and temporal regulation of 3-phosphoinositides by PI 3-kinase and PTEN mediates chemotaxis." Cell 109 (2002): 611-623.
- Fang, Y., Han, S., Mitchell, C., Gupta, S., Studer, E., Grant, S., Hylemon, P., and Dent, P. "Bile acids induce mitochondrial ROS, which promote activation of receptor tyrosine kinases and signaling pathways in rat hepatocytes." Hepatology 40 (2004): 961-971.
- Gesbert, F., Sellers, W., Signoretti, S., Loda, M., and Griffin, J. "BCR/ABL regulates expression of the cyclin-dependent kinase inhibitor p27Kip1 through the phosphatidylinositol 3-Kinase/AKT pathway." Journal of Biological Chemistry 275 (2001): 39223-39230.
- Glaspay, J.A.."Therapeutic options in the management of renal cell carcinoma." Seminars in Oncology 29 (2002): 41-46.
- Godley, P., Taylor M. "Renal cell carcinoma." Current Opinion in Oncology 13 (2001): 199-203.
- Gomez-Navarro, J., and Curiel, D.T. "Conditionally replicative adenoviral vectors for cancer gene therapy." Lancet Oncology 1 (2000): 148-158.
- Grad, J.M., Bahlis, N.J., Reis, I., Oshiro, M.M., Dalton, W.S., and Boise, L.H. "Ascorbic acid enhances arsenic trioxide-induced cytotoxicity in multiple myeloma cells". Blood 98 (2001): 805-813.
- Grant, S., Qiao, L., and Dent, P. "Roles of ErbB family receptor tyrosine kinases, and downstream signaling pathways, in the control of cell growth and survival." Frontiers in Bioscience 7 (2002): 376-389.
- Greenlee, R., Murray, T., and Bolden, S. "Cancer statistics 2000." Cancer Journal of Clinicians 50 (2000): 7-33.
- Gulli, L.F., Palmer, K.C., Chen, Y.Q., and Reddy, K.B. "Epidermal growth factor-induced apoptosis in A431 cells can be reversed by reducing the tyrosine kinase activity." Cell Growth and Differentiation 7 (1996): 173-178.

- Gupta, A., Bakanauskas, V., Cerniglia, G., Cheng, Y., Bernhard, E., and Muschel, R. "The Ras radiation resistance pathway." Cancer Research 61 (2001): 4278-4282.
- Gupta, A., McKenna, W., Weber, C., Feldman, M., Goldsmith, J., and Mick, R. "Local recurrence in head and neck cancer: relationship to radiation resistance and signal transduction." Clinical Cancer Research 8 (2002): 885-892.
- Gupta, S., Stravitz, R.T., Dent, P., and Hylemon, P.B. "Down-regulation of cholesterol 7alpha-hydroxylase (CYP7A1) gene expression by bile acids in primary rat hepatocytes is mediated by the c-Jun N-terminal kinase pathway." Journal of Biological Chemistry 276 (2001): 15816-15822.
- Gupta, S., Yei, L., Kim, D., Kim, C., Chiplunkar, S., and Gollapudi, S. "Arsenic trioxide induces apoptosis in peripheral blood T lymphocyte subsets by inducing oxidative stress: A role of Bcl-2." Molecular Cancer Therapeutics 2 (2003): 711-719.
- Hacki, J., Egger, L., Monney, L., Conus, S., Fellay, L., and Borner, C. "Apoptotic crosstalk between the endoplasmic reticulum and mitochondria controlled by Bcl-2." Oncogene 19 (2000): 2286-2295.
- Hagan, M., Wang, L., Hanley, J., Park, J., and Dent, P. "Ionizing radiation induced mitogen activated protein kinase activation in DU145 prostate carcinoma cells: MAP kinase inhibition enhances radiation-induced cell killing and G2/M phase arrest." Radiation Research 153 (2000): 371-383.
- Hajduch, E., Litherland, G., and Hundal, H. "Protein kinase B (PKB/AKT)-a key regulator of glucose transport?" FEBS Letters 492 (2001): 199-203.
- Halicka, H.D., Smolewski, P., Darzynkiewicz, Z., Dai, W., and Traganos, F. "Arsenic trioxide arrests cells early in mitosis leading to apoptosis." Cell Cycle 1 (2002): 201-209.
- Haviv, Y.S., Blackwell, J.L., Kanerva, A., Nagi, P., Krasnykh, V., Dmitriev, I., Wang, M., Naito, S., Lei, X., Hemminki, A., Carey, D., and Curiel, D.T. "Adenoviral gene therapy for renal cancer requires retargeting to alternative cellular receptors." Cancer Research 62 (2002): 4273-4281.
- Hibi, M., Lin, A., Smeal, T., Minden, A., and Karin, M. "Identification of an oncoprotein- and UV-responsive protein kinase that binds and potentiates the c-Jun activation domain." Genes and Development 7 (1993): 2135-2148.

- Hsieh, C., and Papaconstantinou, J. "Thioredoxin-ASK1 complex levels regulate ROS-mediated p38 MAPK pathway activity in livers of aged and long-lived Snell dwarf mice." The FASEB Journal 20 (2006): 259-268.
- Hsuan, J., Panayotou, G., and Waterfield, M. "Structural basis for epidermal growth factor receptor function." Progress in Growth Factor Research 1 (1989): 23-32.
- Huang, G., Ouyang, X., and Epstein, R. "Proxy activation of protein ErbB2 by heterologous ligands implies a heterotetrameric mode of receptor tyrosine kinase interaction." Biochemical Journal 331 (1998): 113-119.
- Hyun Park, W., Hee Cho, Y., Won Jung, C., Oh Park, J., Kim, K., Hyuck Im, Y., Lee, M.H., Ki Kang, W., and Park, K. "Arsenic trioxide inhibits the growth of A498 renal cell carcinoma cells via cell cycle arrest or apoptosis." Biochemical and Biophysical Research Communications 300 (2003): 230-235.
- Iijima, M., and Devreotes, P. "Tumor suppressor PTEN mediates sensing of chemoattractant gradients." Cell 109 (2002): 599-610.
- Inoki, K., Li, Y., Zhu, T., Wu, J., and Guan, K. "TSC2 is phosphorylated and inhibited by AKT and suppresses mTOR signalling." Nature and Cell Biology 4 (2002): 648-657.
- Iwama, K., Nakajo, S., Aiuchi, T., and Nakaya, K. "Apoptosis induced by arsenic trioxide in leukemia U937 cells is dependent on activation of p38, inactivation of ERK and the Ca²⁺-dependent production of superoxide." International Journal of Cancer 92 (2001): 518-526.
- Janeway, C., Travers, P., Walport, M., and Sclomchik, M. Immunobiology 5th ed. New York: Garland Publishing, 2001.
- Janicke, R., Sprengart, M., Wati, M., and Porter, A. "Caspase-3 is required for DNA fragmentation and morphological changes associated with apoptosis." Journal of Biological Chemistry 273 (1998): 9357-9360.
- Jiang, H., Lin, J., Su, Z., Goldstein, N., and Fisher, P. "Subtraction hybridization identifies a novel melanoma differentiation associated gene, mda-7, modulated during human melanoma differentiation, growth and progression." Oncogene 11 (1995): 2477-2486.
- Jiang, H., Su, Z., Lin, J., Goldstein, N., Young, C., and Fisher, P. "The melanoma differentiation associated gene mda-7 suppresses cancer cell growth."

Proceedings of the National Academy of Science of the United States of America 93 (1996): 9160-9165.

- Jiang, T., and Qiu, Y. "Interaction between Src and a C-terminal proline-rich motif of AKT is required for AKT activation." Journal of Biological Chemistry 278 (2003): 15789-15793.
- Jing, Y., Yang, J., He, R., Gao, F., Sang, H., Tang, X., and Ye, R. "Emodin enhances arsenic trioxide-induced apoptosis via generation of reactive oxygen species and inhibition of survival signaling." Cancer Research 64 (2004): 108-116.
- Juretic, N., Santibanez, J., Hurtado, C., and Martinez, J. "ERK 1,2 and p38 pathways are involved in the proliferative stimuli mediated by urokinase in osteoblastic SaOS-2 cell line." Journal of Cellular Biochemistry 83 (2001): 92-98.
- Kasof, G., and Gomes, B. "Livin, a novel inhibitor of apoptosis protein family member." The Journal of Biological Chemistry 276 (2001): 3238-3246.
- Kato, K., Ito, H., Iwamoto, I., Lida, K., and Inaguma, Y. "Protein kinase inhibitors can suppress stress-induced dissociation of Hsp27." Cell Stress Chaperones 6 (2001): 16-20.
- Kawabe, S., Nishikawa, T., Munshi, A., Roth, J.A., Chada, S., and Meyn, R.E. "Adenovirus-mediated mda-7 gene expression radiosensitizes non-small cell lung cancer cells via TP53-independent mechanisms." Molecular Therapeutics 6 (2002): 637-644.
- Kim, S., Ju, J., Oh, C., Yoon, Y., Song, W., Kim, J., Yoo, Y., Bang, O., Kang, S., and Chun, J. "ERK1/2 and p38 kinase oppositely regulate nitric oxide-induced apoptosis of chondrocytes in association with p53, caspase-3, and differentiation status." Journal of Biological Chemistry 277 (2002): 1332-1339.
- Klein, J., Longo-Guess, C., Rossmann, M., Seburn, K., Hurd, R., Frankel, W., Bronson, R., and Ackerman, S. "The harlequin mouse mutation downregulates apoptosis-inducing factor ." Nature 419 (2002): 367-374.
- Korsmeyer, S., Shutter, J., Veis, D., Merry, D., and Oltvai, Z. "Bcl-2/Bax: a rheostat that regulates an anti-oxidant pathway and cell death." Seminars in Cancer Biology 4 (1993): 327-332.
- Kyriakis, J., App, H., Zhang, X., Banerjee, P., Brautigan, D., Rapp, U., and Avruch, J. "Raf-1 activates MAP Kinase-Kinase." Nature 358 (1992): 417-421.

- Lai, M., Huang, K., Chang, W., and Lai, Y. "Geldanamycin induction of grp78 requires activation of reactive oxygen species via ER stress responsive elements in 9L rat brain tumour cells." Cellular Signalling 6 (2003): 585-595.
- Lebedeva, I., Su, Z., Chang, Y., Kitada, S., Reed, J., and Fisher, P. "The cancer growth suppressing gene mda-7 induces apoptosis selectively in human melanoma cells." Oncogene 21 (2002): 708-718.
- Lebedeva, I., Su, Z., Sarkar, D., Kitada, S., Dent, P., Waxman, S., Reed, J., and Fisher, P. "Melanoma differentiation associated Gene-7, *mda-7*/Interleukin-24, induces apoptosis in prostate cancer cells by promoting mitochondrial dysfunction and inducing reactive oxygen species." Cancer Research 63 (2003): 8138-8144.
- Lee, S., Eom, M., Lee, S., Kim, S., Park, H., and Park, D. "BetaPix-enhanced p38 activation by Cdc42/Rac/PAK/MKK3/6-mediated pathway. Implication in the regulation of membrane ruffling." Journal of Biological Chemistry 276 (2001): 25066-25072.
- Lee, Y., Soh, J., Dean, N., Cho, C., Kim, Tt., and Lee, Y. "Protein kinase C-delta overexpression enhances radiation sensitivity via extracellular regulated protein kinase 1/2 activation, abolishing the radiation-induced G(2)-M arrest." Cell Growth and Differentiation 13 (2002): 237-246.
- Leervers, J., Paterson, H., and Marshall, C. "Requirement for Ras in Raf activation is overcome by targeting Raf to the plasma membrane." Nature 369 (1994): 411-414.
- Levin, V., Gutin, P., and Leibel, S. "Neoplasms of the central nervous system." Cancer: Principles and Practice of Oncology. 4th ed. Philadelphia: Lippincott. 1993. pgs. 1679-1737.
- Lin, T., Genestier, L., Pinkoski, M., Castro, A., Nicholas, S., Mogil, R., Paris, F., Fuks, Z., Schuchman, E., Kolesnick, R., and Green, D. "Role of acidic sphingomyelinase in Fas/CD95-mediated cell death." The Journal of Biological Chemistry 275 (2000): 8657-8663.
- Lin, A., Minden, A., Martinetto, H., Claret, F., Lange-Carter, C., Mercurio, F., Johnson, G., and Karin, M. "Identification of a dual specificity kinase that activates the Jun kinases and p38-Mpk2." Science 268 (1995): 286-290.

- Lipton, S., and Bossy-Wetzel, E. "Dueling activities of AIF in cell death versus survival: DNA binding and redox activity." Cell 111 (2002): 147-150.
- Liu, W., Guo, x., Chen, Q., and Guo, Z. "Opposing effect of p38 and p44/42 signaling on TNF-alpha-induced apoptosis in bovine aortic endothelial cells." Acta Pharmacologica Sinica (APS) 22 (2001): 405-410.
- Liu, Y., Nishikawa, T., Vorburger, S.A., Meyn, R.E., Swisher, S.G., Chada, S., Mirza, N., Hunt, K.K. "Adenoviral-mediated expression of the MDA-7 gene sensitizes breast carcinoma cells to ionizing radiation." Proceedings of the American Association of Cancer Research 62 (2002): 3209.
- Madireddi, M.T., Su, Z.-z., Young, C.S.H., Goldstein, N.I., and Fisher. P.B. "*Mda-7*, a novel melanoma differentiation associated gene with promise for cancer gene therapy." Advanced Experimental Medicine and Biology 465 (2000): 239-261.
- Maizels, E., Mukherjee, A., Sithanandam, G., Peters, C., Cottom, J., Mayo, K., and Hunzicker-Dunn, M. "Developmental regulation of mitogen-activated protein kinase-activated kinases-2 and -3 (MAPKAPK-2/-3) *in vivo* during corpus luteum formation in the rat." Molecular Endocrinology 15 (2001): 716-33.
- Manning, B., Tee, A., Logsdon, M., Blenis, J., and Cantley, L. "Identification of the tuberous sclerosis complex-2 tumor suppressor gene product tuberlin as a target of the phosphoinositide 3-kinase/AKT pathway." Molecular Cell 10 (2002): 151-162
- Mayo, L., and Donners, D. "A phosphatidylinositol 3-kinase/AKT pathway promotes translocation of Mdm2 from the cytoplasm to the nucleus." Proceedings of the National Academy of Science of the United States of America 98 (2001): 11598-11603.
- McKinstry, R., Qiao, L., Yacoub, A., Dai, Y., Decker, R., Holt, S., Hagan, M., Grant, S., and Dent, P. "Inhibitors of MEK1/2 interact with UCN-01 to induce apoptosis and reduce colony formation in mammary and prostate carcinoma cells." Cancer Biology and Therapy 1 (2002): 243-253.
- Mhashilkar, A., Schrock, R., Hindi, M., Liao, J., Sieger, K., Kourouma, F., Zou-Yang, X., Onishi, E., Takh, O., Vedvick, T.S., Fanger, G., Stewart, L., Watson, G., Snary, D., Fisher, P., Saeki, T., Roth, J., Ramesh, R., and Chada, S. "Melanoma differentiation associated gene-7 (*mda-7*): a novel anti-tumor gene for cancer gene therapy." Molecular Medicine 7 (2001): 271-282.

- Miller, W.H. Jr, Schipper, H.M., Lee, J.S., Singer, J., and Waxman, S. "Mechanisms of action of arsenic trioxide." Cancer Research 62 (2002): 3893-3903.
- Miller, W.H. Jr. "Molecular targets of arsenic trioxide in malignant cells." Oncologist 7 (2002): 14-19.
- Milowsky, M.I., and Nanus, D.M. "Advanced renal cell carcinoma." Current Treatment Options in Oncology 2 (2001): 437-445.
- Moodie, A., Willumsen, B., Weber, M., and Wolfman, A. "Complexes of Ras.GTP with Raf-1 and Mitogen-activated Protein Kinase Kinase." Science 260 (1993): 1658-1661.
- Morrison, D., and Cutler, E. "The complexity of Raf-1 regulation." Current Opinion in Cell Biology 9 (1997): 174-179.
- Morishima, N., Nakanishi, K., Takenouchi, H., Shibata, T., and Yasuhiko, Y. "An endoplasmic reticulum stress-specific caspase cascade in apoptosis. Cytochrome c-independent activation of caspase-9 by caspase-12." Journal of Biological Chemistry 277 (2002): 34287-34294.
- Morishima, N., Nakanishi, K., Tsuchiva, K., Shibata, T., and Seiwa, E. "Translocation of Bim to the endoplasmic reticulum (ER) mediates ER stress signaling for activation of caspase-12 during ER stress-induced apoptosis." Journal of Biological Chemistry 279 (2004): 50375-50381.
- Motzer R. J., Bander N. H., Nanus D. M. "Renal-cell carcinoma." New England Journal of Medicine 335 (1996): 865-875.
- Myers, M., Stolarov, J., Eng, C., Li, J., Wang, S., Wigler, M., Parsons, R., and Tonks, N. "P-TEN, the tumor suppressor from human chromosome 10q23, is a dual-specificity phosphatase." Proceedings of the National Academy of Science of the United States of America 94 (1997): 9052-9057.
- Nakanishi, K., Sudo, T., and Morishima, N. "Endoplasmic reticulum stress signaling transmitted by ATF6 mediates apoptosis during muscle development." Journal of Cell Biology 169 (2005): 555-560.
- National Cancer Institute Home Page. <http://www.nci.org> June 20, 2006.

- Navas, T., Baldwin, D., and Stewart, T. "RIP2 is a Raf1-activated Mitogen-activated Protein Kinase Kinase." Journal of Biological Chemistry 274 (1999): 33684-33690.
- Nelson, D., and Cox, M. Lehninger: Principles of Biochemistry. 3rd edition. New York: Worth Publishers, 2000.
- Neri, L., Borgatti, P., Capitani, S., and Martelli, A. "The nuclear phosphoinositide 3-kinase/AKT pathway: a new second messenger system." Biochimica et Biophysica Acta 1584 (2002): 73-80.
- Noguchi, K., Kitanaka, C., Yamana, H., Kokubu, A., Mochizuki, T., and Kuchino, Y. "Regulation of c-Myc through phosphorylation at Ser-62 and Ser-71 by c-Jun N-terminal kinase." Journal of Biological Chemistry 274 (1999): 32580-32587.
- Okegawa, T., Pong, R., Li, Y., Bergelson, J., Sagalowsky, A., Hsieh, J. "The mechanism of the growth-inhibitory effect of coxsackie and adenovirus receptor (CAR) on human bladder cancer: a functional analysis of car protein structure." Cancer Research 61 (2001): 6592-6600.
- Olinski, R., Gackowski, D., Foksinski, M., Rozalski, R., Roszkowski, K., and Jaruga, P. "Oxidative DNA damage: Assessment of the role in carcinogenesis, atherosclerosis, and acquired immunodeficiency syndrome." Free Radical Biology and Medicine 33 (2002): 192-200.
- Paik, S., and Park, C. "HER-2 and choice of adjuvant chemotherapy in breast cancer." Seminars in Oncology 28 (2001): 332-335.
- Park, J., Hill, M., Hess, D., Brazil, D., Hofsteenge, J., and Hemmings, B. "Identification of tyrosine phosphorylation sites on 3-phosphoinositide-dependent protein kinase-1 and their role in regulating kinase activity." Journal of Biological Chemistry 276 (2001): 37459-37471.
- Park, J., Qiao, L., Su, z., Hinman, D., Willoughby, K., McKinstry, R., Yacoub, A., Duigou, G., Young, C., Grant, S., Hagan, M., Ellis, E., Fisher, P., and Dent P. "Ionizing radiation modulates vascular endothelial growth factor (VEGF) expression through multiple mitogen activated protein kinase dependent pathways." Oncogene 20 (2001): 3266-3280.
- Parrish-Novak, J., Xu, W., Brender, T., Yao, L., Jones, C., West, J., Brandt, C., Jelinek, L., Madden, K., McKernan, P.A., Foster, D.C., Jaspers, S., and Chandrasekher, Y.A. "Interleukins 19, 20, and 24 signal through two distinct receptor complexes.

- differences in receptor-ligand interactions mediate unique biological functions.” Journal of Biological Chemistry 277 (2002): 47517-47523.
- Pestka, S., Kotenko, S., and Fisher, P. “IL-24” Encyclopedia of Hormones H.L. Henry and A.W. Norman ed. New York: Academic Press, 2004.
- Pickart, C. “Back to the future with ubiquitin.” Cell 116 (2004): 181-190.
- Ponnazhagan, S., Curiel, D., Shaw, D., Alvarez, R., and Siegal, G. “Adeno-associated virus for cancer gene therapy.” Cancer Research 61 (2001): 6313-6321.
- Qiao, L., Studer, E., Leach, K., McKinstry, R., Gupta, S., Decker, R., Kukreja, R., Valerie, K., Nagarkatti, P., El Deiry, W., Molkentin, J., Schmidt-Ullrich, R., Fisher, P.B., Grant, S., Hylemon, P.B., and Dent P. “Deoxycholic acid (DCA) causes ligand-independent activation of epidermal growth factor receptor (EGFR) and FAS receptor in primary hepatocytes: inhibition of EGFR/mitogen-activated protein kinase-signaling module enhances DCA-induced apoptosis.” Molecular Biology of the Cell 12 (2001): 2629-2645.
- Qin, P., Tang, X., Elloso, M., and Harnish, D. “Bile acids induce adhesion molecule expression in endothelial cells through activation of reactive oxygen species, NF κ B and p38.” American Journal of Physiology, Heart and Circulatory Physiology Mar 31 (2006): Epub ahead of print.
- Rauen, K., Sudilovsky, D., Le, J., Chew, K., Hann, B., Weinberg, V., Schmitt, L., and McCormick, F. “Expression of the coxsackie adenovirus receptor in normal prostate and in primary and metastatic prostate carcinoma: potential relevance to gene therapy.” Cancer Research 62 (2002): 3812-3818.
- Romashkova, J., and Makarov, S. “NF- κ B is a target of AKT in anti-apoptotic PDGF signalling.” Nature 401 (1999): 86-90.
- Saeki, T., Mhashilkar, A., Chada, S., Branch, C., Roth, J.A., and Ramesh, R. “Tumor-suppressive effects by adenovirus-mediated mda-7 gene transfer in non-small cell lung cancer cell *in vitro*.” Gene Therapy 7 (2000): 2051-2057.
- Saeki, T., Mhashilkar, A., Swanson, X., Zou-Yang, H., Sieger, K., and Kawabe, S. “Inhibition of human lung cancer growth following adenovirus-mediated mda-7 gene expression *in vivo*.” Oncogene 21 (2002): 4558-4566.

- Sarkar, D., Su, Z., Lebedeva, I., Sauane, M., Gopalkrishnan, R., Dent, P., and Fisher, P. "Mda-7 (IL-24): signaling and functional roles." Biotechniques October (2002): 30-39.
- Sarkar, D., Su, Z.Z., Lebedeva, I.V., Sauane, M., Gopalkrishnan, R.V., Valerie, K., Dent, P., and Fisher, P.B. "Mda-7 (IL-24) Mediates selective apoptosis in human melanoma cells by inducing the coordinated overexpression of the GADD family of genes by means of p38 MAPK." Proceedings of the National Academy of Science of the United States of America 99 (2002): 10054-10059.
- Sauane, M., Gopalkrishnan, R.V., Sarkar, D., Su, Z.Z., Lebedeva, I.V., Dent, P., Pestka, S., and Fisher, P.B. "MDA-7/IL-24: novel cancer growth suppressing and apoptosis inducing cytokine." Cytokine Growth Factor Review 14 (2003): 35-51.
- Schlesinger, T., Fanger, G., Yujiri, T., and Johnson, G. "The TAO of MEKK." Frontiers of Bioscience 3 (1998): D1181-1186.
- Senju, M., Sueoka, N., Sato, A., Iwanaga, K., Sakao, Y., Tomimitsu, S., Tominaga, M., Irie, K., Hayashi, S., and Sueoka, E. "Hsp90 inhibitors cause G2/M arrest associated with the reduction of Cdc25C and Cdc2 in lung cancer cell lines." Journal of Cancer Research in Clinical Oncology 132 (2006): 150-158.
- Shen, Y., Xie, Q., Norberg, M., Sausville, E., Woude, G., and Wenkert, D. "Geldanamycin derivative inhibition of HGF/SF-mediated Met tyrosine kinase receptor-dependent urokinase-plasminogen activation." Bioorganic & Medicinal Chemistry 13 (2005): 4960-4971.
- Simpson, L., and Parsons, R. "PTEN: life as a tumor suppressor." Experimental Cell Research 264 (2001): 29-41.
- Sirica, Alphonse. "Cholangiocarcinoma: molecular targeting strategies for chemoprevention and therapy." Hepatology 41 (2005): 5-15.
- Srinivasula, S., Datta, P., Fan, X., Fernandes-Alnemri, T., Huang, Z., and Alnemri, E. "Molecular determinants of the caspase-promoting activity of Smac/DIABLO and its role in the death receptor pathway." The Journal of Biological Chemistry 275 (2000): 36152-36157.
- Srivastava, A., and Pandey, S. "Potential mechanism(s) involved in the regulation of glycogen synthesis by insulin." Molecular and Cellular Biochemistry 182 (1998): 135-141.

- Stephens, L., Anderson, K., Stokoe, D., Erdjument-Bromage, H., Painter, G., Holmes, A., Gaffney, P., Reese, C., McCormick, F., Tempst, P., Coadwell, J., and Hawkins, P. "Protein kinase B kinases that mediate phosphatidylinositol 3,4,5-trisphosphate-dependent activation of protein kinase B." Science 279 (1998): 710-714.
- Stern, D. "Tyrosine kinase signaling in breast cancer: ErbB1 family receptor tyrosine kinases." Breast Cancer Research 2 (2000): 176-183.
- Stokoe, D., McCormick, F. "Activation of c-Raf-1 by Ras and Src through different mechanisms: activation *in vivo* and *in vitro*." EMBO JOURNAL 16 (1997): 2384-2396.
- Stokoe, D., Stephens, L., Copeland, T., Gaffney, P., Reese, C., Painter, G., Holmes, A., McCormick, F., and Hawkins, P. "Dual role of phosphatidylinositol-3,4,5-trisphosphate in the activation of protein kinase B." Science 277 (1997): 567-570.
- Stoyanov, B., Volinia, S., Hanck, T., Rubio, I., Loubtchenkov, M., Malek, D., Stoyanova, S., Vanhaesebroeck, B., Dhand, R., and Nurnberg, B. "Cloning and characterization of a G protein-activated human phosphoinositide-3 kinase." Science 269 (1995): 690-693.
- Sturgill, T., Ray, L. "Muscle proteins related to microtubule associated protein-2 are substrates for an insulin-stimulatable kinase." Biochemical and Biophysical Research Communications 134 (1986): 565-571.
- Sturgill, T., Ray, L., Erikson, E., and Maller, J. "Insulin-stimulated MAP-2 Kinase phosphorylates and activates ribosomal Protein S6 Kinase II." Nature 334 (1988): 715-718.
- Su, Z.-z., Lebedeva, I.V., Gopalkrishnan, R.V., Goldstein, N.I., Stein, C.A., Reed, J.C., Dent, P., and Fisher, P.B. "A combinatorial approach for selectively inducing programmed cell death in human pancreatic cancer cells." Proceedings of the National Academy of Science: The United States of America 98 (2001): 10332-10337.
- Su, Z.-z., Lebedeva, I., Sarkar, D., Gopalkrishnan, R., Sauane, M., Sigmon, C., Yacoub, A., Valerie, K., Dent P., and Fisher, P.B. "Melanoma differentiation associated gene-7, *mda-7/IL-24*, selectively induces growth suppression, apoptosis and radiosensitization in malignant gliomas in a *p53*-independent manner." Oncogene 22 (2003): 1164-1180.

- Su, Z.-z., Madireddi, M., Lin, J., Young, C., Kitada, S., Reed, J., Goldstein, N., and Fisher, P. "The cancer growth suppressor gene mda-7 selectively induces apoptosis in human breast cancer cells and inhibits tumor growth in nude mice." Proceedings of the National Academy of Science of the United States of America 95 (1998): 14400-14405.
- Susin, S., Lorenzo, H., Zamzami, N., Marzo, I., Snow, B., Brothers, G., Mangion, J., Jacotot, E., Costantini, P., Loeffler, M., Larochette, N., Goodlet, D., Aebersold, R., Siderovski, D., Penninger, J., Kroemer, G. "Molecular characterization of mitochondrial Apoptosis-inducing Factor." Nature 397 (1999): 441-446.
- Szegezdi, E., Fitzgerald, U., and Samali, A. "Caspase-12 and ER stress mediated apoptosis: The story so far." Annals of the New York Academy of Science 1010 (2003): 186-194.
- Taher, M., Hershey, C., Oakley, J., and Valerie, K. "Role of the p38 and MEK1/2/p42/p44 MAP kinase pathways in the differential activation of human immunodeficiency virus gene expression by ultraviolet and ionizing radiation." Photochemistry and Photobiology 71 (2000): 455-459.
- Tamm, I., Kornblau, S., Segall, H., Krajewski, S., Welsh, K., Kitada, S., Scudiero, D., Tudor, G., Qui, Y., Monks, A., Andreeff, M., and Reed, J. "Expression of prognostic significance of IAP-family genes in human cancers and myeloid leukemias." Clinical Cancer Research 6 (2000): 1796-1803.
- Torres, J., and Pulido, R. "The tumor suppressor PTEN is phosphorylated by the protein kinase CK2 at its C-terminus. Implications for PTEN stability to proteasome-mediated degradation." Journal of Biological Chemistry 276 (2001): 993-998.
- Tournier, C., Whitmarsh, A., Cavanagh, J., Barret, T., and Davis, R. "The MKK7 gene encodes a group of c-Jun NH2-terminal kinase kinases." Molecular and Cellular Biology 19 (1999): 1569-1581.
- Trottier, J., Milkiewicz, P., Kaeding, J., Verreault, M., and Barbier, O. "Coordinate regulation of hepatic bile acid oxidation and conjugation by nuclear receptors." Molecular Pharmaceutics 3 (2006): 212-222.
- Tzahar, E., Levkowitz, G., Karunagaran, D., Yi, L., Peles, E., Lavi, S., Chang, D., Liu, N., Yayon, A., Wen, D. and Yarden, Y. "ErbB3 and ErbB4 Function as the Respective Low and High Affinity Receptors of All Neu Differentiation Factor/hergulin Isoforms." Journal of Biological Chemistry 269 (1994): 25226-25233.

- Vazquez, F., Ramaswamy, S., Nakamura, N. and Sellers, W. "Phosphorylation of the PTEN tail regulates protein stability and function." Molecular and Cellular Biology 20 (2000): 5010-5018.
- Vivanco, I. and Sawyers, C. "The phosphatidylinositol 3-Kinase AKT pathway in human cancer." Nature Reviews Cancer 2 (2002): 489-501.
- Vlahos, C., Matter, W., Hui, K., and Brown, R. "A specific inhibitor of phosphatidylinositol 3-kinase, 2-(4-morpholinyl)-8-phenyl-4H-1-benzopyran-4-one (LY294002)." Journal of Biological Chemistry 269 (1994): 5241-5248.
- Vogelzang N., and Stadler W. "Kidney cancer." Lancet 352 (1998): 1691-1696.
- Wang, M., Tan, Z., Zhang, R., Kotenko, S.V., and Liang, P. "Interleukin 24 (MDA-7/MOB-5) signals through two heterodimeric receptors, IL-22R1/IL-20R2 and IL-20R1/IL-20R2." Journal of Biological Chemistry 277 (2002): 7341-7347.
- Waterman, H., Alroy, I., Strano, S., Seger, R., and Yarden, Y. "The c-terminus of the kinase-defective neuregulin receptor ErbB3 confers mitogenic superiority and dictates endocytic routing." EMBO JOURNAL 18 (1999): 3348-3358.
- Webb, C., Hose, C., Koochekpour, S., Jeffers, M., Oskarsson, M., Sausville, E., Monks, A., and Woude, G. "The geldanamycins are potent inhibitors of the hepatocyte growth factor/scatter factor-Met-Urokinase plasminogen activator-plasmin proteolytic network." Cancer Research 60 (2000): 342-349.
- Welsh, G., Wilson, C., and Proud, C. "GSK3: a SHAGGY frog story." Trends in Cell Biology 6 (1996): 274-279.
- Wiggin, G., Soloaga, A., Foster, J. Murray-Tait, Cohen, P. and Arthur, J. "MSK1 and MSK2 are required for the mitogen- and stress-induced phosphorylation of CREB and ATF1 in fibroblasts." Molecular and Cellular Biology 22 (2002): 2871-81.
- Williams, M., Arthur, J., Balendran, A., Van der Kaay, J., Poli, V., Cohen, P., and Alessi, D. "The role of 3-phosphoinositide-dependent protein kinase 1 in activating AGC kinases defined in embryonic stem cells." Current Biology 10 (2000): 439-448.
- Wu, Y., Zhang, X., and Zehner, Z. "c-Jun and the dominant-negative mutant, TAM67, induce vimentin gene expression by interacting with the activator Sp1." Oncogene 22 (2003): 8891-8901.

- Xia, Z., Dickens, M., Rainegeaud, J., Davis, R., and Greenberg, M. "Opposing effects of ERK and JNK-p38 MAP kinases on apoptosis." Science 270 (1995): 1326-1331.
- Yacoub, A., Park, J., Qiao, L., Dent, P., and Hagan, M. "MAPK dependence of DNA damage repair: ionizing radiation and the induction of expression of the DNA repair genes XRCC1 and ERCC1 in DU145 human prostate carcinoma cells in a MEK1/2 dependent fashion." International Journal of Radiation Biology 77 (2001): 1067-1088.
- Yacoub, A., Mitchell, C., Brannon, J., Rosenberg, E., Qiao, L., McKinstry, R., Linehan, W., Su, Z., Sarkar, D., Lebedeva, I., Valerie, K., Gopalkrishnan, R., Grant, S., Fisher, P., Dent, P. "MDA-7 (Interleukin-24) inhibits the proliferation of renal carcinoma cells and interacts with free radicals to promote cell death and loss of reproductive capacity." Molecular Cancer Therapeutics 2 (2003): 623-632.
- Yacoub, A., Mitchell, C., Lister, A., Lebedeva, I.V., Sarkar, D., Su, Z.-z., Sigmon, C., McKinstry, R., Qiao, L., Broaddus, W.C., Gopalkrishnan, R., Grant, S., Fisher, P.B., and Dent, P. "MDA-7 (IL-24) inhibits the growth and enhances the radiosensitivity of glioma cells *in vitro* and *in vivo*." Clinical Cancer Research 9 (2003): 3272-3281.
- Yang, E., Zha, J., Jockel, J., Boise, L., Thompson, C., and Korsmeyer, S. "Bad, a heterodimeric partner for Bcl-XL and Bcl-2, displaces Bax and promotes cell death." Cell 80 (1995): 285-291.
- Yin, X., Wang, K., Gross, A., Zhao, Y., Zinkel, S., Klocke, B., Roth, K., and Korsmeyer, S. "Bid-deficient mice are resistant to Fas-induced hepatocellular apoptosis." Nature 400 (1999): 886-891.
- Yin, X. "Bid, a critical mediator for apoptosis induced by the activation of Fas/TNF-R1 death receptors in hepatocytes." Journal of Molecular Medicine 78 (2001): 203-211.
- Yosimichi, G., Nakanishi, T., Nishida, T., Hattori, T., Takano-Yamamoto, T., and Takigawa, M. "CTGF/Hcs24 induces chondrocyte differentiation through a p38 mitogen-activated protein kinase (p38MAPK), and proliferation through a p44/42 MAPK/extracellular-signal regulated kinase (ERK)." European Journal of Biochemistry 268 (2001): 6058-6065.
- Young, J., Moarefi, I., and Hartl, F. "Hsp90: a specialized but essential protein-folding tool." The Journal of Cell Biology 154 (2001): 267-273.

- Yu, C., Wang, Z., Dent, P., and Grant, S. "MEK1/2 inhibitors promote Ara-C-induced apoptosis but not loss of Deltapsi(m) in HL-60 cells." Biochemical and Biophysical Research Communications 286 (2001): 1011-1018.
- Yustein, J., Li, D., Robinson, D., and Kung, H. "KFC, a Ste20-like kinase with mitogenic potential and capability to activate the SAPK/JNK pathway." Oncogene 19 (2000): 710-718.
- Zhang, X., Silva, E., Gershenson, D., and Hung, M. "Amplification and rearrangement of c-erb B proto-oncogenes in cancer of human female genital tract." Oncogene 4 (1989): 985-989.
- Zhou, B., Liao, Y., Xia, W., Spohn, B., Lee, M., and Hung, M. "Cytoplasmic localization of p21Cip1/WAF1 by AKT-induced phosphorylation in HER-2/neu-overexpressing cells." Nature Cell Biology 3 (2001): 245-252.

Vita

Clint Mitchell was born on October 3, 1980 in Birmingham, Alabama to Larry and Biki Mitchell. He graduated from Atlee High School in Hanover, Virginia in June of 1998. He received his Bachelor of Science in Biomedical Engineering from Virginia Commonwealth University in Richmond, Virginia in 2002. He received his Master of Science in Biomedical Engineering from Virginia Commonwealth University in May of 2005. He currently works as a lab specialist in the Biochemistry / Radiation Oncology Department of Massey Cancer Center.

Caron, R., Yacoub, A., Zhu, X., **Mitchell, C.**, Han, S., Sasazuki, T., Shirasawa, S., Kozikowski, A., Hagan, M., Grant, S., and Dent, P. "H-RAS V12-induced radioresistance in HCT116 colon carcinoma cells is heregulin dependent." Molecular Cancer Therapeutics 4 (2005): 243-255.

Caron, R., Yacoub, A., Li, M., Zhu, X., **Mitchell, C.**, Hong, Y., Hawkins, W., Sasazuki, T., Shirasawa, S., Kozikowski, A., Dennis, P., Hagan, M., Grant, S., and Dent, P. "Activated forms of H-RAS and K-RAS differentially regulate membrane association of PI3K, PDK-1, and AKT and the effect of therapeutic kinase inhibitors on cell survival." Molecular Cancer Therapeutics 4 (2005): 257-270.

Caron, R., Yacoub, A., **Mitchell, C.**, Zhu, X., Hong, Y., Sasazuki, T., Shirasawa, S., Hagan, M., Grant, S., and Dent, P. "Radiation-stimulated ERK1/2 and JNK1/2 signaling can promote cell cycle progression in human colon cancer cells." Cell Cycle 4 (2005): 456-464.

Dai, Y., Rahmani, M., Xin-Yan, P., Khanna, P., Han, S., **Mitchell, C.**, Dent, P., and Grant, S. "Farnesyl-transferase inhibitors interact synergistically with the Chk1 inhibitor UCN-01 to induce apoptosis in human leukemia cells through interruption of both AKT and MEK/ERK pathways and activation of Sek1/JNK." Blood 105 (2005):1706-1716.

Dent, P., Fang, Y., Gupta, S., Studer, E., **Mitchell, C.**, Spiegel, S., and Hylemon, P. "Conjugated bile acids promote ERK1/2 and AKT activation via a pertussis toxin-sensitive mechanism in murine and human hepatocytes." Hepatology 42 (2005): 1291-1299.

Dent, P., Han, S., **Mitchell, C.**, Studer, E., Yacoub, A., Grandis, J., Grant, S., Krystal, G., and Hylemon, P. "Inhibition of insulin/IGF-1 receptor signaling enhances bile acid toxicity in primary hepatocytes." Biochemistry Pharmacology 70 (2005): 1685-1696.

Fang, Y., Han, S., **Mitchell, C.**, Gupta, S., Studer, E., Grant, S., Hylemon, P., and Dent, P. "Bile acids induce mitochondrial ROS, which promote activation of receptor tyrosine kinases and signaling pathways in rat hepatocytes." Hepatology 40 (2004): 961-971.

Hawkins, W., **Mitchell, C.**, McKinstry, R., Gilfor, D., Starkey, J., Dai, Y., Dawson, K, Ramakrishnan, V., Roberts, J., Yacoub, A., Grant, S., and Dent, P. "Transient exposure of mammary tumors to PD184352 and UCN-01 causes tumor cell death *in vivo* and prolonged suppression of tumor regrowth." Cancer Biology and Therapy 4 (2005): 1275-1284.

Yacoub, A., Park, M., Hanna, D., Hong, Y., **Mitchell, C.**, Pandya, A., Harada, H., Powis, G., Chen, C., Koumenis, C., Grant, S., and Dent, P. "OSU-03012 promotes caspase-independent, PERK-, cathepsin B-, BID- and AIF-dependent killing of transformed cells." Molecular Pharmacology (2006): Epub April 18 ahead of print.

Yacoub, A., **Mitchell, C.**, Hong, Y., Gopalkrishnan, R., Su, Z., Gupta, P., Sauane, M., Lebedeva, I., Curiel, D., Mahasreshti, P., Rosenfeld, M., Broaddus, W., James, C., Grant, S., Fisher, P., and Dent, P. "MDA-7 regulates cell growth and radiosensitivity *in vitro* of primary (non-established) human glioma cells." Cancer Biology and Therapy 3 (2004): 739-751.

Yacoub, A., **Mitchell, C.**, Lebedeva, I., Sarkar, D., Su, Z., McKinstry, R., Gopalkrishnan, R., Grant, S., Fisher, P., and Dent, P. "MDA-7 (IL-24) inhibits growth and enhances radiosensitivity of glioma cells *in vitro* via JNK signaling." Cancer Biology and Therapy 2 (2003): 347-53.

Yacoub, A., **Mitchell, C.**, Lister, A., Lebedeva, I., Sarkar, D., Su, Z., Sigmon, C., McKinstry, R., Ramakrishnan, V., Qiao, L., Broaddus, W., Gopalkrishnan, R., Grant, S., Fisher, P., and Dent, P. "Melanoma differentiation-associated 7 (interleukin 24) inhibits growth and enhances radiosensitivity of glioma cells *in vitro* and *in vivo*." Clinical Cancer Research 9 (2003): 3272-81.

Yacoub, A., **Mitchell, C.**, Brannon, J., Rosenberg, E., Qiao, L., McKinstry, R., Linehan, W., Su, Z., Sarkar, D., Lebedeva, I., Valerie, K., Gopalkrishnan, R., Grant, S., Fisher, P., and Dent, P. "MDA-7 (interleukin-24) inhibits the proliferation of renal carcinoma cells and interacts with free radicals to promote cell death and loss of reproductive capacity." Molecular Cancer Therapeutics 2 (2003): 623-32.